Evolutionary Patterns of Trilobites Across the End Ordovician Mass Extinction

by

Curtis R. Congreve
B.S., University of Rochester, 2006
M.S., University of Kansas, 2008

Submitted to the Department of Geology
and the Faculty of the Graduate School of
The University of Kansas in partial
fulfillment on the requirements for the
degree of Doctor of Philosophy
2012

Advisory Committee:

_____
Bruce Lieberman, Chair

_____
Paul Selden

_____
David Fowle

_____
Ed Wiley

_____
Xingong Li

Defense Date: December 12, 2012

The Dissertation Committee for Curtis R. Congreve certifies
that this is the approved Version of the following thesis:

Evolutionary Patterns of Trilobites Across the End Ordovician Mass Extinction

Advisory Committee:

_____

Bruce Lieberman, Chair

_____

Paul Selden

_____

David Fowle

_____

Ed Wiley

_____

Xingong Li

Accepted: April 18, 2013

Abstract: The end Ordovician mass extinction is the second largest extinction event in the history or life and it is classically interpreted as being caused by a sudden and unstable icehouse during otherwise greenhouse conditions. The extinction occurred in two pulses, with a brief rise of a recovery fauna (*Hirnantia* fauna) between pulses. The extinction patterns of trilobites are studied in this thesis in order to better understand selectivity of the extinction event, as well to understand the effect of the extinction of the evolution of various trilobite groups. To study these patterns two phylogenetic analyses of sphaerexochines and ceraurids were generated and the overall data was combined with two older analyses of homalonotids and deiphonines from my Masters Thesis. Speciation and extinction rates were estimated in the deiphonines and sphaerexochines (two closely related cheirurid clades) to understand the different patterns of extinction and survivorship in greater detail. Then, utilizing the phylogenetic analyses, the end Ordovician is reinterpreted as a large scale analog of Vrba's Relay Model, referred to herein as the Cladal Turnover Model.

This thesis is dedicated to my family (who have always supported me in all of my idiotic flights of fancy), my friends (who for some reason consistently tolerate me), and my advisor. I couldn’t have done this without any of you.

Table of Contents

Introduction

Curtis R. Congreve

The Importance of Mass Extinctions and Climatic Oscillations

In 1985, Steven Jay Gould wrote about a concept that he referred to as the Paradox of the First Tier. He noted that, despite the ubiquity of natural selection, the history of life is not predictable or progressive but rather marked by a strong signature of chance. If the day-to-day battles of natural selection were the sole factors guiding evolution through deep time, one would expect a consistent grade of predictable and progressive change as life continued to combat its way to better and better adaptability. Instead, the history of life seems to be mostly a story of survival of the luckiest, with massively successful clades being snuffed out seemingly at random (the untimely death of the dinosaurs and subsequent rise of the scrappy mammals is perhaps the best example of this phenomenon). He concluded then, that processes affecting evolution might exist at various hierarchies (or tiers), with the processes operating at higher tiers muting or canceling out the effects of lower tiers. In the paper he defined three tiers; the first being natural selection, the second being processes affecting birth and death of species, and the third being mass extinctions. In this framework, processes operating at the short time scale of natural selection, while very important in the day to day struggle of an individual population, are less important during longer time scales as the effects are muted by processes affecting differential success of species. In turn, while a species (or clade) could prove successful during normal conditions, the random culling of species in mass extinction events can profoundly reset the

rules, making successful clades into evolutionary losers and vice versa. As such, mass extinction events may represent incredibly important turning points in life history, and a general understanding of their impact and effects are vital to evolutionary biology.

While Gould's tiers (Gould 1985) were intended to designate a distinct discontinuity in evolution, the tiers themselves can be united if we instead view each tier as a response to climatic cycles or oscillations of increasing time and intensity. Looking at the first tier (natural selection), short term climatic cycles such as the wet and dry cycles of El Niño and La Niña can have dramatic effects on selection, as evidenced in the dramatic morphological changes of beak morphology through time witnessed in Darwin's finches (Grant and Grant 2002), with dry conditions pushing finches towards favoring one beak morphology and wet conditions pushing the population towards a different morphology. These patterns then seem to oscillate back and forth in step with the climate. Looking at the second tier (processes affecting speciation and extinction), longer and more intense climatic cycles (possibly associated with orbital cycles like Milankovitch cycles) have been suggested as motors of speciation and extinction, resulting in pulsed turnovers of taxa (Vrba 1985, 1992, 1995; van Dam 2006). As climate oscillates into extremes, species ranges become fractionated as habitable areas become scarce. This fractionation results in increased potential for extinction, but it also increases the potential for populations of species to become isolated, thereby speciating due to allopatric speciation. Looking at the third tier, mass extinctions may also be correlated with even longer term cycles. Raup and Sepkoski (1982) argued that there is a 26 million year extinction cycle, and Rohde and Muller (2005) presented a new analysis suggesting that there is a 62 million year cycle in biodiversity. Lieberman and Melott (2007, 2012) reconsidered these analyses and found strong evidence for the 62 million year cycle and some evidence, albeit less profound, for a 26 million

year and 32 million year cycle (Lieberman and Melott 2007). They proposed that the potential cause of this 62 million year cycle is the Earth's position in the universe. The Earth becomes more or less susceptible to extreme cosmogenic radiation and bolide impacts depending upon its position in the universe, and these astronomical factors can cause extreme and sudden shifts in the climate (Lieberman and Melott 2007, 2009, Alvarez et al. 1980, Melott et al. 2004). By placing Gould's tiers into this framework, we can envision the history of life as a series of nested hierarchies with evolutionary change driven by climatic oscillations; more intense longer cycles define higher tiers and mute the effects of shorter scale oscillations that dominate lower tiers.

Since the processes occurring during mass extinctions are similar to those occurring in species turnover (i.e. extreme shifts in climate result in habitat degradation) it might be expected that the patterns of extinction and speciation during mass extinctions might be analogous to those that occur during species turnover. In this fashion, it is possible that mass extinctions could be viewed as large scale analogs of species turnover, and patterns of extinction and survivorship during these events may best be understood using a model akin to Vrba's Turnover Pulse (1985) or Vrba's Relay Model (1992). These models suggest that major shifts in climate should result in pulses of extinction and speciation, with some species being adversely affected by the environmental shift while other species flourish. One mass extinction event that might show this pattern of pulsed extinction and speciation is the End Ordovician mass extinction.

The Ordovician Mass Extinction Event

The end Ordovician marks the second largest mass extinction, in terms of percent genera and families extinguished, in the history of life (Sepkoski 1996). The cause of this extinction has classically been interpreted as the formation of a sudden and unstable icehouse in the middle of

otherwise greenhouse conditions, which occurs contemporaneously with the extinction event (Berry and Boucot 1973, Sheehan 1973, Brenchley et al. 1994, Sheehan 2002). The extinction is seen as occurring in two major pulses, related to the initial onset of glaciation and the return to greenhouse conditions (Hallam and Wignall 1997). The first extinction pulse has traditionally been interpreted to have been caused by habitat degradation due to a combination of the draining of epicontinental seaways (Sheehan 1973) and the shrinking of the tropical climatic belt (Berry and Boucot 1973, Stanley 1984). After this pulse, there is a proliferation of survivor taxa, referred to as the *Hirnantia* taxa. The second pulse of extinction has been interpreted to have resulted from a sudden return to warmer, pre-glacial conditions, with the newly icehouse-adapted taxa going extinct. More specifically, the presence of major glaciation may have increased ocean circulation, oxygenating oceanic deep water and opening up this habitat to oxygen demanding taxa (Hallam and Wignall 1997). When the glaciers quickly receded, dysoxic conditions may have returned to the ocean bottoms, killing off taxa with high oxygen requirements (Rong and Harper 1988, Briggs et al. 1988, Fortey 1989, Sheehan 2002; Bapst 2012). While the interpreted cause of the extinction (ice maxima during the Hirnantian period) has remained consistent, modern studies have refined the timing. Modern geochemical evidence from carbon isotopes (Saltzman 2005, Finnegan et al. 2011), zooplankton biogeography (Vandenbroucke et al. 2010), and the results of ocean circulation modeling of the Ordovician (Hermann et al. 2004) suggests that the Ordovician icehouse transition likely occurred during the late Ordovician (Sandbian or early Katian), with a polar front positioned between 55º -70ºS. However, tropical sea surface temperature estimates remain high throughout the late Ordovician and only drop sharply at the extinction event (Finnegan et al. 2011). The Hirnantian glaciation is then interpreted as an

extreme glacial maximum within this late Ordovician icehouse, rather than a completely sudden transition from icehouse to greenhouse.

Introduction to the Thesis

In this thesis, new phylogenetic studies of Ordovician cheirurid trilobites are conducted with the intention of better understanding the effects of the mass extinction event. First a phylogenic analysis is conducted on sphaerexochine trilobites (Chapter 1) and then a full monographic revision is conducted on ceraurid trilobites (Chapter 3). This data is then subsequently combined with data previously assembled for my Masters Thesis to look at changes in rates of speciation and extinction during the mass extinction event (Chapter 2). From this data a model is proposed, named the Cladal Turnover Model, as one possible explanation for the extinction patterns occurring at the end Ordovician (Chapter 4) and the thesis concludes with an overview of recurring patterns of trilobite extinction and survivorship as well as plans for future study.

References

Alvarez, L.W. and W. Alvarez, F. Asaro, H.V. Michel. 1980. Extraterrestrial Cause for the Cretaceous-Tertiary Extinction. *Science* 208(4448):1095-1108.

Bapst, D.W., P.C. Bullock, M.J. Melchin, H.D. Sheets, C.E. Mitchell. 2012. Graptoloid diversity and disparity became decoupled during the Ordovician mass extinction. *PNAS* vol. 109 no. 9:3428-33

Berry, W.B.N. and A.J. Boucot. 1973. Glacio-eustatic control of the Late Ordovician-Early Silurian platform sedimentation and faunal changes. *Geological Society of America Bulletin* 84:275-284.

Brenchley, P.J., J.D. Marshall, G.A.F. Carden, D.B.R. Robertson, D.G.F. Long. 1994. Bathymetric and isotopic evidence for a short-lived Late Ordovician glaciation in a greenhouse period. *Geology* 22:295-298.

Briggs, D.E.G., R.A. Fortey, E.N.K. Clarkson. 1988, Extinction and the fossil record of the arthropods. *In* Larwood, GP. (ed) Extinction and Survival in the Fossil Record. Clarendon. Oxford.

Finnegan, S. and K. Bergmann, J.M. Eiler, D.S. Jones, D.A. Fike, I. Eisenman, N.C. Hughes, A.K. Trípati, W.W. Fischer. 2011. The Magnitude and Duration of Late Ordovician-Early Silurian Glaciation. *Science*. 331:903-906.

Fortey, R.A. 1989. There are extinctions and extinctions: examples from the lower Palaeozoic. *Philosophical Transactions of the Royal Society of London B* 325:327-355.

Gould, S.J. 1985. The Paradox of the first tier: an agenda for paleobiology. Paleobiology. 2-12.

Grant, P.R. and B.R. Grant. 2002 Unpredictable Evolution in a 30-Year Study of Darwin's Finches. *Science*. 296:707-711.

Hallam, A. and P.B. Wignall. 1997. Mass Extinctions and Their Aftermath. Oxford University Press. New York.

Hermann, A.D. and B.J. Haupt, M.E. Patzkowsky, D. Seidov, R.L. Slingerland, 2004, Response of Late Ordovician paleoceanography to changes in sea level, continental drift, and atmospheric pCO_2: Potential causes for long-term cooling and glaciation. Palaeogeography, Palaeoclimatology, Palaeoecology. 210:385-401.

Lieberman, B. S. and A. L. Melott. 2007. Considering the case for biodiversity cycles: reexamining the evidence for periodicity in the fossil record. *PLoS One* 2(8) e759:1-9.

——., and A. L. Melott. 2012. Whilst this planet goes cycling on: What role for periodic astronomical phenomena in large scale patterns in the history of life? In J. Talent (Ed.), *Earth and Life: Global Biodiversity, Extinction Intervals, and Biogeographic Perturbations Through Time*. Springer, Berlin. In press.

Rong, J. and D.A.T. Harper. 1988. A global synthesis of the latest Ordovician Hirnantian brachiopod faunas. *Transactions of the Royal Society of Edinburgh* 79:383-402.

Saltzman, M.R. and S.A. Young, 2005, Long-lived glaciation in the Late Ordovician? Isotopic and sequence-stratigraphic evidence from western Laurentia. Geology. 33(2):109-112.

Sepkoski, J.J. 1996. Patterns of Phaneroxoic extinction: a perspecitve from global data bases. *In* Valentine, JW (ed). Global Events and Stratigraphy in the Phanerozoic. Princeton University Press, Princeton.

Sheehan, P.M. 1973. The relation of Late Ordovician glaciation to the Ordovician-Silurian changeover in North American brachiopod faunas. *Lethaia* 6:147-154.

——., 2002. The Late Ordovician Mass Extinction. *Annual Review Earth Planet Science* 29:331-364.

Stanley, S.M. 1984. Temperature and biotic crises in the marine realm. *Geology* 23:205-208.

Vandenbroucke, T.R.A. and H.A. Armstrong, M. Williams, F. Paris, J.A. Zalasiewicz, K. Sabbe, J. Nõlvak, T.J. Challands, J. Verniers, T. Servais. 2010. Polar front shift and atmospheric CO_2 during the glacial maximum of the Early Paleozoic Icehouse. PNAS. 107(34):14983-14986.

van Dam, J.A. and H.A. Aziz, M.A.A. Sierra, F.J. Hilgen, L.W. van den Hoek Ostende, L.J. Lourens, P. Mein, A.J. van der Meulen, P. Pelaez-Campomanes. 2006. Long-period astronomical forcing of mammal turnover. *Nature*. 443:687-691.

Vrba, E. 1985. Environment and evolution: alternative causes of the temporal distribution of evolutionary events. *South African Journal of Science* 81:229-236.

——., 1992. Mammals as a Key to Evolutionary Theory. *Journal of Mammalogy* vol. 73,1:1-28

——., 1995. The fossil record of African Antelopes (Mammalia, Bovidae) in relation to human evolution and paleoclimate. *In* Vrba, E.S. and G.H Denton, T.C. Partridge, L.H. Burckle (eds). Paleoclimate and evolution, with emphasis on human origins Yale University Press

Chapter 1- Phylogenetic and Biogeographic Analysis of Sphaerexochine Trilobites

Curtis R. Congreve, Bruce S. Lieberman

(Formatted for submission to PLOSOne)

Abstract:

Background

Sphaerexochinae is a speciose and widely distributed group of cheirurid trilobites. Their temporal range extends from the earliest Ordovician through the Silurian, and they survived the end Ordovician mass extinction event (the second largest mass extinction in Earth history). Prior to this study, the individual evolutionary relationships within the group had yet to be determined utilizing rigorous phylogenetic methods. Understanding these evolutionary relationships is important for producing a stable classification of the group, and will be useful in elucidating the effects the end Ordovician mass extinction had on the evolutionary and biogeographic history of the group.

Methodology/Principal Findings

Cladistic parsimony analysis of cheirurid trilobites assigned to the subfamily Sphaerexochinae was conducted to evaluate phylogenetic patterns and produce a hypothesis of relationship for the group. This study utilized the program TNT, and the analysis included thirty-one taxa and thirty-nine characters. The results of this analysis were then used in a Lieberman-modified Brooks Parsimony Analysis to analyze biogeographic patterns during the Ordovician-Silurian.

Conclusions/Significance

The genus *Sphaerexochus* was found to be monophyletic, consisting of two smaller clades (one composed entirely of Ordovician species and another composed of Silurian and Ordovician species). By contrast, the genus *Kawina* was found to be paraphyletic. It is a basal grade that also contains taxa formerly assigned to *Cydonocephalus*. Phylogenetic patterns suggest Sphaerexochinae is a relatively distinctive trilobite clade because it appears to have been largely unaffected by the end Ordovician mass extinction. Finally, the biogeographic analysis yields two major conclusions about *Sphaerexochus* biogeography: Bohemia and Avalonia were close enough during the Silurian to exchange taxa; and during the Ordovician there was dispersal between Eastern Laurentia and the Yangtze block (South China) and between Eastern Laurentia and Avalonia.

INTRODUCTION

The Cheiruridae are a diverse family of phacopine trilobites with a long geologic history spanning the latest Cambrian to the Middle Devonian. Although the group is believed to be monophyletic, the individual species level relationships are largely unknown due to a paucity of phylogenetic studies within the group [1], [2]. Lane [3] provided the most recent taxonomic revision of the entire family, and recognized seven subfamilies within the Cheiruridae. One subfamily is the diverse, Ordovician-Silurian Sphaerexochinae; it is diagnosed by its possession of a wide axis, three pairs of glabellar furrows with S1 being longer and more incised than S2 or S3, eyes positioned close to the axial furrows, triangular free cheek, wide and short rostral plate,

thoracic and pygidial doublure extending to the axial furrow, and a hypostome with small anterior wings and a gently inflated middle body and a shallow notch on the posterior border [4]. There are four genera that are readily referable to this subfamily, and a phylogenetic analysis of these will be the focus of this study. The first genus is the eponymous *Sphaerexochus*; the monophyly of *Sphaerexochus* is supported by several apomorphies including a highly inflated glabella that is subcircular in outline, S1 deeply incised and curving sharply towards L0, S2 and S3 faintly incised, free cheeks small and vertical, and a hypostome that is trapezoidal in outline [3], although monophyly had not been previously tested using a phylogenetic approach. It has been proposed that the genus can be further divided into four subgenera (two of which are monotypic): *S. (Sphaerexochus), S. (Korolevium), S. (Parvixochus),* and *S. (Onukia)* [5], [6]. Three other sphaerexochine genera are *Kawina*, *Cydonocephalus*, and *Forteyops*. *Kawina* had previously been treated as closely related to *Sphaerexochus* on the basis of reduced triangular free cheeks, wide axis of the exoskeleton, eyes situated close to the axial furrow, rostral plate wide (transverse) and short, S1 furrows deeper and longer than S2 and S3, a pygidial and thoracic doublure extending to the axial furrow, and a pygidium with two to three axial rings, a semi-circular outline, a pronounced terminal axial piece, and three pleural spines [4]. Adrain and Fortey [7] reclassified *Cydonocephalus* as a junior synonym of *Kawina*, see also Jell and Adrain [8]**.** The type species of the monotypic *Forteyops*, *Forteyops sexapugia*, was originally grouped within *Kawina* [9] until Pribyl *et al.* [6] moved it into its own genus. The monophyly and relationships of these genera have not been previously tested using a phylogenetic approach. One taxon formerly assigned to the sphaerexochines by Lane [3], *Hyrokybe*, has since been shown to be more closely related to a different cheirurid subfamily: the Acanthoparyphinae (see [1]), and therefore will not be considered herein. The affinities of *Nieszkowskia* also likely

lie with this subfamily as well. Other taxa that have been previously assigned to the Sphaerexochinae, such as *Xystocrania* and *Pompeckia*, are either known from limited material or have dubious affinities, and therefore will not be considered herein. Here we present a phylogenetic analysis of the Sphaerexochinae as part of a larger systematic revision of the Cheiruridae, and use the resulting phylogeny to consider biogeographic patterns spanning the Ordovician-Silurian and discern patterns of survival during the end Ordovician mass extinction.

The end Ordovician mass extinction event is considered to be the second largest mass extinction in the history of life and is classically interpreted as being caused by a brief, unstable icehouse during otherwise greenhouse conditions [10]–[12]. The event is particularly important for trilobites, as its selectivity profoundly affected the evolution of the group. Previous research suggests that trilobites with a planktonic larval stage are more strongly affected by the extinction event than trilobites with benthic larvae [13]. Furthermore, trilobite groups with a presumed pelagic adult stage completely go extinct at the Ordovician-Silurian boundary. To put this research into a broader context, the sphaerexochines are a group that survives the event and they have been interpreted as having benthic larvae [14].

MATERIALS AND METHODS

Phylogenetic Analysis

Morphological terminology follows Whittington et al. [15] (see Fig. 1 and Fig. 2 for line drawings of trilobites with the relevant parts labeled). Material was examined from the Yale University Peabody Museum of Natural History (YPM), the Museum of Comparative Zoology, Harvard University (MCZ), the University of Kansas Museum of Invertebrate Paleontology

(KUMIP), the Naturhistoriska Riksmuseet, Stockholm, Sweden (AR), the Paleontological Museum of the University of Oslo, Norway (PMO), the VSEGEI in Saint Petersburg, Russia, and the Swedish Geological Survey, Uppsala (SGU).

Taxa Analyzed.

A total of thirty-one taxa were included in this analysis. *Forteyops* s*exapugia* was chosen as the outgroup as it appears to represent a basal sphaerexochine distinguished by its very early stratigraphic appearance, and it can be distinguished from all other ingroup sphaerexochines by its possession of dagger-shaped pygidial pleurae (a character common in other cheirurid trilobites but not found in other sphaerexochine species). All well-preserved members of the Sphaerexochinae for which material was available were considered in the phylogenetic analysis. Meriting special mention here is *Sphaerexochus britannicus*, which was included as a distinct species despite Thomas's [16] claim that the species is a synonym of *S. mirus*. Although Thomas [16] argued that the differences in the proportions of the pygidia between the two forms arose solely because the pygidia represented different developmental stages, Ramsköld [17] demonstrated that these differences could not be attributed to ontogenetic changes. Another noteworthy species is *S. scabridus*. Ramsköld [17] argued that this species might be dimorphic as he identified a few long-spined pygidia. However, he noted that these long-spined specimens were rare and that there was insufficient material to conclude if these specimens were in fact dimorphs of *S. scabridus* or if instead they belonged to a different species. Following his cautions, in our analysis we coded only the short-spined specimens of *S. scabridus*, since these are most similar to the neotype established by Ramsköld [17]. Finally, special mention should be given to the potentially dimorphic species, *S. dimorphus*. This taxon was analyzed twice in our study, the first time coding the species as a dimorphic taxon and the

second time with each morph coding as a separate species. This procedure investigated whether or not there was sufficient phylogenetic evidence to split *S. dimorphus* into two separate species. Because the character codings for each of the two morphs were distinct from the codings of all other taxa considered in the analysis, these morphs could not be synonymized with any other species. The net relationships suggested by both of these two analyses are identical; however, the analysis that split the two morphs into separate species had slightly worse resolution, with both morphs grouped together in a large polytomy. Coupling this result with the fact that the two morphs only differ in three of the characters used for phylogenetic analysis, we chose to treat *S. dimorphus* as a single dimorphic taxon for the purposes of this paper.

Specific Taxa Analyzed.

(Relevant material examined is listed where appropriate. In instances where museum material was not examined, species were coded using photographs from scientific publications.) *Forteyops* s*exapugia* (YPM 18289, 18291, 18293);*"K." arnoldi*; *"K." divergens*; *K. vulcanus* (YPM 170174, 227101, 227109–227112); *"K." griphus*; *"K." torulus*; *"K." prolificus*;*"K."mercurius; "K." scrobiculus; "K." prominulus; Sphaerexochus latifrons* (AR 30060, 30063, 30065, 30067, 51316–51318, 51320–51322, 51324; YPM 183971–183973); *S. molongloensis*; *S. scarbridus* (AR 29991, 30016, 30042, 30068, 30074, 30075, 30078, 30144, 30187, 30193, 30194, 51305, 51307–51309, 51311–51313, 51315, 51338–51343, 53232–53236; SGU 1401, 1402); *S. atacius*; *S. eurys*; *S. calvus* (SGU 4133–4135; AR 11256–11263, 11375, 11376, 49250); *S. laciniatus* (AR 29831, 29857, 29858, 29860, 29862, 29866, 29882, 30059, 30072, 30112, 51325); *S. johnstoni*; *S. mirus* (AR 39276, 39477–39482, 39484–39486, 39553 a, b; MCZ 1325, 1328, 196479, 196484, 196498; YPM 6573, 183982–183984, 183998–194000) (Fig. 3); *S. britannicus*; *S. pulcher*; *S. parvus*; *S. brandlyi*; *S.*

romingeri (KUMIP 105187–105190; MCZ 195135, 195139, 195144, 195146, 195190, 195195, 195535, 195541, 195546, 195548, 195555, 195565; YPM 183978–183981, 184003); *S. fibrisulcatus*; *S. hapsidotus*; *S. dimorphus*; *S. glaber*; *S. hiratai*; and *S. arenosus.*

Characters.

The characters used in phylogenetic analysis are listed below in approximate order from anterior to posterior position on the organism. A complete character matrix is given in Table S1. Characters emphasize the adult, holaspid stage as there are only a limited number of taxa for which early ontogenetic stages are available.

Cephalon

1. S1; 0: contacts S0, 1: does not contact S0.
2. Space between the proximal edges of both L1 lobes measured transversely (dorsal view); 0: wide (distance between the proximal edges of L1/posterior glabellar margin transverse width = 0.5), 1: narrow (distance between the proximal edges of L1/posterior glabellar margin transverse width = 0.33).
3. Point of maximum glabellar convexity (lateral view); 0: medial, 1: anterior.
4. S2 and S3; 0: strongly incised, 1: weakly incised, 2: indistinct or absent.
5. Genal spines; 0: present; 1: absent or reduced to small thorn-like projections.
6. Angle formed by the intersection of the anterior and lateral glabellar margins, in anterior view; 0: relatively broad (115–120 degrees), 1: relatively narrow (105–110 degrees).
7. Tubercle on center of L0; 0: present, 1: absent.
8. Shape of S1 close to the lateral glabellar margins; 0: S-shaped, 1: straight.

9. Border of librigena; 0: wide (ratio of exsagittal width of librigena to border width is 0.4–0.5); 1: narrow (ratio of exsagittal width of librigena to border width is 0.2–0.33).
10. L0; 0: wide (maximum glabellar width (tr.)/L0 (tr.) is 1.2–1.4), 1: narrow (maximum glabellar width (tr.)/L0 (tr.) is 1.6–1.8).
11. S1; 0: strongly incised, 1: weakly incised to indistinct.
12. Anterior glabellar margin (in anterior view); 0: roughly straight, 1: strongly convex.
13. Glabella between S0 and S1 (in lateral view); 0: curves uniformly with the rest of the glabella, 1: inflates dramatically.
14. S1 orientation; 0: runs roughly transverse, 1: curves posteriorly.
15. Shape of medial part of S0; 0: straight, 1: concave anteriorly.
16. Lateral margins of the glabella immediately anterior of S1 (in dorsal view); 0: roughly parallel, 1: strongly converging, 2: strongly diverging.
17. Border furrow on librigena; 0: pencil thin (ratio of exsagittal width of librigena to border furrow width is 0.1), 1: narrow (ratio of exsagittal width of librigena to border furrow width is 0.15–0.22), 2: wide (ratio of exsagittal width of librigena to border furrow width is 0.27–0.33).

Hypostome

1. Middle body furrow; 0: does not intersect or only faintly contacts outer border furrow, 1: prominently intersects outer border furrow.
2. Middle body furrow of hypostome; 0: prominently intersects entire middle body, 1: restricted to the lateral edges of the middle body.

3. Posterior margin; 0: possesses a strongly concave pocket, 1: is straight or with concave pocket strongly reduced to absent.

Pygidium (Note, all measurements of the terminal axial piece use the notch on the lateral edges of the terminal axial piece as the anteriormost point of the axial piece if the segment has been fused to the axial ring.)

1. Pleural spines; 0: terminate close to each other, forming a pygidial shield, 1: separate from each other distally.
2. Inter-pleural furrows; 0: wide, 1: narrow (pencil thin).
3. Anteriormost set of pleural spines; 0: has proximal “kink” associated with a 60–80 degree angle change and a long crescent shaped notch on the anterior side of the spine, 1: gradually curves proximally, with the notch absent or reduced.
4. Distal pleural tips; 0: flat, 1: rounded, 2: subtriangular.
5. Width (tr.) of terminal axial piece; 0: narrow (tr.) (transverse width of the anteriormost part of the axial piece ~ three quarters of its length (sag.)), 1: wide (tr.) (transverse width of the anteriormost part of the axial piece ~ two times its length (sag.)), 2: average (tr.) (transverse width of the anteriormost part of the axial piece ~ its length (sag.)).
6. Pygidial convexity (posterior view); 0: vaulted, 1: nearly flat.
7. Pygidial dimensions; 0: wide and short (pygidial width (tr.) divided by length (sag.) is roughly 2.1–2.2), 1: long and narrow (pygidial width (tr.) divided by length (sag.) is roughly 1.6–1.8), 2: very long (pygidial width (tr.) divided by length (sag.) is roughly 1–1.3).
8. First axial ring; 0: wide (width (tr.) of axial ring divided by width (tr.) of pleural field ~1.5–1.7), 1: narrow (width (tr.) of axial ring divided by width (tr.) of pleural field ~1).

9. Posteriormost part of terminal axial piece in dorsal view; 0: rounded, 1: pointed.
10. Maximum convexity of terminal axial piece, in lateral view; 0: anterior, 1: medial, 2: posterior.
11. Interpleural furrows; 0: deep, 1:shallow.
12. Lateral margins of second set of pleural spines at approximate spine midpoint; 0: strongly curved, 1: weakly curved to straight.
13. Terminal axial piece size; 0: small (length (sag.) < length (sag.) of first axial ring), 1: large (length (sag.) >1.5 length (sag.) of first axial ring).
14. Distal tips of pleural spines; 0: hooked (i.e., sharply curved near distal ends), 1: straight.
15. Distal ends of the posteriormost pleural spines; 0: dramatically inflate laterally, 1: remain relatively the same size.
16. Angle the pygidial axial furrow along axial ring 1 and 2 forms with a sagittal line, 0: shallow (~20°), 1: sharp (>30°).
17. Furrow on proximal end of first pleural spine; 0: visible in dorsal view, 1: not visible in dorsal view.
18. Lateral edges of terminal axial piece; 0: straight sided, 1: strongly curved.
19. Third axial ring; 0: fused completely to terminal axial piece, forming a notch, 1: partially fused (ring partly visible), 2: ring distinct (not fused).

Methods.

The data were analyzed using TNT v1.1 [18]. A traditional search algorithm using TBR with 10,000 replications, 1 random seed, and 10 trees saved per replication was used to determine the most parsimonious trees for the data matrix. All characters were unweighted and all multistate characters were treated as unordered as there were no obvious criteria for ordering them. To

assess tree support, bootstrap, jackknife, and Bremer [19] support values were calculated in TNT. Bootstrap and jackknife tests were analyzed using 10,000 replicates and a traditional search (13 characters, 33 percent of the data, were removed during the jackknife test). The matrix data were compiled into Nexus files using Mesquite v.2.01 [20] and trees were generated using FigTree v.1.1.2 [21].

Biogeographic Analysis

The results from phylogenetic analysis were used in biogeographic analysis by applying Lieberman-modified Brooks Parsimony Analysis (LBPA) [22]. This method is described in detail in Lieberman and Eldredge [23], and Lieberman [24], [25]; the method has been used to investigate biogeographic patterns in a variety of fossil taxa, (e.g. [23], [24], [26]–[28]). An area cladogram was created by replacing the names of the terminal taxa on the consensus most parsimonious tree with the geographic areas where these taxa were found. The areas used in the analysis are: Avalonia (present day Great Britain and Ireland); Eastern (E.) and Northwestern (N.W.) Laurentia; Bohemia (Central Europe); Yangtze block (South China and Japan); Australia; and Baltica (present day Norway, Sweden, eastern Russia, and Finland) (Fig. 4). These areas represented distinct geological regions and also contained large numbers of endemic taxa during the Ordovician and Silurian; in effect these definitions follow the area designations of Scotese and McKerrow [29], Fortey and Cocks [30], Harper [31], Torsvik et al. [32], [33], and Zhou and Zhen [34]. One of the species used in the analysis, *Sphaerexochus eurys*, is found in Scotland (in the Midland Valley Terrane- Girvan). For the purposes of this analysis, Scotland was treated as part of Eastern Laurentia based on paleomagnetic and faunal studies that suggest the Midland Valley Terrane stayed peripheral to Laurentia throughout the Ordovician [33], [35]. Next, the

geographic locations for the ancestral nodes of the area cladogram were optimized using a modified version of the Fitch [36] parsimony algorithm (Fig. 5). The area cladogram was then used to generate two data matrices, one to code for congruent patterns of geodispersal (Table S2) and the other to code for congruent patterns of vicariance (Table S3). The former provides information about the relative time that barriers formed, isolating regions and their respective biotas; the latter provides information about the relative time that barriers fell, allowing biotas to congruently expand their range [23]–[25]. Each matrix was then analyzed using the exhaustive search function of PAUP* 4.0 [37] as well as the implicit enumeration function in TNT v1.1 [18]. PAUP* was used in addition to TNT because the exhaustive search function in PAUP* calculates the g_1 statistic, which can be used to gauge whether the results were significantly different from randomly generated data. Both programs yielded the same trees. The method results in the generation of two trees, one tree showing congruent patterns of range expansion (the geodispersal analysis) and the other tree showing congruent patterns of range contraction (the vicariance analysis).

RESULTS

Phylogenetic Analysis

The analysis generated 29 most parsimonious trees of length 115 steps, with CI (excluding uninformative characters) and RI values of 0.405 and 0.715 respectively. A strict consensus of these trees (Figs. 5, 6) suggests that taxa traditionally assigned to *Kawina* and *Cydonocephalus* form a paraphyletic grade at the base of a monophyletic *Sphaerexochus*. Species relationships within part of *Sphaerexochus* are uncertain; however, there are at least two smaller clades within this monophyletic group, with the more

resolved clade consisting entirely of mid Ordovician species and the polytomy consisting of Silurian species and the Ordovician species *S. calvus*, *S. fibriculatus*, and *S. eurys*.

Part of the lack of resolution in Silurian *Sphaerexochus* can be attributed to *S. romingeri*. If this taxon is removed from the analysis, TNT generates a single most parsimonious tree of 112 steps. However, since *S. romingeri* is well preserved and known from ample material, there seems to be no clear grounds for excluding it from the analysis.

Biogeographic Analysis

Results of the analysis.

The LBPA yielded three most parsimonious geodispersal trees of length 69 steps (Fig. 7). The strict consensus of these three trees results in two resolved nodes uniting E. Laurentia and the Yangtze Block, and Avalonia and Bohemia. In addition, a single most parsimonious vicariance tree of length 60 steps was also recovered. The tree has three resolved nodes uniting N.W. Laurentia and Avalonia, E. Laurentia and the Yangtze Block, and Baltica with a combined E. Laurentia-Yangtze Block.

We used the test of Hillis [38], the g_1 statistic, to determine whether the results of our analysis differ from those produced by random data. The g_1 statistics for the geodispersal and vicariance components of the LBPA were −1.175 and −1.005 respectively, suggesting that our results differ from random data with a significance value of 0.01.

DISCUSSION

Phylogenetic Analysis

Our analysis suggests that the genus *Sphaerexochus* as originally defined is monophyletic. By contrast, *Kawina* and *Cydonocephalus*form one large grade at the base of *Sphaerexochus*, and are therefore paraphyletic. We suggest that *Kawina* be redefined as a monotypic genus including its type species *K. vulcanus,* and that all other species originally placed within *Kawina* and *Cydonocephalus* be placed within *"Kawina*", with the quote marks denoting paraphyly following the convention of Wiley [39]. We are hesitant to lump all of the species originally assigned to *Kawina* and *Cydonocephalus* into *Sphaerexochus* because relationships within *"Kawina"* may be more complex than this analysis suggests. Therefore, we consider it prudent to differentiate them from *Sphaerexochus* until a larger scale phylogeny can piece apart the complete taxonomic relationships of other taxa including *Xystocrania* and *Nieszkowskia*.

The topology suggests that there are at least two smaller clades within the genus *Sphaerexochus,* giving partial support to some of the previously identified subgeneric groupings within the genus (*sensu* [6]). The smaller of the two clades contains *S. arenosus*, *S. atacius*, *S. pulcher*, and *S. parvus*, all of which are species that were originally placed by Pribyl *et al.* [6] into the subgenera *S. (Korolevium)* and *S. (Parvixochus).* Thus, *S. (Korolevium)* as it was originally defined is a monophyletic group. The monotypic *S. (Parvixochus),* which contains the species *S. parvus*, maps basally to the *S. (Korolevium)* clade. Since the placement of *S. (Parvixochus)* on the tree does not reduce *S. (Korolevium)* to a paraphyletic group, there is no sufficient evidence to suggest synonymy of these two groups. The second clade consists of species placed within *S. (Sphaerexochus)* and is also monophyletic as originally defined. The phylogenetic placement of

the monotypic subgenus *S. (Onukia)* [5] could not be assessed in this analysis because the type species of the group is based on poorly preserved and deformed specimens that could not be analyzed phylogenetically.

The tree topology suggests that the genus *Sphaerexochus* was relatively unaffected by the mass extinction event at the end Ordovician. While the *S (Korolevium)-S. (Parvixochus)* clade consists entirely of Ordovician species, these species go extinct during the Middle Ordovician so the mass extinction event cannot be invoked to explain the clade's disappearance. The *S. (Sphaerexochus)* clade contains Silurian and Ordovician species and further supports the hypothesis that this group passed through the mass extinction event essentially unscathed. Even though our analysis of this clade resulted in a large polytomy, no matter how the polytomy is resolved, the implications are generally the same. For instance, if the Ordovician species map out basal to the Silurian species, this implies that the common ancestors of these Ordovician species survived the event and gave rise to the new Silurian forms. If, however, one or more of the Ordovician species maps nested within the Silurian species, then it implies that the diversification within the Silurian clade has its roots in the Middle or Late Ordovician. This is true even if *S. romingeri* is removed from the analysis because then the taxon *S. calvus* (a Late Ordovician species) maps out nested within the Silurian forms; this would actually suggest that the end Ordovician may have been a time of significant diversification for species within *Sphaerexochus*. This type of extinction resistance of select groups of trilobites across the end Ordovician mass extinction is not entirely unique, as it has been observed by other authors, such as Adrain *et al.* [40].

Phylogenetic analysis reveals interesting patterns of character evolution within *Sphaerexochus*. Holloway [41] argued that Silurian species of *Sphaerexochus* showed little difference in their cephala, concluding that the cephalon could not provide diagnostic characters for species identification in Silurian species. Our results mirror this assessment: species grouping within the large Silurian polytomy all code similarly for cephalic characters, varying only in the width of the free cheek border and the width of the free cheek furrow. This fixation in the characters of the cephalon might suggest an evolutionary bottleneck. Potentially, one source of that bottleneck might be preferential extinction at the end Ordovician. However, the phylogeny suggests that the *Sphaerexochus* clade was not especially affected by the mass extinction event; instead, the bottleneck might have occurred in the Middle Ordovician. It is also possible that the fixation of cephalic characters could be due to some sort of evolutionary burden or developmental constraints *sensu* Riedl [42] and Gould [43], but such a possibility at this time remains untestable.

Systematic Paleontology

Kawina Barton, 1916 [44].

Type species.

Kawina vulcanus (Billings, 1865 [45]).

Diagnosis.

Medial portion of S0 strongly concave anteriorly. Lateral margins of the glabella strongly converge anterior of S1. Border of the librigena narrow (tr.). Border furrow of the librigena pencil thin. For addition diagnostic criteria see the diagnosis of *K. vulcanus* in Whittington [46].

Discussion.

Because the phylogenetic analysis indicates *Kawina* is paraphyletic, we propose that the genus be redefined as a monotypic taxon including its type species. All other species originally placed within the genus *Kawina* (or its junior synonym *Cydonocephalus*) are placed within "*Kawina*".

Sphaerexochus Beyrich, 1845 [47].

Type species.

Sphaerexochus mirus Beryich, 1845 [47].

Diagnosis.

See Lane [3].

Discussion.

Some species that have traditionally been placed within the genus *Sphaerexochus* could not be considered in phylogenetic analysis because they were poorly preserved or very incomplete. For example, *S. eximius, S. parabibrisulcatus,* and *S. trisulcatus* were excluded from the analysis because they are based only on glabellar material. *Sphaerexochus sugiyamai, S. planirachis, S. lanei, S.? shallochensis,* and *S. balclatchiensis* were excluded because their holotype specimens were strongly crushed and/or deformed. *Sphaerexochus lorum* was excluded from analysis because its pygidia and cranidia were severely crushed and eroded. *Sphaerexochus bridgei* and *S. arcuatus* were excluded from the analysis because their pygidia were incomplete and effaced. The assignment of these taxa, excluding *S.? shallochensis*(whose generic affinity cannot be determined because its type consists of a crushed thorax), to *Sphaerexochus*, however, is valid based on the presence of the following characters: wide spacing between medial tips of S1; S2

and S3 weakly incised to absent; shape of S1 straight close to the lateral glabellar margins; strongly convex anterior glabellar border; and the third axial ring of the pygidium is partially or completely fused to the terminal axial piece. In addition, *Sphaerexochus angustifrons* was treated as synonymous with *S. calvus* following Warburg [48].

The species that have been previously referred to as *S. desertus*and *S. bohemicus* were excluded from analysis because their affinities do not appear to lie with *Sphaerexochus*; in particular, the pygidium of *S. bohemicus* shows significant similarities with eccoptochilinids and *S. desertus* has been classified as an asaphid. *Sphaerexochus centeo* and *S. akimbo* unfortunately could not be considered in phylogenetic analysis.

Biogeographic Analysis

The vicariance tree suggests a close relationship between N.W. Laurentia and Avalonia that is not replicated in the geodispersal tree. This relationship is governed by the condition of the basal node of the phylogeny, which was reconstructed as a combined E. Laurentia-N.W. Laurentia-Avalonia. The node is temporally constrained to the Early Ordovician, when Avalonia was separated from Laurentia and peripheral to Gondwana [49]. Since there is no paleomagnetic evidence to suggest that Avalonia and Laurentia were joined during the Late Cambrian/Early Ordovician, we interpret this result as being caused by a long distance dispersal event. The geodispersal tree suggests a close relationship between Avalonia and Bohemia. The pattern could potentially be the result of the movement of Bohemia towards the equatorial Laurentia-Baltica-Avalonia complex during the Late Ordovician/Silurian [49]. Previous work on the Deiphoninae, another group of cheirurid trilobites, suggests a similar geodispersal event between Laurentia and Bohemia [2]. However, based on the area cladogram, the relationship between Avalonia and

Bohemia is only supported by the biogeographic states of two taxa (*S. britannicus* and *S. mirus*), so it would be prudent not to make too much of this pattern.

The geodispersal tree also suggests a close relationship between E. Laurentia and the Yangtze block. This relationship is replicated in the vicariance tree, suggesting that the processes affecting geodispersal and vicariance between these two regions were the same, potentially implicating cyclical processes such as sea-level rise and fall. However, paleomagnetic and other faunal evidence suggest that these two regions were far apart [34], [49]. The pattern may be governed by the fact that the ancestral node of the large polytomy in Figure 5 was reconstructed as a combined E. Laurentia-Yangtze, thereby resulting in each end member taxon in the polytomy being derived via vicariance or geodispersal from the combined ancestral area of E. Laurentia-Yangtze. In order to test the effects of this polytomy, the biogeographic analysis was run again but using the phylogeny that excluded *S. romingeri*. This time, the close relationship between E. Laurentia and Yangtze is only recovered in the geodispersal tree, although other area relationships within the biogeographic analysis change as well, suggesting reasonably that any relationship between E. Laurentia and Yangtze is attributable to long distance dispersal. A similar long distance dispersal event has been observed in deiphonine trilobites between N.W. Laurentia and Australia during the late Ordovician [2].

Conclusions

A phylogenetic analysis of the sphaerexochines suggests that the genus *Sphaerexochus* is monophyletic as originally defined, while the genera *"Kawina"* and *"Cydonocephalus"* form a paraphyletic grade at the base of *Sphaerexochus*. The topology of the tree also suggests that the sphaerexochines were barely affected by the end Ordovician mass extinction event. Since the

group is presumed to have had benthic larvae, this result agrees with the previous study by Chatterton and Speyer [13] on trilobite survivability across the extinction event. Compared to the extinction patterns observed in related groups, like the deiphonine trilobites [2], the sphaerexochines are particularly exceptional because they not only appear to suffer little extinction, but potentially proliferate during or immediately after the event. The biogeographic patterns of the group do not strongly suggest a biogeographic pattern in survival across the extinction event. The biogeographic analysis does suggest, however, that the sphaerexochines may have been capable of fairly long-distance dispersal, despite their benthic larval and adult life strategies. This could be the result of a planktonic-benthic larval life strategy, which has been hypothesized by Chatterton and Speyer [13] as an alternative interpretation of cheirurid ontogeny. To test this claim, further biogeographic analyses on cheirurid trilobites will be necessary to see if multiple cheirurid groups exhibit this pattern in long-distance dispersal.

ACKNOWLEDGMENTS

We thank Susan Butts from the YPM, Jessica Cundiff from the MCZ, Stefan Bengtson and Christiana Frauzen-Bengtson from the AR, David Bruton and Franz-Josef Lindemann from the PMO, Linda Wickström from the SGU, and Ivan Gogin from the VSEGEI for providing access to study material that was vital for the completion of this study, and also for loaning relevant material. Thanks to Jonathan Adrain for information on taxonomic composition of the sphaerexochines, to David Bruton for information on specimen repositories and providing relevant references, and to Brian Chatterton, Malte C. Ebach, and one anonymous reviewer for comments that greatly improved the quality of this manuscript.

REFERENCES

1. Adrain JM (1998) Systematics of the Acanthoparyphinae (Trilobita), with species from the Silurian of Arctic Canada. Journal of Paleontology 72: 698–718.
2. Congreve CR, Lieberman BS (2010) Phylogenetic and Biogeographic Analysis of Deiphonine Trilobites. Journal of Paleontology 84: 128–136.
3. Lane PD (1971) British Cheiruridae (Trilobita). London: Palaeontographical Society. 95 p.
4. Whittington HB (1965) Trilobites of the Ordovician Table Head Formation, Western Newfoundland. Bulletin of the Museum of Comparative Zoology, Harvard University 132: 275–442.
5. Kobayashi T, Hamada T (1976) A new Silurian trilobite from Ofunato, North Japan. Proceedings of the Japanese Academy 52: 367–370.
6. Pribyl A, Vanek J, Pek I (1985) Phylogeny and taxonomy of family Cheiruridae (Trilobita). Acta Universitatis Palackianae Olomucensis Facultatis Medicae 83: 107–193.
7. Adrain JM, Fortey RA (1997) Ordovician trilobites from the Tourmakeady Limestone, western Ireland. Bulletin of the Natural History Museum Geology Series 53: 79–115.
8. Jell PA, Adrain JM (2003) Available generic names for trilobites. Memoirs of the Queensland Museum 48: 331–553.
9. Ross RJ Jr (1951) Stratigraphy of the Garden City Formation in north-eastern Utah, and its trilobite faunas. Bulletin of the Peabody Museum of Natural History, Yale University, New Haven No. 6: i–vi. 1-161.
10. Berry WBN, Boucot AJ (1973) Glacio-Eustatic Control of Late Ordovician Early Silurian Platform Sedimentation and Faunal Changes. Geological Society of America Bulletin 84: 275–284.
11. Sheehan PM (1973) Relation of Late Ordovician Glaciation to Ordovician-Silurian Changeover in North-American Brachiopod Faunas. Lethaia 6: 147–154.
12. Sheehan PM (2001) The Late Ordovician mass extinction. Annual Review of Earth and Planetary Sciences 29: 331–364.
13. Chatterton BDE, Speyer SE (1989) Larval Ecology, Life-History Strategies, and Patterns of Extinction and Survivorship among Ordovician Trilobites. Paleobiology 15: 118–132.
14. Speyer SE, Chatterton BDE (1989) Trilobite larvae and larval ecology. Historical Biology 3: 27–60.
15. Whittington HB, Chatterton BDE, Speyer SE, Fortey RA, Owens RM, et al. (1997) Part O; Arthropoda 1; Trilobita, revised; Volume 1, Introduction, order Agnostida, order Redlichiida. In: Kaesler RL, editor. Treatise on Invertebrate Paleontology. Lawrence, KS: The University of Kansas Press and the Geological Society of America. 530 p.
16. Thomas AT (1981) British Wenlock trilobites. Part 2. Palaeontographical Society Monographs (London) 134: 57–99.
17. Ramsköld L (1983) Silurian cheirurid trilobites from Gotland. Palaeontology (Oxford) 26: 175–210.
18. Goloboff PA, Farris JS, Nixon KC (2008) TNT, a free program for phylogenetic analysis. Cladistics 24: 774–786.
19. Bremer K (1994) Branch Support and Tree Stability. Cladistics-the International Journal of the Willi Hennig Society 10: 295–304.
20. Maddison WP, Maddison DR (2007) Mesquite: a modular system for evolutionary analysis. 2.72 ed. 11: Available:http://mesquiteproject.org. Accessed: 2009 Dec.

21. Rambaut A (2008) FigTree. 1.1.2 ed. 19: Available:http://tree.bio.ed.ac.uk/software/figtree. Accessed: 2009 Dec.
22. Maguire KC, Stigall AL (2008) Paleobiogeography of Miocene Equinae of North America: a phylogenetic biogeographic analysis of the relative roles of climate, vicariance, and dispersal. Palaeogeography, Palaeoclimatology, Palaeoecology 267: 175–184.
23. Lieberman BS, Eldredge N (1996) Trilobite biogeography in the Middle Devonian: Geological processes and analytical methods. Paleobiology 22: 66–79.
24. Lieberman BS (2000) Paleobiogeography: Using Fossils to Study Global Change, Plate Tectonics, and Evolution. New York: Plenum/Kluwer Academic. 207 p.
25. Lieberman BS (2003) Biogeography of the Trilobita during the Cambrian radiation: deducing geological processes from trilobite evolution. Special Papers in Palaeontology 70: 59–72.
26. Rode AL, Lieberman BS (2005) Integrating evolution and biogeography: a case study involving Devonian crustaceans. Journal of Paleontology 79: 267–276.
27. Hembree DI (2006) Amphisbaenian paleobiogeography: evidence of vicariance and geodispersal patterns. Palaeogeography Palaeoclimatology Palaeoecology 235: 340–354.
28. Lee SB, Lee DC, Choi DK (2008) Cambrian-Ordovician trilobite family Missisquoiidae Hupe, 1955: Systematic revision and palaeogeographical considerations based on cladistic analysis. Palaeogeography Palaeoclimatology Palaeoecology 260: 315–341.
29. Scotese CR, McKerrow WS (1991) Ordovician plate tectonic reconstructions. In: Barnes CR, Williams SH, editors. Geological Surey of Canada Paper 90-09. pp. 271–282.
30. Fortey RA, Cocks LRM (1992) The Early Palaeozoic of the North Atlantic region as a test case for the use of fossils in continental reconstruction. Tectonophysics 206: 147–158.
31. Harper DAT (1992) Ordovician Provincial Signals from Appalachian-Caledonian Terranes. Terra Nova 4: 204–209.
32. Torsvik TH, Tait J, Moralev VM, Mckerrow WS, Sturt BA, et al. (1995) Ordovician Paleogeography of Siberia and Adjacent Continents. Journal of the Geological Society 152: 279–287.
33. Torsvik TH, Smethurst MA, Meert JG, VanderVoo R, McKerrow WS, et al. (1996) Continental break-up and collision in the Neoproterozoic and Palaeozoic - A tale of Baltica and Laurentia. Earth-Science Reviews 40: 229–258.
34. Zhou ZY, Zhen YY (2008) Trilobite-constrained Ordovician biogeography of China with reference to faunal connections to Australia. Proceedings of the Linnean Society of New South Wales 129: 183–195.
35. Armstrong HA, Owen AW (2001) Terrane evolution of the paratectonic Caledonides of northern Britain. Journal of the Geological Society 158: 475–486.
36. Fitch WM (1971) Toward Defining Course of Evolution - Minimum Change for a Specific Tree Topology. Systematic Zoology 20: 406–416.
37. Swofford D (1998) PAUP. 4.0 ed. 2: Available:http://PAUP.csit.fsu.edu/. Accessed: 2011 Jun.
38. Hillis DM (1991) Discriminating Between Phylogenetic Signal and Random Noise in DNA Sequences. In: Miyamoto MM, Cracraft J, editors. Phylogenetic analysis of DNA sequences: Oxford University Press. pp. 278–294.
39. Wiley EO (1979) An annotated Linnaean hierarchy, with comments on natural taxa and competing sytems. Systematic Zoology 28: 308–337.

40. Adrain JM, Fortey RA, Westrop SR (1998) Post-Cambrian trilobite diversity and evolutionary faunas. Science 280: 1922–1925.
41. Holloway DJ (1980) Middle Silurian trilobites from Arkansas and Oklahoma USA - part 1. Palaeontographica Abteilung A Palaeozoologie-Stratigraphie 170: 1–85.
42. Riedl R (1978) Order in living organisms. 1–313. A systems analysis of evolution; Riedl R, editor: John Wiley & Sons, Chichester, New York etc. i-xx.
43. Gould SJ (1980) Is a new and general theory of evolution emerging? Paleobiology 6: 119–130.
44. Barton DC (1916) A revision of the Cheirurinae with notes on their evolution. St Louis Washington University Studies 3: (101–151).
45. Billings E (1861) Palaezoic fossils of Canada: Geologic Survey of Canada.
46. Whittington HB (1963) Middle Ordovician trilobites from Lower Head, Western Newfoundland. Bulletin of the Museum of Comparative Zoology, Harvard University 129: 1–118.
47. Beyrich E (1845) Ueber einige böhmische Trilobiten. Berlin. G Reimer. 47 p.
48. Warburg E (1925) The Trilobites of the Leptaena Limestone in Dalarne. With a discussion of the zoological position and the classification of the Trilobita. Bulletin of the Geological Institution of the University of Uppsala 17: v+446.
49. Cocks LRM, Torsvik TH (2002) Earth geography from 500 to 400 million years ago: a faunal and palaeomagnetic review. Journal of the Geological Society 159: 631–644.
50. Scotese CR (2007) PaleoGIS. 2: Available:http://www.scotese.com/software.htm. Accessed: 2011 Jun.

FIGURES AND TABLES

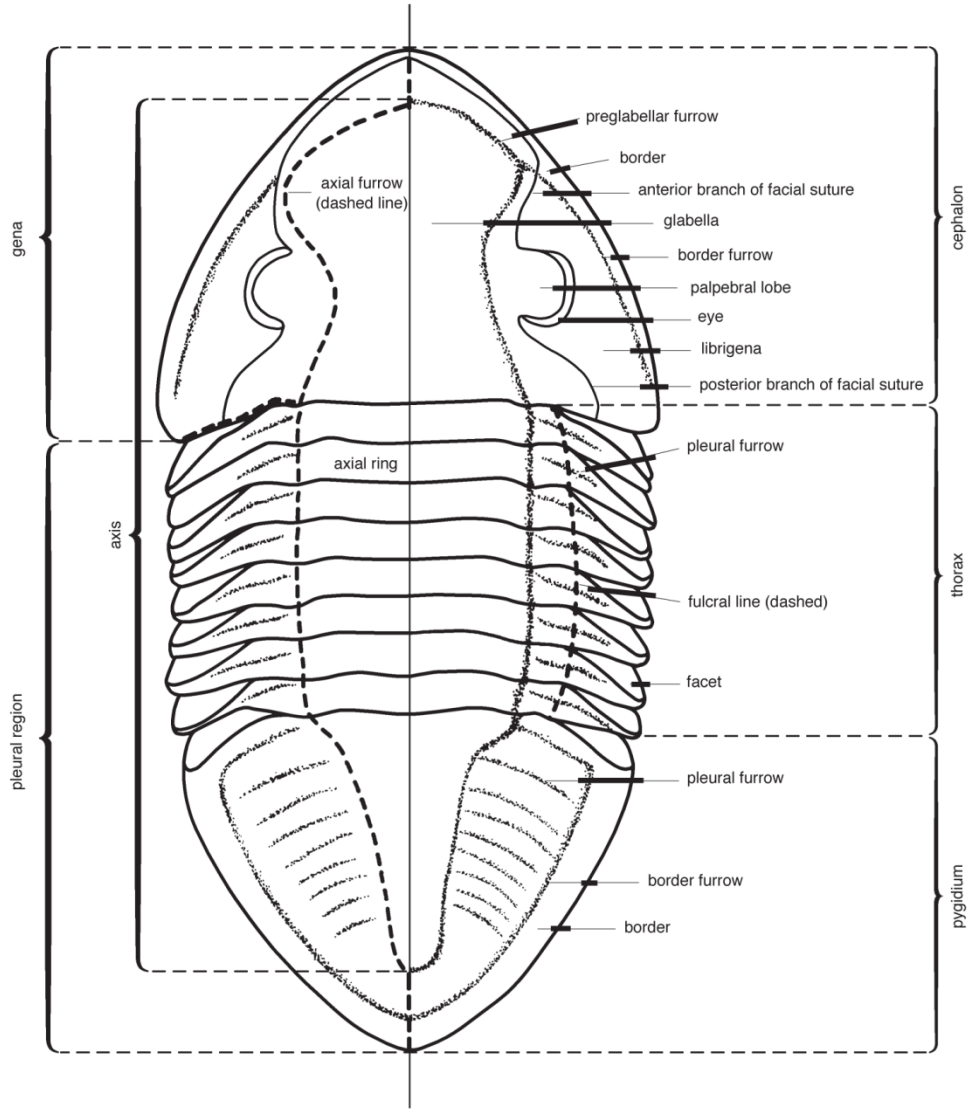

Figure 1. Line drawing of the Ordovician trilobite *Isotelus* with basic anatomical parts labeled. From Treatise on Invertebrate Paleontology, courtesy of ©1997, The Geological Society of America and The University of Kansas.

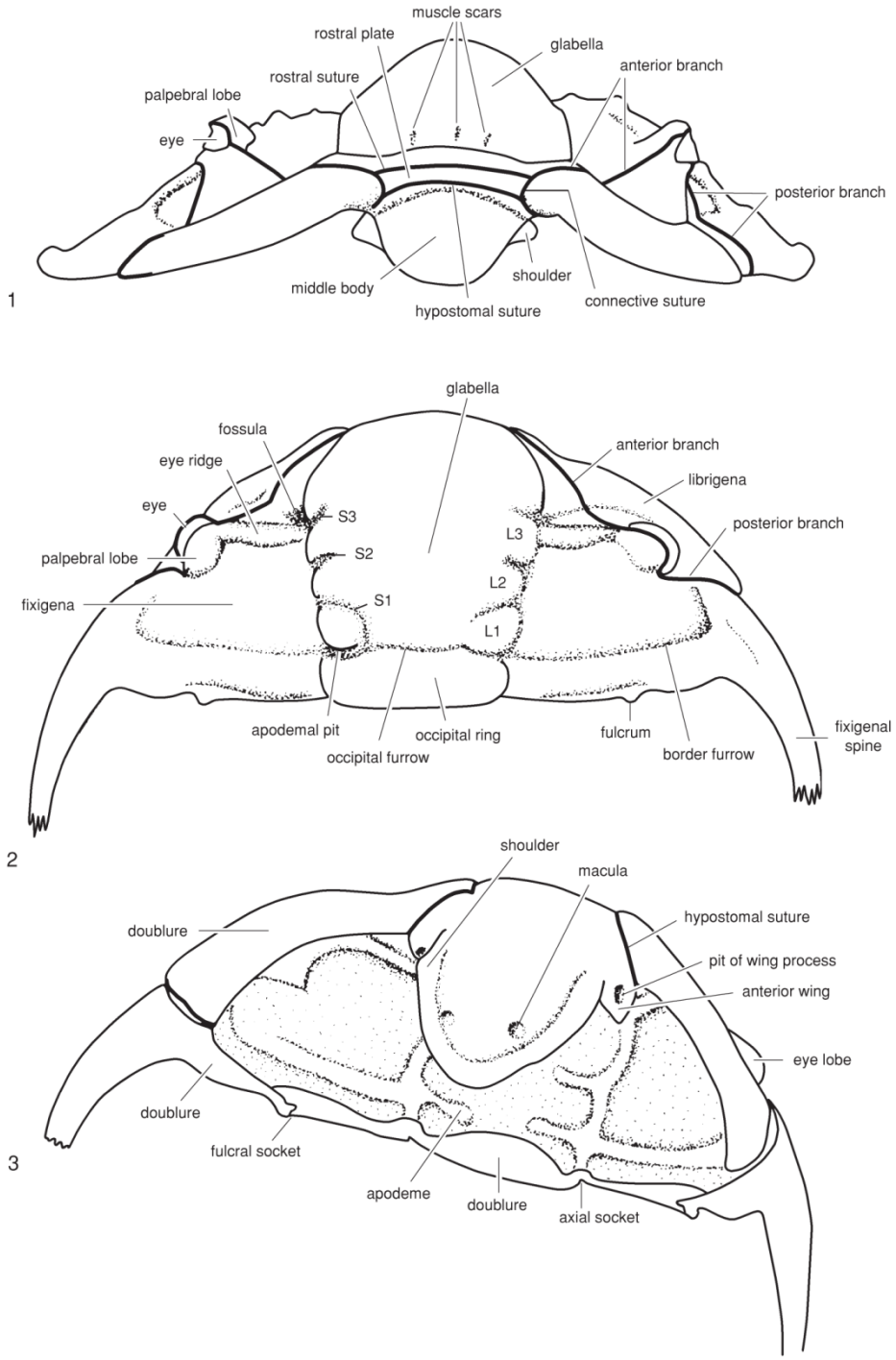

Figure 2. Line drawing of the cephalon of Ordovician cheirurid trilobite *Ceraurus monteyensis* with anatomical terminology labeled. From Treatise on Invertebrate Paleontology, courtesy of ©1997, The Geological Society of America and The University of Kansas.

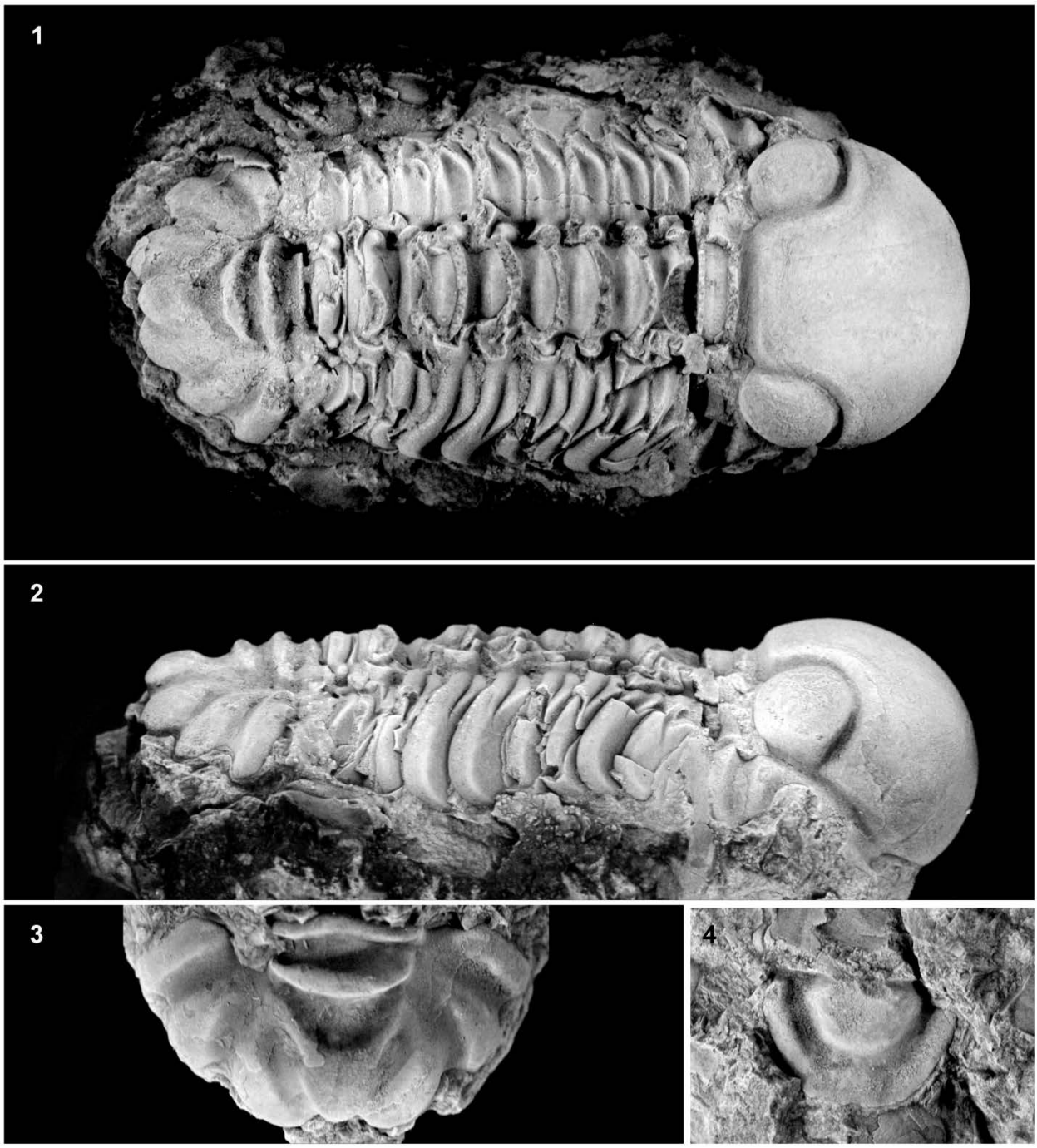

Figure 3. *1*) Complete specimen of *Sphaerexochus mirus* (MCZ 196479) in dorsal view, 3x. *2*) Complete specimen of *Sphaerexochus mirus* (MCZ 196479) in lateral view, 2.25x. *3*) Pygidium of *Sphaerexochus mirus* (MCZ 196498), 3.2x. *4*) Hypostome of *Sphaerexochus mirus* (MCZ196484), 3.25x.

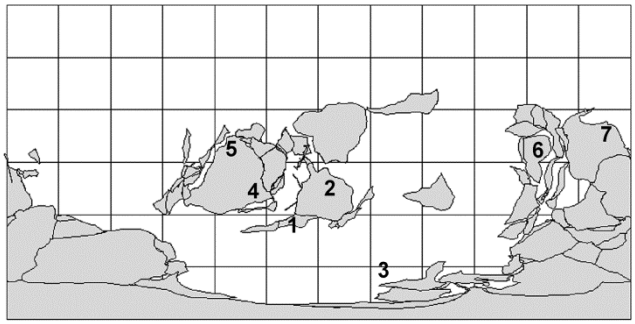

Figure 4. Paleogeographic reconstruction for the Late Ordovician (Caradoc) generated using ArcView 9.2 and PaleoGIS [50]. The biogeographic areas used in this analysis are shown where *1* = Avalonia, *2* = Baltica, *3* = Bohemia, *4* = Eastern Laurentia, *5* = Northwestern Laurentia, *6* = Yangtze block, and *7* = Australia.

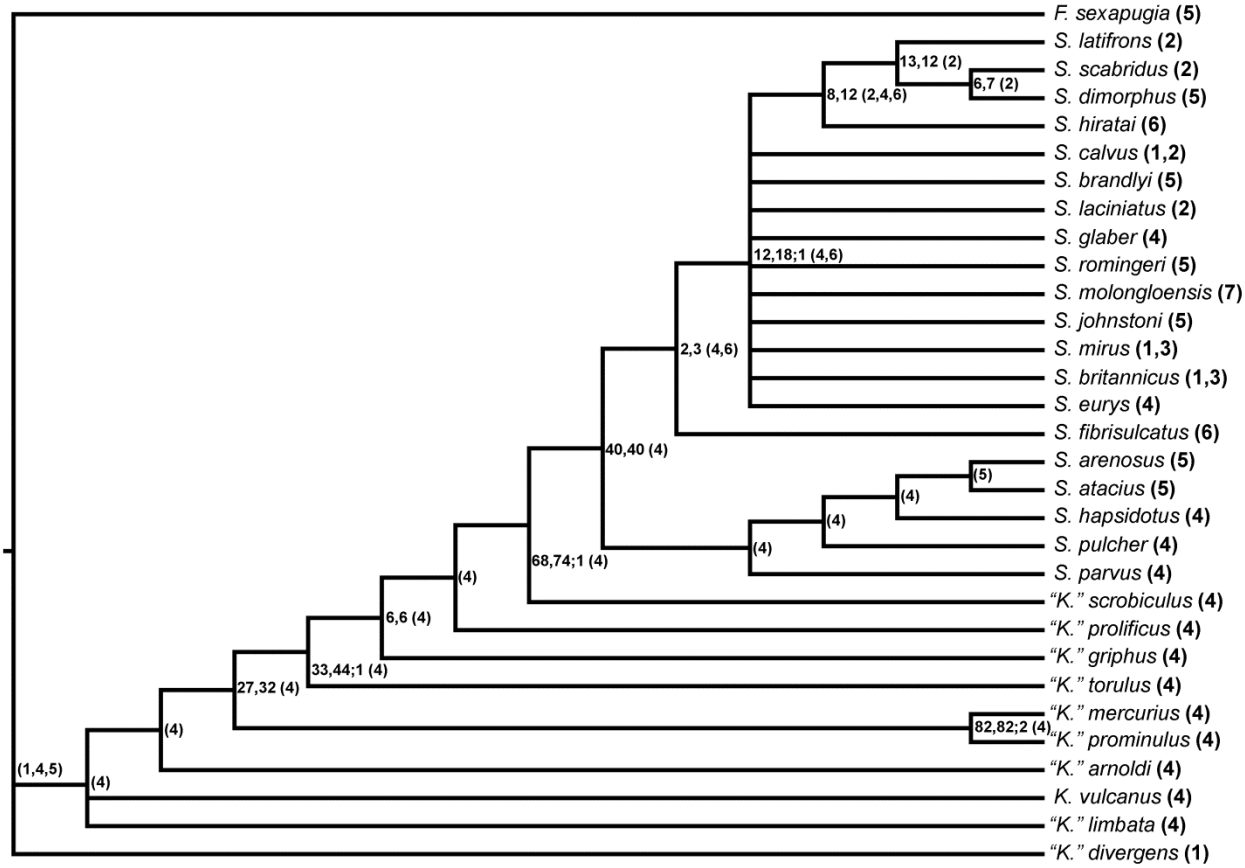

Figure 5. Results from parsimony analysis showing strict consensus of 29 most parsimonious trees of length 116 steps. Tree graphics generated using FigTree v.1.1.2 [21] with genera labeled and paraphyletic genus identified using quotations following Wiley [39]. The values written in plain text are bootstrap, jackknife, and Bremer Support values respectively; the values that are bracketed, i.e., (*1, 2*, …), are the areas used in the biogeographic analysis, coded as follows: *1* = Avalonia; *2* = Baltica; *3* = Bohemia; *4* = Eastern Laurentia; *5* = Northwestern Laurentia; *6* =Yangtze; and *7* = Australia.

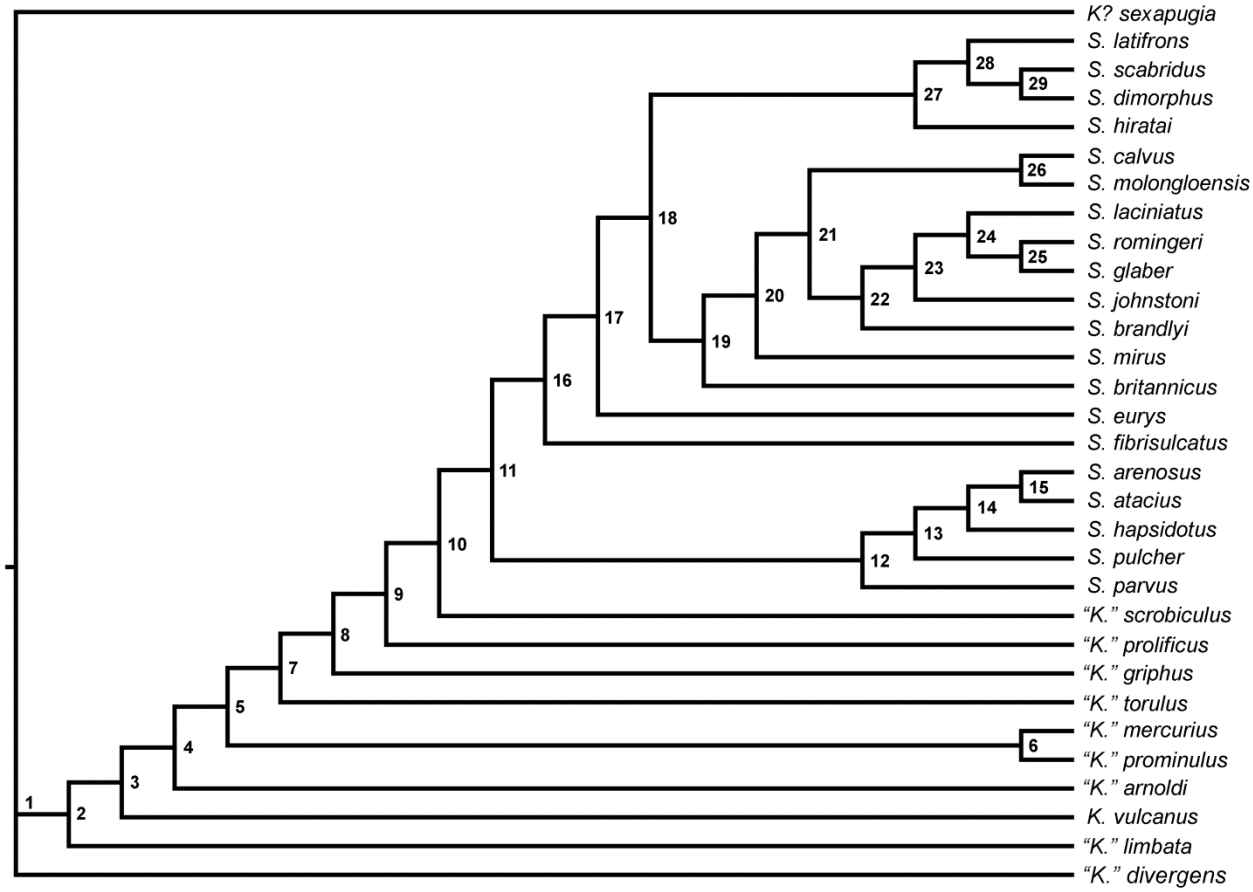

Figure 6. One of the 29 most parsimonious trees with characters mapped on the tree; parentheses denote unambiguous optimizations and brackets denote ambiguity. *Node 1*: 1 [0,1]; 5 [0,1]; 28 (1). *Node 2*: 1 (1); 5 (1); 16 (1); 21 [0,1]; 27 (2); 28 (0). *Node 3*: 9 [0,1]; 21

(0). *Node 4*: 15 (1); 19 (1); 33 (1); 34 (0). *Node 5*: 3 (1); 9 (1); 24 [0,1,2]; 27 [1,2]; 39 [1,2]. *Node 6*: 13 (1); 14 (1). *Node 7*: 6 (0); 17 (1). *Node 8*: 7 (0). *Node 9*: 16 (0). *Node 10*: 4 (1); 5 [0,1]; 12 (1). *Node 11*: 2 (0); 5 (0); 8 (1); 27 (1) 39 (1). *Node 12*: 9 [0,1]; 20 (0); 31 (0). *Node 13*: 21 (1); 24 (1); 27 (0); 35 [0,1]. *Node 14*: 22 [0,1]; 23 [0,1]; 30 [0,1]; 36 (1); 37 (0). *Node 15*: 9 (1); 12 (0); 16 (2); 33 (0). *Node 16*: 4 (2); 24 (1); 26 [0,1]. *Node 17*: 1 (0); 10 (1); 26 (0); 29 (0). *Node 18*: 38 (1); 39 (0). *Node 19*: 32 (0). *Node 20*: 22 (0). *Node 21*: 38 (0). *Node 22*: 30 (0). *Node 23*: 21 [0,1]; 23 (0). *Node 24*: 17 (2); 32 [0,1]. *Node 25*: 25 (0); 31 (0). *Node 26*: 9 (0); 35 (0). *Node 27*: 34 (0). *Node 28*: 31 (0). *Node 29*: 27 (0).

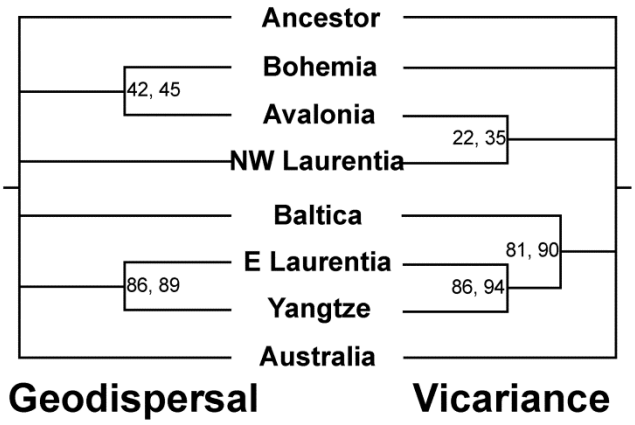

Figure 7. Results from biogeographic analysis: on the left the strict consensus of the three most parsimonious geodispersal trees; and on the right the most parsimonious vicariance tree.

Table S1

Character/taxon	1	2	3	4	5	6	7	8	9	10	11	12	13	14	15	16	17	18	19	20	21	22	23	24	25	26	27	28	29	30	31	32	33	34	35	36	37	38	39
S. latifrons	0	0	1	2	?	0	0	1	?	1	0	1	0	0	0	0	?	?	?	?	0	1	1	1	2	0	1	0	0	1	0	1	1	0	1	0	1	1	0
S. molongloensis	0	0	1	2	?	0	0	1	0	1	0	1	0	0	0	0	1	?	?	?	0	1	1	1	2	?	1	0	0	?	1	1	1	1	0	0	1	0	0
S. scabridus	0	0	1	2	?	0	0	1	?	1	0	1	0	0	0	0	0 & 2	?	1	1	?	0	1	1	1	1	0	0	0	0	1	0	1	1	0	1	0	1	1	0
S. atacius	1	0	0	1	0	0	0	1	1	0	0	0	0	0	0	0	2	1	0	1	0	0	1	1	0	2	1	0	0	?	?	0	1	0	1	0	1	0	?	1
S. eurys	0	0	1	?	0	0	?	1	1	1	0	1	0	0	0	0	1	?	?	1	0	1	0	1	2	0	0	0	0	?	1	1	0	1	1	1	1	0	1
S. calvus	0	0	1	1	0	0	?	1	0	1	0	1	0	0	0	0	2	?	?	?	0	0	1	1	1	0	1	0	0	1	1	0	1	1	0	0	1	0	0
S. lacianatus	0	0	1	2	?	0	0	1	1	0	0	1	0	0	0	0	2	1	1	1	1	0	0	1	2	0	1	0	0 & 1	0	1	1	1	0	1	0	1	1	0
S. johnstoni	0	0	1	2	0	0	0	1	1	1	0	1	0	0	0	0	1	?	?	?	1	1	0	1	2	0	1	0	0	0	1	0	1	1	1	0	1	0 & 1	0
S. mirus	0	0	1	2	0	0	0	1	?	1	0	1	0	0	0	0	0	?	?	?	1	1	0	1	1	2	0	1	0	0	1	1	0	1	1	1	0	1	1	0
S. britanicus	0	0	1	2	0	0	0	1	1	1	0	1	0	0	0	0	0	1	?	?	?	0	1	?	1	2	0	0	0	0	1	1	0	?	1	1	0	?	1	0
S. pulcher	0	0	1	1	0	0	0	1	0	0	0	1	0	0	0	0	0	1	0	1	0	1	1	1	1	2	1	0	1	1	1	0	1	1	1	1	0	1	0	1
S. parvus	0 & 1	0	1	1	0	0	0	1	0	0	0	1	0	0	0	0	0	1	1	0	0	0	1	1	0	?	?	1	0	?	?	0	1	?	1	1	0	1	?	?
S. brandlyi	0	0	1	2	0	0	0	1	1	1	0	?	0	0	0	?	1	1	0	?	0	0	1	1	0	0	1	1	0	0	1	0	1	1	1	0	0	0	0
S. romingeri	0	0	1	2	0	0	0	1	1	1	0	1	0	0	0	0	0	2	?	?	?	0	0	0	1	2	0	1	0	0	0	0	0	1	1	1	1	0	1	0	0
S. fibrisulcatus	1	0	?	2	?	0	?	1	?	0	1	0	0	0	0	?	?	?	?	?	0	1	?	1	1	?	1	0	1	?	1	1	1	1	0	0	?	0	1
S. hapsidotus	0 & 1	0	1	1	0	0	0	1	0 & 1	0	0	1	0	0	0	0	0	1	1	1	0	1	0	0	1	2	1	0	0	1	0	0	1	1	1	0	1	0	0	0
S. glaber	0	0	1	2	?	0	?	1	?	1	0	1	0	0	0	0	0	?	?	?	?	0	0	0	1	1	?	0	0	0	0	0	0	0	1	1	1	0	1	0	0
S. arenosis	0 & 1	0	1	1	0	0	0	1	1	0	0 & 1	0	0	0	0	2	2	1	0	0	1	0	0	1	2	?	0	1	1	?	1	1	0	1	1	1	0	0	1
S. dimorphus	0	0	1	2	0	0	0	1	1	1	0	1	0	0	0	0	1	1	1	1	0 & 1	1	0	1	2	0	0 & 2	0	0	0 & 1	0	1	1	0	1	0	1	1	0

Character state distributions for taxa used in phylogenetic analysis. Characters and character states are as listed in the text. Missing data are indicated by "?". Character numbers are listed at top of table.

Table S2

Taxon/Character	1	2	3	4	5	6	7	8	9	10	11	12	13	14	15	16	17	18	19	20	21	22	23	24	25	26	27	28	29	30	31	32	33	34	35	36	37	38	39	40	41	42	43	44	45	46	47	48
Ancestor	0	0	0	0	0	0	0	0	0	0	0	0	0	0	0	0	0	0	0	0	0	0	0	0	0	0	0	0	0	0	0	0	0	0	0	0	0	0	0	0	0	0	0	0	0	0	0	0
Avalonia	1	1	0	0	0	0	0	0	0	0	0	0	0	0	0	0	0	0	0	0	0	0	0	0	0	0	0	0	0	0	0	0	0	0	2	2	0	0	2	0	0	0	0	0	0	0	0	0
Baltica	0	0	0	0	0	0	0	0	0	0	0	0	0	0	0	0	0	0	0	0	0	0	0	0	0	0	0	0	0	0	0	0	0	0	0	0	0	0	2	0	0	2	0	1	1	1	1	1
Bohemia	0	0	0	0	0	0	0	0	0	0	0	0	0	0	0	0	0	0	0	0	0	0	0	0	0	0	0	0	0	0	0	0	0	0	2	2	0	0	0	0	0	0	0	0	0	0	0	0
E. Laurentia	1	0	1	1	1	1	1	1	1	1	1	1	1	1	1	1	1	1	1	1	1	1	1	1	1	1	0	0	1	0	1	1	1	1	1	1	1	1	1	1	1	0	0	0	0	0	0	0
NW. Laurentia	1	0	0	0	0	0	0	0	0	0	0	0	0	0	0	0	0	0	0	0	0	0	0	0	0	2	1	1	0	0	0	0	2	2	0	0	2	0	0	0	0	0	0	0	0	0	2	0
Yangtze	0	0	0	0	0	0	0	0	0	0	0	0	0	0	0	0	0	0	0	0	0	0	0	0	0	0	0	0	2	1	1	0	1	1	1	1	1	1	1	0	1	1	1	0	0	0	0	0
Australia	0	0	0	0	0	0	0	0	0	0	0	0	0	0	0	0	0	0	0	0	0	0	0	0	0	0	0	0	0	0	0	0	0	0	0	0	0	0	0	2	0	0	0	0	0	0	0	0

Geodispersal matrix derived from the area cladogram in Figure 2. "0" represents the primitive state, absent from all areas, and "1" and "2" represent the derived states, where are all characters are treated as ordered. The outgroup is the all "0" ancestor, primitively absent from all areas.

Table S3

Taxon/Character	1	2	3	4	5	6	7	8	9	10	11	12	13	14	15	16	17	18	19	20	21	22	23	24	25	26	27	28	29	30	31	32	33	34	35	36	37	38	39	40	41	42	43	44	45	46	47	48
Ancestor	0	0	0	0	0	0	0	0	0	0	0	0	0	0	0	0	0	0	0	0	0	0	0	0	0	0	0	0	0	0	0	0	0	0	0	0	0	0	0	0	0	0	0	0	0	0	0	0
Avalonia	1	2	1	0	0	0	0	0	0	0	0	0	0	0	0	0	0	0	0	0	0	0	0	0	0	0	0	0	0	0	0	0	0	0	1	1	0	0	1	0	0	0	0	0	0	0	0	0
Baltica	0	0	0	0	0	0	0	0	0	0	0	0	0	0	0	0	0	0	0	0	0	0	0	0	0	0	0	0	0	0	0	0	0	0	0	0	0	1	1	0	0	1	1	2	1	1	0	1
Bohemia	0	0	0	0	0	0	0	0	0	0	0	0	0	0	0	0	0	0	0	0	0	0	0	0	0	0	0	0	0	0	0	0	0	0	1	1	0	0	0	0	0	0	0	0	0	0	0	0
E. Laurentia	1	1	2	1	1	1	1	1	1	1	1	1	1	1	1	1	1	1	1	1	1	1	1	1	1	0	0	0	1	1	1	2	0	0	0	0	0	0	0	2	0	1	1	1	0	0	0	0
NW. Laurentia	1	1	1	0	0	0	0	0	0	0	0	0	0	0	0	0	0	0	0	0	0	0	0	0	0	1	1	1	0	0	0	0	1	1	0	0	1	0	0	0	0	0	0	0	0	0	1	0
Yangtze	0	0	0	0	0	0	0	0	0	0	0	0	0	0	0	0	0	0	0	0	0	0	0	0	0	0	0	0	1	2	1	1	0	0	0	0	0	0	0	1	0	1	2	1	0	0	0	0
Australia	0	0	0	0	0	0	0	0	0	0	0	0	0	0	0	0	0	0	0	0	0	0	0	0	0	0	0	0	0	0	0	0	0	0	0	0	0	0	0	0	1	0	0	0	0	0	0	0

Vicariance matrix derived from the area cladogram in Figure 2."0" represents the primitive state, absent from all areas, and "1" and "2" represent the derived states, where are all characters are treated as ordered. The outgroup is the all "0" ancestor, primitively absent from all areas.

Chapter 2 - Speciation and extinction rates of Ordovician cheirurid trilobites and their implications for survivability during the end Ordovician mass extinction event

Curtis R. Congreve and Bruce S. Lieberman

(Formatted for submission to Paleobiology)

Abstract.— The end Ordovician extinction event is the second largest mass extinction in the history of life. The extinction has classically been interpreted as being caused by a brief, sudden onset glacial period that occurred during the otherwise greenhouse conditions of the Late Ordovician. Previous research suggests that the extinction event had a particularly interesting effect on the evolutionary history of trilobites, strongly selecting against trilobites with nektonic or planktonic life strategies. Free-swimming trilobites went entirely extinct at the event, and trilobite groups with presumed planktonic larval stages were more likely to go extinct than trilobites with presumed benthic larvae. While this pattern has been studied broadly at the family level, there have been no detailed phylogenetically constrained estimates of speciation and extinction rates through time for any of these late Ordovician trilobite clades. This analysis focuses on extinction and speciation rates within two different clades (Deiphoninae, Sphaerexochinae) of cheirurid trilobites, a speciose group that is presumed to have had both a benthic larval and adult life strategy and that spans this time interval. The results from the analysis of extinction rates are used to evaluate competing theories for the cause of the End Ordovician extinction event (ie: habitat loss from lowering sea levels, gamma ray burst, etc.) to determine which cause best fits the data. Further, we consider how speciation and extinction rates co-vary, and compare these results with those gleaned from earlier phylogenetic

biogeographic studies, to consider how speciation mode and rates of speciation are themselves related both before, during, and after the crisis interval. Our results suggest that there is a definite phylogenetic signature affecting the survivability of trilobites across the event, with deiphonines showing a characteristic response to the extinction event while the sphaerexochines appear to be barely affected.

Introduction

The end Ordovician is considered to be the second largest period of mass extinction, in terms of percent genera and families lost, in Earth history (Sepkoski 1996). The extinction has classically been interpreted as being the result of a rapid onset, unstable glacial period during otherwise greenhouse conditions (Berry and Boucot 1973, Sheehan 1973, Brenchley et al 1994, Sheehan 2002). The extinction has been split into two major pulses; the first pulse related to the initial advancement of the glaciers, which drained epicontinental seaways by trapping water in continental ice sheets, thereby degrading available ecospace (Berry and Boucot 1973, Sheehan 1973, Stanley 1984, Hallam and Wignall 1997). The second pulse of extinction is associated with the sudden recession of the glaciers, which dramatically changed ocean circulation, flooding the deep ocean with dysoxic waters and potentially killing deeper water organisms that had previously moved into these environments during the glacial event when ocean deep water had become more oxygenated (Rong and Harper 1988, Briggs et al 1988, Hallam and Wignall 1997, Sheehan 2002). The smoking gun for this sudden onset glacial event is still a matter of debate, with causes ranging from decreased pCO_2 concentrations due to silicate weathering in Gondwanan mountain building events (Kump et al 1999) to dramatic atmospheric changes due to the effects of a nearby gamma ray burst (Melott et al 2004).

This extinction was particularly impactful on the evolution of trilobites (Adrain et al 1998), which have an interesting pattern of survivability across the extinction event. Chatterton and Speyer (1989) studied survivorship of taxonomic groups of trilobites across the event and compared survivorship with life strategy. They noted that trilobites with inferred benthic larvae were more likely to survive the mass extinction event than those groups with inferred planktonic larvae. Also, all trilobites that had an inferred pelagic adult life strategy went extinct at the event (Chatterton and Speyer 1989). In addition to this pattern, the study of Adrain et al (2000) on trilobite alpha diversity across the extinction event indicates that, despite taxonomic diversity of trilobites being profoundly cut by the event, regional alpha diversity was barely affected by the extinction and quickly returned to normal levels in the Silurian. This result implicates a breakdown of provinciality or endemism during the extinction event, with surviving taxa increasing their biogeographic range and filling the available ecological space (Adrain et al 2000); a pattern that has also been suggested from other paleontological evidence (Whittington and Hughes 1972, Cocks and Fortey 1988).

In order to better understand the affects this mass extinction had on trilobite evolution, as well as to tease apart the causal factors affecting survivability across this event, this study calculates speciation and extinction rates for two related groups of trilobites that originate in the Ordovician and survive the extinction event, the Deiphoninae and the Sphaerexochinae. Both groups are monophyletic clades of trilobites belonging to the same family, Cheiruridae, which have previously been studied using modern phylogenetic and biogeographic methods (Congreve and Lieberman 2010, 2011). According to these analyses, both the deiphonines and sphaerexochines inhabit similar biogeographic regions and undergo similar patterns of dispersal during the end Ordovician, and both groups are presumed by Chatterton and Speyer (1989) to

have had benthic larval and adult life strategies. By incorporating these biogeographic and phylogenetic studies into an analysis on speciation and extinction rates, we can better piece apart the role of abiotic factors versus intrinsic biotic factors controlling the patterns of survivability across the end Ordovician biodiversity crisis. Phylogenetic information, in particular, is essential for calculating speciation rates because in order to obtain a rate one first needs to know which taxa give rise to other taxa. Further, phylogenetic information can be used to provide additional temporal information about when species originate through the establishment of ghost lineages (Edgecombe 1992, Smith 1994, Lieberman 2001).

Methods

A total of fifty one taxa were included in this analysis. Information on the species assignments and phylogeny of the groups can be found in Congreve and Lieberman (2010, 2011). This method assumes an ontological definition of species as unique phylogenetic trajectories through time, often referred to as the evolutionary species concept (Wiley 1978, Wiley and Lieberman 2011). Stage divisions within the Ordovician and Silurian follow the global standard established by Gradstein et al. (2004). Since stage divisions have been difficult to establish globally, past stage definitions often varied across geographic regions (Cowie et al. 1972, Williams et al. 1972, Cocks et al. 1971). Most of the species included in this analysis were described before the formation of the new global standard, and occurrence data originally used local geologic stages. Therefore, the species ranges for this study were correlated to the most recent global standard ages for the Ordovician and Silurian (Gradstein et al. 2004) using the work of Cocks et. al. (2010); a study correlating the traditional local geologic stages to the modern geologic stages. Species were binned into the geologic stages with which their temporal

ranges overlapped, using the most constrained range data possible given the data provided. This age correlated data was then combined with the phylogenetic data (Congreve and Lieberman 2010, 2011) to create ghost lineages by constraining the timing of cladogenetic events; no species are assumed to be directly ancestral because they do not have the characteristics of metataxa, since each species is both diagnosably distinct and possesses unique synapomorphies or autapomorphies.

These data were utilized to estimate speciation and extinction rates using a standard birth/death model (Stanley 1979). This method has previously been applied to the fossil record with positive results (Lieberman 2001, Rode and Lieberman 2005, Nee 2006, Abe and Lieberman 2009). A general rate of diversity change, measured in taxonomic diversity per million year (r), was estimated from the following birth/death model:

$$N_{final} = N_0 e^{rt}$$

in which "N" represents taxonomic diversity and "t" represents time in million years. The initial diversity for a given time period is considered to be equivalent to the final diversity of the previous time period. In this manner, the effects of singleton taxa (taxa that do not cross time boundaries and are constrained only to one time bin) are removed as per the provisions outlined in Foote (2000a, 2000b), thereby ensuring conservative extinction estimations. Speciation rates were then estimated using the same birth/death model, but this time including the effects of singleton taxa (ie: N_{final} is equal to the total number of taxa that persist during the time bin). Given the general rate of taxonomic diversity change (r) and speciation rate, the rate of extinction can be calculated from the equation: $r = speciation\ rate + extinction\ rate$. The rate calculations for the analyses of the deiphonine and sphaerexochine trilobites are shown in Table 1 and Table 2 respectively.

Results

In the Deiphoninae, the rate of diversity change (fig 1) began positive in the Middle Ordovician (Dapinigian) and became strongly negative at the end Ordovician extinction event in the Hirnantian. There was a brief positive recovery period in the Early Silurian, before the rate of diversity change dipped strongly negative again and the clade went extinct. Splitting the data into its constituent speciation and extinction rates (fig 2), the factors affecting the changes in rate through time can be more finely analyzed. The Middle Ordovician (Dapinigian) had a pronounced speciation rate and no extinction. This is likely an edge effect (Foote 2000a), as the spike corresponds with the first occurrence of the group in the fossil record. Speciation rates then steadily dropped throughout the Ordovician, while extinction rates remained relatively low. At the extinction event (Hirnantian), the speciation rate reached zero and the extinction rate jumped dramatically. Post extinction event, there was no net change in the Llandovery, followed by an increased speciation and extinction rate in the Wenlock. Speciation then plummeted while extinction remained high, and the group went extinction in the Ludlow.

In the Sphaerexochinae, the rate of diversity change (fig 3) started slightly positive in the Early Ordovician (Floian), with a dramatic positive spike in the Dapinigian. Rates then became strongly negative in the Darwillian and Sandbian, before becoming positive again in the Late Ordovician (Katian). Little net change occurred at the extinction event (Hirnantian) or immediately following the event (Llandovery), but the rate steadily dropped during the Silurian until the group went extinct in the Ludlow. Parsing out the speciation and extinction rates (fig 4), a large spike in speciation rate can be observed in the Dapinigian, followed by a dramatic drop in speciation and a rise in extinction in the Darwillian and Sandbian. During the Late Ordovician

(Katian) speciation rates increased again and extinction dramatically decreased. Very little speciation or extinction occurred at the extinction event (Hirnantian) or during the subsequent period (Llandovery). By the Wenlock, speciation within the group ceased and extinction rates steadily rose until the clade went extinct.

Discussion

The patterns of diversity change in the Deiphoninae follow a trend that would be expected from a group that was strongly affected by the Hirnantian extinction event. Speciation dropped substantially just before the event, and extinction rates dramatically increased during the event. After the Hirnantian, speciation rates increased as the group underwent a period of the recovery. At least a portion of the dramatic spike in both rates during the Wenlock is likely to be artificially inflated because this particular study did not sample any deiphonine specimens from the Llandovery, due the absence of well-preserved specimens that could be incorporated into the phylogenetic analysis. Age estimations for ghost lineages could not be pulled back into the Llandovery, therefore it is likely that some of the increase in diversity could have occurred during the Llandovery immediately after the extinction event.

In contrast, the pattern of diversity change in the Sphaerexochinae suggests that the group may not have been affected by the extinction event at all. Rather, the sphaerexochines may have instead gone through a small extinction event during the Middle Ordovician (Darwillian-Sandbian) and subsequently diversified during the Late Ordovician (Katian). During the Hirnantian event, the sphaerexochines experienced minimal extinction, suggesting that the environmental perturbations that caused the extinction event had little effect on the clade.

However, in the Silurian, the group no longer speciated and extinction rates climbed, in a response similar to Jablonski's (2002) "dead clade walking".

Both groups are closely related (Lieberman and Karim 2010) with similar inferred larval and adult life strategies (Chatterton and Speyer 1989), but they each have markedly different responses to the mass extinction. Furthermore, both the deiphonines and sphaerexochines lived in similar biogeographic regions. While each group originated in different regions, the sphaerexochines likely originated in Laurentia and the deiphonines likely originated in Baltica, both groups had dispersed to roughly the same biogeographic regions by the Upper Ordovician, living predominantly in the equatorial complex of Laurentia, Avalonia, and Baltica during the extinction event (Congreve and Lieberman 2010, Congreve and Lieberman 2011). Since both groups were living in similar regions during the extinction event, a refugium hypothesis cannot be implicated to explain this difference in survivability. Instead, the data suggest that a biological signature unique to each group is affecting survivorship during the extinction event. This result follows in line with previous research that suggests clades tend to have individualistic responses to environmental perturbations, as discussed by Vrba (1985), Jablonski (1986), Lieberman and Vrba (1995), and Gould (1980).

Conclusions

Chatterton and Speyer's (1989) study on survivability across the end Ordovician mass extinction suggested the presence of a unique biological signature intrinsic within large groups of trilobites (larval life strategy) that was selected for during the mass extinction event. The results of our study suggest that, even among closely related taxa, there is an individualistic response to the cataclysmic environmental changes that occurred during the end Ordovician. Since both

groups lived in similar biogeographic regions, it is likely that abiotic factors are not the cause of this discrepancy in the patterns of survivability, thereby implicating an intrinsic biological factor associated with the group. While it is difficult to determine what biotic factors could be affecting the extinction patterns of these groups during the end Ordovician, it is possible that the more morphologically conserved sphaerexochines may also have been more ecologically generalized than the deiphonines. A larger niche breadth may have helped the sphaereoxchines to weather the extinction event. We are currently working on future research that will study the effects of geographic range and niche breadth on survivability of the mass extinction event. This study indicates that multiple biological factors could be affecting extinction in trilobites across the end Ordovician event, thereby bringing to light the inherent difficulty in determining causal factors for extinction and survival during mass extinctions.

Acknowledgments

This research was supported by National Science Foundation DEB-0716162 and the Panorama fund of the Biodiversity Institute of the University of Kansas. We thank Susan Butts from the YPM, Brenda Hunda from the Cincinnati Museum Center, Scott Lidgard from the FMNH, Jessica Cundiff from the MCZ, Stefan Bengtson and Christiana Frauzen-Bengtson from the AR, David Bruton and Franz-Josef Lindemann from the PMO, Linda Wickström from the SGU, and Ivan Gogin from the VSEGEI for providing access to study material that was vital for the completion of this study, and also for loaning relevant material.

References

Abe, F. R., and B. S. Lieberman. 2009. The Nature of evolutionary radiations: A case study involving Devonian trilobites. Evolutionary Biology 36:225-234.

Adrain, J.M and R.A. Fortey, S.R. Westrop, 1998, Post-Cambrian trilobite diversity and evolutionary faunas. Science, 280:1922-1925

Adrain, J.M. and S.R. Westrop, B.D.E. Chatterton, L. Ramsköld, 2000, Silurian trilobite alpha diversity and the end-Ordovician mass extinction. Paleobiology, 26:625-646.

Berry, W.B.N. and A.J. Boucot 1973, Glacio-eustatic control of the Late Ordovician-Early Silurian platform sedimentation and faunal changes. Geological Society of America Bulletin 84:275-284.

Brenchley, P.J., J.D. Marshall, G.A.F. Carden, D.B.R. Robertson, D.G.F. Long. 1994. Bathymetric and isotopic evidence for a short-lived Late Ordovician glaciation in a greenhouse period. Geology 22:295-298.

Briggs, D.E.G. and R.A. Fortey, E.N.K. Clarkson. 1988, Extinction and the fossil record of the arthropods. In Larwood, GP. (ed) Extinction and Survival in the Fossil Record. Clarendon. Oxford.

Chatterton, B.D.E. and S.E. Speyer, 1989, Larval Ecology, Life-History Strategies, and Patterns of Extinction and Survivorship among Ordovician Trilobites. Paleobiology 15: 118-132.

Cocks, L.R.M. and C.H. Holland, R.B. Bickards, I. Strachan, 1971, A correlation of Silurian rocks in the British Isles. Journal of the Geological Society, London. 127:103-36.

Cocks, L.R.M., and R.A. Fortey, A.W.A. Rushton, 2010, Correlation for the Lower Palaeozoic. Geology Magazine. 147 (2):171-180.

Cocks, L.R.M. and R.A. Fortey, 1988, Lower Palaeozoic facies and faunas around Gondwana. Geological Socity, London Special Publications. 37:183-200.

Congreve, C.R. and B.S. Lieberman, 2010, Phylogenetic and Biogeographic Analysis of Deiphonine Trilobites. Journal of Paleontology 84: 128-136.

Congreve, C. R., and B. S. Lieberman. 2011. Phylogenetic and biogeographic analysis of sphaerexochine trilobites. PloS One 6:e21304.

Cowie, J.W., and A.W.A. Rushton, C.J. Subblefield, 1972, A correlation of Cambrian rocks in the British Isles. Geological Society, London Special Report. 2:1-42.

Edgecombe, G.D., 1992. Trilobites and the Cambrian-Ordovician "event": cladistic reappraisal, p. 144-177. In M. J. Novacek and Q. D. Wheeler (eds.), Extinction and Phylogeny. Columbia University Press, New York.

Foote, M. 2000a. Origination and extinction components of taxonomic diversity: general problems. Paleobiology 26 (supplement to No. 4): 74-102.

Foote, M. 2000b. Origination and extinction components of taxonomic diversity: Paleozoic and post Paleozoic dynamics. Paleobiology 26:578-605.

Gould, S.J., 1980, Is a new and general theory of evolution emergin? Paleobiology, 6(1):119-130.

Gradstein, F. and J. Ogg, A. Smith, 2004, A Geological Time Scale 2004. Cambridge University Press.

Hallam, A. and P.B. Wignall. 1997. Mass Extinctions and Their Aftermath. Oxford University Press. New York.

Jablonski, D.,1986. Background and mass extinctions: The alternation of macroevolutionary regimes. Science 231: 129-133

Jablonski, D. 2002, Survival without recovery after mass extinctions, PNAS. 99(12):8139-44.
Kump, L.R. and M.A. Arthrus, M.E. Patzkowsky, M.T. Gibbs, D.S. Pinkus, P.M. Sheehan, 1999, A weathering hypothesis for glaciation at high atmospheric pCO_2 during the Late Ordovician. Palaeogeography, Palaeoclimatology, and Palaeoecology. 152:173-187.
Lieberman, B.S., 2001, Phylogenetic analysis of the Olenellina Walcott, 1890 (Trilobita, Cambrian). Journal of Paleontology, 75:96-115
Lieberman, B. S., and T. S. Karim. 2010. Tracing the trilobite tree from the root to the tips: a model marriage of fossils and phylogeny. Arthropod Structure & Development 39:111-123.
Lieberman, B. S., and E. Vrba. 1995. Hierarchy theory, selection, and sorting: a phylogenetic perspective. BioScience 45:394-399.
Melott, A.L. and B.S. Lieberman, C.M. Laird, L.D. Martin, M.V. Medvedev, B.C. Thomas, J.K. Cannizzo, N. Gehrels, C.H. Jackman. 2004. Did a gamma-ray burst initiate the late Ordovician mass extinction? International Journal of Astrobiology. 3(1):55-61
Nee, S. 2006. Birth-death models in macroevolution. Annu. Rev. Ecol. Syst. 37:1–17.
Rode A.L. and B.S. Lieberman, 2005, Integrating evolution and biogeography: a case study involving Devonian crustaceans. Journal of Paleontology 79: 267-276
Rong, J. and D.A.T. Harper. 1988. A global synthesis of the latest Ordovician Hirnantian brachiopod faunas. Transactions of the Royal Society of Edinburgh 79:383-402.
Sepkoski, J.J., 1996. Patterns of Phaneroxoic extinction: a perspecitve from global data bases. In Valentine, JW (ed). Global Events and Stratigraphy in the Phanerozoic. Princeton University Press, Princeton.
Sheehan, P.M., 1973, The relation of Late Ordovician glaciation to the Ordovician-Silurian changeover in North American brachiopod faunas. Lethaia 6:147-154.
Sheehan, P.M., 2000, The Late Ordovician Mass Extinction. Annual Review Earth Planet Science 29:331-364.
Smith, A.B., 1994, Systematics and the Fossil Record: Documenting Evolutionary Patterns, Wiley Blackwell Science Ltd, Oxford.
Stanley, S.M., 1979, Macroevolution: Pattern and Proces, San Francisco: Freeman
Stanley, S.M., 1984, Temperature and biotic crises in the marine realm. Geology 23:205-208.
Whittington, H.B. and C.P. Hughes, 1972, Ordovician Geography and Faunal Provinces Deduced from Trilobite Distribution. Philosophical Transactions of the Royal Society of London. Series B, Biological Sciences. 263(850):235-270.
Williams, A. and I Strachan, D.A. Bassett, W.T. Dean, J.K. Ingham, A.D. Wright, H.B. Whittington, 1972, A correlation of Ordovician rocks in the British Isles. Geological Society of London Special Report 3:1-74.
Wiley, E.O. 1978, The Evolutionary Species Concept Reconsidered, Systematic Biology. 27(1):17-26.
Wiley, E.O. and B.S. Lieberman, 2011, Phylogenetics: Theory and Practice of Phylogenetic Systematics, Wiley-Blackwell. Hoboken, New Jersey.
Vrba, E.S., 1985, Environment and evolution: alternative causes of the temporal distribution of evolutionary events. South African Journal of Science 81:229-236.

Figures and Tables

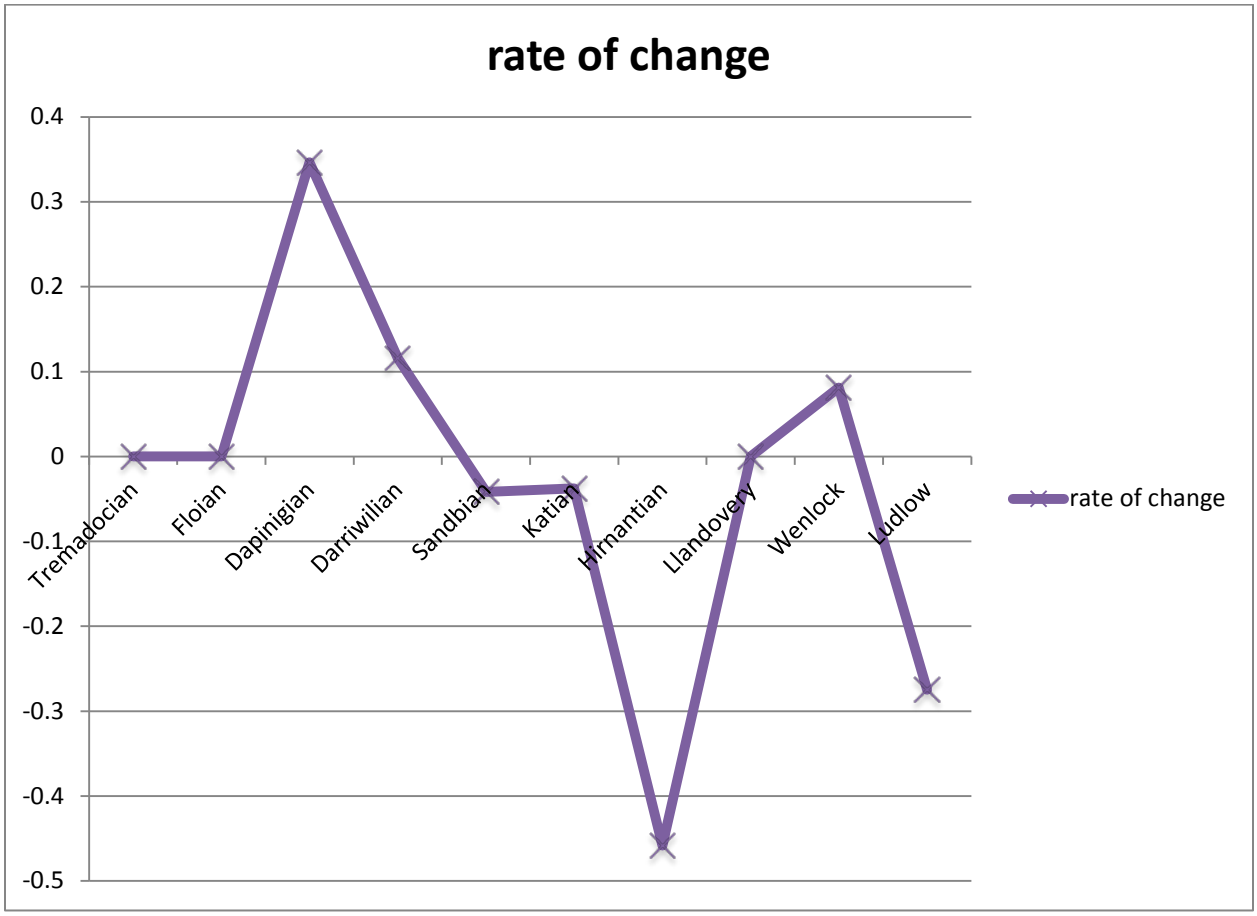

Figure 1: Rates of change in biodiversity through time in the Deiphoninae.

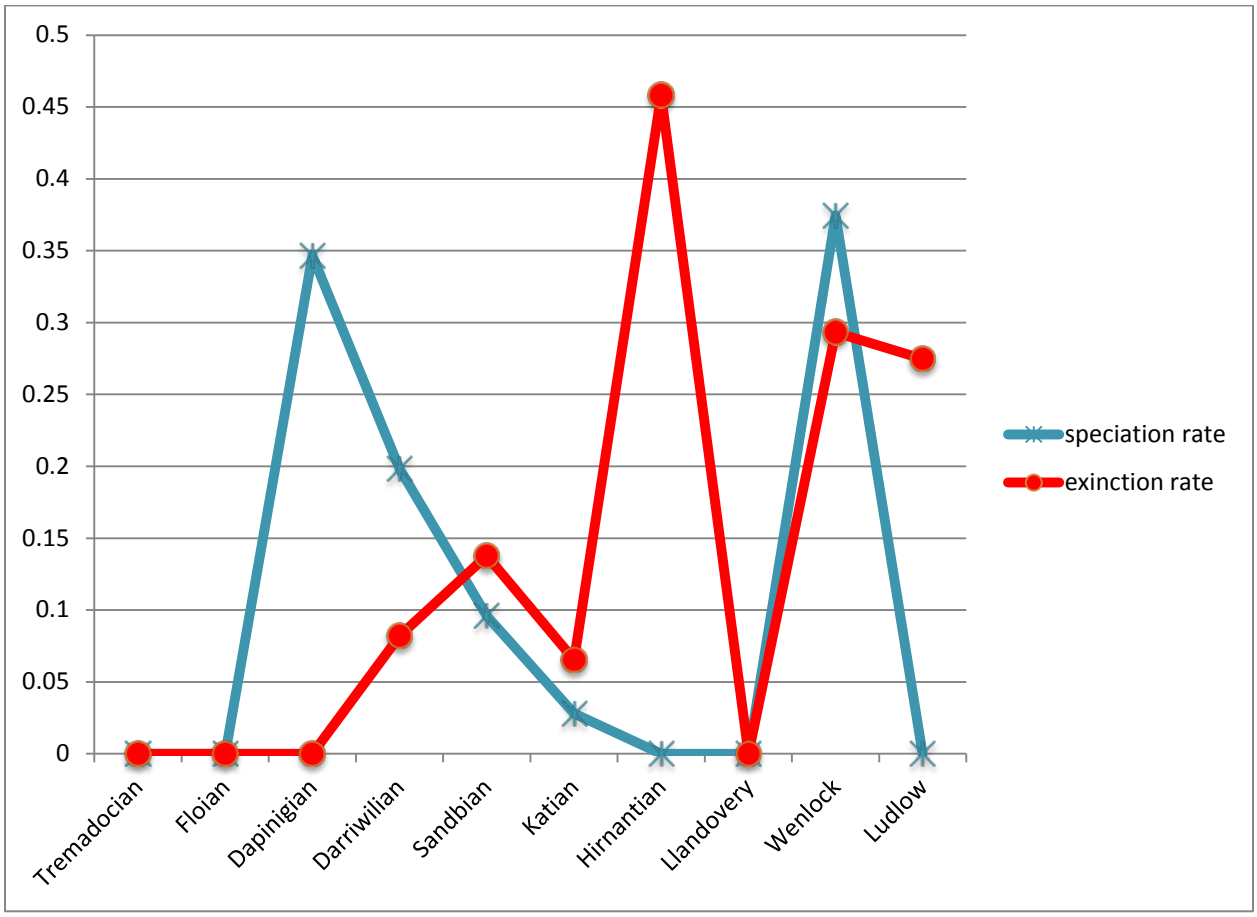

Figure 2: Speciation and extinction rates through time in the Deiphoninae.

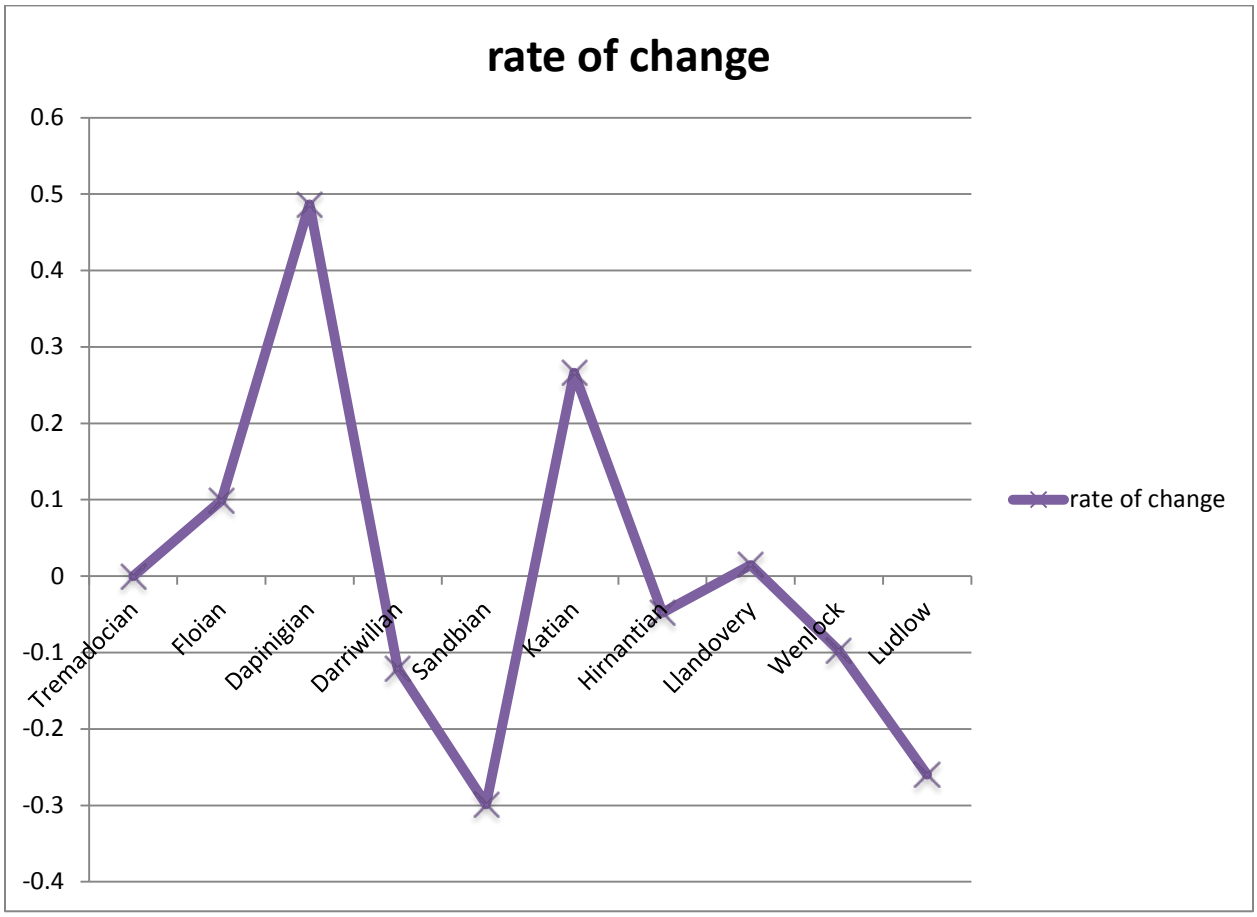

Figure 3: Rates of change in biodiversity through time in the Sphaerexochinae.

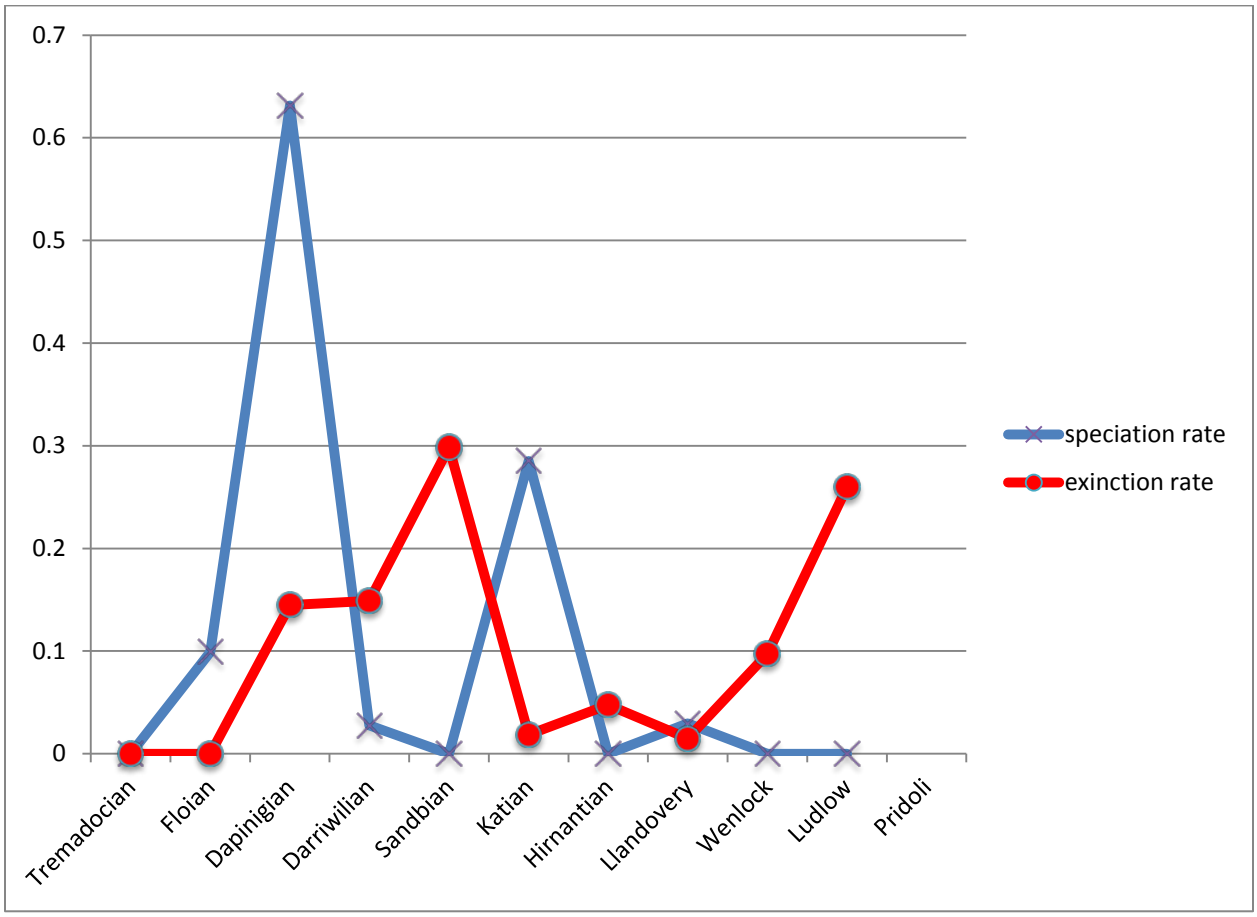

Figure 4: Speciation and extinction rates through time in the Sphaerexochinae.

Table 1: Rates of change in biodiversity through time in the Deiphoninae.

Age	Time	N0	Nf	rate of change	speciation rate	extinction rate
Tremadocian	8	0	0	0	0	0
Floian	7	0	0	0	0	0
Dapinigian	4	0	4	0.34657359	0.34657359	0
Darriwilian	7	4	16	0.115847174	0.198042052	0.082194878
Sandbian	6	9	16	-0.041885738	0.095894024	0.137779762
Katian	9	7	9	-0.037385804	0.027923825	0.065309629
Hirnantian	2	5	5	-0.458145366	0	0.458145366
Llandovery	18	2	2	0	0	0
Wenlock	5	2	13	0.081093022	0.374360435	0.293267414
Ludlow	4	3	3	-0.274653072	0	0.274653072

Table 2: Speciation and extinction rates through time in the Deiphoninae.

Age	Time	N0	Nf	rate of change	speciation rate	extinction rate
Tremadocian	8	0	0	0	0	0
Floian	7	0	2	0.099021026	0.099021026	0
Dapinigian	4	2	25	0.486477537	0.631432161	0.144954624
Darriwilian	7	14	17	-0.121042551	0.027736573	0.148779125
Sandbian	6	6	6	-0.298626578	0	0.298626578
Katian	9	1	13	0.266432808	0.284994373	0.018561565
Hirnantian	2	11	11	-0.04765509	0	0.04765509
Llandovery	18	10	17	0.014575792	0.029479347	0.014903555
Wenlock	5	13	13	-0.097101563	0	0.097101563
Ludlow	8	8	8	-0.259930193	0	0.259930193

Chapter 3 - A Phylogenetic and Taxonomic Revision of the Ceraurid Trilobites

Curtis R. Congreve and Gerald Kloc

(Formatted for submission to Zootaxa)

ABSTRACT: The genus *Ceraurus* Green, 1832 is a speciose group of cheirurid trilobites from the Ordovician of North America. Over the years, taxonomists have split this large genus into various genera (*Gabriceraurus* Pribyl, Vanek, and Pek, 1985, *Bufoceraurus* Hessin, 1989, *Leviceraurus* Hessin, 1988a, etc.), suggesting "*Ceraurus*" might actually be better considered a tribe of related forms, however this hypothesis has not previously been tested phylogenetically. This study uses specimen based phylogenetic analysis to elucidate the relationships between species within this potential "ceraurid tribe". To this end, a larger scale phylogenetic analysis was first conducted on the subfamily containing the ceraurids, the Cheirurinae Hawle and Corda, 1947, in order to understand the positions of the groups within the clade. Then, smaller phylogenies were conducted on the various clades of ceraurids in order to understand interspecific relationships, as well as to test the monophyly of the genera. The results of these analyses suggest *Ceraurus* forms a monophyletic genus while *Gabriceraurus* is shown to be paraphyletic, and is thus redefined as a monotypic genus including its type species. Species originally grouped within *Bufoceraurus* form a monophyletic group. However, the genus *Bufoceraurus* was assigned to a type species that is closely aligned with *Ceraurus*, and therefore the genus, as originally defined, is a synonym of *Ceraurus*. The species formerly assigned to *Bufoceraurus* which form a clade are assigned to a new genus, *Eubufoceraurus* gen. nov.. New material collected from Wisconsin, Iowa, Missouri, New York, and Ontario is used to name

several new species of ceraurid trilobites (*Eubufoceraurus scheeri* sp. nov., *Ceraurus kirchmeieri* sp. nov., *C. paraplattinensis* sp. nov., *C. jenlorum* sp. nov., *C. napaneei* sp. nov., *C. hillieri* sp. nov., *C. wilsoni* sp. nov., *C. ottawaensis* sp. nov., and *Ceraurus furca* sp. nov.) and is also used to revise established taxa, most notably the type species of the genus, *Ceraurus pleurexanthemus* Green, 1835. Photographs of the original type specimens suggest the species is more closely aligned with *Ceraurus monteyensis* Evitt, 1953, rather than the material from the Walcott Rust Quarry, as had been previously suggested by Raymond and Barton. We therefore synonymize *C. monteyensis* into *C. pleurexanthemus* and treat the material from the Walcott Rust Quarry as a new species named *C. walcotti* sp. nov.. This revision of the ceraurids is part of a larger, ongoing study of cheirurid trilobites that seeks to both revise the taxonomy of the cheirurids as well as generate phylogenetic hypotheses that can be used to better understand the macroevolutionary significance of the End Ordovician Mass Extinction on the evolution of the group as a whole.

INTRODUCTION

The genus *Ceraurus* Green 1832 is a speciose group of Ordovician trilobites belonging to the subfamily Cheiruridae. The genus is likely endemic to Laurentia and likely represents a monophyletic group based on several unique synapomorphies of the glabella, thorax, and pygidium. However, there are two large problems with the current taxonomic structuring of the group. The first problem is the uncertain relationship of *Ceraurus* to other, similar genera. Over the years the genus has been redefined, and species that were originally placed within this one genus have been divided up into multiple genera (Raymond and Barton 1913, Barton 1913, Cooper 1953, Ludvigsen 1976, Whittington 1954, Pribyl, Vanek, and Pek 1985, Hessin 1989,

Hessin 1988a). However, species within the genus *Ceraurus* still share many characteristics of the cephalon, thorax, and pygidium found in the species now placed within these newer, separate genera (*Bufoceraurus* Hessin, 1989, *Gabriceraurus* Pribyl, Vanek, and Pek, 1985, *Leviceraurus* Hessin, 1988a, *Borealaspis* Ludvigsen, 1976, *Whittakerites* Ludvigsen, 1976, *Hapsiceraurus* Whittington, 1954, *Ceraurinella* Cooper, 1953, *Ceraurinus* Barton, 1913). As such, it could be inferred that some or all of these genera could in fact belong to a larger related group of *Ceraurus*-like trilobites, a ceraurid tribe (while not expressly stated as such, Lespérance and Desbiens (1995) discuss the ceraurids as though the genera were a related group). The first priority of this monograph is to conduct a phylogenetic analysis to use as a framework for a larger scale revision of *Ceraurus* and its related genera. This is the first time a phylogenetic approach has been used to test the legitimacy of these genera.

Furthermore, species classifications within *Ceraurus* have been problematic, owing in part to an inconsistent diagnosis of the type species *C. pleurexanthemus* Green, 1832. The original type specimen was considered too poorly preserved or prepared to be a useful specimen, and was therefore redescribed by Raymond and Barton (1913) with new material from the Walcott Rust Quarry (Brett *et al*. 1999). However, modern preparative techniques have been applied to the type specimens (Whitely and Kloc 2002) and the original types have been shown to be markedly different from the material used by Raymond and Barton. This is only the most glaring example where new knowledge suggests dramatic changes in the original taxonomic definitions. The second priority of this manuscript will be to revise the majority of ceraurid species, as well as naming new species from new material collected from Iowa, Wisconsin, Missouri, New York, Ontario, and Quebec.

Morphological terminology discussed in this monograph follows Whittington *et al.* 1997 unless expressly stated.

HIGHER LEVEL TAXONOMY AND PHYLOGENY

Before species relationships within the ceraurid tribe could be adequately assessed, the placement of the ceraurids within the entirety of the cheirurids needed to be understood. Lane (1971) placed *Ceraurus* and its related forms into the subfamily Cheirurinae Hawle and Corda, 1847, based largely upon the synapomorphy of an exsagittally positioned furrow on the pleurae of the thoracic segments, as well as similarities in the trapezoidal shape of the glabella. The authors concur with this assignment, although acknowledge that a large scale phylogenetic analysis of the entirety of the cheirurids has not yet been attempted and could suggest different evolutionary groupings (although more recent taxonomic work from Lane (2002) and Parnaste (2003, 2004, 2008) have added more taxonomic evidence to better define the taxonomic groupings within the cheirurids). Such a large scale analysis is beyond the scope of this monograph, and therefore we use the current taxonomic placement as our assumption for the higher level relationships within the cheirurids. Therefore, in order to better understand the relationships of the ceraurids to the rest of the Cheirurinae, a phylogenetic analysis of the subfamily was conducted. The purpose of this analysis was two-fold. First, the analysis was meant to determine which “ceraurid” genera should be grouped within separate lineages and which genera should be grouped into a larger tribe. Second, the results of the analysis were used to determine which taxa would function as suitable outgroup taxa for our detailed analysis of the ceraurids.

This analysis included twenty seven species sampled from genera traditionally grouped within the Cheirurinae; *Lehua* Barton, 1916, *Hadromeros* Lane, 1971, *Ktenoura* Lane, 1971, *Cheirurus* Beyrich, 1845, *Laneites* Pribyl, Vanek, and Pek, 1985, *Xylabion* Lane, 1971, *Ceraurinus* Barton, 1913, *Osekaspis* Prantl and Pribyl, 1947, *Ceraurinella* Cooper, 1953, *Cerauropeltis* Pribyl, Vanek, and Pek, 1985, *Paraceraurus* Männil, 1958, *Gabriceraurus* Pribyl, Vanek, and Pek, 1985, *Bufoceraurus* Hessin, 1989, *Borealaspis* Ludvigsen, 1976, *Whittakerites* Ludvigsen, 1976, *Hapsiceraurus* Whittington, 1954, *Ceraurus* Green, 1832, and *Leviceraurus* Hessin, 1988a. Species from the genus *Cerauroides* Prantl and Pribyl, 1946 were not included in this analysis because the specimens were poorly preserved and often tectonically deformed, so they were not useful for phylogenetic coding. *Anacheirurus fredrichi* Whittard, 1967 was selected as the outgroup since the taxon shares apomorphies found in early Ordovician cheirurine genera, such as the elongation of the posterior-most thoracic pleurae into long spines, but lacks the thoracic pleural furrow common to all of the cheirurine trilobites.

Specific Taxa Analyzed: *Anacheirurus fredrichi* Whittard, 1967, *Lehua vincula* (Barrande, 1872), *L. argus* Whittington, 1963, *Hadromeros subulatus* (Linnarsson, 1869), *H. keisleyensis* (Reed, 1896), *Ktenoura retrospina* Lane, 1971, *Cheirurus centralis* Salter, 1853, *Laneites polydorus* (Billings, 1865), *Xylabion sexermis* (Öpik, 1937), *Ceraurinus glaber* (Whittington, 1954), *C. serratus* Ludvigsen, 1979, *C. icarus* (Billings, 1860), *C. marginatus* Barton, 1913, *Osekaspis comes* Prantl and Vanek, 1964, *Ceraurinella arctica* Ludvigsen, 1979, *Ce. chondra* Whittington and Evitt, 1954, *Ce. typa* Cooper, 1953, *Cerauropeltis ruedemanni* (Raymond, 1916), *Paraceraurus aculeatus* Männil, 1958, *Gabriceraurus gabrielsi* (Ludvigsen, 1979), *G. dentatus* (Raymond and Barton, 1913), *Eubufoceraurus pustulosus* sp. nov., *Whittakerites*

planatus Ludvigsen, 1976, *Borealaspis biformis*, Ludvigsen, 1976, *Ceraurus walcotti* sp. nov., *Hapsiceraurus, hispidus* Whittington, 1954, *Leviceraurus mammiloides*, Hessin ,1988a.

Characters: The majority of the characters used in the phylogenetic analysis come from the dorsal side of the mineralized exoskeleton. The characters are listed below in approximate order from anterior to posterior position on the organism. A complete character matrix is given in Table 1.

Cephalic Characters

Character 1. Cephalic outline, 0: semicircular (cephalic border is expanding anteriorly upon intersecting a sagittal line drawn from the medial portion of the eye ridge); 1: subrectangular (cephalic border roughly is roughly transverse upon intersecting a sagittal line drawn from the medial point of the eye ridge).

Character 2. A anterior lobe of the glabella, 0: strongly reduced so that the glabella nearly terminates after S3 (percentage of sagittal glabellar length beyond the S3 furrow 23%-25%), 1: anterior lobe is approximately the same sagittal length as other glabellar lobes (percentage of sagittal glabellar length beyond the S3 furrow 32%-35%), 2: anterior lobe of the glabella inflated and larger than any other glabellar lobes (percentage of sagittal glabellar length beyond the S3 furrow 39%-42%), 3: anterior lobe dramatically inflated so that sagittal length of the anterior lobe nearly as large as the sagittal length of all other

glabellar lobes combined (percentage of sagittal glabellar length beyond the S3 furrow 47%-50%)

Character 3. Posterior border of the genae, 0: straight; 1: bulges posteriorly as the border approaches the genae.

Character 4. Anterior glabellar border, 0: strongly expands beyond the cephalic border; 1: remains within the cephalic border

Character 5. Genal spines, 0: long (ratio of exsagittal width of the genal spines to the sagittal width of L0 >5); 1: reduced to small thorns (ratio of exsagittal width of the genal spines to the sagittal width of L0 =2.2-2.5).

Character 6. Posterior and medial portions of the lateral margins of the glabella, 0: straight sided (position of distal edge of L3 is parallel to L1), 1: expands anterio-laterally.

Character 7. Angle of the posterior and medial portions of the lateral margins of the glabella, 0: roughly parallel to the sagittal line (angle the lateral margin makes with the sagittal line is 0-10 degrees); 1: sharp angle (angle the lateral margin makes with the sagittal line is ~30 degrees); 2: weak angle (angle the lateral margin makes with the sagittal line is ~20 degrees).

Character 8. Paired pits arranged transverse anterior to S3 (dorsal exoskeleton), 0: absent; 1: present.

Character 9. Paired tubercules arranged transverse running along the sagittal axis of the glabella, 0: absent; 1: present.

Character 10. Anterior border of the cephalon, 0: wide (exsagittal width of anterior border ~ sagittal width of L0); 1: reduced (exsagittal width of anterior border ~ 0.5 sagittal width of L0).

Character 11. Glabella anterior of S3, 0: expands laterally (diagnosed by a marked angular change in the lateral glabellar margins at S3); 1: does not expand or begins to converge (diagnosed by a consistent angle of attack for lateral glabellar margin across S3).

Character 12. Eye position, 0: medial section of the eye ridge adjacent to the medial section of L2; 1: medial section of the eye ridge adjacent to S2; 2: medial section of the eye ridge adjacent to the medial section of L3

Character 13. S1, 0: strongly cuts S0; 1: does not intersect or very weakly intersects S0

Character 14. Anterior border of the glabella, 0: curved; 1: straight

Character 15. S2 and S3, 0: strongly penetrate the sagittal (furrows cut approximately 75% of the distance towards the center of the glabella); 1: constrained to the lateral borders or reduced; 2: gently penetrates the sagittal (furrows cut approximately 50% of the distance towards the center of the glabella).

Character 16. Direction of the lateral-most section of S1, 0: relatively transverse; 1: strongly exsagittally (points posteriorly at 30° relative to the transverse)

Character 17. Paired nodes arranged sagittally between the eye ridge and glabella, 0: present; 1: absent.

Character 18. S2 and S3, 0: relatively straight and squared off at the edges, 1: curved and triangular in shape.

Character 19. Ornamentation of the glabella, 0: tubercated; 1: smooth or granulated.

Hypostomal Characters

Character 20. Lateral margins of the hypostome, 0: terminate at a posterior margin, giving a trapezoidal shape to the hypostome; 1: converge together at a single point posteriorly, giving the hypostome a semi-triangular shape.

Character 21. Angle the lateral edges of the hypostome make with a sagittal line measured at the lateral kink, 0: shallow (~20 degrees); 1: moderate (28-30 degrees); 2: sharp (37-40 degrees).

Character 22. Middle body, 0: pinched in laterally by apodemal furrow; 1: lateral edges continuous.

Character 23. Small spines protruding from the posterior edges of the hypostome, 0: present; 1: absent.

Thoracic Characters

Character 24. Thoracic pleural furrow, 0: roughly transverse; 1: extends at an angle from posterior to anterior edge.

Character 25. Paired nodes running transversely along the axial ring of the thorax, 0: present; 1: absent.

Character 26. Final two pairs of thoracic pleurae, 0: extend dramatically longer than the other pleurae; 1: are indistinguishable from other pleurae.

Pygidial Characters

Character 27. First pygidial spines length, 0: short (exsagittal length of the first pleurae from the axial ring furrow to the distal end / sagittal length of the first axial ring = 5.5-8); 1: long. (exsagittal length of the first pleurae from the axial ring furrow to the distal end / sagittal length of the first axial ring = 12-15)

Character 28. Anterior axial furrow of the terminal axial ring, 0: triangular with the pointed end facing anterior; 1: trapezoidal.

Character 29. Distal edge of first pygidial spine, 0: smoothly curved; 1: tapers down into a roughly triangular shape.

Character 30. Second set of pygidial spines, 0: short but prominently extend beyond the pygidial border; 1: strongly reduced or do not extend off of the pygidial border; 2: long (comparable in length to thoracic pleurae).

Character 31. Proximal portion of pygidial spine forms a strong shoulder, 0: present, 1: absent

Character 32. Maximum convexity of the first pair of pygidial spines, 0: proximal; 1: medial; 2: distal.

Character 33. Small ridge runs exsagittally along the length of the first pair of pygidial spines spine, 0: absent; 1: present.

Character 34. Distal edges of the second/third set of pygidial pleural spines, 0: rounded; 1: triangular, 2: barely expand beyond the pygidial border.

Character 35. Posterior-most pygidial set of pleurae, 0: partially or completely fused together forming a single inflated and posteriorly directed terminal axial spine; 1: remain distinct entities.

Methods: The analysis was run in TNT v1.1 (Goloboff et al., 2008) using the traditional search function, with a random seed of 1, TBR, and 10,0000 replicates, saving 10 trees per replicate. Characters were treated as unordered and of equal weight since there was no *a priori* information to suggest any ordering or weight. Bootstrap and Jackknife values were calculated using a traditional search and 10,000 replicates. Bremer support values were also calculated using TNT. Matrix data was compiled into nexus files using Mesquite v2.75 (Maddison and Maddison, 2007) and trees were generated using Figtree v.1.3.1 (Rambaut, 2008).

Results: The analysis resulted in two most parsimonious trees with 119 steps and CI and RI values of 0.228 and 0.354 respectively. A strict consensus is shown in figure 1, and one of the two most parsimonious trees is shown in figure 2. Our analysis suggests there are at least five large subclades within the Cheirurinae. The genus *Lehua* likely forms a group basal to the entirety of the group. A larger clade that includes *Hadromeros*, *Ktenoura,* and *Cheirurus* plots sister to the taxa classically referred to as "ceraurid-like". Both *Ceraurinus* and *Ceraurinella* are shown to be distinct monophyletic genera. Finally, the genera *Ceraurus, Eubufoceraurus, Leviceraurus, Whittakerites, Borealaspis, Hapsiceraurus,* and *Gabriceraurus* group together in one larger clade with *Cerauropeltis* and *Paraceraurus* plotting basal.

Our analysis suggests that several of the "ceraurid" genera do group together into a larger clade; a ceraurid tribe which consists of species assigned to the genera *Ceraurus, Eubufoceraurus, Leviceraurus, Whittakerites, Borealaspis, Hapsiceraurus,* and *Gabriceraurus.* *Cerauropeltis ruedemanni* and *Paraceraurus aculeatus* plot basal to the ceraurid tribe and both are potentially useful outgroups for the ceraurid analysis. This "ceraurid tribe" is defined by possessing the following synapomorphies: paired apodemal pits on the glabella; glabellar furrows deeply incised, nearly straight, squared off at the end proximal to the glabella; lateral borders of the glabella are not completely parallel and instead expand anterio-laterally; generally long genal spines (although this character varies slightly within the group); triangularly shaped hypostome; prominent anterior pygidial spines with rest of the pygidial pleurae forming small reduced lappets or for these spines to be completely effaced.

The genera *Ceraurinus* and *Ceraurinella* are closely related to this "ceraurid tribe", however they are distinct monophyletic clades. *Ceraurinus* is defined by the combination of several synapomorphies, including the subrectangular shape of the cephalon, broad and rounded

distal edges of the pygidial pleural spines, and a small ridge that runs down the center of the anterior-most set of pygidial pleural spines. *Ceraurinella*, meanwhile, is defined by a the following characters: posterio-lateral margins of the glabella nearly parallel with a dramatic lateral swelling anterior of S3; pygidial pleurae form distinct spines with the anterior-most spines being the longest and the posterior-most spines partially or completely fused together to form a roughly triangular terminal spine (often bifurcated when the two pleurae are not completely fused). It is also interesting to note that there is a deeply rooted division between the Ordovician "ceraurid-like" forms and the Ordovician/Silurian "*Cheirurus*-like" forms, something that taxonomists have suggested for years (Raymond 1913, Ludvigsen 1979).

EVOLUTION OF THE CERAURIDS

CERAURUINELLA PHYLOGENETIC ANALYSIS

A second phylogenetic analysis was then conducted on the monophyletic sister group to the "ceraurid" tribe, the *Ceraurinella*. This genus, along with *Ceraurinus*, was originally formed from species split from the genus *Ceraurus*. The group has been considered to be among the *Ceraurus*-related genera (Shaw 1968), so a detailed analysis of the evolutionary patterns of the group was deemed important to gain a greater understanding of the entirety of ceraurid evolution. A more in depth analysis of *Ceraurinus* was not conducted because all available valid species assigned to the genus were included in the higher level phylogeny.

This analysis included fourteen taxa belonging to the genus *Ceraurinella* We presume these taxa to all be accurately assigned to the genus based upon the following shared synapomorphies, posterio-lateral margins of the glabella nearly parallel with a dramatic lateral swelling anterior of S3; pygidial pleurae form distinct spines with the anterior-most spines being the longest and the posterior-most spines partially or completely fused together to form a roughly triangular terminal spine (often bifurcated when the two pleurae are not completely fused). The taxa *Ceraurinella peregrinus* Dean, 1966 was excluded from the analysis, partly because the specimen was poorly preserved, and partly because the species lacks the lateral swelling expansion of the glabella anterior of S3. *C. oepiki* Edgecombe *et al.* 1999a and *C. magnilobata* Tripp, 1967 were excluded from analysis because they are poorly preserved and tectonically deformed, however the authors consider these species to be correctly placed within *Ceraurinella*. The species *C. buttsi* Cooper, 1953 was excluded from the analysis since it is only known from one partial cranidium, but we also considered to be correctly placed within *Ceraurinella*.

Osekaspis comes was chosen as the outgroup for this analysis based on the close sister relationship between *Osekaspis* and *Ceraurinella* based upon the topology of our higher level phylogeny, as well as the shared synapomorphy of fusing the posterior-most pygidial pleural spines into a single terminal spine.

Specific Taxa Analyzed: *Osekaspis comes, Ceraurinella necra* Ludvigsen, 1979, *C. scofieldi* (Barton, 1913), *C. templetoni* DeMott 1987, *C. typa* Cooper 1953, *C. latipyga* Shaw, 1968, *C. arctica* Ludvigsen, 1979, *C. brevispina* Ludvigsen, 1979, *C. chondra* Whittington and Evitt, 1954, *C. zhoui* Edgecombe *et al.*, 1999b, *C. kingstoni* Chatterton and Ludvigsen, 1976, *C.*

longispina Ludvigsen, 1979, *C. nahanniensis* Chatterton and Ludvigsen, 1976, *C. seriata* Ludvigsen, 1979.

Characters: The majority of the characters used in the phylogenetic analysis come from the dorsal side of the mineralized exoskeleton. The characters are listed below in approximate order from anterior to posterior position on the organism. A complete character matrix is given in Table 2.

Cephalic Characters

Character 1. S2 and S3, 0: sharply incised; 1: weakly incised

Character 2. Angle of the posterior and medial portions of the lateral margins of the glabella, 0: roughly parallel to the sagittal line (angle the lateral margin makes with the sagittal line is 0-10 degrees); 1: weak angle (angle the lateral margin makes with the sagittal line is ~20 degrees)

Character 3. Anterior border of the cephalon, 0: wide (exsagittal width of cephalic border ~ sagittal width of L0) ; 1: reduced (exsagittal width of cephalic border ~ ½ sagittal width of L0).

Character 4. S1, 0: strongly cuts S0; 1: does not intersect or very weakly intersects S0

Character 5. S2 and S3, 0: strongly penetrate the sagittal (furrows cut approximately 75% of the distance towards the center of the glabella); 1: gently penetrates the sagittal (furrows cut approximately 50% of the distance towards the center of the glabella).

Character 6. Direction of the lateral-most section of S1, 0: relatively transverse; 1: strongly exsagittally (points posteriorly at 30° relative to the transverse)

Character 7. Genal spines, 0: long (2x sag OC); 1: short (1x sag OC)

Character 8. Glabella expands laterally beyond S3, 0: present, 1: absent

Character 9. Genal spines depart from the cephalon at an angle of, 0: ~30 degrees, 1: 0-10 degrees.

Hypostomal Characters

Character 10. Middle body, 0: pinched in laterally by apodemal furrow; 1: lateral edges continuous.

Character 11. Angle the lateral edges of the hypostome make with a sagittal line measured at the lateral kink, 0: shallow (~20 degrees); 1: moderate (28-30 degrees); 2: sharp (37-40 degrees).

Character 12. Small spines protruding from the posterior edges of the hypostome, 0: present; 1: absent.

Pygidial Characters

Character 13. First pygidial spines length, 0: short (exsagittal length of the first pleurae from the axial ring furrow to the distal end / sagittal length of the first axial ring = 5.5-8); 1: long. (exsagittal length of the first pleurae from the axial ring furrow to the distal end / sagittal length of the first axial ring = 12-15)

Character 14. Distal edge of first pygidial spine, 0: lobate; 1: tapers down into a roughly triangular shape.

Character 15. Maximum convexity of the first pair of pygidial spines, 0: proximal; 1: medial; 2: distal.

Character 16. Distal edges of the second/third set of pygidial pleural spines, 0: rounded; 1: triangular.

Character 17. Posterior-most pygidial set of pleurae, 0: fused together forming a single inflated and posteriorly directed terminal axial spine; 1: partly fused or remain completely distinct entities.

Character 18. Terminal pygidial spine formed from the posterior-most set of pleurae, 0: pleurae fused completely, 1: pleurae incompletely fused resulting in a bifurcation of the structure or completely separated.

Methods: The analysis was run in TNT using the implicit enumeration function, which searches the entire parsimony landscape for optimal tree topologies. Characters were treated as unordered and of equal weight since there was no a priori information to suggest an ordering or weight. Bootstrap, Jackknife, and Bremer (1994) values were calculated using a traditional search and 10,000 replicates. Bremer support values were also calculated using TNT. Matrix data was compiled into nexus files using Mesquite v2.75 (Maddison and Maddison, 2007) and trees were generated using Figtree v.1.3.1 (Rambaut, 2008).

Results: Our analysis resulted in one MPT of 43 steps, with a CI and RI value of 0.442 and 0.538 respectively (fig 3). The topology is mostly pectinate, without any major clade divisions within the group. A few pairs of taxa plot in close sister relationships, including *C. seriata-C.*

nahanniensis, *C. kingstoni*-*C. longispina*, and *C. chondra*-*C. zhoui*. The sister group relationships of this final group, *C. chondra*- *C. zhoui*, is particularly interesting since *C. chondra* is a Laurentian species while *C. zhoui* is Gondwanan. Since this relationship is found derived in the phylogeny (and not an artifact of a basal Gondwanan origin), it implies that there may have been dispersal of *Ceraurinella* between Laurentia and Gondwana during the Ordovician.

"CERAURID TRIBE" PHYLOGENETIC ANALYSIS

A final phylogenetic analysis was conducted on the remaining ceraurid taxa which grouped together in the higher level phylogeny as a "ceraurid tribe". The analysis included 23 ingroup taxa originally assigned to the genera *Bufoceraurus*, *Gabriceraurus*, *Leviceraurus*, *Borealaspis*, *Whittakerites*, *Hapsiceraurus*, and *Ceraurus*. *Ceraurus hudsoni* Raymond, 1905 was not included in the analysis because it is represented by only one poorly preserved, incomplete crandium collected from an unknown locality. *C. proicens* Tripp, 1967, *C. elginensis* Slocom, 1913, *C. binodosus* Cooper and Kindle, 1936, *C. misneri* Foerste, 1909, *C. savagei* Walter, 1924, and *C. simmonsi* Hussey, 1926 were also not included in this analysis because they are known from a few poorly preserved cranidia, however the authors consider the placement of these taxa within the genus *Ceraurus* to be correct. Furthermore, *C. misneri* and *C. savagei* are likely synonyms of *C. milleranus* Miller and Gurley, 1894 and *C. elginensis* respectively that were named based on taphonomic differences rather than true synapomorphies or autapomorphies. *C. hermanni* Walter, 1924 was excluded from the analysis because the type specimen was in a

private collection that has since been lost, thereby turning the species into a *nomen nudum*. The species *C. trapezoidalis* Esker, 1964 and *C. breviceps* Cooper, 1953 were not included partly because of poor preservation and partly because the species were synonymized with *C. ruidus* Cooper, 1953 by Shaw (1974). We tentatively accept Shaw's synonymy, however we acknowledge that Shaw's claim should be treated with caution due to the incompleteness of the original type of *C. ruidus* and that collection of new material from the Edinburg Limestone from Virginia is necessary to ascertain if these synonymies are indeed legitimate (sadly this field work was outside of the scope of this monograph). In order to accommodate any error that could have been the result of an incorrect synonymy, characters were only coded from Cooper's original types. *Gabriceraurus mifflinensis* DeMott, 1987 was not included in the analysis because our field work suggests that there are at least two ceraurid species found in the locality from which this taxon was described (one of which is described as a new species, *C. jenlorum*, from complete specimens). Since *G. mifflinensis* was described from an isolated cranidium and an isolated pygidium, we were unable to ascertain with complete confidence whether or not the original holotype and paratype material are in fact mismatched without first describing a complete specimen from the locality. *Ceraurus whittingtoni* Evitt, 1953, *Gabriceraurus blussoni* (Ludvigsen, 1979), and *Ceraurus tuberosus* Troedsson, 1928 were not included because adequate specimen photographs were not available (specimen photos were small, and in the case of *C. whittingtoni*, poorly contrasted) and we were unable to visit the original type specimens or collect any new topotype material. Finally, *Borealaspis numitor* (Billings, 1866) was not included in the analysis because it is only known from one poorly preserved partial cranidia. The species has some characteristics in common with other ceraurids (short and deeply incised glabellar furrows, possible paired exsagittally positioned nodes close to the eye, subrectangular

L1, L2, and L3) but is unique in having a strongly curved S3 and a slightly rounded outline of the glabella. For the purposes of this monograph we consider *B. numitor* to likely be a derived ceraurid and agree with Ludvigsen (1976) that it is likely closely related to the other species designated as *Borealaspis*, however more complete specimens need to be discovered before this problem can be addressed fully.

As will be discussed later in the Systematic Paleontology section of the monograph, several of the species included in this analysis are new species split from previously described taxa. Hessin's (1989) *C.* cf. *plattinensis* is treated as unique taxon since it differs from the original Midwestern material it resembles in six distinct characters and are therefore is assigned to a new species, *Ceraurus paraplattinensis* sp. nov. *Ceraurus bispinosus* Raymond and Barton, 1913 is not considered to be synonymous with Hessin's (1989) *Bufoceraurus* material, and as such Hessin's material is renamed *Eubufoceraurus pustulosus* sp. nov.. *Ceraurus monteyensis* Evitt, 1953 is considered to be synonymous with Green's (1832) original type specimens of *C. pleurexanthemus*, however specimens from the Walcott Rust Quarry originally assigned to *Ceraurus pleurexanthemus* by Raymond and Barton (1913) are instead treated as unique taxa and are renamed *C. walcotti* sp. nov..

Cerauropeltis ruedemanni was designated as the outgroup in TNT, however *Paraceraurus aculeatus* was also included in the analysis with the expectation that the taxon would likely plot basally and function as a second outgroup, allowing for better character optimizations.

Specific Taxa Analyzed: *Cerauropeltis ruedemanni* (Raymond, 1916), *Paraceraurus aculeatus* Männil, 1958, *Gabriceraurus gabrielsi* (Ludvigsen, 1979), *G. dentatus* (Raymond and Barton,

1913), *G. hirsuitus* (Ludvigsen, 1979), *Eubufoceraurus pustulosus* sp. nov., *E. scheeri* sp. nov., *E. cetus* (Dean, 1979) *Whittakerites planatus* Ludvigsen, 1976, *Borealaspis biformis* Ludvigsen, 1976, *Borealaspis whittakerensis* Ludvigsen, 1976, *Ceraurus walcotti* sp. nov., *C. kirchmeieri* sp. nov., *C. ruidus* Cooper, 1953, *C. mackensiensis* Ludvigsen, 1979, *C. matranseris* Sinclair, 1947, *C. pleurexanthemus* Green, 1832, *C. globulobatus* Bradley, 1930, *C. jenlorum* sp. nov., *C.* cf. *globulobatus* Bradley, 1930, *C. milleranus* Miller and Gurley, 1894, *C. plattinensis* Foerste 1920, *C. paraplattinensis* sp. nov., *Hapsiceraurus hispidus* Whittington, 1954, *Leviceraurus mammiloides* Hessin, 1988a, *L.? furca* sp. nov.

Characters: The majority of the characters used in the phylogenetic analysis come from the dorsal side of the mineralized exoskeleton. The characters are listed below in approximate order from anterior to posterior position on the organism. A complete character matrix is given in Table 3.

The position of the eyes relative to the glabella was an important character utilized in the phylogeny. While this has historically been viewed as a useful characteristic for discerning ceraurid species (Raymond and Barton 1913), the character was criticized by Lespérance and Desbiens (1995) as being highly variable within the ceraurids. In our experience, the eye position relative to the glabella is mostly constant within species, and when the character does appear to vary, it does so in conjunction with other synapomorphic or autapomorphic characteristics, which suggests that there are two species in the same area. Therefore the presumed variability of eye position in ceraurids is likely due to the taxonomic error of over-lumping species (e.g. *Ceraurus pleurexanthemus*) and not because of a real biological variation. It is also possible the character may appear variable in the literature due to authors having their own individual metrics

for aligning the position of the eye to the glabella (i.e. if one author interprets the eye alignment by using the posterior border of the eye, while another uses the center line of the eye, this would result in inconsistencies in interpretation). As such, throughout this monograph we will be interpreting the position of the eye based on a transverse line drawn from the center of the base of the palpebral lobe to the glabella and reinterpreting diagnoses and descriptions to fit this determination.

The organization of nodes and tubercles on the posterior border of the cephalon are incredibly diverse in form and tend to be consistent within species, and are therefore useful characteristics for diagnosing species. However, because the ornamentation is so complex and diverse, it was difficult to accurately code all of the relevant variability without creating multistate characters so large as to be parsimony uninformative. Furthermore, it is occasionally difficult to tease apart the ornamentation that is unique to the posterior cephalic border, and the ornamentation that results from the entire exoskeleton being covered in tubercles/granules. Future workers may find the ornamentation of the posterior cephalic border a useful character, but for our analysis we felt we were unable to accurately characterize it, and therefore excluded it from the analysis.

Cephalic Characters

Character 1. Large prominent glabellar tubercles paired across the glabella, 0: visible; 1: absent or ornamentation is randomly arranged.

Character 2. Ornamentation of the glabella, 0: mostly evenly covered in small granules or effaced; 1: mostly evenly covered in large tubercles; 2: large tubercles concentrated on the anterior side of the glabella.

Character 3. Angle of departure for the genal spines, 0: stay close to the body (15-20 degrees from sag); 1: moderately expand away from the body (25-30 degrees from sag); 2: dramatically depart from the body (40-45 degrees from sag).

Character 4. Glabella curvature (lateral view), 0: strongly vaulted resulting in a dome-like glabella; 1: low relief glabella.

Character 5. Lateral portion of the posterior margin of the cephalon, 0: possesses small posteriorly directed spines; 1: posterior border does not have a posteriorly directed spine.

Character 6. Glabellar spine near the occipital ring, 0: large spine protrudes off of the glabella from near the occipital ring; 1: the occipital ring possesses no large spine.

Character 7. Cheek ornamentation, 0: granulose; 1: tubercose; 2: warty (warty texture has very large tubercles that are raised to a point and nearly resemble small spines).

Character 8. Genal spines, 0: strongly curved; 1: nearly straight

Character 9. Cephalic outline, 0: semicircular (cephalic border is expanding anteriorly upon intersecting a sagittal line drawn from the medial portion of the eye ridge); 1: subrectangular (cephalic border roughly is roughly transverse upon intersecting a sagittal line drawn from the medial point of the eye ridge)

Character 10. Posterior border of the genae, 0: straight; 1: bulges posteriorly as the border approaches the genae, 2: curves anteriorly before reaching genal spine.

Character 11. Genal spines, 0: long (ratio of exsagittal width of the genal spines to the sagittal width of L0 >5); 1: reduced to small thorns (ratio of exsagittal width of the genal spines to the sagittal width of L0 =2.5-3.5)

Character 12. Angle of the posterior and medial portions of the lateral margins of the glabella, 0: glabella barely expands anteriorly with the sides being roughly parallel to the sagittal line (5-10 degrees); 1: glabella prominently expands with the lateral margins forming a sharp angle with the sagittal (15-20 degrees).

Character 13. Anterior border of the cephalon, 0: wide (exsagittal width of anterior border ~ sagittal width of L0); 1: reduced (exsagittal width of anterior border ~ ½ sagittal width of L0).

Character 14. Eyes position, 0: medial section of the eye ridge adjacent to the medial section of L2; 1: medial section of the eye ridge adjacent to S2; 2: medial section of the eye ridge adjacent to the medial section of L3

Character 15. Anterior border of the glabella, 0: curved; 1: straight

Character 16. S2 and S3 furrows, 0: prominently encroach on the sagittal line of the glabella; 1: are constrained to the lateral borders of the glabella.

Character 17. Paired nodes arranged sagittally between the eye ridge and glabella, 0: present; 1: absent.

Character 18. Ornamentation of the genal spines and cephalic border, 0: smooth or covered in imperceptibly small granules; 1: covered in prominent large granules or very small tubercles; 2: densely covered in large pustules.

Hypostomal Characters

Character 19. Angle the lateral edges of the hypostome make with a sagittal line measured at the lateral kink, 0: moderate (28-30 degrees); 1: sharp (37-40 degrees).

Character 20. Middle body furrow of the hypostome, 0: prominently cuts lateral edge of the middle body; 1: lateral edge of the middle body is continuous and the furrow is absent or reduced.

Thoracic Characters

Character 21. Paired nodes running transversely along the axial ring of the thorax, 0: present; 1: absent or strongly reduced.

Pygidial Characters

Character 22. Furrow cutting into the first pygidial pleurae proximal to the pygidial axis, 0: strongly incised, 1: weakly incised or effaced.

Character 23. Axial furrow of the pygidium, 0: weakly incised; 1: sharply incised, nearly pinching out the pleurae at the point proximal to the axis.

Character 24. Angle of departure of the first pygidial pleural spines from the pygidium (angles measured from the pleural furrow on the spine), 0: wide (50-60 degrees from the sagittal line), 1: narrow (30-40 degrees from the sagittal line), 2: spine departs from the pygidium directly posterior.

Character 25. Curvature of the first set of pygidial spines, 0: strongly curved; 1: weakly curved.

Character 26. Anterior axial furrow of the terminal axial ring, 0: triangular with the pointed end facing anterior; 1: Trapezoidal.

Character 27. Second and third set of pygidial spines, 0: short but prominently extend beyond the pygidial border forming small lappets; 1: strongly reduced or do not extend off of the pygidial border, 2: long spines nearly as long as the anterior pygidial spines.

Character 28. First pygidial pleural spine, 0: strongly curves proximal to the axis of the pygidium, 1: curves strongest in the medial section of the spine

Character 29. Posterior-most pygidial set of pleurae, 0: form a fused, inflated expansion posterior of the pygidium; 1: remain distinct spines or do not extend beyond the border of the pygidium.

Character 30. Outline of the pygidium, 0: strongly curved forming a nearly semicircular outline; 1: weakly curved forming a nearly trapezoidal outline.

Character 31. Shape of the 2nd and 3rd pygidial pleural spines, 0: triangular, 1: lobate, 2: spines fused or indistinct.

Methods: The analysis was run in TNT using the traditional search function, with a random seed of 1, TBR, and 10,0000 replicates, saving 10 trees per replicate. Characters were treated as unordered and of equal weight since there was no a priori information to suggest an ordering or weight. Bootstrap, Jackknife, and Bremer (1994) values were calculated using a traditional search and 10,000 replicates. Bremer support values were also calculated using TNT. Matrix data was compiled into nexus files using Mesquite v2.75 (Maddison and Maddison, 2007) and trees were generated using Figtree v.1.3.1 (Rambaut, 2008).

Results: Our analysis resulted in 16 MPTs of 113 steps, with CI and RI values of 0.354 and 0.631 respectively. A strict consensus of these results is shown in Figure 4, and one of the most parsimonious trees is shown in Figure 5. Taxa originally grouped within the genus *Eubufoceraurus* are shown to form a monophyletic group, united by the combination of the following synapomorphies: warty tubercles covering the exoskeleton; eyes aligned with 3L of the glabella; small pair of spines protruding posteriorly from the lateral position of the posterior border of the glabella; the medial and posterior pygidial pleurae develop distinct lappets/short spines. *Gabriceraurus*, as it is traditionally defined, is a basal paraphyletic grade whose defining characteristics (eyes aligned with 2L, shallowly expanding lateral margins of the glabella, trapezoidal furrow around the terminal axial piece of the pygidium) are plesiomorphic. All of the taxa assigned to the other genera plot in one large clade including all of *Ceraurus*, *Leviceraurus, Whittakerites, Hapsiceraurus, Borealaspis,* and *Leviceraurus*. Both *Borealaspis* and *Leviceraurus* plot out as small derived clades nestled within other species originally grouped into

Ceraurus. While these taxa do represent monophyletic clades, treating them as unique genera turns *Ceraurus* into a polyphyletic group, requiring the creation of multiple monotypic genera. Therefore, we propose that the most conservative approach is for all of these species to be subsumed into a broader defined *Ceraurus*. This clade is highly variable, and therefore is diagnosed by the majority of the taxa sharing the following synapomorphies: semicircular cephalic outline; prominent paired nodes positioned close the eye and arranged roughly sagittal to each other; glabellar furrows constrained to the lateral margins of the glabella; glabellar furrows deeply incised, and squared off; lateral margins of the middle body of the hypostome smooth with the middle body furrow effaced; pygidium with one prominent set of pygidial spines on the anterior pleurae with the other pleural lappets strongly reduced or completely absent; triangular shaped furrow on the anterior of the terminal axial piece of the pygidium.

SYSTEMATIC PALEONTOLOGY

Museum abbreviations used below are as follows: Yale Peabody Museum (YPM), Museum of Comparative Zoology (MCZ), Cincinnati Museum Center (CMNH), Royal Ontario Museum (ROM), Geological Survey of Canada (GSC), Field Museum of Natural History (FMNH, also specimens sometimes labeled UC), New York State Museum (NYSM), and American Museum of Natural History (AMNH).

Family CHEIRURIDAE Hawle and Corda, 1847

Subfamily CHEIRURINAE Hawle and Corda, 1847

Genus GABRICERAURUS Pribyl, Vanek, and Pek, 1985

Type Species .-- *Ceraurus gabrielsi* Ludvigsen, 1979

Other Taxa Included .-- "*Gabriceraurus*" *dentatus* (Raymond and Barton, 1913), "*G.*" *blussoni* (Ludvigsen, 1979), "*G.*" *hirsuitus* (Ludvigsen, 1979).

Diagnosis .-- The diagnosis follows Ludvigsen's (1979) original diagnosis for the type species, *Gabriceraurus gabrielesi*, except for one character. Ludvigsen states the position of the eye is aligned with S2. However, drawing a transverse line from the center of the eye demonstrates that the eye is aligned with L1.

Discussion .-- The results of our phylogenetic analysis show the genus *Gabriceraurus* to be a basal paraphyletic grade. Since the genus, as classically defined by Pribyl, Vanek, and Pek (1985), does not represent a monophyletic group, it is not a real evolutionary unit. The name, however, is still useful for taxonomic purposes. Therefore, we follow the conventions of Wiley (1979) and redefine the genus *Gabriceraurus* as a monotypic genus including its type specimen. The other taxa originally grouped within *Gabriceraurus* are referred to as "*Gabriceraurus*" with the quote marks denoting that they represent a grade.

GABRICERAURUS GABRIELSI (Ludvigsen, 1979)

Ceraurus gabrielsi LUDVIGSEN, 1979, pp. 29-32, pl. 12, figs 1-44, pl. 12, figs 1-49

Gabriceraurus gabrielsi PRIBYL, VANEK, AND PEK, 1985, p. 161

Holotype .--Nearly complete cranidium GSC 44074.

Occurrence .-- Middle and upper Esbataottine Formation, Sunblood Range and Whittaker Ranger. Upper Sunblood Formation, Natla River.

Diagnosis .-- See Ludvigsen (1979).

Discussion.-- Using the phylogeny to observe character evolution, it is interesting to note that *Gabriceraurus gabrielsi* has a plesiomorphic pygidium. Particularly, the nature of the anterior pygidial pleural spines is similar to the spines in *Paraceraurus aculeatus* and *Ceratropeltis ruedemanni*. The anterior pygidial pleural spines dramatically curve proximal to the pygidium, but are roughly straight medially and distally. Furthermore, the proximal portions of the spines fuse onto the attachment point of the pygidium, creating the appearance of a large shoulder on the lateral anterior edges of the pygidium. No other ingroup taxa included in the analysis shared this character; however the character is shared with "*G.*" *blussoni*, suggesting that the two species are likely closely related.

"GABRICERAURUS" HIRSUITUS (Ludvigsen, 1979)

Ceraurus aff. *dentatus* LUDVIGSEN, 1975, pl. 4, figs 3-4.

Ceraurus hirsuitus LUDVIGSEN, 1979, pp.32-34, pl. 14, figs 1-25.

Gabriceraurus hirsuitus PRIBYL, VANEK, AND PEK, 1985, p. 161

non *Gabriceraurus hirsuitus* HESSIN, 1989, pp. 1204-1208, pl. 1, figs 1-7.

Holotype .-- Incomplete cranidium GSC 40415.

Occurrence .-- Upper Esbataottine Formation, Sunblood Range and Flood Creek.

Diagnosis .-- Our diagnosis follows Ludvigsen (1979) with the following additions: large prominent node on the posterior border of the cephalon positioned close to the eye; pygidium subrectangular in outline; medial and posterior pleural lappets weakly defined and rounded.

"GABRICERAURUS" DENATATUS (Raymond and Barton, 1913)

Plate 1, Figures 1-3

Ceraurus dentatus RAYMOND AND BARTON, 1913, pp. 534-535, pl. 1, fig 2.

Gabriceraurus dentatus PRIBYL, VANEK, AND PEK, 1985, p. 161

? *Gabriceraurus dentatus* DEMOTT, 1987, p. 78, pl. 9, figs 1-7, pl. 10 figs 1-3.

Gabriceraurus hirsuitus HESSEN, 1989, pp. 1204-1208, pl. 1, figs 1-7.

Gabriceraurus dentatus LESPÉRANCE AND DESBIENS, 1995, pp. 15-16, fig 5.

Holotype .-- Original holotype lost. Three paratype specimens including incomplete exoskeleton AMNH 29511, incomplete pygidium AMNH 29509, and nearly complete exoskeleton GSC 1769b.

Occurrence .-- Collected from the Trenton Formation Middleville, Herkimer County, New York and Cobourg, Ontario. Possibly collected from the Guttenberg Formation near Fennimore Wisconsin.

Diagnosis .-- No complete diagnosis has been proposed for this species, however our proposed diagnosis uses the original types and material from New York and Ontario, as well as useful descriptions from Raymond and Barton (1913) and Lespérance and Desbiens (1995): cephalon subrectangular in outline; eyes positioned far back on the head with the center of the eye aligned

with L2; glabella and cheeks covered in randomly arranged, low relief tubercles while the rest of the exoskeleton is densely covered in fine granules; glabella subrectangular in outline, lateral margins expand anteriorly at approximately 15-20º, and anterior border nearly straight in dorsal view; glabellar furrows deeply incised, roughly straight, and gently penetrate into the glabella nearly half the distance to the sagittal line; anterior border of the cephalon wide and broadly defined by a deeply incised anterior border furrow; posterior cephalic border with a line of faint tubercles close to the glabella but lacking any prominent raised nodes as seen in other ceraurids; genal spines long and depart from the cephalon at approximately 20º angle with the sagittal and gently curve until the distal end of the spine is pointing almost directly posterior; axial ring of the thorax smooth; three nodes associated with the thoracic pleural furrows large and inflated, gently rising above pleurae; pygidium subtrapezoidal in outline, with one large set of pygidial pleural spines on the anterior pleurae and small, reduced, subtriangular lappets on the medial and posterior pleurae; pygidial spines depart the pygidium at roughly 45º, triangular in shape, and curve medially until distal tips of the spines spine point nearly directly posterior; pleural furrow on the proximal section of the pygidial spine deeply incised; furrow anterior of the terminal axial piece trapezoidal in shape.

Discussion.-- Hessin (1989) synonymized "*Gabriceraurus" dentatus* with "*G." hirsuitus* because the original holotype of "*G." dentatus* was lost. Lespérance and Desbiens (1995) argued that this was inappropriate taxonomic procedure and instead redescribed the species using the original paratypes as replacements for the holotype. We concur with Lespérance and Desbiens' (1995) treatment of "*G.*" *dentatus*.

DeMott (1987) reported *"G." dentatus* material from Wisconsin which is similar to the Ontario and New York specimens and lacks any obvious autapomorphies that would distinguish

it. However, DeMott's specimens are mostly broken cranidia and pygidia, and thereby do not have cheeks, genal spines, and thoracic segments to compare with. As such, we cautiously accept DeMott's designation of his material as *"G." dentatus* but acknowledge that new *"G." dentatus* material from Wisconsin is necessary to determine if this assignment is correct.

"GABRICERAURUS" BLUSSONI (Ludvigsen, 1979)

Ceraurus hirsuitus LUDVIGSEN, 1979, p.34, pl. 13, figs 9-29

Gabriceraurus hirsuitus PRIBYL, VANEK, AND PEK, 1985, p. 161

Holotype .-- Cranidia GSC 44129.

Occurrence .-- Collected from the upper Sunblood Formation, Mary Range.

Diagnosis .-- Our diagnosis follows Ludvigsen (1979), with one addition: center of the eyes aligned with L2.

Discussion.-- The species is assigned to "*Gabriceraurus*" based upon similarities between this specimen and the type of the genus, *G. gabrielsi*. Particularly, the pygidium of *"G." blussoni* is similar to the pygidium of *G. gabrielsi*, with both specimens exhibiting pygidial pleural spines that sharply curve proximal to the pygidium and fuse slightly to the attachment site of the pygidium, forming a pronounced "shoulder".

Genus EUBUFOCERAURUS gen. nov.

Etymology .-- Named from the Latin for sharp or spike, spiculum.

Type Species .-- *Eubufoceraurus pustulosus* sp. nov. (originally named by Hessin, 1989 as *Bufoceraurus bispinosus* (Raymond and Barton, 1913))

Other Taxa Included .-- *Eubufoceraurus cetus* (Dean, 1979), *Eubufoceraurus scheeri* sp. nov..

Diagnosis .-- Exoskeleton densely covered in raised, warty pustules/tubercles; eyes positioned far forward on the cephalon, with the center of the eye aligned with L3; glabellar furrows prominently cut inwards towards the center of the glabella; small, posteriorly directed spines on the posterior border of the cephalon close to the genal spines; anterior set of pygidial pleural spines large and prominent, while the other pleurae have strongly differentiated lappets which prominently extend beyond the pygidial border.

Discussion .--The specimens that Hessin (1989) originally described as *Bufoceraurus bispinosus* do clade together with similar trilobites in the analysis, forming a monophyletic group. This gives credence to Hessin's original idea that his specimens represent a unique genus, *Bufoceraurus*. However, Hessin incorrectly synonymized his material with *Ceraurus bispinosus* (discussed below) and then named *C. bispinosus* as the type species for the genus. When this error is corrected, *Bufoceraurus* becomes a synonym of *Ceraurus* because the genus is tied to its type species, *C. bispinosus*. As such, even though Hessin's material does represent a real monophyletic genus, *Bufoceraurus* is not a valid name because it was defined based on material incorrectly assigned to a different species. Since the old name is no longer available, we propose a new genus, *Eubufoceraurus*, with its type species assigned as a new species named from Hessin's material, *Eubufoceraurus pustulosus*.

Also, in Hessin's original diagnosis, he synonymized all specimens that shared similar characteristics to his proposed *Bufoceraurus* within one species, thereby hierarchically reducing

the species to the level of the genus. We consider this to be inappropriate taxonomically since there are distinct species within the group. Therefore, we treat taxa that were originally synonymized within Hessin's monotypic *Bufoceraurus* as independent species.

EUBUFOCERAURUS PUSTULOSUS sp. nov.

Plate 2, Figure 1

Bufoceraurus bispinosus HESSIN, 1989, pp.1208-1213, pl. 2, figs 1-4, 6-7.

non *Ceraurus bispinosus* RAYMOND AND BARTON, 1913, pp. 536-538, pl. 1, fig, 3,4.

non *Ceraurus cetus* DEAN, 1979, pp. 5-6, pl. 2, figs 1-5, 9, pl. 4, fig 10.

non *Ceraurus*? sp. BRADLEY, 1930, p.276, pl.30, fig 44.

Etymology .-- The species is named after the large pustules that cover the exoskeleton.

Holotype .-- Incomplete exoskeleton ROM 46068a.

Other Material .-- Incomplete exoskeleton ROM 46068b, incomplete exoskeleton ROM 52739, hypostome ROM 46070. A cranidium with paired tubercles running up the glabella (ROM 46069) is placed within the species with a degree of uncertainty.

Occurrence .-- Bobcaygeon Formation collected at Carden quarry, 6 km northeast of Brechin, Ontario.

Diagnosis .-- Our diagnosis for the species follows Hessin's (1989) diagnosis of the genus *Bufoceraurus*, with the addition of three characters: posterior border of the cephalon remains

transverse as it approaches the genal spines; spines on the posterior border positioned very close to the genal spines; glabella densely covered in randomly arranged tubercles.

Description .-- While examining private trilobite collections, it became apparent that Hessin's description of *Bufocerarus* was based on two different species. In Hessin's (1989) original description, he utilized a specimen from a private collection to draw his reconstruction and inform his descriptions that was not figured in photographs. This specimen has paired nodes running sagittally up the glabella, which is only seen in one of Hessin's photographed specimens (ROM 46069). This resulted in two different species being used to describe *Eubufoceraurus* from the Bobcaygeon.As such, we consider it prudent to redescribe the species based only off of the material which best fits the new holotype. This redescription is shorter (given in part to the fragmentary material available), and eschews information from the incomplete cranidium ROM 46069.

Exoskeleton, cheeks, and glabella densely covered in large, prominent warty pustules. Eyes positioned far forward on the cephalon, aligned with S3. Cephalon semicircular in outline. Glabella subrectangular in shape with lateral margins that prominently expand. S1, S2, and S3 straight, deeply incised, squared at the ends, and dramatically incised into the sagittal of the glabella. Some specimens exhibit larger randomly arranged pustules on the anterior-most section of the glabella. While most specimens do not preserve it, a small posteriorly directed spine on the posterior border of the cephalon is visible on the right lateral cheek of the holotype specimen. Posterior border of the cephalon separated from the cheek by a strongly incised narrow furrow, and heavily ornamented (however all specimens are lightly effaced so it cannot be determined if there are diagnostic patterns of ornamentation on the border). Occipital ring roughly one third of

the transverse width of the cephalon, and similar in sagittal width to the posterior cephalic border and the first axial rings of the thorax.

Hypostome subtriangular in shape. Middle body oval in shape and covered in round tubercles. Middle body furrow absent or strongly effaced. Furrow around the middle body strongly incised and narrow.

11 thoracic segments. Axial ring of the thorax eroded or damaged in most specimens, so it is difficult to determine if the species exhibits raised paired nodes on the axis that are present in some other ceraurids. Exsagittally arranged furrow on the thoracic pleurae long, and strongly incised. Lateral-most lobe formed from the furrow appears to raise gently into a prominent node.

Pygidium semicircular to subtriangular in outline with three prominent pygidial segments and a prominent terminal axial piece. All three pygidial pleurae form strongly defined pygidial spines, which are strongly curved medially, lobate, and with the anterior-most pygidial spine being the longest and the posterior-most spine being the shortest. Axial furrow thin but prominently incised. Pleural furrows strongly incised. Furrow between the axis and the terminal axial piece strongly incised and strongly triangular in shape. Terminal axial piece inflated into a small, lobate terminal spine.

Discussion.-- Hessin's (1989) synonymy of this material with *Ceraurus bispinosus* Raymond and Barton, 1913 is dubious. While *Ceraurus bispinosus* is only known from a poorly preserved cranidia, a close examination of the specimen reveals that *C. bispinosus* and Hessin's material are drastically different. First, *C. bispinosus* does not have the three sets of paired tubercles running sagittally up the glabella that are found in Hessin's original paratypes. Second, there is an inflation on the right side of the glabella of *C. bispinosus* that appears similar to the paired inflations seen in *C. maewestoides* Ludvigsen, 1979, *C. biformis* (Ludvigsen, 1976), *C.*

whittakerensis (Ludvigsen, 1976), and *C. binodosus* Cooper and Kindle, 1936. Unfortunately, the left side of the glabella is worn off so it cannot be confirmed if this character is indeed a paired inflation as observed in those other taxa. Still, no such inflation can be seen on Hessin's material. Finally, while the lateral sides of the original type for *C. bispinosus* are broken off, the posterior-most portion of the palpebral ridge remains, showing that the eye was roughly aligned with S2 on the glabella, which is further back than Hessin's material. In light of this evidence, the only characteristic that Hessin's material shares with the type of *C. bispinosus* is the fact that both are ornamented with large tubercles or pustules, but even this characteristic is suspect. Hessin's material is consistently more densely ornamented than *C. bispinosus*, and the tubercles on *C. bispinosus* are smaller and have generally less vertical relief than the large, warty, almost spine-like pustules found on Hessin's material. While this difference in ornamentation could be a function of ontogeny (since the type specimen of *C. bispinosus* is dramatically smaller than Hessin's material), we find this explanation to be unsatisfactory based upon our material of the new species *Eubufoceraurus scheerorum*. We observe and illustrate specimens of *E. scheerorum* from many different ontogenetic stages, and while it is true that the pustules grow in size relative to the body, they retain a raised, warty like characteristic even in smaller specimens. Therefore, we conclude that *Ceraurus bispinosus* is not a synonym of Hessin's material and that Hessin's material is henceforth renamed *Eubufoceraurus pustulosus*. These sentiments are echoed by Lespérance and Desbiens (1995).

It is possible that this mistaken classification could be due to an over reliance on Raymond and Barton's (1913) original reconstructions and interpretations of the *Ceraurus bispinosus* holotype. Raymond and Barton's reconstruction of the holotype has several inaccuracies when compared to the original specimen. First, the reconstruction gives the

appearance that the raised inflations of the glabella found in the holotype specimen are actually paired tubercles. This makes it appear as though *C. bispinosus* had paired tubercles running up the glabella, as seen in Hessin's material, when this conclusion is actually false. Second, the reconstruction gives the illusion that the break on the anterior right side of the cranidium of the holotype is actually a notch in the cranidium where the eye would sit if the free cheek was connected. This gives the inaccurate impression that the eye of *C. bispinosus* was positioned strongly anteriorly forward, adjacent to L3 as seen in Hessin's material. Finally, as discussed above the original specimen has a piece of the palpebral ridge preserved, positioned far back on the cephalon relative to Hessin's material, but the original reconstructions of the animal incorrectly interpret this ridge as a small tubercle. These inaccuracies in Raymond and Barton's reconstruction all suggest characters that would, if correct, make *C. bispinosus* a likely synonym of *Eubufoceraurus pustulosus*. However, when looking at the actual specimens, these two species do not resemble each other.

One final note, only one of Hessin's cephala (ROM 46069) clearly exhibits pairs of tubercles/pustules running sagittally down the glabella. The other two specimens are badly crushed and worn down around the glabella, so it is difficult to determine if the absence of the character in the other specimens is taphonomic or biologically significant (Hessin attributes this absence to variability within the species in his description). Given information discussed above from private collections, we do not accept Hessin's original claim that this characteristic is a synapomorphy of the species, however we acknowledge that future material is necessary to properly separating out the two species of *Eubufoceraurus* in the Bobcaygeon.

EUBUFOCERAURUS SCHEERORUM sp. nov.

Plate 2, Figure 2; Plate 3, Figures 1-5; Plate 4, Figures 1-2

Etymology .-- This species is named after the father and son who first discovered it, Al and Caleb Scheer.

Holotype .-- One large, incomplete cephalon. KUMIP 325579.

Other Material .-- Three isolated incomplete cranidia KUMIP 325582, 325584, 325585 two incomplete pygidia KUMIP 325581, 325583, and two ventral genal spines and fixigenae KUMIP 325580, 325585.

Occurrence .-- Mifflin Member of the Plattville Group collected near Fennimore, Wisconsin.

Diagnosis .-- Roughly parallel sided glabella; posterior border of the cephalon curves anteriorly as it approaches the genal spines; glabellar tubercles/pustules randomly arranged; spine on the posterior border of the cephalon present but reduced to a small, thorn-like structure; two large raised nodes medially positioned on the occipital ring; pleural furrows of the pygidium deeply incised; lappets on the medial and posterior pleurae of the pygidium short in length and sharply triangular in shape.

Description .-- Exoskeleton densely covered in large warty tubercles/pustules with strong vertical relief, giving them the appearance of spines. Cephalon roughly subrectangular in outline, but with the anterior border of the cephalon curving anteriorly as it approaches the genal spines. Small, posteriorly directed, thorn-like spines positioned on the lateral edges of the posterior border of the cephalon close to the attachment site of the thorax. Anterior border of the cephalon broad and separated from the cheek by a shallow, slightly effaced border furrow. Genal spines depart from the cephalon at approximately 35º, are triangular in shape, and strongly curve medially with the distal ends of the spine pointing inwards towards the animal. Eyes positioned

far forward, aligned with S3. Eye size cannot be determined because no complete eyes are preserved. Cheeks on the some specimens bulge ventrally (KUMIP 325579, 325584), while the cheeks of other specimens have lower vertical relief (KUMIP 325582, 325585). Glabella subrectangular in outline with gently expanding lateral margins (5-10º) and straight anterior border. Glabellar furrows deeply incised, moderately penetrate into the center of the glabella, straight, and squared off at the end proximal to the glabella. L1, L2, and L3 roughly equal sized, subrectangular in shape, and large relative to the size of the glabella. Tubercles/pustules on the glabella randomly arranged. Glabella has low relief in lateral view. Occipital ring slightly more vaulted than the glabella, and has two faint raised nodes positioned medially.

Pygidia specimens broken in half but the available information is sufficient to ascertain the pygidial outline without genal spines is subtrapezoidal. Anterior pygidial pleural spines depart from the pygidium at approximately 45º, triangular in shape and strongly curved medially. Medial pleural furrow on the anterior pygidial pleurae strongly incised. Medial and posterior pygidial pleural lappets triangular, short but prominently project beyond the pygidial border. Interpleural furrows sharply incised. Furrow anterior of the terminal axial piece of the pygidium triangular in shape.

Discussion .-- This is the first *Bufoceraurus* named from the Mifflin, and may be the first time this type of material has been documented from the area.

EUBUFOCERAURUS CETUS (Dean, 1979)

Plate 5, Figure 1

Ceraurus cetus DEAN, 1979, pp. 5-6, pl. 2, figs 1-5, 9, pl. 4, fig 10.

non *Bufoceraurus bispinosus* HESSIN, 1989, pp.1208-1213, pl. 2, figs 1-7.

Holotype .-- Incomplete cranidium GSC 38633.

Other Material .-- Paratype cranidium GSC 38634.

Occurrence .-- Lourdes Limestone Formation collected from Port au Port Peninsula, Newfoundland.

Diagnosis .-- Our diagnosis follows Dean's (1979) with the following additions: two posteriorly directed spines on the posterior border of the cephalon, lobate in shape, and large spine close to the attachment of the thorax to the cephalon and a small thorn-like spine positioned close to the genal spines; center of the eyes aligned with S3 of the glabella in dorsal view; lateral margins of the glabella expand outwards anteriorly at about 20º.

Genus CERAURUS Green 1832

Type Species .-- *Ceraurus pleurexanthemus* Green, 1832

Synonyms .-- *Leviceraurus* Hessin, 1988a, *Whittakerites* Ludvigsen, 1976, *Borealaspis* Ludvigsen, 1976, *Hapsiceraurus* Whittington, 1954, *Bufoceraurus* Hessin, 1989.

Other Taxa Included .-- *Ceraurus walcotti* sp. nov., *C. milleranus* Miller and Gurley, 1894 , *C. planatus* (Ludvigsen, 1976), *C. mackensiensis* Ludvigsen, 1979, *C. whittakerensis* (Ludvigsen, 1976), *C. biformis* (Ludvigsen, 1976), *C. plattinensis* Foerste, 1920, *C. proicens* Tripp, 1967, *C. simmonsi* Hussey, 1926, *C. savagei* Walter, 1924, *C. misneri* Foerste, 1909, *C. furca* sp. nov., *C. whittingtoni* Evitt, 1953, *C. mammiloides* Hessin, 1988a, *C. tuberosus* Troedsson, 1928, *C. kirchmeieri* sp. nov., *C. globulobatus* Bradley, 1930, *C. hispidus* (Whittington, 1954), *C. ruidus*

Cooper, 1953, *C. bispinosus* Raymond and Barton, 1913, *C. binodosus* Cooper and Kindle, 1936, *C. maewestoides* Ludvigsen 1979, *C. matranseris* Sinclair, 1947, *C. elginensis* Slocom, 1913, *C. paraplattinensis* sp. nov., *C. mifflinensis* DeMott, 1987, *C.*? *numitor* (Billings, 1866), *C. jenlorum* sp. nov., *C. napaneei* sp. nov., *C. hillieri* sp. nov., *C. wilsoni* sp. nov., *C. ottawaensis* sp. nov..

Diagnosis .-- The clade is highly variable, and therefore is diagnosed by the majority of the taxa sharing the following synapomorphies: semicircular cephalic outline; prominent paired nodes positioned close the eye and arranged roughly sagittal to each other; glabellar furrows constrained to the lateral margins of the glabella, deeply incised, and squared off; lateral margins of the middle body of the hypostome smooth with the middle body furrow effaced; pygidium with one prominent set of pygidial spines on the anterior pleurae and with the other pleural lappets strongly reduced or completely absent; triangular shaped furrow on the anterior of the terminal axial piece of the pygidium.

Discussion .-- Some of the genera subsumed into *Ceraurus* do form smaller groups within the genus, particularly *Leviceraurus* and *Borealaspis*. However, despite the morphological similarities of these species, the groups are not separate lineages and instead represent derived ceraurids (i.e. *Leviceraurus* is a *Ceraurus* with a subrectangular cephalic outline and unique thin spines, *Borealaspis* is a *Ceraurus* with prominent inflations on the anterior of the glabella, posterior glabellar spines, and slightly curved S3). Furthermore, due to the topology of the tree, acknowledging these taxa as unique genera would result in a polyphyletic *Ceraurus*, necessitating the creation of multiple monotypic genera. As such, we consider it taxonomically prudent to synonymize *Leviceraurus, Whittakerites*, and *Borealaspis* into *Ceraurus*.

CERAURUS PLUEREXANTHEMUS Green, 1832

Plate 5, Figure 2; Plate 6, Figures 1-4; Plate 7, Figures 1-5; Plate 8, Figures 1-3

Ceraurus pleurexanthemus GREEN, 1832, p. 84,5, fig. 10.

Ceraurus pleurexanthemus var. *monteyensis* EVITT, 1953, pp. 38-39, pl. 5, figs 9-12, pl. 6, figs 1-10, pl. 7, figs 3, 5-12, 21-28, pl. 8, figs 1-4, 8-16.

non *Ceraurus pleurexanthemus* RAYMOND AND BARTON, 1913, pp. 528-533, pl. 2, figs 1, 2, 7. EVITT 1953, pl. 7, figs. 1, 2, pl. 8, figs 5-7. BRETT *ET AL.*, 1999, p. 300, figs 8.3, 8.5, 8.7.

Holotype .-- A complete exoskeleton and a paratype exoskeleton NYSM 4203. Specimens currently missing, however photographs of the specimens were taken by Thomas Whitely (Whitely and Kloc 2002), and are included in this monograph.

Other Material .-- Topotype cranidia originally assigned to *Ceraurus pleurexanthemus monteyensis* collected from “Glens Falls” at Chazy Landing, Clinton County, New York KUMIP 325594-6, Incomplete exoskeleton and various cranidia from the Sugar River Formation at Watertown, Jefferson County, New York KUMIP 325587-93 and MCZ 120103.

Occurrence .-- Collected from the lower Trenton Formation around Newport, New York, as well as the “Glens Falls” at Chazy Landing, Clinton County, New York, and the Sugar River Formation at Watertown, Jefferson County, New York.

Diagnosis .-- Center of the eyes aligned with S2; cheeks smooth except for paired exsagittally arranged nodes close to the eyes; glabella strongly vaulted in lateral view, and sparsely covered in tubercles, with a set of three paired tubercles running up the sagittal line of the glabella’

glabellar furrows deeply incised, straight, and restricted to the lateral edges of the glabella; one faint node on the posterior cephalic border, positioned close to the eye; genal spines depart from the cephalon at an angle of approximately 20º and gently curve medially, staying close to the body; axial rings of the thorax smooth; pronounced pygidial border formed from a fusing of the medial and posterior pygidial pleurae; pygidial pleural spines gently curve medially until the distal tips point roughly directly posterior.

Description .-- Cephalic outline semicircular. Exoskeleton mostly smooth or covered in fine granules. Cheeks mostly smooth, but with a pair of exsagittally arranged nodes positioned close to the eyes. Center of the eyes aligned with S2. Large Eye Index 0.316. Glabella subrectangular in shape, lateral margins strongly expanding at an angle of 20º, strongly vaulted in lateral view, and sparsely covered in tubercles, with a set of three paired tubercles running up the sagittal line of the glabella. Glabellar furrows deeply incised, straight, and restricted to the lateral edges of the glabella. Anterior cephalic border broad and separated from the cheek by a deeply incised border furrow. Posterior cephalic border with one faint raised node positioned close to the eye. Lateral edges of the posterior cephalic border run transverse into the genal spines. Genal spines depart from the cephalon at an angle of approximately 20º and gently curve medially, staying close to the body.

11 thoracic segments. Axial rings of the thorax smooth, lacking any raised nodes.

Hypostome subtriangular in shape, roughly 1.3x longer than wide, with lateral edges sharply converging at an angle of 30º with the sagittal. Middle body covered in maculae, but lacks a prominent middle body furrow.

Pygidium semicircular in outline. Pronounced pygidial border formed from the fusing of the medial and posterior pygidial pleurae. Interpleural furrows strongly incised. Axial furrows

weakly incised. Posterior pygidial pleural spines depart from the pygidium at an angle of approximately 30º and gently curve until the distal tips of the spines point roughly posterior.

Discussion.-- The original type specimens of *Ceraurus pleurexanthemus,* when prepped out of the rock (Whitely and Kloc 2002), are immediately distinct from the Rust formation material coming from Trenton Falls (Walcott Rust Quarry). The eyes of the Walcott Rust Quarry specimens are positioned far forward and aligned with the L3, while the eyes of the types are further back and aligned with S2. The genal spines of the Walcott Rust Quarry specimens depart at an angle of approximately 45º and are nearly straight, while the genal spines of the types depart at an angle of approximately 20º and gently curve medially until the tips point inwards towards the specimen. The axial rings of the thorax of the Walcott Rust Quarry specimens have prominent pairs of raised nodes, while the axial rings of the types are smooth and do not have any prominent nodes. The pygidium of the type specimens has a pronounced border likely formed from the fusing of distal ends of the medial and posterior pleurae, while the Walcott Rust Quarry specimens do not have this pronounced border, with the pleurae sharply terminating at the end of the pygidium. Finally, the pygidial pleural spines of the Walcott Rust Quarry specimens are barely curved and splay outwards, while the pygidial pleural spines of the type specimens gently curve medially until the distal tips point roughly directly posterior. Because of these differences, we conclude that the Walcott Rust Quarry ceraurids are not the same as the type specimens of *Ceraurus pleurexanthemus,* and therefore should be treated as a new species, described below as *C. walcotti*.

When Raymond and Barton (1913) set out to redescribe *C. pleurexanthemus,* they logically decided to utilize the copious ceraurid collections of the MCZ from the Rust Formation at Trenton Falls. Since the original type specimen was poorly prepped out, they cannot be faulted

for assuming that the Trenton Falls material was roughly comparable to Green's original types because, at the time, the type specimen was effectively useless. However, Trenton Falls was not an ideal place to look for equivalent material to Green's specimens, since the trilobites in the quarry are from the Rust Formation. Around Newport (the proposed topotype location for Green's original material), there are no exposed beds of the Rust Formation, which is higher stratigraphically in the Trenton, but there are exposures of the lower Trenton up to and including the Sugar River Formation (Brett *et al.* 1999, Brett and Baird 2002). Therefore, we concluded that the lower Trenton would be a better place look for an equivalent to the type.

A subspecies, *C. pleurexanthemus monteyensis*, was named by Evitt (1953) from the lower Trenton, specifically the "Glens Falls", a unit of undifferentiated Trenton that includes beds equivalent to the Sugar River Formation (Brett and Baird 2002). We have collected topotype material of *C. pleurexanthemus monteyensis*, as well as new material from the Sugar River Formation at Watertown, New York, that is morphologically equivalent to the topotype material. When comparing these specimens to the original types of *C. pleurexanthemus*, the two species are shown to be equivalent. Specifically, all of the characteristics that separate the type of *C. pleurexanthemus* from the Walcott Rust Quarry material are shared with *C. pleurexanthemus monteyensis*. Therefore, we propose that the two species are the same and synonymize *C. pleurexanthemus monteyensis* into *C. pleurexanthemus.*

It is interesting to note that one of the specimens collected from the topotype locality of *C. pleurexanthemus monteyensis* (Pl. 7, Fig. 3) exhibits a second raised nodes on the posterior border of the cephalon positioned close to the genal spine. No other specimens collected from the locality exhibit this second raised node. Either this character represents variability within the species *C. pleurexanthemus*, or there may be two different species from this locality.

CERAURUS WALCOTTI, n. sp.

Plate 9, Figure 1; Plate 10, Figures 1-2; Plate 11, Figures 1-3

Ceraurus pleurexanthemus RAYMOND AND BARTON, 1913, pp. 528-533, pl. 2, figs 1, 2, 7. EVITT, 1953, pl. 7, figs. 1, 2, pl. 8, figs 5-7. BRETT *ET AL.*, 1999, p. 300, figs 8.3, 8.5, 8.7.

Etymology .-- This species is named after Charles Walcott, as well as the type locality (Walcott Rust Quarry) from which the specimen occurs.

Holotype .-- A complete exoskeleton MCZ 111708.

Other Material .-- Assorted exoskeletons and cranidia from the Walcott Rust quarry including MCZ 185368, 186008, 185979, 185978, 185970, 185961, 111119, 186061, 134301 and YPM 6571, 183913,6571, 183961-2,183901-3.

Occurrence .-- Collected from the Rust Formation at Trenton Falls (Walcott Rust Quarry) and Grondines member of the Neuville Formation at Neuville, Quebec.

Diagnosis .-- A *Ceraurus* species with the following characters: center of the eyes aligned with L3; cheeks smooth except for paired exsagittally arranged nodes close to the eyes; glabella strongly vaulted in lateral view, and sparsely covered in tubercles, with a set of three paired tubercles running up the sagittal line of the glabella; glabellar furrows deeply incised, straight, and restricted to the lateral edges of the glabella; one prominent node on the posterior cephalic border, positioned close to the eye; genal spines depart from the cephalon at an angle of approximately 45º and are nearly straight; prominent paired nodes on the axial rings of the

thorax; pygidial pleural spines nearly straight and splay outwards with the distal tips pointing dramatically abaxial.

Description .-- See Raymond and Barton's (1913) description of *Ceraurus pleurexanthemus*.

Discussion.-- For the reasons cited above in the redescription and discussion of *C. pleurexanthemus*, the Walcott Rust Quarry material originally assigned to *C. pleurexanthemus* is removed from said species and considered to be its own unique taxon, *C. walcotti*. Furthermore, *Ceraurus* material collected from the Grondines member of the Neuville Formation near Neuville, Quebec that was originally designated as *C.* cf. *pleurexanthemus* exhibits all of the diagnostic characters of *C. walcotti* and therefore we reclassify this material as *C. walcotti*.

CERAURUS MACKENSIENSIS Ludvigsen, 1979

Ceraurus cf. *pleurexanthemus* TROEDSSON, 1928, p. 68, pl. 16. fig 22. (not figs 20, 21)

Ceraurus mackensiensis LUDVIGSEN, 1979, pp. 34-36, pl. 15, figs 1-44

Holotype .-- Incomplete cranidium GSC 44156.

Occurrence .-- Lower Whittaker Formation, Funeral Range and Whittaker Range.

Diagnosis .-- Our diagnosis follows Ludvigsen (1979) with the following modification: center of the eye aligned with L2.

CERAURUS PLANATUS (Ludvigsen, 1976)

Whittakerites planatus LUDVIGSEN, 1976, pp. 950-953, pl. 1, figs 1-14. LUDVIGSEN 1979, p. 38, pl. 16, figs 1-47.

Holotype .-- Incomplete cranidium GSC 44191.

Occurrence .-- Collected from the Lower Whittaker Formation, Whittaker and Dusky Range.

Diagnosis .-- See Ludvigsen (1976).

Discussion.-- *C. planatus* does possess a few autapomorphies when compared to other ceraurids, particularly the strongly convex anterior border of the glabella (the structure of the pygidium is not considered to be autapomorphous because it is the result of the expression of two phylogenetic characters, a subtrapezoidal pygidial outline and the fusion of pleural lappets into a pronounced pygidial border). Since the genus *Whittakerites* was only known from one species, it is possible that the inability to code these autapomorphic characteristics into the analysis could have resulted in the group plotting out more basal than it should. However, since all phylogenetic analyses, like taxonomy, are working hypotheses, we accept the genus's synonymy within *Ceraurus* and acknowledge that new material may change this assignment.

CERAURUS WHITTAKERENSIS (Ludvigsen, 1976)

"Ceraurus" cf. *numitor* LUDVIGSEN, 1975, pl. 5, fig. 11.

Borealaspis whittakerensis LUDVIGSEN, 1976, 34-36, pl. 15, figs 1-44. LUDVIGSEN, 1979, p. 39, pl. 17, figs 1-12.

Holotype .-- Incomplete cranidium GSC 40450

Occurrence .-- Collected from the Lower Whittaker Formation, Funeral Range.

Diagnosis .-- See Ludvigsen (1976)

Discussion.-- While the glabellae of *C. whittakerensis* and *C. biformis* are slightly more circular in outline than most ceraurids, they are not as bulbously rounded as *C*?. *numitor*. Coupled with the presence of paired exsagittally arranged nodes on the cheek close to the eyes (a uniquely ceraurid character), and a ceraurid-like pygidium, we feel relatively confident in the synonym of these two species into *Ceraurus*.

CERAURUS BIFORMIS (Ludvigsen, 1976)

Ceraurus bituberculatus TROEDSSON, 1928, p. 69, pl. 17, fig 11

Borealaspis biformis LUDVIGSEN, 1976, p. 957, pl. 2, figs 8-18. LUDVIGSEN, 1979, p. 39, pl. 17, figs 13-33.

Holotype .-- Incomplete cranidium GSC 44230

Occurrence .-- Collected from the Lower Whittaker Formation, Funeral, Whittaker, and Dusky Range.

Diagnosis .-- See Ludvigsen (1976).

CERAURUS HISPIDUS (Whittington, 1954)

Hapsiceraurus hispidus WHITTINGTON, 1954, p. 125, pl. 59, figs 1-7, pl. 60, fig 19.

Holotype .-- Incomplete exoskeleton USNM 28169a.

Occurrence .-- Upper Ordovician of Sillman's Fossil Mount, Baffin Island.

Diagnosis .-- See Whittington (1954).

Discussion.-- The genus *Hapsiceraurus* is synonymized into *Ceraurus*, based on the monotypic species (*Hapsiceraurus hispidus*) plotting derived within the genus. This synonymy is in agreement with Lespérance and Desbiens' (1995) original assessment of the genus and thus represents an excellent example of phylogeny reinforcing and testing systematic hypotheses.

CERAURUS PLATTINENSIS Foerste, 1920

Plate 12, Figures 1-6; Plate 13, Figures 1-3; Plate 14, Figures 1-4; Plate 15, Figures 1-4

Ceraurus plattinensis FOERSTE, 1920, p. 217, pl. 21, figs 20A, 20B, pl. 23, figs 3a, 3b. DEMOTT, 1963, p. 144, pl. 9, figs 17-24, pl. 10, figs 8-10. DEMOTT, 1987, p. 77, pl. 9, figs 17-24, pl. 10, figs 8-10.

non *Ceraurus plattinensis* HESSIN, 1988b, figs 1A-1D. HESSIN, 1989, pp. 1213-1217, pl.3 fig 1-7

Holotype .-- Incomplete exoskeleton USNM 78441.

Other Material .-- One nearly complete exoskeleton missing the pygidium KUMIP 325602, and multiple assorted cephala, hypostomes, and pygidia KUMIP 325597-601, 325603-10.

Occurrence .-- Collected from Plattin Limestone from New London, Ralls County, Missouri, and Decorah group

Diagnosis .-- Cephalic outline semicircular; exoskeleton covered in fine granules; glabella covered in tubercles that are sparsely spaced on the posterior of the glabella and densely packed on the anterior border of the glabella; center of the eye aligned with L2; posterior cephalic border smooth, with one very faint node positioned close to the eyes; lateral edge of the posterior cephalic border gently expands posteriorly forming a convex bulge; axial rings of the thorax lack raised nodes; pygidium subtrapezoidal in outline; furrow on the anterior of the terminal axial piece triangular in shape.

Description .-- Cephalic outline semicircular. Exoskeleton covered in fine granules. Glabella covered in tubercles that are sparsely spaced on the posterior of the glabella and densely packed on the anterior border of the glabella. Cheeks mostly smooth or covered in granules. Small exsagittally positioned tubercles on the cheek positioned close to the eye. Center of the eye aligned with L2. Glabella subrectangular in shape, anterior border gently curved, low relief in lateral view, and lateral margins very gently expand at an angle of approximately 5-10º. Glabellar furrows deeply incised, straight, and restricted to the lateral margins of the glabella. Posterior cephalic border smooth, with one very faint node positioned close to the eyes. Lateral edge of the posterior cephalic border gently expands posteriorly forming a convex bulge. Genal spines depart from the cephalon at approximately 40º, broad in shape, and dramatically curve medially until the distal end of the spine points posteriorly. Occipital ring vaulted in lateral view, raised higher than the thoracic axial rings.

11 thoracic segments. Axial rings of the thorax smooth, lacking any distinct raised nodes. Lobes associated with the thoracic pleural furrows barely inflated.

Hypostome subtriangular in shape, 1.2x longer than wide, and lateral edges of the structure converge at a shallow angle of 20º with the sagittal. Middle body covered in maculae, and lacks a prominently defined middle body furrow.

Pygidium subtrapezoidal in outline with three prominent pygidial segments and a strongly reduced terminal axial piece. Anterior pygidial pleural spines depart from the glabella at an angle of approximately 30º with the sagittal, triangular in shape, and strongly curve medially until the distal ends of the spines point roughly posterior. Axial furrows weakly incised. Interpleural furrows strongly incised. Medial and posterior pleurae do not form distinct lappets. Furrow on the anterior of the terminal axial piece triangular in shape.

Discussion.-- DeMott (1987) suggested that the holotype for *C. plattinensis* was lost, however comparisons of museum specimens with Foerste's (1920) original figures shows that the specimen is presently housed in the Smithsonian collections. Hessin (1989) defined material from Brechin, Ontario as plesiotypes of *C. plattinensis.* While the material from Ontario does share some of the characteristics found in *C. plattinensis* from the Decorah Formation of the Midwestern United States (most noticeably the position of the eyes, the broadly curved genal spines, and the small posteriorly directed lobe on the lateral edge of the posterior cephalic border), it differs from the Midwestern material in the expansion of the lateral margins of the glabella, the nature of the glabellar furrows, the nodes on the posterior border of the cephalon and the axial rings of the thorax, and the pygidial pleural lappets. These differences are discussed in more depth below. Comparing Hessin's material to our newly collected material from the Decorah group (particularly material from New London, Ralls County the topotype locality), we reject Hessin's plesiotypes and instead treat his material as a new species, *C. paraplattinensis*, described below.

It is interesting to note that one of the most iconic characteristics of the species, the small posteriorly directed lobe on the lateral edges of the posterior cephalic border, is continuously variable in its expression within the species, with some specimens in a population exhibiting a strongly pronounced lobe while others barely expressing it all, instead possessing only a faint convex bulge proximal to the genal spines. A similar variability is also seen in the *C. paraplattinensis* material from Ontario, which is to be expected considering that the two species have a close evolutionary relationship. It is also interesting to note that, while large holaspid pygidia of *C. plattinensis* do not exhibit distinct pygidial lappets on the medial and anterior pleurae, a few of the very small pygidia do form distinct lappets. The expression of the lappets into large holaspid specimens in *C. paraplattinensis* may then be due to pedomorphosis.

CERAURUS PARAPLATTINENSIS sp. nov.

Plate 16, Figures 1-2; Plate 17, Figures 1-2; Plate 18, Figure 1; Plate 40, Figure 1

Ceraurus plattinensis HESSIN, 1988b, figs 1A-1D. HESSIN, 1989, pp. 1213-1217, pl.3 fig 1-7

Etymology .-- The name is chosen to designate that this species is morphologically similar to *C. plattinensis*.

Holotype .-- Nearly complete specimen ROM 48775.

Other Material .-- Hessin's original material including two nearly complete exoskeletons ROM 46071, 46073 and a pygidium ROM 46072.

Occurrence .-- Collected from the Bobcaygeon Formation at Brechin, Ontario.

Diagnosis .-- Similar to *Ceraurus plattinensis*, but with the following distinctions: glabella dramatically expands anteriorly, with the lateral margins forming roughly a 20º angle with the sagittal line; glabellar furrows deeply incised, straight, and prominently cut into the glabella nearly half the distance to the sagittal line; one prominent node on the posterior border of the cephalon positioned close to the eye; paired nodes on the axial ring of the thorax; pygidial pleural spines depart from the pygidium at a wide angle, approximately 50º; medial and posterior pygidial pleurae have prominent, subtriangular lappets.

Description .-- See Hessin's (1989) description of *C. plattinensis*.

Discussion.-- Hessin's material is treated as a new species based on the fact that it differs from *C. plattinensis* in six distinct characteristics detailed above in the diagnosis.

CERAURUS MAEWESTOIDES Ludvigsen, 1979

Ceraurus maewestoides LUDVIGSEN, 1979, p. 36, pl. 13, figs 30-33.

Holotype .-- Incomplete cranidium GSC 44142

Occurrence .-- Lower Whittaker Formation, Dusky Range.

Diagnosis .-- See Ludvigsen (1979).

Discussion.-- This species exhibits two interesting characteristics. It shares the large inflations on the anterior lobe of the glabella found in *Ceraurus maewestoides* Ludvigsen, 1979, *C. biformis* (Ludvigsen, 1976), *C. whittakerensis* (Ludvigsen, 1976), *C. binodosus* Cooper and Kindle, 1936, and *C. bispinosus* Raymond and Barton, 1913. Also, the sculpture of the glabella is finely granulose with two prominently defined set of tubercles running up the glabella, similar to the

glabellar sculpture found in *C. mammiloides* Hessin, 1988a and *C. furca* sp. nov. Because *C. maewestoides* represents a conglomeration of seemingly synapomorphic characters, it implies that either these two groups of taxa have similar affinities, or that at least one of these characteristics evolved multiple times. More complete specimens of *C. maewestoides* are necessary to tease apart the phylogenetic placement of the species relative to *C. biformis-C. whittakerensis* and *C. mammiloides-C. furca.*

CERAURUS BINODOSUS Cooper and Kindle, 1936

Ceraurus binodosus COOPER AND KINDLE, 1936, 369, pl. 53, fig 20.

Holotype .-- Incomplete cranidium USNM 91799.

Occurrence .--Whitehead Formation of Percé, Quebec.

Diagnosis .-- See Cooper and Kindle (1936).

Discussion.-- The type specimen is an incomplete glabella, however it is similar enough to other ceraurid glabella to classify it as a *Ceraurus* species. Despite the poor preservation, the species exhibits one interesting characteristic: the paired inflations on the anterior of the glabella also found in *Ceraurus maewestoides* Ludvigsen, 1979, *C. biformis* (Ludvigsen, 1976), *C. whittakerensis* (Ludvigsen, 1976), and *C. bispinosus* Raymond and Barton, 1913. The species is closest in appearance to *C. bispinosus*, but more complete specimens need to be collected in order to determine if these two species are closely related.

CERAURUS BISPINOSUS Raymond and Barton, 1913

Plate 19, Figures 1-2

Ceraurus bispinosus RAYMOND AND BARTON, 1913, p. 536, pl. 1, figs 3-4.

WILSON, 1947, p. 49, pl. 9, fig 1. LUDVIGSEN, 1978, pl. 3, fig 26.

non *Bufoceraurus bispinosus*, HESSIN, 1989, pp.1208-1213, pl. 2, figs 1-7.

Holotype .-- Fragmentary cranidium ROM 18682.

Occurrence .--Leray? beds in Tetreauville, Quebec.

Diagnosis .-- Our diagnosis follows Raymond and Barton (1913), with the following modifications: exoskeleton covered in small tubercles, with larger, randomly arranged tubercles/pustules on the glabella; glabella subrectangular, with at least one inflation on the anterior lobe (and an effaced mark that implies a second inflation); glabellar furrows deeply incised, straight, and constrained to the lateral margins; a small portion of the occipital ridge preserved in the specimen suggests the center of the eye aligned with S2.

Discussion.-- As discussed above, *C. bispinosus* is separated from *Eubufoceraurus* and treated as a unique taxon. Also as discussed above, it shares similarities with *C. binodosus*, although more complete specimens of both are necessary before the evolutionary relationships of these taxa can be assessed.

CERAURUS MATRANSERIS Sinclair, 1947

Plate 19, Figures 3-6; Plate 20, Figure 1

Ceraurus matranseris SINCLAIR, 1947, p. 254, pl. 1, figs 3-6. DESBIENS AND LESPÉRANCE, 1989, p.1191, fig 2M, 2N. LESPÉRANCE AND DESBIENS, 1995, p. 13, figs 4.1-4.13.

Holotype .-- Small holotype cranidium GSC 110333.

Occurrence .--Collected in the Shipshaw Formation 1 mile north of Roberval, Lac Sain-Jean, Quebec and the Lindsay Formation near Picton, Ontario.

Diagnosis .-- Our diagnosis follows Lespérance and Desbiens (1995) with the following modifications; center of the eye aligned with L3; pair of prominently enlarged nodes on the posterior border positioned between the eye and glabella, and one enlarged node positioned close to the genal spines; genal spines broad proximal to the cephalon and taper into a triangular shape distally, curved strongly medially so distal points of the spine tend to point inwards towards the animal; hypostome lacks a prominent middle body furrow; interpleural furrows of the pygidium strongly incised.

Description .-- See Lespérance and Desbiens (1995).

Discussion.-- The position of the eye in Sinclair's holotype specimen is positioned further back on the cephalon (aligned with L2) than all other topotype and paratype *C. matranseris* material. Since the holotype specimen is an exceptionally small cranidium, and since the holotype only differs in the position of the eyes, it is highly probable that the specimen is not a holaspid specimen and instead may be meraspid stage. As such, eye position in the species may start further back and move forward when the species becomes an adult.

CERAURUS GLOBULOBATUS Bradley, 1930

Plate 20, Figures 2-4

Ceraurus globulobatus BRADLEY, 1930, p. 274, pl. 30, figs 33-36, 39-42.

Ceraurus globulobatus LESPÉRANCE AND DESBIENS, 1995, p. 13, figs 4.14-4.23.

non *Ceraurus* cf. *globulobatus* HESSIN, 1989, p. 1217, pl. 4, figs 1-7.

Holotype .-- Internal mold of incomplete cranidium UC 20709

Other Material .-- Internal molds of incomplete cranidia and pygidia, UC 29103,28956, 20709B, 20719A, 20696, 20695C, 20695B, and internal molds of incomplete cranidia KUMIP 325663-5.

Occurrence .-- Collected from the Kimmswick Formation at Glen Park, Missouri.

Diagnosis .-- Our diagnosis follows Lespérance and Desbiens (1995) with the following additions: eye (when visible) aligned with S2; lateral margins of the glabella gently expand at an angle of approximately 5-10º; glabella subrectangular in shape, very gently vaulted in lateral view, and covered in randomly arranged tubercles; genal spines thin, depart from the glabella at an angle of approximately 20º, and nearly straight; posterior cephalic border with one prominent raised node positioned close to the eye and one prominent raised node positioned close to the genal spines; prominent pygidial border likely formed from the fusing of pygidial pleural lappets.

Discussion.-- *C. globulobatus* is known exclusively from the Kimmswick, a sparry limestone that is particularly harsh on the fossils. As such, the majority of the specimens of *C. globulobatus* are broken and slightly eroded internal molds, making comparisons with other ceraurid material difficult.

CERAURUS CF. GLOBULOBATUS Bradley, 1930

Plate 21, Figure 1; Plate 22, Figures 1-3

Ceraurus cf. *globulobatus* HESSIN, 1989, p. 1217, pl. 4, figs 1-7.

Other Material .-- Nearly complete exoskeleton ROM 46075, three complete exoskeletons ROM 48566, complete specimen GSC 13713.

Occurrence .-- Collected from the Bobcaygeon Formation at Brechin, Ontario.

Discussion.-- Hessin's (1989) material is very similar morphologically to *C. globulobatus* but differs in the following characteristics: lateral margins of the glabella strongly expand at an angle of approximately 20º; posterior border of the cephalon has one very faint node positioned close to the eyes and one very faint node positioned close to the genal spines. Lespérance and Desbiens (1995) also suggested that the prominence of the eye in Hessin's *C.* cf. *globulobatus* material was another distinguishing characteristic separating the two taxa, however we are wary of the real importance of this character given that the absence of the eye ridge in the Kimmswick material of *C. globulobatus* is likely due to taphonomic processes. In the phylogeny, the two taxa plot out as sisters and differ in one phylogenetic character (the expansion of the lateral margins of the glabella). Due to the incompleteness of the *C. globulobatus* material, it is impossible to determine if *C.* cf. *globulobatus* is synonymous with *C. globulobatus* or represents a unique sister taxon. Therefore, we concur with Hessin's original designation and refer to the Ontario material as *C.* cf. *globulobatus*.

CERAURUS RUIDUS Cooper, 1953

Plate 22, Figures 4-5

Ceraurus ruidus COOPER, 1953, p. 27, pl. 11, figs 1, 2, 4, 12, 15, pl. 12, fig 6.

Ceraurus breviceps COOPER, 1953, p. 28, pl. 11, figs 8, 10, 11, 13.

Ceraurus convexus COOPER, 1953, p. 28, pl. 11, fig 3.

Ceraurus trapezoidalis ESKER, 1964, p. 201, pl. 2, figs 1-4.

Holotype .-- Nearly complete cranidia USNM 111783.

Occurrence .-- Type locality from the Edinburg Formation, 1.5 miles north of Strasburg, Shenandoah County, Virginia. Also found in Edinburg Formation 4 miles east of Catawba Sanitorium, Roanoke County, Virginia, as well as the Bromide Formation in Carter County, Oklahoma (following Shaw's (1974) synonymy).

Diagnosis .-- Our diagnosis follows Cooper (1953) with the following additions: glabella and cheeks densely covered in tubercles, while the rest of the exoskeleton covered in granules or small tubercles; central position of the eye aligned with S2; genal spines thin, long, and curve medially until the distal end of the spine roughly points posteriorly; interpleural furrows and axial furrows of the pygidium strongly incised; furrow anterior of the terminal axial piece of the pygidium triangular in shape.

Discussion.-- Shaw's synonymy of *Ceraurus ruidus* with Cooper's other Virginia species (*C. convexus* and *C. breviceps*) is considered to be well founded, as the differences between the species are likely due to differences in preservation. The synonymy of *C. ruidus* with *C. trapezoidalis* is more tentatively accepted. No obvious characteristics separate the two species, however it should be noted that Cooper's *C. ruidus* material is not as complete as Esker's *C.*

trapezoidalis material, lacking free cheeks or thoracic characters. For the time we accept Shaw's synonymy of the two species, however we acknowledge that new material from the Edinburg Formation of Virginia needs to be collected to confirm this synonymy.

CERAURUS MIFFLINENSIS (DeMott, 1987)

Plate 23, Figures 1-2, 4-6; Plate 24, Figures 1-5; Plate 25, Figures 1-3

Ceraurus mifflinensis DEMOTT, 1963, p. 137, pl. p, figs 8-15, pl. 10, figs 4-7.

Gabriceraurus mifflinensis DEMOTT, 1987, p. 78, pl. 9, figs 8-16, pl. 10, figs 4-7.

Holotype .-- Incomplete cranidium MCZ 8994

Other Material .-- Assorted cranidia, pygidia, thorax and hypostomes KUMIP 325619-20, 325622-33.

Occurrence .-- Collected from the Mifflin Member of the Plattville Group collected near Fennimore, Wisconsin.

Diagnosis.-- Center of the eyes aligned with L2; glabella subrectangular, low vertical relief in ventral view, lateral margins gently expand at approximately 10º, anterior border gently convex, and surface covered in randomly arranged low relief tubercles; glabellar furrows short, deeply incised, and constrained to the lateral edges of the glabella; cheeks mostly smooth, with scattered small tubercles/granules; paired prominent exsagittally arranged nodes close to the eye; posterior border of the cephalon with one prominently raised node positioned close to the eye and a line of faint tubercles positioned close to the genal spine; genal spines depart from the cephalon at approximately 45º and covered in sparsely spaced and faint tubercles; axial ring of the thorax has

prominent paired nodes that are raised to a spine-like point; nodes along the thoracic pleural furrows also raised into pointed spines; semicircular pygidial outline; pygidial axial furrow weakly incised; furrow anterior of the terminal axial piece of the pygidium strongly triangular in shape.

Discussion.-- *Ceraurus mifflinensis* is removed from *Gabriceraurus* and placed into *Ceraurus* based on the presence of paired exsagittally arranged nodes next to the eye and the triangular shaped furrow anterior of the terminal axial piece of the pygidium, as well as the fact that the characteristics used to place the species in *Gabriceraurus* (eyes aligned with L2, cephalic outline subrectangular) have been shown to be plesiomorphic,

DeMott's (1987) original material is broken and weathered and the type specimen lacks potentially informative characteristics of the cheeks, posterior cephalic border, and the genae. However, our new material collected from the Mifflin of Wisconsin allows for a more complete understanding of the species. Many of the specimens collected show strong morphological similarities with DeMott's (1987) original type specimen. However, a large proportion of specimens collected (and one of Demott's specimens MCZ 8996) exhibit consistently different suits of morphological characters from the type of *C. mifflinensis*, so we conclude that that there is significant evidence that two *Ceraurus* species occur in the Mifflin. The presence of two different species within the Mifflin presents a potential problem assigning hypostoma and pygidia to *C.* mifflinensis, given that the type of *C. mifflinensis* is an isolated cranidium. Thankfully two complete specimens have been collected of this second species (described below) which demonstrate that this second species has a hypostome and pygidium that are distinctly unique from the *C. mifflinensis* material described by DeMott (1987). Therefore, we

accept that the pygidium (MCZ 9003) and hypostome (MCZ 9004) figured in DeMott (1987) are correctly assigned to *C. mifflinensis*.

CERAURUS JENLORUM sp. nov.

Plate 23, Figure 3; Plate 26, Figures 1-2; Plate 27, Figures 1-4; Plate 28, Figures 1-4

Etymology .-- This species is named after Jennifer and Lori Scheer.

Holotype .-- Complete specimen KUMIP 325634. Paratype complete specimen KUMIP 325635.

Other Material .-- Assorted cranidia, pygidia, and hypostomes KUMIP 325621, 325636-42.

Occurrence .-- Collected from the Mifflin Member of the Plattville Group collected near Fennimore, Wisconsin.

Diagnosis.-- Two raised nodes on the posterior border positioned between the eye and occipital ring; eyes aligned with S2; exoskeleton covered in large granules, while the cheeks have prominent and densely packed tubercles; glabella nearly parallel sided and densely covered in large, randomly arranged tubercles; genal spines depart from the cephalon at approximately 45 degree angle and strongly curve medially until they point nearly transversely into the organism's thorax; hypostome has a pair of small triangular shaped projections on the posterior border; prominent paired nodes on the rings of the thoracic segments; pygidium subtrapezoidal in outline and with a strongly pronounced pygidial border formed from the fusing of the medial and posterior-most pygidial pleurae; pygidial axial furrow strongly incised to the point where the medial pygidial pleurae is nearly pinched out at the base; pygidial furrow separating the axial rings from the terminal axial piece very weakly triangular (forms a strongly obtuse angle).

Description.--Exoskeleton mostly covered in dense, large granules. Cephalon semicircular in outline with genal spines that depart from the cephalon at an angle of ~45º, are broad at the base, have lines of gently raised tubercles running down the length, and strongly curve medially to the point where the tips are nearly pointing directly into the thorax. Cheeks gently vaulted and densely covered in large tubercles. Two larger exsagittally arranged nodes positioned close to the eyes on the cheeks are barely discernible from the densely packed tubercles. Glabella subrectangular in shape, with very gently expanding lateral margins, nearly straight anterior border, low vertical relief, and densely covered in randomly arranged tubercles. L1, L2, and L3 roughly equal in length, short, straight, strongly incised, squared off at the ends, and gently penetrate the sagittal line of the glabella. Eyes aligned with S2 and spread far apart from the glabella, close to the anterior border. Large Eye Index 0.3-0.35. Anterior border of the cephalon broad and separated from the cheeks by a strongly incised furrow. Posterior border of the cephalon has two faintly raised nodes positioned close to the occipital ring and one large node near the genal spines (often associated with a line of tubercles).

Hypostome subtriangular in outline and covered in dense granulation. Middle body oval in shape, lacking any noticeable middle body furrow. Two small, triangular spine-like structures protrude from the posterior border of the hypostome.

Thorax consists of 11 segments. Axial rings have two prominent, nearly spine-like paired nodes. Three nodes are prominent on the thoracic pleurae (all associated with the exsagittally arranged pleural furrow), with the lateral-most node being raised far more prominently than the medial and proximal nodes.

Pygidium subtrapezoidal in outline with three prominent pygidial segments and a strongly reduced terminal axial piece. One large set of pygidial spines derived from the anterior-

most pygidial pleurae. Medial and posterior-most pleurae flatted into lappets and fuse together, forming a pronounced pygidial border. Interpleural furrows weakly incised. Axial furrow sharply incised, nearly pinching the medial pleurae out at the base. Intrapleural furrow on the pygidial spine weakly incised. Pygidial spines triangular in shape and depart from the pygidium at an angle of roughly 40º, strongly curving medially until the distal points of the spines adaxial. Furrow separating the terminal axial piece from the axis triangular in shape, with a strongly obtuse angle. DeMott (1987) illustrates this hypostomes (Plate 10, Fig. 17-19) and incorrectly assigns it to *Ceraurinella scofieldi*. However, the hypostome of *Ceraurus jenlorum* is easily distinguishable from the hypostome of *Ceraurinella scofieldi* in that *Ceraurus jenlorum* lacks the faintly incised middle body furrow that is found in all *Ceraurinella* hypostomes.

Discussion.-- This species is easily differentiated from *Ceraurus mifflinensis* with the following characteristics: center of the eyes aligned with S2; two gently raised nodes on the posterior border of the cephalon positioned close to the eyes and lacks a line of tubercles running close to the genal spines; genal spines very long and depart from the cephalon at a wide angle (approximately 55º), strongly curved medially until the distal ends of the spines point nearly transversely into the thorax; cheeks densely covered in small but prominent tubercles; hypostome has two small triangular protrusions on the posterior border axial border of the hypostome; pygidium subtrapezoidal in outline; axial furrows of the pygidium strongly incise, nearly pinching out the medial pygidial pleurae at the base; medial and posterior-most pygidial pleurae flatten to form lappets and fuse together forming a pronounced pygidial border.

The hypostome of *C. jenlorum* is particularly interesting when compared to other species of the genus *Ceraurus*. While the general outline of the hypostome is very similar in shape (subtriangular) to a standard *Ceraurus* hypostome, the small triangular barbs on the posterior

border of *C. jenlorum* are unique and vaguely resemble the barbs found in more distantly related cheirurids, like species assigned to *Ceraurinella*. Therefore, it is likely that these barbs either represent a re-evolution of more plesiomorphic characteristic, or a deep seeded parallelism.

CERAURUS ELGINENSIS Slocom, 1913

Ceraurus elginensis SLOCOM, 1913, p. 73, pl. 17, figs 4, 5. SLOCOM, 1916, p. 224, pl. 18, figs 4, 5. WALTER, 1924, p. 245, pl. 19, figs 10.

Holotype .-- Two incomplete cranidia FMNH 16630.

Occurrence .-- Collected from the Elgin member of the Maquoketa Formation, near Bloomfield, Iowa and also Clermont, Iowa.

Diagnosis .-- See Walter (1924).

Discussion.-- We agree with Walter's (1924) opinion that the possession of two to three tubercles positioned close to or on the base of the genal spine is a unique characteristic among ceraurids. In fact, the only ceraurid specimens that have a similar characteristic are the specimens Slocom (1913) originally designated as *C. milleranus* from (see a discussion of this material below) and *C. mifflinensis*.

CERAURUS CF. ELGINENSIS Slocom, 1913

Plate 29, Figures 1-6; Plate 30, Figures 1-3

Ceraurus milleranus SLOCOM, 1913, p. 71, pl. 17 figs 1-3.

Material .-- Partial cranidia FMNH 16853, 17056 and upside down pygidium FMNH 16958 as well as assorted cranidia KUMIP325643-51.

Occurrence .-- Clermont Member of the lower Maquoketa Formation near Clermont, Iowa.

Discussion.-- Slocom (1913) originally designated this material as *C. milleranus*. The material does share some similarities with the type specimen of *C. milleranus*, particularly the position of the eyes relative to the glabella (aligned with S2) and the tubercated glabella and cheeks. However, these characteristics are not diagnostic as they are also shared by *C. elginensis*, which is distinctly different from the Cincinnati *C. milleranus* material. Closer examination of the Clermont material reveals that it shares more characteristics in common with *C. elginensis*, than *C. milleranus*. The posterior border of the cephalon of the Clermont material has two paired raised nodes positioned close to the eyes, with two to three tubercles close to the base of the genal spines, which is also observed in *C. elginensis* but not observed in *C. milleranus*. Also, the ornamentation of the Clermont material is more similar to *C. elginensis* in that the tubercles are large, rounded, and have a large degree of vertical relief, whereas the tubercles of *C. milleranus* are smaller and less spine-like. In fact, except for the size (the Clermont material is always smaller than *C. elginensis*) the two species are nearly identical. Since the Elgin overlies the Clermont, it is possible that these two species have been distinguished more by stratigraphic position than by actual biological differences. However, at present there is insufficient material from both horizons to determine the morphological variability within these populations, and therefore we acknowledge that a definitive species definition cannot yet be made.

CERAURUS MILLERANUS Miller and Gurley, 1894

Plate 30, Figures 4-5

Ceraurus milleranus RAYMOND AND BARTON, 1913 p. 538, pl. 1, figs, 6-8.

CASTER *ET AL.*, 1955, pl. 3, fig. 28.

non *Ceraurus milleranus* SLOCOM, 1913, p. 71, pl. 17 figs 1-3.

Holotype .-- Complete specimen UC 6062.

Occurrence .-- Collected from the Richmond Group and Cincinnatian near Cincinnati Ohio, and Butler County, Ohio.

Diagnosis .-- Our diagnosis follows the observations and revisions from Raymond and Barton (1913) with the following additions: semicircular cephalic outline; glabella and the cheeks moderately covered in large, low relief tubercles; center of the eyes aligned with S2; lateral margins of the glabella gently expand anteriorly at an angle of approximately 10º; anterior border of the glabella rounded in dorsal view; posterior border of the cephalon has two paired nodes positioned close to the eye, with the lateral-most node strongly defined and the node closest to the glabella faint; genal spines depart from the cephalon at shallow angle (approximately 20º), short, and nearly straight; faint paired nodes on the axial rings of the thoracic segments; pygidial outline semicircular; pleural spines depart from the pygidium at approximately 30º and gently curve until the distal ends point roughly posterior; furrow anterior of the terminal axial piece triangular in shape.

Discussion.-- Subsequent authors (Slocom 1913, Ludvigsen 1979) have attempted to extend the geographic range of *C. milleranus* to other localities outside of the Cincinnati basin, and while these specimens may look similar to *C. milleranus* on a cursory level, detailed comparison with the original type specimen and other Cincinnati material reveals significant differences (as

discussed above and below). Therefore, we constrict the geographic range of *C. milleranus* to the Cincinnati basin and assign Slocom's material to *C.* cf. *elginensis* and Ludvigsen's material to *C.* cf. *milleranus*.

CERAURUS CF. MILLAERANUS Miller and Gurley, 1894

Ceraurus milleranus LUDVIGSEN, 1979, p. 36, pl. 15 figs 45-57.

Material .-- One cranidium GSC 44183, two hypostomes GSC 44184-5, two pygidia GSC 44186, 44188, and one free cheek GSC 44187.

Occurrence .--Lower Whittaker Formation, Dusky Range.

Discussion.-- Ludvigsen's (1979) *C. milleranus* material from the McKenzie Mountains shares many characteristics with specimens from Cincinnati, particularly the paired exsagittally arranged nodes next to the eye, the posteriorly directed genal spines, one prominent node on the posterior border of the cephalon, and randomly arranged tubercles on the glabella and cheeks. It differs from the Cincinnati material in the position of the eyes (which are further forward in the McKenzie Mountains material and aligned with S3), the dramatically expanding glabella (which expands at an angle of approximately 20^{o}), and the curvature of the pygidial pleural spines (which strongly bow outwards medially, while the Cincinnati material is faintly curved). Given the incomplete nature of the specimens, and since there is insufficient material at present to assess the variability of the McKenzie Mountains material, we find that these differences indicate that the assignment of the McKenzie Mountains species to *C. milleranus* is not definitive, hence the designation *C.* cf. *milleranus*.

CERAURUS WHITTINGTONI Evitt, 1953

Ceraurus pleurexanthemus WHITTINGTON, 1941, p. 498, pl. 72, figs 1-3, 9-40.

Ceraurus whittingtoni EVITT, 1953, p. 39, pl. 5 figs 13-16, pl. 6, figs 11-24, pl. 7, figs 3, 13-20, pl. 8, figs 17-25.

Holotype .-- Incomplete pygidium USNM 116692-a. Paratypes are disassociated silicified parts USNM 116692-b through z.

Occurrence .-- Collected from Middle Trentonian rocks four miles north-northeast of Spring hill, Augusta County, Virginia.

Diagnosis .-- A detailed description can be found in Whittington's (1941) description of *Ceraurus pleurexanthemus* and a refinement of this diagnosis, as well as a comparative analysis of *C. whittingtoni* with other ceraurid specimens, can be found in Evitt (1953).

Discussion.-- The other ceraurid trilobite described from Virginia is *Ceraurus ruidus*. *C. whittingtoni* is easily distinguished from *C. ruidus* with the following characteristics: the eyes of *C. whittingtoni* are positioned far forward on the glabella (with the center line of the eyes aligned with S3) while the eyes of *C. ruidus* are positioned further back; the cheeks of *C. ruidus* are densely covered in randomly arranged tubercles, while the cheek ornamentation of *C. whittingtoni* is sparse; exsagittally arranged prominent paired nodes/tubercles are positioned close to the eyes in *C. whittingtoni*, while these nodes are either not present in *C. ruidus* or are not significantly larger in size than the other tubercles that cover the cheeks.

CERAURUS MAMMILOIDES (Hessin, 1988a)

Leviceraurus mammiloides HESSIN, 1988a, p. 90, figs, 3.1-3.6, 4.1, 4.4 only.

non *Leviceraurus mammiloides* HESSIN, 1988a, p. 90, figs 4.2, 4.3 only.

Holotype .-- Incomplete exoskeleton ROM 45225.

Occurrence .-- Collected from the Cobourg Formation near Bowmanville and Colborne, Ontario.

Diagnosis .-- Our diagnosis follows Hessin's (1988a) original diagnosis for the genus *Leviceraurus* with the following additions: anterior border of the glabella straight to very gently convex in dorsal view; cephalic outline subrectangular; center of the eye aligns with S2; thin pygidial pleural spines depart from the pygidium at shallow angle of approximately 30º.

Description .-- See Hessin's (1988a) description of *Leviceraurus mammiloides*, excluding information from specimen ROM 45224.

Discussion.-- We agree with most of Hessin's (1988a) description of *C. mammiloides*. However, new material collected from the Cobourg Formation suggests that one of Hessin's specimens (ROM 45224) belongs to a different species described below.

CERAURUS FURCA, sp. nov.

Plate 31, Figures 1-2

Leviceraurus mammiloides HESSIN, 1988a, p. 90, figs 4.2, 4.3 only.

Etymology .-- This species is named after the Latin word for fork, referring to its unique tuning-fork shaped pygidial spines.

Holotype .-- Complete specimen KUMIP 325617

Other Material .-- Nearly complete exoskeleton ROM 45224, complete exoskeleton ROM 45128.

Occurrence .-- Collected in Cobourg Formation near Georgian Bay, Collingwood, Ontario.

Diagnosis .-- Cephalic outline subrectangular; glabella subrectangular in shape, strongly vaulted in lateral view, anterior border strongly convex in dorsal view, lateral margins faintly expand anteriorly at an angle of approximately 5º, and covered in fine granules with three large pairs of tubercles arranged sagittally; eyes substantially raised and aligned with S2; ventral doublure of the anterior cephalic border smooth, lacking the raised nodes found in *C. mammiloides*; paired nodes on the axial rings of the thorax; pygidial pleural spines depart from the pygidium directly posteriorly, with the uncrushed specimen showing the spines curving ventrally as they depart from the pygidium.

Description .-- Cephalic outline subrectangular. Exoskeleton smooth or covered in fine granules. Ventral doublure of the anterior cephalic border smooth, lacking the raised nodes found in *C. mammiloides*. Eyes substantially raised and aligned with S2. Large Eye Index 0.36. Glabella subrectangular in shape, strongly vaulted in lateral view, anterior border strongly convex in dorsal view, lateral margins faintly expand anteriorly at an angle of approximately 5º, and covered in fine granules with three large pairs of tubercles arranged sagittally. Glabellar furrows deeply incised, straight, squared off at the ends, and restricted to the lateral edges of the glabella. Genal spines depart from the cephalon at a shallow angle (roughly 20º), remain fairly straight, and curve towards the ventral distally. Anterior border of the cephalon wide and separated from

the cheeks by a faint border furrow. Occipital ring similar in size to thoracic axial rings in dorsal view, and is the same vertical relief in ventral view. Posterior cephalic border smooth, lacking any prominent nodes, and transverse close to the genal spines.

11 thoracic segments. Axial rings narrow, vaulted, and have faint paired nodes. One raised node on the lateral edge of the thoracic pleural furrow.

Pygidial outline subtriangular or semicircular (difficult to tell in hand specimen) with three prominent pygidial segments and a strongly reduced terminal axial piece. Pygidial pleural spines very thin and long, depart from the pygidium directly posterior and immediately curve ventrally before bowing out abaxially and curve adaxially distally. In the crushed specimen (ROM 45224), the spines point directly posteriorly, although they still curve adaxially at the distal ends. Other pygidial characters poorly preserved or covered by the pleural spines.

Discussion.-- *C. furca* is differentiated from *C. mammiloides* in the following characters; *C. furca* has a glabella with a strongly convex anterior border, smooth anterior cephalic doublure, and pygidial spines that depart from the pygidium nearly directly posteriorly and curve ventrally. The pygidium in the specimen ROM 45224 (Hessin 1988a figs 4.2, 4.3) is crushed and pushed underneath the exoskeleton, making it impossible to determine precisely whether or not the pygidial spines most closely resemble *C. furca* or *C. mammiloides*. However interpolation of the trajectory of the spines implies a shallower angle of departure (relative to the sagittal line) from the pygidium than shown in the *C. mammiloides* specimen ROM 45226 (Hessin 1988a figs 3.5, 3.6). Coupled with the strongly convex anterior margin of the glabella, we propose that ROM 45224 should be classified as *C. furca*.

CERAURUS KIRCHMEIERI, sp. nov.

Plate 32, Figure 1

Etymology .-- This species is named after Michael J. Kirchmeier, the original collector of the type specimen.

Holotype .-- One complete holotype exoskeleton KUMIP 325618

Occurrence .-- Found in the Elgin Member of the Maquoketa Formation in Fillmore County Minnesota.

Diagnosis .-- Exoskeleton sculpture densely granulated; strongly effaced paired glabellar tubercles; eyes positioned opposite L3; cheeks posterior border of the cephalon lacks any prominent nodes; lightly expanding glabella with low convexity; genal spines depart the cephalon at about 20º, barely curved, and triangular in outline; strongly effaced paired tubercles along the axial thoracic ring.

Description .-- Exoskeleton evenly covered in dense granulation, but characteristic ornamentation common in other ceraurid trilobites is effaced or absent (i.e.: lacks nodes/tubercles close to the eye, and also lacks any tubercles on the posterior border of the cephalon). Cephalon semicircular in outline. Anterior cephalic border broad and separated from the cheek by a well-defined furrow. Eyes positioned far forward on the cephalon, with the transverse center of the eye aligned with the transverse center of L3. Eyes dramatically raised above the cephalon. Large Eye Index is 0.31-0.37 (varies between eyes). Palpebral ridge leading to the glabella faintly preserved. Lateral margins of the glabella gently expand anteriorly at an angle of approximately 20 degrees with the sagittal line in dorsal view. Glabella subrectangular in outline, with a gently convex anterior border. Glabellar furrows deeply incised, straight,

squared off at the end proximal to the glabella, and restricted to the lateral borders of the glabella. L1, L2, and L3 roughly similar sizes and expressed as small squared off lobes. Three sets of strongly effaced paired tubercles follow the sagittal line of the glabella. Pair of apodemal glabellar pits aligned with S3. Glabella weakly convex in lateral view. Occipital ring similar in size to the axial rings of the subsequent thoracic segments, and exhibits low dorsal relief. Posterior border of the cephalon near the genal spine is nearly transverse. Genal spines long, broad at the base, straight in dorsal view, triangular in shape, and depart at an angle of approximately 20 degrees, staying close to the thorax. Tips of genal spines curve slightly dorsally.

11 thoracic segments. Paired nodes along the axial ring of the segments are visible upon close inspection, but are strongly effaced. Paired nodes along the pleural furrows strongly reduced in size, barely raised up above the rest of the pygidial pleurae. Axial ring of the thorax wide and with low dorsal relief relative to the rest of the specimen.

Pygidial border semicircular in outline with three prominent pygidial segments and a strongly reduced terminal axial piece. One prominent pair of pygidial spines originates from the anterior set of pygidial pleurae. Subsequent pygidial pleurae do not form any spines or lappets. Axial and interpleural furrows weakly incised. Pleural spines depart from pygidium at roughly 45 degrees and strongly curve medially until tips point nearly directly posterior. Spines triangular in shape.

Discussion .-- *Ceraurus kirchmeieri* is distinctly different from the only other *Ceraurus* species named from the Elgin, *Ceraurus elginensis*. The eyes of *C. kirchmeieri* are positioned further forward than the eyes of *C. elginensis,* which are aligned with S2. Despite being highly effaced, *C. kirchmeieri* has paired nodes running up the sagittal line of the glabella, while these nodes are

absent in *C. elginensis*. Also, the sculpture of the exoskeletons of the two species are dramatically different; *C. kirchmeieri* is covered in fine granules as opposed to the large raised tubercles that cover the exoskeleton of *C. elginensis*. Finally, the posterior border of the cephalon of *C. kirchmeieri* lacks any large raised nodes, whereas the posterior border of the cephalon of *C. elginensis* has two large paired nodes located proximal to the glabella, and three smaller tubercles running close to the genal spines. Because of these differences, we consider it highly unlikely that *C. kirchmeieri* merely represents a more complete specimen *C. elginensis*.

When compared with every other species of *Ceraurus, C. kirchmeieri* is particularly unique due to its effacement. While characteristics such as paired nodes on the glabella and thorax are present in *C. kirchmeieri*, they have been dramatically effaced. Since so much of the detailed granulation of the exoskeleton is preserved, we find it unlikely that this effacement is due solely to taphonomic biases. No other known *Ceraurus* species show this type of effacement, and therefore it is likely an autapomorphous characteristic.

CERAURUS NAPANEEI, sp. nov.

Plate 33, Figures 1-2; Plate 34, Figures 1-5; Plate 35, Figures 1-4

Etymology .-- Named after the Napanee Member of the Trenton from which this species is found.

Holotype .-- Complete specimen KUMIP 325652. Paratype cranidium KUMIP 325658 and pygidium KUMIP 325656.

Other Material .--Assorted cranidia, pygidia, and hypostomes KUMIP 325653-5, 7, 325659-61

Occurrence .-- The Napanee Member near Boonville, New York.

Diagnosis .-- Glabella strongly vaulted and densely covered in randomly arranged tubercles; eyes aligned with 3L; posterior cephalic border has prominent paired nodes positioned close to the eye and one prominent node positioned close to the genal spines (some specimens have small tubercles running across the entirety of the posterior border as well); genal spines depart from the cephalon at an angle of approximately 20 degrees and barely curve medially; small, faintly expressed paired nodes on the axial rings of the thorax; pronounced pygidial border formed from the fusing of the flattened lappets of the medial and posterior-most pygidial pleurae.

Description .-- Exoskeleton mostly smooth or covered in faint, small granules. Cephalon roughly semi-circular in dorsal outline (type specimen cephalon is crushed, making the cephalon appear slightly more boxy due to the splaying out of the cheeks). Cheeks lightly covered in small, widely spaced tubercles. Two large paired tubercles, arranged exsagittally, positioned close to the eyes. Glabella subrectangular in outline, strongly vaulted, covered in large randomly arranged tubercles, and with a gently curved anterior border and lateral margins that greatly expand at approximately 20º. S1, S2, S3 roughly similar in size, deeply incised, wide, squared at the ends, and short (restricted to the lateral margins of the glabella). Eyes positioned far forward on the head and aligned with L3. Large Eye Index 0.35-0.37. Genal spines triangular in shape, gently curve proximally and are nearly straight medially, and depart from the cephalon at an angle of approximately 20º. Anterior cephalic border wide and separated from the cheek by a sharply defined furrow. Posterior cephalic border has two paired nodes positioned close to the occipital ring, with the lateral-most node being the most prominent. A second faint node positioned close to the genal spines is present on most specimens.

Hypostome subtriangular in outline. Middle body oval shaped and densely covered in maculae. Middle body lacks any prominent middle body furrow. Furrow separating the middle

body from the outer body strongly incised and wide. Lateral margins of the hypostome converge at an angle of roughly 30º.

11 thoracic segments. Axial ring has two, faintly expressed paired nodes arranged transversely. Exsagittally running furrow on the proximal section of the thoracic pleurae. Area around the exsagittal furrow gently inflated, but not prominently raised into nodes as seen in other ceraurids.

Pygidial border strongly curved, semicircular to subtriangular in outline with three prominent pygidial segments and a strongly reduced terminal axial piece. Anterior-most pygidial pleurae extended into long triangular spines that depart from the pygidium at an angle of roughly 45º, and remain relatively straight medially (with a slight bend). Intrapleural furrows on the first pair of spines effaced or strongly reduced. Axial furrow barely expressed, while the interpleural furrows are deeply incised and wide. Furrow separating the terminal axial piece from the pygidial axis triangular in shape. Medial and posterior-most pleurae flatten into lappets and fuse together forming a prominent pygidial border.

Discussion .-- *Ceraurus napaneei* is distinct from other ceraurids collected from the Trenton, particularly with its paired nodes on the posterior border of the cephalon and the randomly arranged tubercles on the glabella (characteristics that are not found in either *C. pleurexanthemus* or *C. walcotti*). Looking at the cephalon alone, the species bears some resemblance to *C. milleranus*, except that the eyes are positioned much further forward in *C. napaneei*. The pygidium, however, is completely distinct from *C. milleranus*, with its strongly pronounced pygidial border formed from the fusing of the pygidial lappets (a characteristic *C. napaneei* shares with both *C. pleurexanthemus* and *C. globulobatus*).

CERAURUS HILLIERI, sp. nov.

Plate 36, Figure 1

Etymology .-- Named after the Hillier Member from which the holotype specimen of this species is found.

Holotype .-- Nearly complete specimen NYSM 17000

Occurrence .-- From the top of the Hillier Limestone, Gulf Stream near Rodman, Jefferson Co., New York.

Diagnosis .-- Large randomly arranged tubercles on the glabella; very large and raised eyes aligned with S2; S1, S2, and S3 restricted to the lateral margins of the glabella; one faint node on the posterior border of the cephalon positioned between the eye and the occipital ring; pygidium semicircular in outline and covered in small tubercles; intrapleural furrows on the anterior-most pygidial pleurae strongly incised.

Description .-- Exoskeleton mostly smooth or covered in faint, small granules. Cephalon roughly semi-circular in dorsal outline. Cheeks poorly preserved on holotype but available material suggests that they are mostly smooth or covered in fine granules. Two large paired tubercles, arranged exsagittally, positioned close to the eyes. Glabella subrectangular in outline, strongly vaulted, covered in large randomly arranged tubercles, and with a gently curved anterior border and lateral margins that greatly expand at approximately 20º. S1, S2, S3 roughly similar in size, deeply incised, wide, squared at the ends, and short (restricted to the lateral margins of the glabella). Eyes very large and aligned with S2. Large Eye Index 0.4-0.42. Genal spines triangular in shape, gently curve proximally and are nearly straight medially, and depart from the cephalon

at an angle of approximately 20º. Anterior cephalic border wide and separated from the cheek by a sharply defined furrow. Posterior cephalic border has one faint node positioned close to the occipital ring.

11 thoracic segments. The holotype specimen is the only collected specimen with thoracic segments, and they are slightly eroded, so it cannot be determined if the species has paired nodes on the axial rings of the thorax.

Pygidium semiciruclar in outline with three prominent pygidial segments and a strongly reduced terminal axial piece and covered in small tubercles. Anterior-most pygidial pleurae form large spines, while the medial and posterior-most pleurae barely extend beyond the pygidial border. Pygidial spines depart from the pygidium at roughly 40º and faintly curve medially. Intrapleural furrow on the anterior-most pleurae strongly incised. Interpleural furrows strongly incised and wide, while the axial furrow is faintly incised. Furrow separating the terminal axial piece from the axis triangular in outline.

Discussion .-- The large eyes of *C. hillieri* are a unique characteristic of this species, as no other ceraurid exhibits eyes that are as large relative to the size of the body. This characteristic is not merely the result of some strange ontogenetic development, as the relative eye size remains large across different sized individuals.

CERAURUS WILSONI, sp. nov.

Plate 37, Figure 1; Plate 38, Figure 1

Etymology .-- Named after Canadian paleontologist Alice Evelyn Wilson.

Holotype .-- Complete specimen ROM 45129.

Other Material .-- Nearly complete exoskeleton GSC 137134.

Occurrence .-- Lindsay Formation at Ogden Point Quarry, Ontario and the Cobourg Formation at the St. Isidore Quarry, Ontario.

Diagnosis .-- Glabella densely covered in large tubercles, with even larger pairs tubercles running sagittally up the glabella; small tubercles randomly arranged on the genal spines and anterior cephalic border; eyes aligned with S2; small tubercles evenly spaced across the cheeks, with two larger, exsagittally arranged tubercles positioned close to the eyes; genal spines depart from the cephalon at roughly 20º and faintly curve medially; posterior border has one prominent node positioned close to the eyes with a line of faint tubercles leading to the occipital ring and one prominent node positioned close to the genal spines.

Description .-- Cephalon roughly semi-circular in dorsal outline. Cheeks densely covered in small tubercles. Two larger paired tubercles, arranged exsagittally, positioned close to the eyes. Glabella subrectangular in outline, densely covered in large tubercles with even larger pairs of tubercles running sagittally up the glabella, and with a gently curved anterior border and lateral margins that gently expand at approximately 10º. S1, S2, S3 roughly similar in size, deeply incised, wide, squared at the ends, and gently penetrate into the sagittal of the glabella. Eyes aligned with S2. Large Eye Index 0.25-0.28. Genal spines triangular in shape, covered in small tubercles, gently curve proximally and are nearly straight medially, and depart from the cephalon at an angle of approximately 20º. Anterior cephalic border wide, covered in randomly arranged small tubercles, and separated from the cheek by a sharply defined furrow. Posterior cephalic border has one prominent node positioned close to the eye with a line of small tubercles running towards the occipital ring, and one prominent node positioned close to the genal spine.

11 thoracic segments. Axial ring has two, faintly expressed paired nodes arranged transversely. Exsagittally running furrow on the proximal section of the thoracic pleurae. Area around the exsagittal furrow gently inflated, but not prominently raised into nodes as seen in other ceraurids.

Pygidium semicircular in outline with three prominent pygidial segments and a strongly reduced terminal axial piece. Anterior-most pygidial pleurae extended into long triangular spines that depart from the pygidium at an angle of roughly 30º, and remain gently curve medially. Intrapleural furrows on the first pair of spines effaced or strongly reduced. Axial furrow shallowly incised. Interpleural furrows deeply incised. Furrow separating the terminal axial piece from the pygidial axis triangular in shape. Medial and posterior-most pleurae flatten into lappets and fuse together forming a prominent pygidial border.

Discussion .-- The crushed specimen from St. Isidore appears to differ from the holotype specimen in that the genal spines appear to be substantially shorter. Close examination of the specimen suggests that the spines may be broken, giving the appearance of coming to a point prematurely. It is possible, however, that this interpretation could be incorrect and the St. Isidore specimen could represent a related species to the holotype. Despite the difference in genal spine length, the two specimens are incredibly similar, specifically sharing the pronounced tubercation of the glabella, as well as the arrangement of nodes and tubercles on the posterior border of the cephalon.

CERAURUS OTTAWAENSIS, sp. nov.

Plate 39, Figure 1; Plate 40, Figure 1

Etymology .-- Named after the city of Ottawa, near which the holotype specimen was collected.

Holotype .-- One complete specimen KUMIP 325662.

Other Material .-- Two nearly complete specimens GSC 137135-6.

Occurrence .-- Lower Bobcaygeon near Ottawa, Ontario.

Diagnosis .-- Glabella ornamented with small tubercles; eyes aligned with S3; posterior border has two paired nodes positioned close to the occipital ring and one positioned close to the genal spines; genal spines depart from the cephalon at approximately 45º and dramatically curve medially until the spines point nearly adaxially; prominent paired nodes on the axial rings of the thorax; pygidial spines depart from the pygidium at around 45º and dramatically curve medially until the spines points roughly adaxially.

Description .-- Exoskeleton mostly smooth or covered in faint, small granules. Cephalon roughly semicircular to subtriangular in dorsal outline. Cheeks sparsely covered in small tubercles. Two large paired tubercles, arranged exsagittally, positioned close to the eyes. Glabella subrectangular in outline, covered in large randomly arranged tubercles, and with a gently curved anterior border and lateral margins that gently expand at approximately 10º. S1, S2, S3 roughly similar in size, deeply incised, wide, squared at the ends, and short (restricted to the lateral margins of the glabella). Eyes aligned with L3. Large Eye Index 0.28. Genal spines triangular in shape, strongly curved medially, and depart from the cephalon at an angle of approximately 45º. Anterior cephalic border wide and separated from the cheek by a sharply defined furrow. Posterior cephalic border has a pair of prominent nodes positioned close to the occipital ring and one other node positioned close to the genal spines.

11 thoracic segments. Axial ring has two, prominently expressed paired nodes arranged transversely. Exsagittally running furrow on the proximal section of the thoracic pleurae. Area around the exsagittal furrow gently inflated, but not prominently raised into nodes as seen in other ceraurids.

Pygidium is crushed or incomplete in most specimens, however some character data can be ascertained. Pygidium roughly semi-circular in outline. Genal spines depart from the pygidium at approximately 45º and strongly curve medially until they point nearly adaxially. *Discussion* .-- The splayed out and strongly curved genal spines of *C. ottawaensis* most closely resemble those found in *C. jenlorum*. However, the two species are easily distinguished from each other as they differ in nearly every other possible manner.

ACKNOWLEDGMENTS

The authors would like to thank Susan Butts (YPM), Jessica Cundiff (MCZ), Brenda Hunda (CMNH), Janet Waddington (ROM), Michelle Coyne (GSC), Paul Mayer (FMNH), Ed Landing (NYSM), and Bushra Hussaini (AMNH) for access to museum specimens and for loaning out material that was vital to completing this monograph. We would like to thank Tom Whitely for informative discussions on ceraurids, as well as access to his collection of high-quality specimen photographs. We would also like to thank Al, Caleb, and Lory Scheer for their help and expertise on Midwestern fossils, but also for their warmth and hospitality. We would also like to thank George Kampouris for allowing us access to his extensive collection of Ontario material and for his detailed knowledge of the geology of the Ottawa area. Similarly, we would like to thank Mark Bourie for sharing his expertise on Ontario trilobites, as well as also sharing

his knowledge of the geology of Ottawa. We would also like to thank Bruce Stinchcomb for providing excellent specimens of Missouri trilobites from the Kimmswick. Finally, we would like to thank Cori Myers, Erin Saupe, Francine Abe, Wes Gapp, James Lamsdell, and Bruce Lieberman for support and advice throughout the writing of this monographic work. Funding for this monograph was provided by the NSF (DEB-0716162), the Association for Women Geoscientists (AWG), the KU Biodiversity Institute, the KU Geology Department, the Paleontological Society, and the Kansas and Missouri Paleontological Society.

REFERENCES

Barrande, J. (1872) *Systéme Silurien du centre de la Boheme, lére partie, Supplement au Vol. 1. Trilobites, Crustacés divers et Poissons*, Parah, Paris.

Barton, D.C. (1913) A new genus of Cheiruridae, with description of some new species, *Bulletin of the Museum of Comparative Zoology at Harvard College*, 54:545-556.

Barton, D.C. (1916) *A revision of the Cheirurinae with notes on their evolution*, St Louis Washington University Studies 3: pp. 101-151.

Beyrich, E. (1845) *Ueber einige böhmische Trilobiten*, Berlin, 47 p

Billings, E. (1861-1865) *Palaezoic fossils of Canada*, Geologic Survey of Canada.

Bradley, J.H. Jr. (1930) Fauna of the Kimmswick Limestone of Missouri and Illinois, *Contributions from the Walker Museum*, 2:i-v, 219-290.

Bremer, K. (1994) Branch Support and Tree Stability, *Cladistics-the International Journal of the Willi Hennig Society*, 10: 295-304.

Brett, C.E. and Whiteley, T.E., Allison, P.A., Yochelson, E.L. (1999) The Walcott-Rust Quarry: Middle Ordovician trilobite konservat-lagertätten, *Journal of Paleontology*, 73(2): 288-305.

Brett, C.E. and Baird, G.C. (2002) Revised stratigraphy of the Trenton Group in its type area, central New York State: sedimentology and tectonics of a Middle Ordovician self-to-basin succesion, *Physics and Chemistry of the Earth*, 27: 231-263.

Chatterton, B.D.E. andLudvigsen, R. (1976) Silicified Middle Ordovician trilobites from the South Nahanni River area, District of Mackenzie, Canada, *Palaeontographica, Abteilung A*, 154:1-106.

Cooper, G.A. (1953) Trilobites from the Lower Champlainian Formations of the Appalachians Valley, *Geological Society of America Memoir*, 55, 69 p.

Cooper, G.A. and Kindle, C.H. (1936) New brachiopods and trilobites from the Upper Ordovician of Percé, Quebec, *Journal of Paleontology*, 10:348-372.

Dean, W.T. (1966) The Lower Ordovician stratigraphy and trilobites of the Landeyran Valley and the neighbouring district of the Montagne Noirse, south-western France, *Bulletin of the British Museum (Natural History) Geology*, 12(6):245-353.

Dean, W.T. (1979) Trilobites from the Long Point Group (Ordovician), Port au Port Peninsula, southwestern Newfoundland, *Geological Survey of Canada Bulletin*, 290, 53 p.

DeMott, L.L, 1963, Middle Ordovician trilobites of the Upper Mississippi Valley; Unpublished Ph.D. thesis, Harvard University.

DeMott, L.L. *Edited by* Sloan, R.E., Shaw, F.C., Tripp, R.P. (1987) Platteville and Decorah trilobites from Illinois and Wisconsin, *in* Sloan, R.E. (ed.), Middle and Late Ordovician lithostratigraphy and biostratigraphy of the Upper Mississippi Valley, *Minnesota Geological Survey, Report of Investigations* 35, p. 63-98

Desbiens, S. and Lespérance, P.J. (1989) Stratigraphy of the Ordovician of the Lac Saint-Jean and Chicoutimi outliers, Quebec, *Canadian Journal of Earth Sciences*, 26:1185-1202.

Edgecombe, G.D. and Chatterton, B.D.E., Vaccari, N.E., Waisfeld, B.G. (1999a) Ordovician cheirurid trilobites from the Argentine Precordillera, *Journal of Paleontology*, 73(6):115-1175.

Edgecombe, G.D.B. and Banks, M.R., Banks, D.M. (1999b) Upper Ordovician Phacopida (Trilobita) from Tasmania, *Alcheringa: An Australasian Journal of Palaeontology*, 23(4): 235-257.

Esker, G.E. III, (1964) New species of trilobites from the Bromide Formation (Pooleville Member) of Oklahoma, *Oklahoma Geology Notes*, 24:195-209.

Evitt, W.R. (1953) Observations on the trilobite *Ceraurus*, *Journal of Paleontology*, 27:33-48.

Foerste, A.F. (1909) Preliminary notes on Cincinnatian and Lexington fossils, *Bulletin of the Scientific Laboratory of Denison University*, 14:298-324.

Foerste, A.F. (1920) The Kimmswick and Plattin Limestones of Northeastern Missouri, *Journal of the Scientific Laboratories of Denison University*, 19:175-224

Goloboff, P.A. and Farris, J.S., Nixon, K.C. (2008) TNT, a free program for phylogenetic analysis, *Cladistics*, 24: 774-786

Green, J. (1832) *Monograph of the trilobites of North America*, J. Brano, Philadelphia, 93 p.

Hawle, I. and Corda, A.J. (1847) *Prodrom einer Monographie der böhmischen Trilobiten*, Abhandlungen Böhmischen Gesellschaft Wissenschaften Prague, 5:117-292.

Hessin, W.A. (1988a) *Leviceraurus*, a new cheirurinae trilobite from the Cobourg Formation (Middle-Upper Ordovician), Southern Ontario, Canada, *Journal of Paleontology*, 62:87-93.

Hessin, W.A. (1988b) Partial regeneration of a genal spine by the trilobite *Ceraurus plattinensis*, *Lethaia*, 21:285-288.

Hessin, W.A. (1989) *Ceraurus* and related trilobites from the Middle Ordovician Bobcaygeon Formation of south-central Ontario, Canada, *Canadian Journal of Earth Sciences*, 26:1203-1219.

Hussey, R.C. (1926) *The Richmond Formation of Michigan*, Museum of Paleontology, The University of Michigan, 2(8):113-187.

Lane, P.D. (1971) *British Cheiruridae (Trilobita)*, Palaeontographical Society Monographs, 95 p.

Lane, P.D. (2002) The taxonomic position and coaptive structures of the Lower Ordovician trilobite *Cyrtometopus*, *Special Papers in Palaeontology*, 67:153-169.

Lespérance, P.J. and Desbiens, S. (1995) Selected Ordovician Trilobites from the Lake St. John District of Quebec and Their Bearing on Systematics, *Paleontological Society Memoirs*, vol 42:1-19.

Linnarsson, J.G.O. (1869) *Om Vestergötlands cambriska och siluriska aflagringar*.

Ludvigsen, R. (1975) Ordovician formations and faunas, southern Mackenzie Mountains, *Canadian Journal of Earth Sciences*, 12: 663-697.

Ludvigsen, R. (1976) New cheirurinid trilobites from the lower Whittaker Formation (Ordovician), southern Mackenzie Mountains, *Canadian Journal of Earth Sciences*, 13:947-959.

Ludvigsen, R. (1978) Towards an Ordovician trilobite biostratigraphy of Southern Ontario, *Michigan Basin Geological Society, Special Paper*, 3:73-84.

Ludvigsen, R. (1979) A trilobite zonation of Middle Ordovician rocks, Southwestern District of Mackenzie, *Geological Survey of Canada Bulletin*, 312, 99 p.

Maddison, W.P. and Maddison, D.R. (2007) Mesquite: a modular system for evolutionary analysis, 2.72 ed, Available: http://mesquiteproject.org (accessed 2010)

Männil, R. (1958) Trilobites of the families Cheiruridae and Encrinuridae from Estonia, *ENSV Teaduste Akadeemia Geoloogia Instituudi Uurimused*, 3:165-212.

Miller, S.A. and Gurley, W.F.E. (1894) Description of some new species of invertebrates from the Palaeozoic rocks of Illinois and adjacent states, *Illinois State Museum of Natural History Bulletin*, 3, 81 p.

Öpik, A. (1937) Trilobiten aus Estland, *Acta et Commentationes Universitatis Tartuensis, A*, 32: 1-163.

Parnaste, H. (2003) The Lower Ordovician trilobite *Krattaspis*: the earliest cyrtometopinid (Cheiruridae) from the Arenig of the East Baltic, *Special Paper in Palaeontology*, 70: 241-257.

Parnaste, H. (2004) Revision of the Ordovician cheirurid trilobite genus *Reraspis* with the description of the earliest representative, *Proceedings of the Estonian Academy of Sciences, Geology*, 53(2):125-138.

Parnaste, H. (2008) *Xylabion* and related genera, pp. 307-312 *in* Rábano, I., Gozalo, R., García-Bellido, D. (eds) *Advances in Trilobite Research*, Instituto Geológico y Minero de España, Madrid.

Prantl, F. and Pribyl, A. (1946) Classification and division of the genus *Scutellum* Pusch, 1833 from the Barrandian (Central Bohemia), *Bulletin international de l'Académie tchèque des Sciences*, 47(9): 1-32.

Prantl, F. and Pribyl, A. (1947) Classification of some Bohemian Cheiruridae (Trilobitae). Sborn. Narodn. Musea v. Praze, vol 3, B, no. 1.

Pribyl A., Vanek, J., Pek, I. (1985) Phylogeny and taxonomy of family Cheiruridae (Trilobita), *Acta Universitatis Palackianae Olomucensis Facultatis Medicae*, 83:107-193.

Rambaut, A. (2008) *FigTree. 1.1.2 ed.* Available: http://tree.bio.ed.ac.uk/software/figtree (accessed 2011)

Raymond, P.E. (1905) Trilobites of the Chazy limestone, *Annals of the Carnegie Museum*, 3(2).

Raymond, P.E. (1916) A new *Ceraurus* from the Chazy, *New York State Museum Bulletin*, 189:121-126.

Raymond, P.E. and Barton, D.C. (1913) A revision of the American species of Ceraurus, *Bulletin of the Museum of Comparative Zoology at Harvard College*, 54:523-543.

Reed, F.R.C. (1896) The fauna of the Keisley limestone; Pt. 1, *Quarterly Journal of the Geological Society, London*, 52:407-437.
Salter, J.W. (1853) Figures and descriptions illustrative of British organic remains, *Memoirs of the Geological Survey of Great Britain.*
Shaw, F.C. 1968, Early Middle Ordovician Chazy trilobites of New York. New York Sate Museum and Science Service, Memoir 17, 163 p.
Shaw, F.C. 1974, Simpson Group (Middle Ordovician) trilobites of Oklahoma. The Paleontological Society Memoir, 6, 54 p.
Sinclair, G.W. 1947, Two examples of injury in Ordovician trilobites. American Journal of Science, 245:250-257.
Slocom, A.W. 1913, New trilobites from the Maquoketa Beds of Fayette County, Iowa. Field Museum of Natural History, Publication 171, Geological Series, 4:41-83.
Slocom, A.W. 1916, New trilobites from the Maquoketa Beds of Fayette County, Iowa. Iowa Geologic Survey, vol 25: 183-249.
Tripp, R.P. 1967, Trilobites from the Albany division (Ordovician) of the Girvan district, Ayrshire. Palaeontology, 8:577-603.
Troedsson, G.F. 1928, I. On the Middle and Upper Ordovician faunas of Northern Greenland. Part II. Jubilæumsekspeditionen Nord om Grønland 1920-23, number 7, 197 p.
Walter, O.T. (1924) Trilobites of Iowa and some related Palaeozoic forms, *Annual Report of the Iowa Geological Survey*, 31:173-351.
Wiley, E.O. (1979) An annotated Linnaean hierarchy, with comments on natural taxa and competing systems, *Systematic Zoology*, 28:308-337.
Whiteley, T.E. and Kloc, G.J. (2002) The Holy Holotype, *American Paleontologist*, vol 10 (August):3-5
Whittard, W.F. (1967) The trilobite *Anacheirurus frederici* (Salter) from the Tremadoc Series of North Wales, *Geology Magazine*, 104(3):284-289.
Whittington, H.B. (1941) Silicified Trenton Trilobites, *Journal of Paleontology*, 15(5): 492-522.
Whittington, H.B. (1954) Ordovician trilobites from Silliman's fossil mount, *in* A.K. Miller, W. Youngquist, C. Collinson (eds), Ordovician Cephalopod Fauna of Baffin Island. Geological Society of America Memoire, 62. p. 119-149.
Whittington, H.B. (1963) Middle Ordovician trilobites from Lower Head, Western Newfoundland, *Bulletin of the Museum of Comparative Zoology, Harvard University* 129:1-118.
Whittington, H.B. and Evitt, W.R. (1954), Silicified Middle Ordovician trilobites, *Geological Society of America Memoirs*, 59, 137 p.
Whittington, H.B. and Chatterton, B.D.E., Speyer, S.E., Fortey, R.A., Owens, R.M. et al. 1997 Part O; Arthropoda 1; Trilobita, revised; Volume 1, Introduction, order Agnostida, order Redlichiida. In: Kaesler, RL, (editor) *Treatise on Invertebrate Paleontology*. Lawrence, KS: The University of Kansas Press and the Geological Society of America
Wilson, A.E. (1947) Trilobita of the Ottawa Formation of the Ottawa-St. Lawrence Lowland, *Geological Survey of Canada Bulletin*, 9:1-86.

FIGURE AND PLATE CAPTIONS

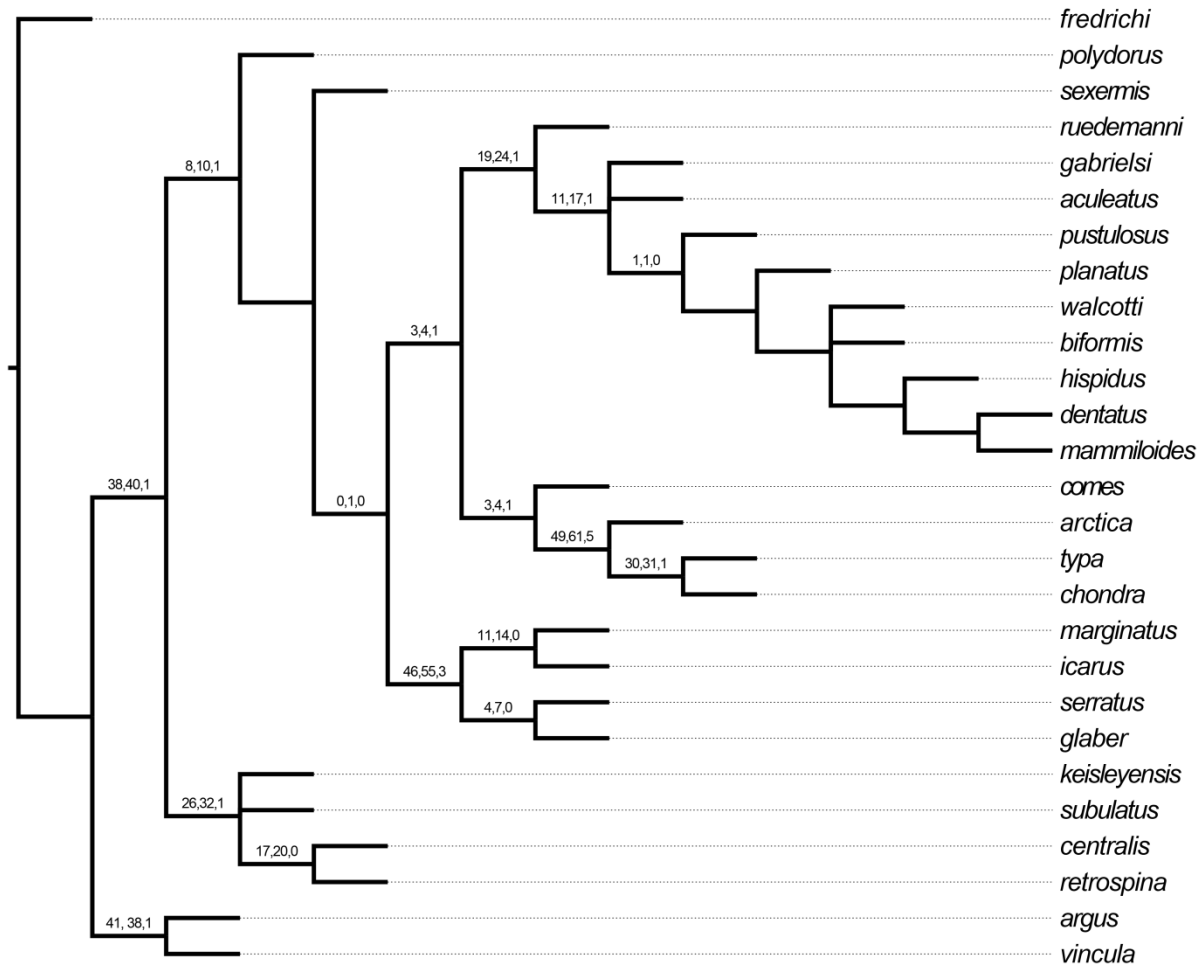

Figure 1: The strict consensus of the two most parsimonious trees of the Cheirurinae analysis. Numbers on the branches are support values from Bootstrap, Jackknife, and Bremer analyses and are listed in that order.

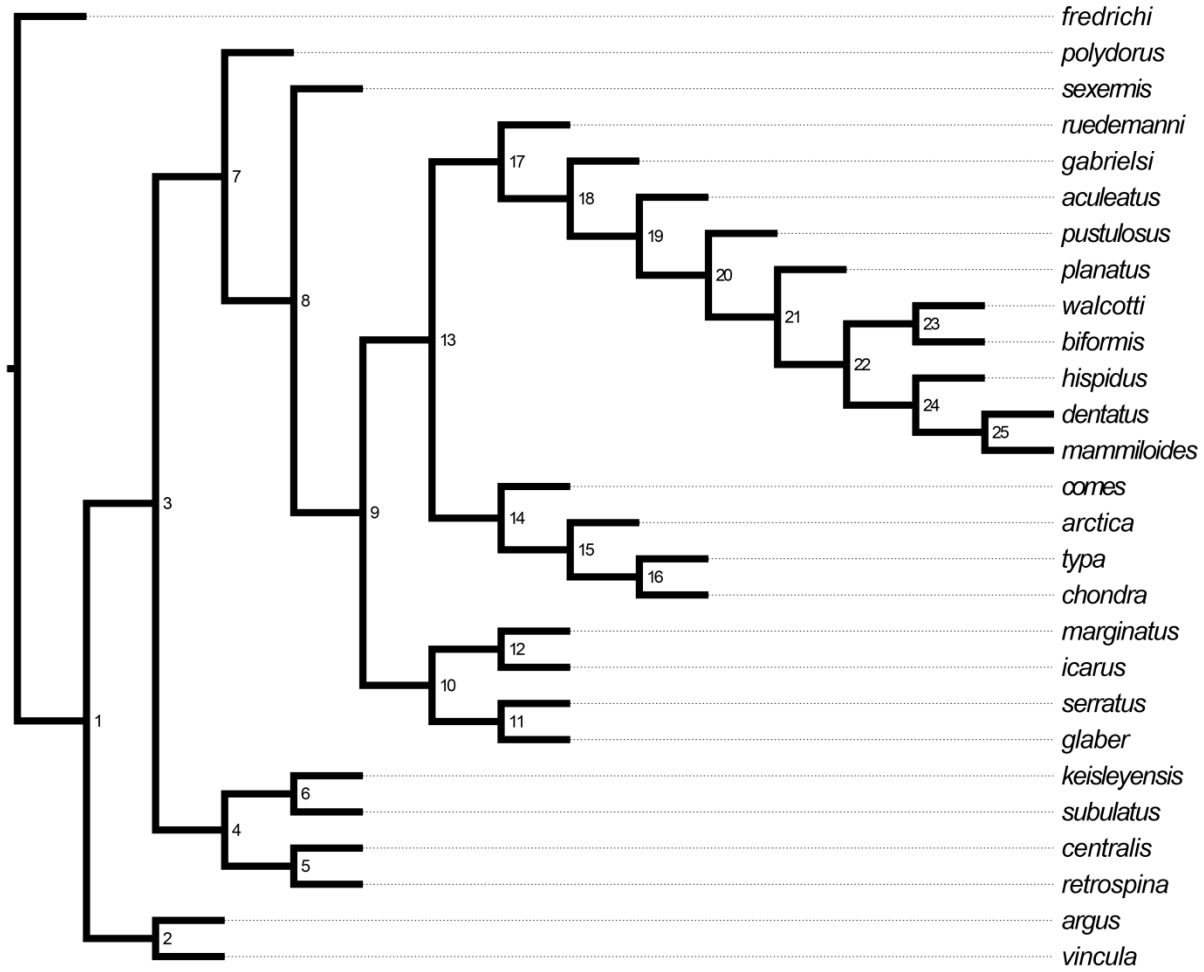

Figure 2: One of the two most parsimonious trees of the Cheirurinae analysis with the individual nodes on the tree numbered.

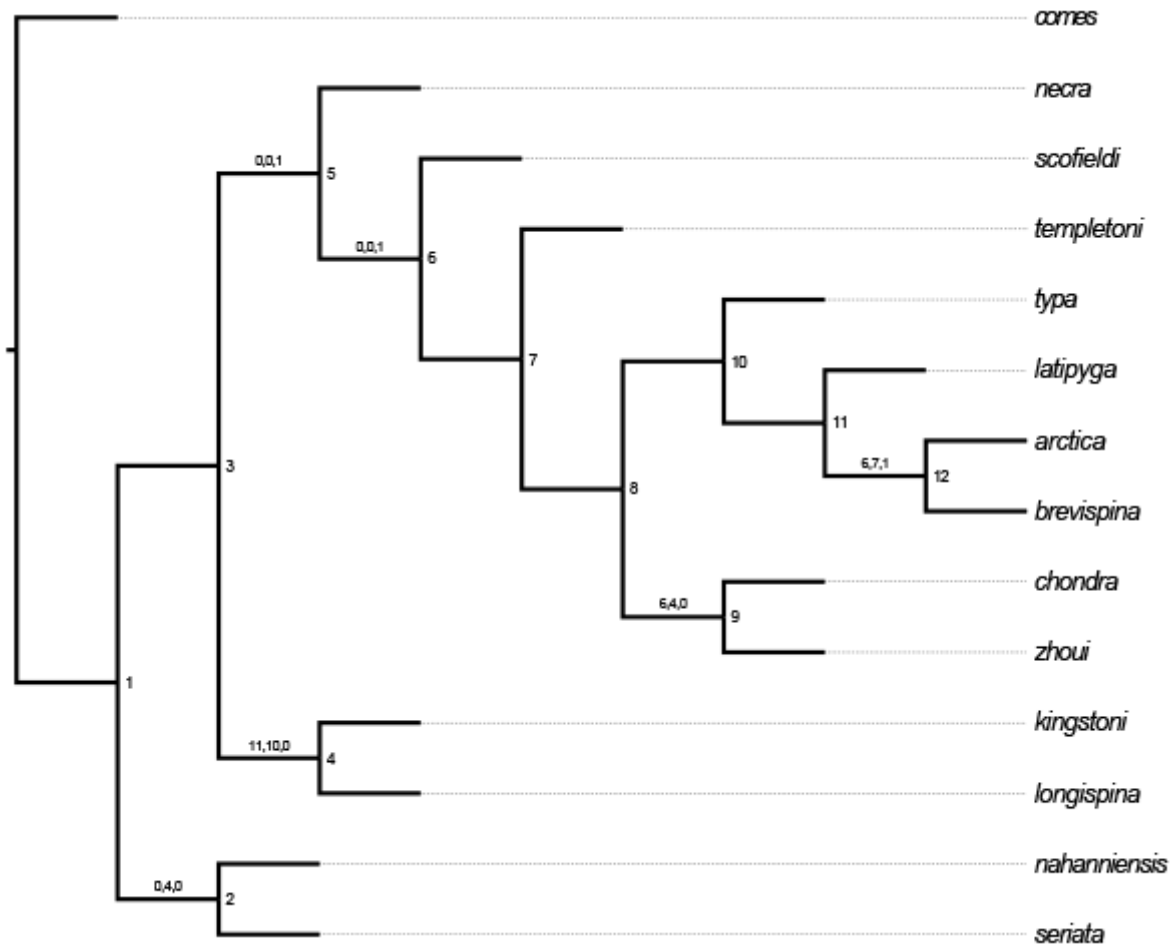

Figure 3: The most parismonious tree of the *Ceraurinella* analysis. Numbers on the branches are support values from Bootstrap, Jackknife, and Bremer analyses and are listed in that order.

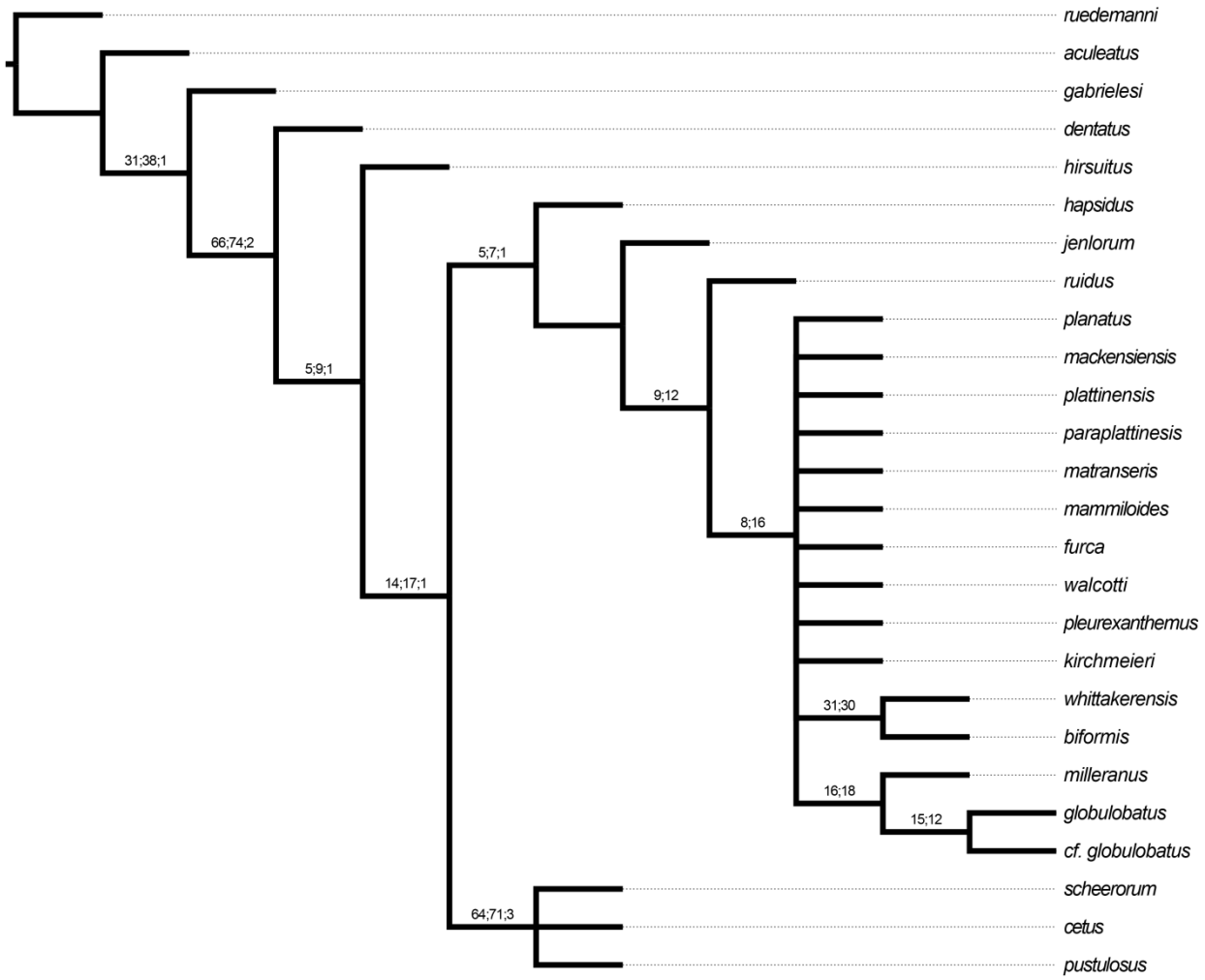

Figure 4: The strict consensus of the 16 most parsimonious trees of the “ceraurid-tribe” analysis. Numbers on the branches are support values from Bootstrap, Jackknife, and Bremer analyses and are listed in that order.

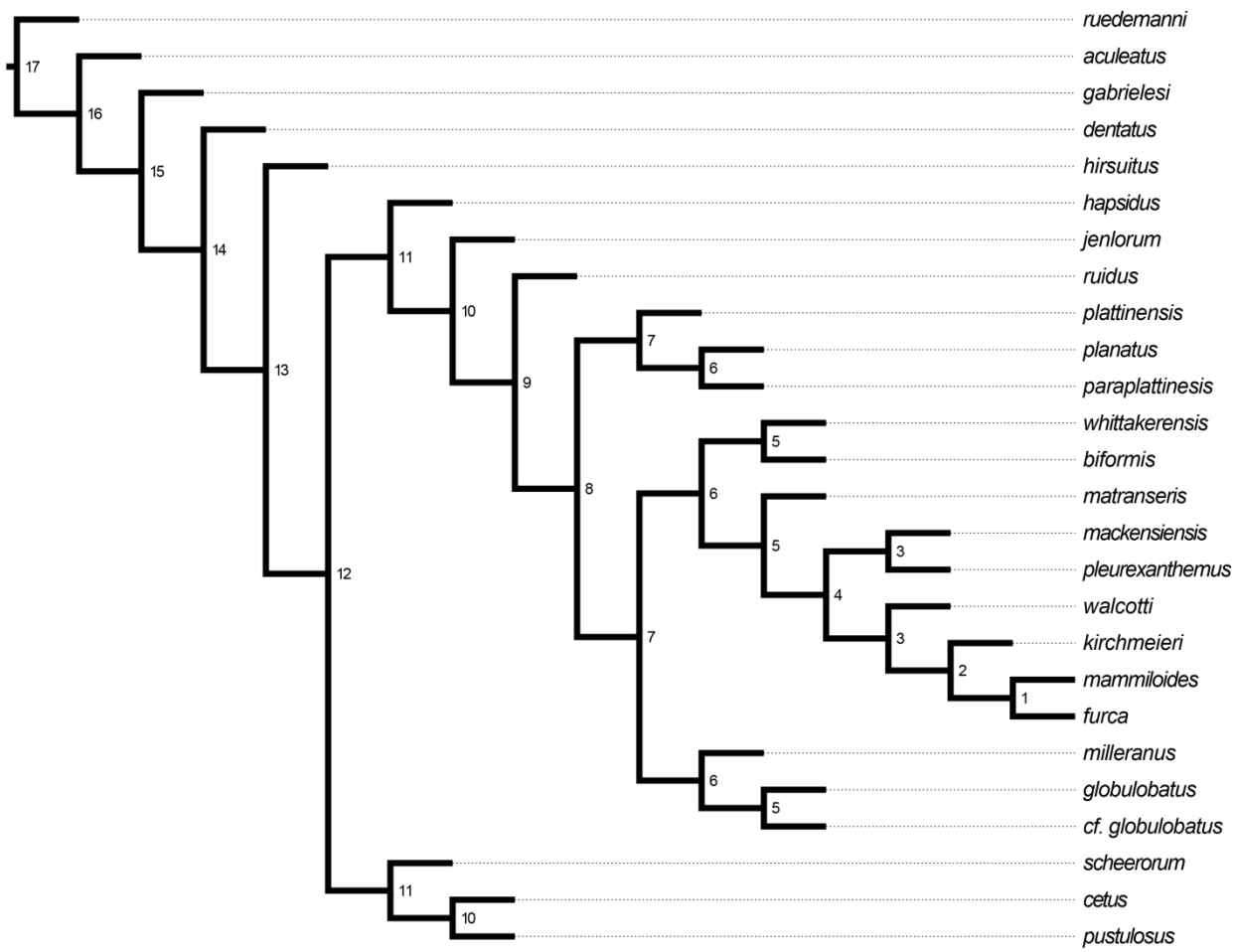

Figure 5: One of the four most parsimonious trees of the “ceraurid-tribe” with the nodes on the tree numbered.

Plate 1

"*Gabriceraurus*" *dentatus* (Raymond and Barton, 1913)

Figure 1: Dorsal view of nearly complete exoskeleton from Trenton Group rocks of Hull, Quebec ROM 18740, ×1.6.

Figure 2: Dorsal view of paratype exoskeleton from Cobourg Formation at Cobourg, Ontario GSC 1769b, ×0.7. Photograph from Thomas Whitely.

Figure 3: Dorsal view of paratype pygidium from Trenton Limestone of Watertown, New York MCZ 100802, ×1.1 Photograph from Thomas Whitely.

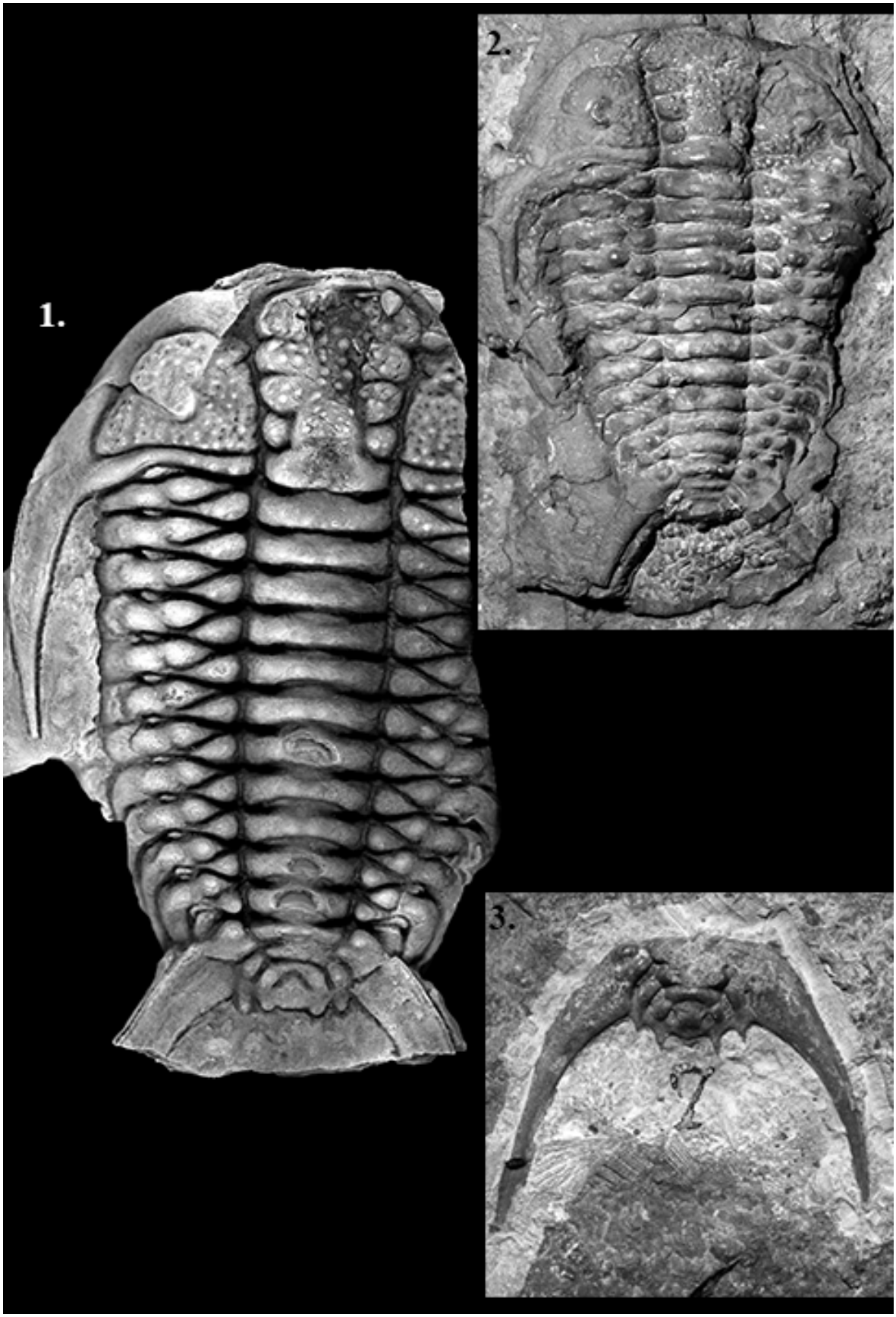
1.
2.
3.

Plate 2

Eubufoceraurus pustulosus sp. nov.

Figure 1: Dorsal view of incomplete exoskeleton from the Bobcaygeon Formation at Brechin, Ontario ROM 52739, ×2.3.

Eubufoceraurus scheerorum sp. nov.

Figure 2: Dorsal view of holotype type cranidium from the Mifflin Member at Fennimore, Wisconsin KUMIP 325579, ×2.5.

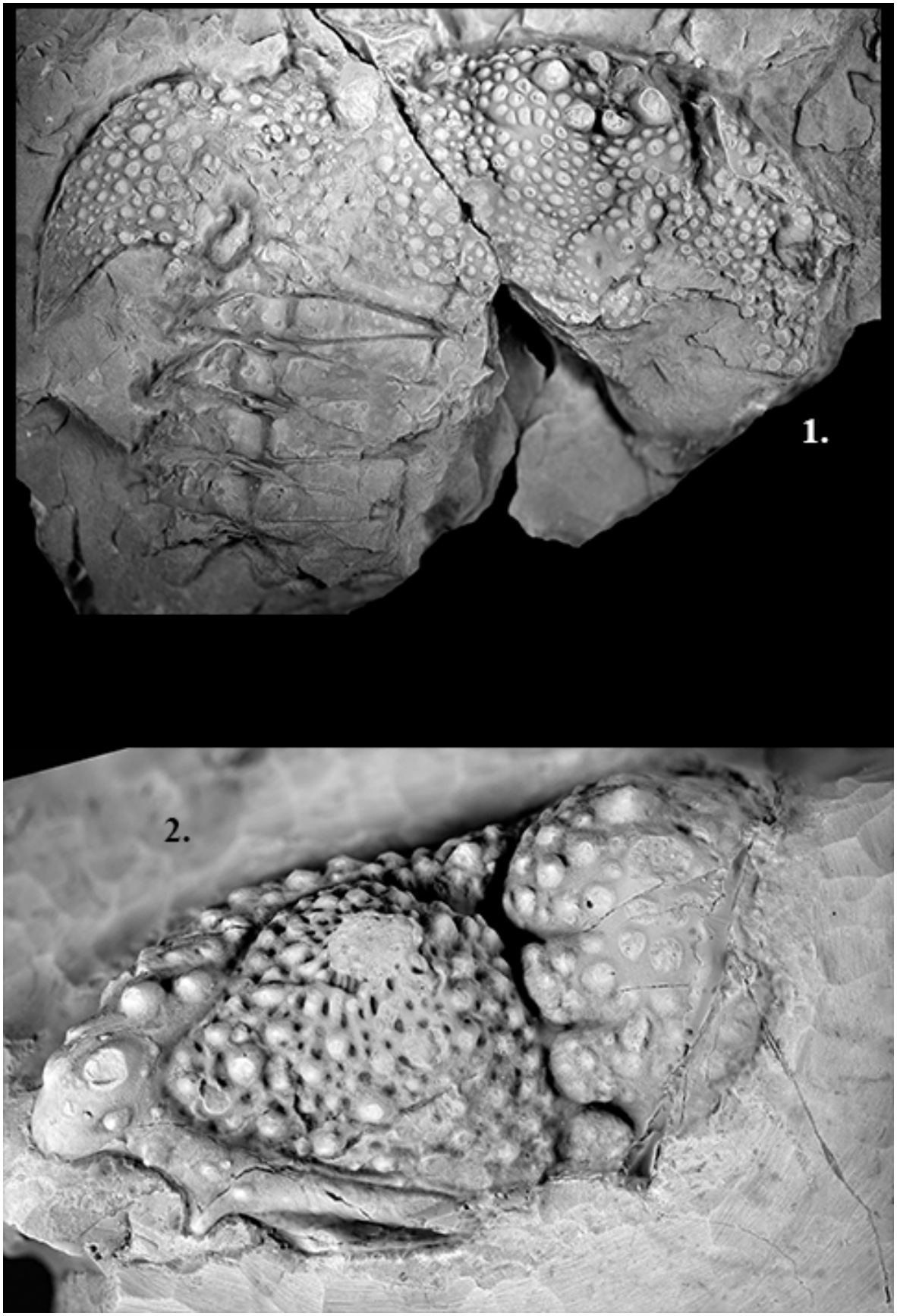
1.
2.

Plate 3

Eubufoceraurus scheerorum sp. nov.

Figure 1: Ventral genal spine and cheek with posterior border spine preserved from the Mifflin Member at Fennimore, Wisconsin KUMIP 325580, ×1.8.

Figure 2: Partial pygidium from the Mifflin Member at Fennimore, Wisconsin KUMIP 325581, ×3.1.

Figure 3: Small crandium from the Mifflin Member at Fennimore, Wisconsin KUMIP 325584, ×4.3.

Figure 4: Crushed pygidium from the Mifflin Member at Fennimore, Wisconsin KUMIP 325583, ×3.1

Figure 5: Cranidium from the Mifflin Member at Fennimore, Wisconsin KUMIP 325582, ×4.22.


1.
2.
3.
4.
5.

Plate 4

Eubufoceraurus scheerorum sp. nov.

Figure 1: Partial cranidium from the Mifflin Member at Fennimore, Wisconsin KUMIP 325585, ×3.9.

Figure 2: Partial cheek and genal spine from the Mifflin Member at Fennimore, Wisconsin KUMIP 325586, ×4.6.

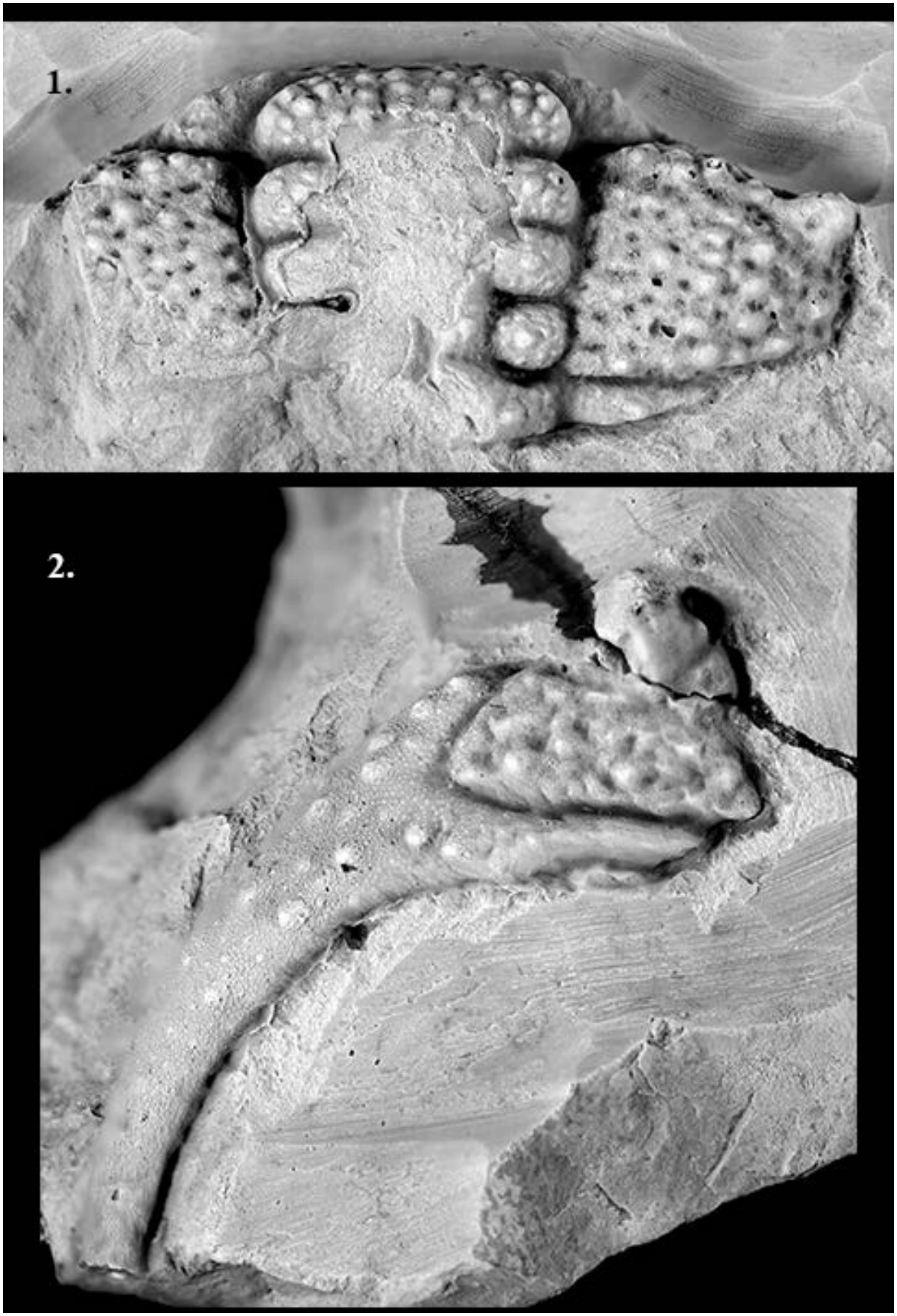
1.
2.

Plate 5

Eubufoceraurus cetus (Dean, 1979)

Figure 1:Holotype cranidium from the Lourdes Formation at Port au Port Peninsula, Newfoundland GSC 38633, ×1.2. Photograph from Thomas Whitely.

Ceraurus pleurexanthemus Green, 1832

Figure 2: Holotype exoskeleton from the lower Trenton Group near Newport, New York NYSM 4203, ×6.7. Photograph from Thomas Whitely.

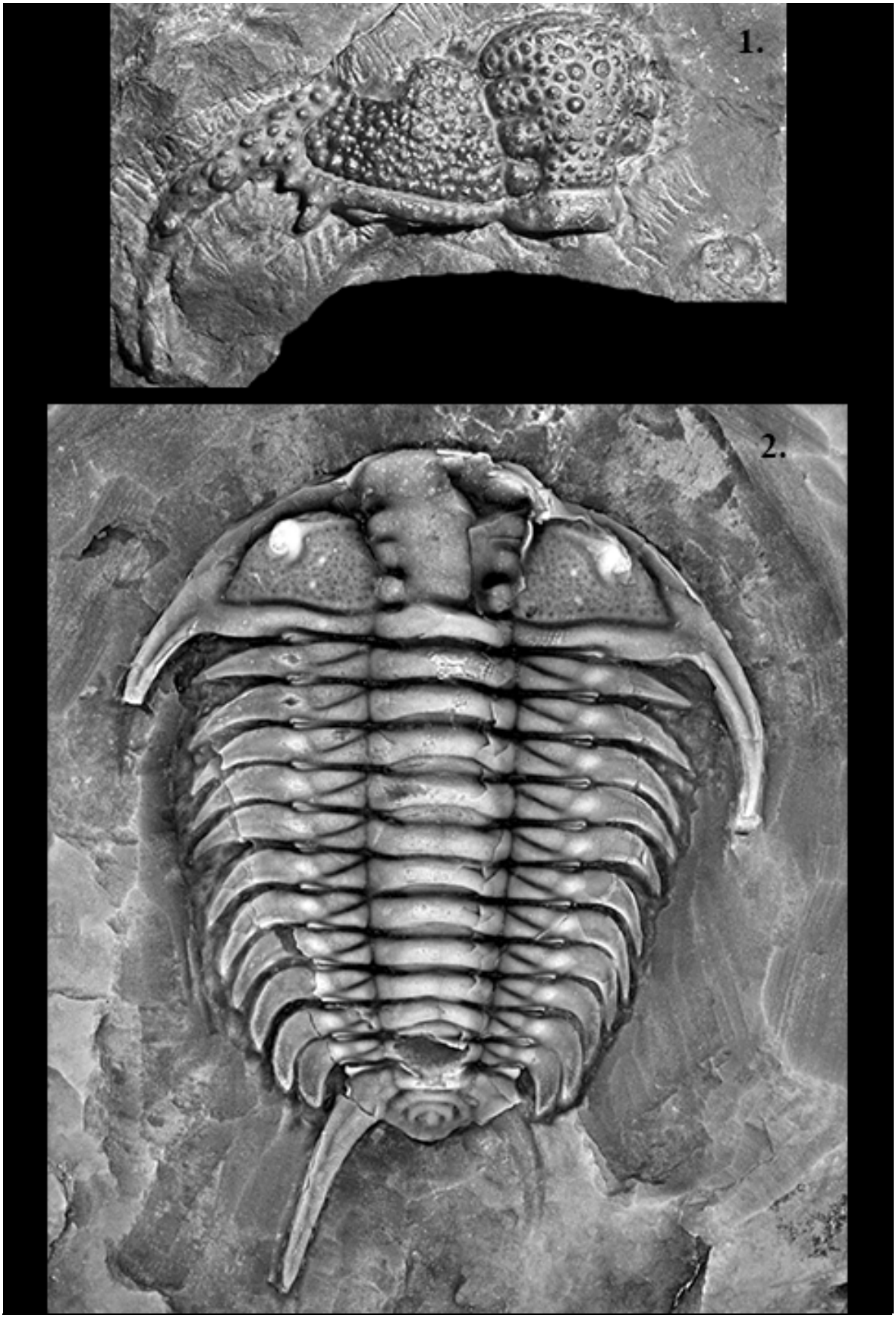
1.
2.

Plate 6

Ceraurus pleurexanthemus Green, 1832

Figure 1: Holotype exoskeleton from the lower Trenton Group near Newport, New York NYSM 4203, ×3.5. Photograph from Thomas Whitely.

Figure 2: Nearly complete exoskeleton from the Sugar River Formation near Watertown, New York KUMIP 325587, ×3.6.

Figure 3: Paratype exoskeleton from the lower Trenton Group near Newport, New York NYSM 4203, ×2.8. Photograph from Thomas Whitely.

Figure 4: Hypostome on paratype exoskeleton from the lower Trenton Group near Newport, New York NYSM 4203, ×7. Picture from Thomas Whitely.

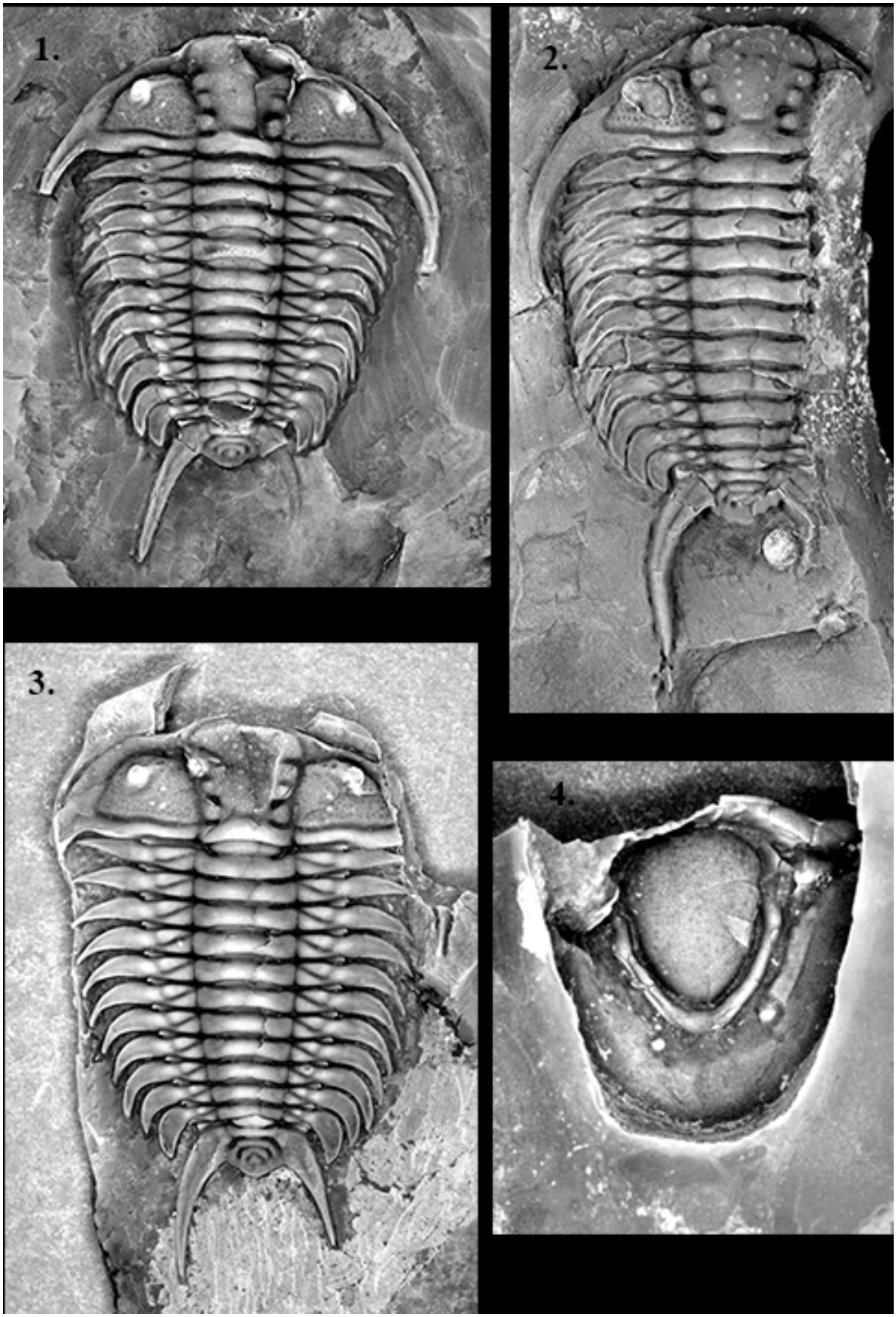
1.
2.
3.
4.

Plate 7

Ceraurus pleurexanthemus Green, 1832

Figure 1: Two incomplete cranidia from the Sugar River Formation near Watertown, New York KUMIP 325588-9, ×3.1.

Figure 2: Nearly complete exoskeleton from Sugar River Formation near Watertown, New York KUMIP 325590, ×5.4.

Figure 3: Hypostome from the Sugar River Formation near Watertown, New York KUMIP 325591, ×4.7.

Figure 4: Partially crushed cranidium from the Sugar River Formation near Watertown, New York KUMIP 325592, ×2.3.

Figure 5: Cranidium from the Sugar River Formation near Watertown, New York KUMIP 325593, ×4.75.

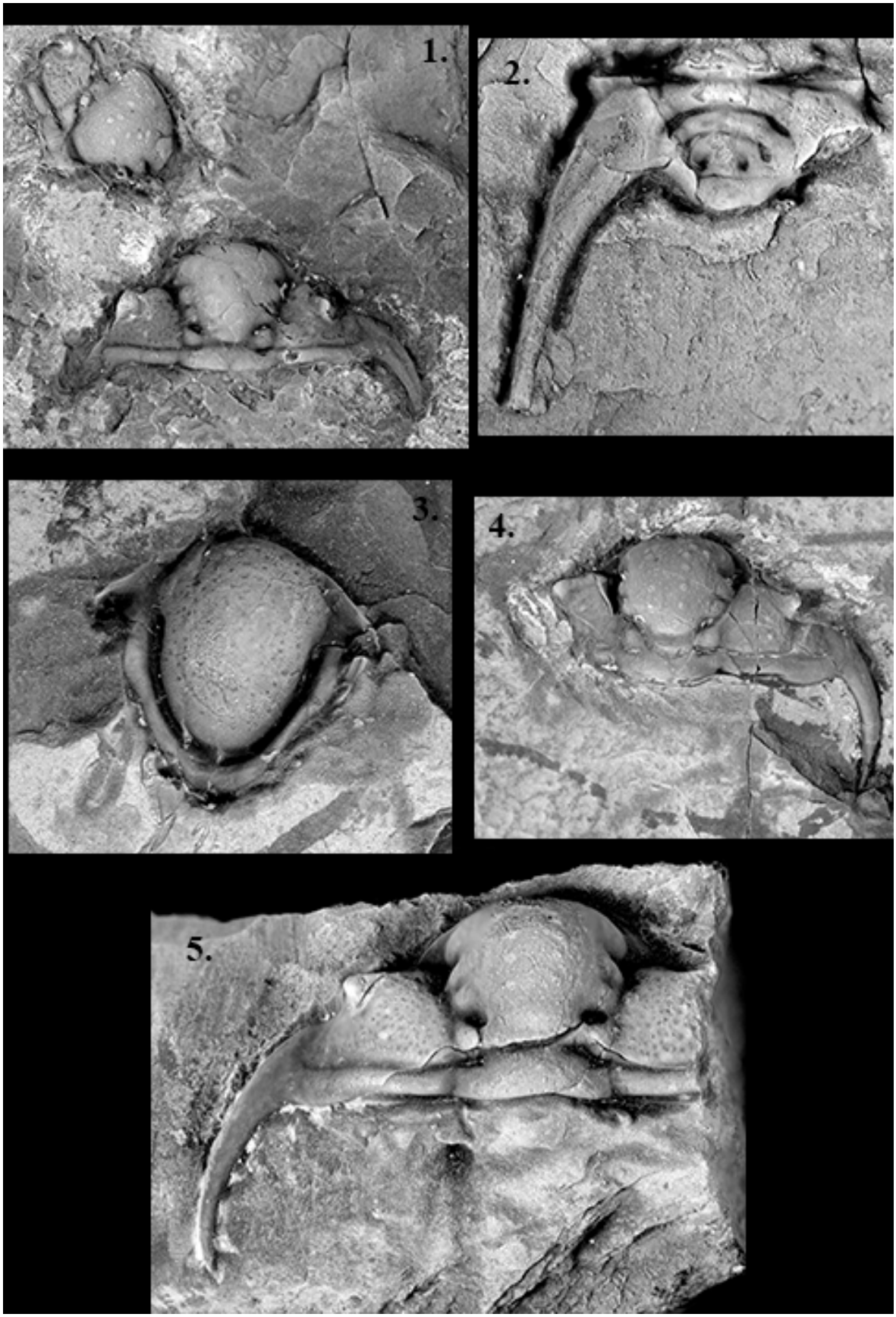
1.
2.
3.
4.
5.

Plate 8

Ceraurus pleurexanthemus Green, 1832

Figure 1: Cranidium from the Glens Falls Formation near Chazy Landing, New York KUMIP 325594, ×5.7.

Figure 2 Cranidium from the Glens Falls Formation near Chazy Landing, New York KUMIP 325595, ×5.5.

Figure 3: Cranidium from the Glens Falls Formation near Chazy Landing, New York KUMIP 325596, ×5.3.

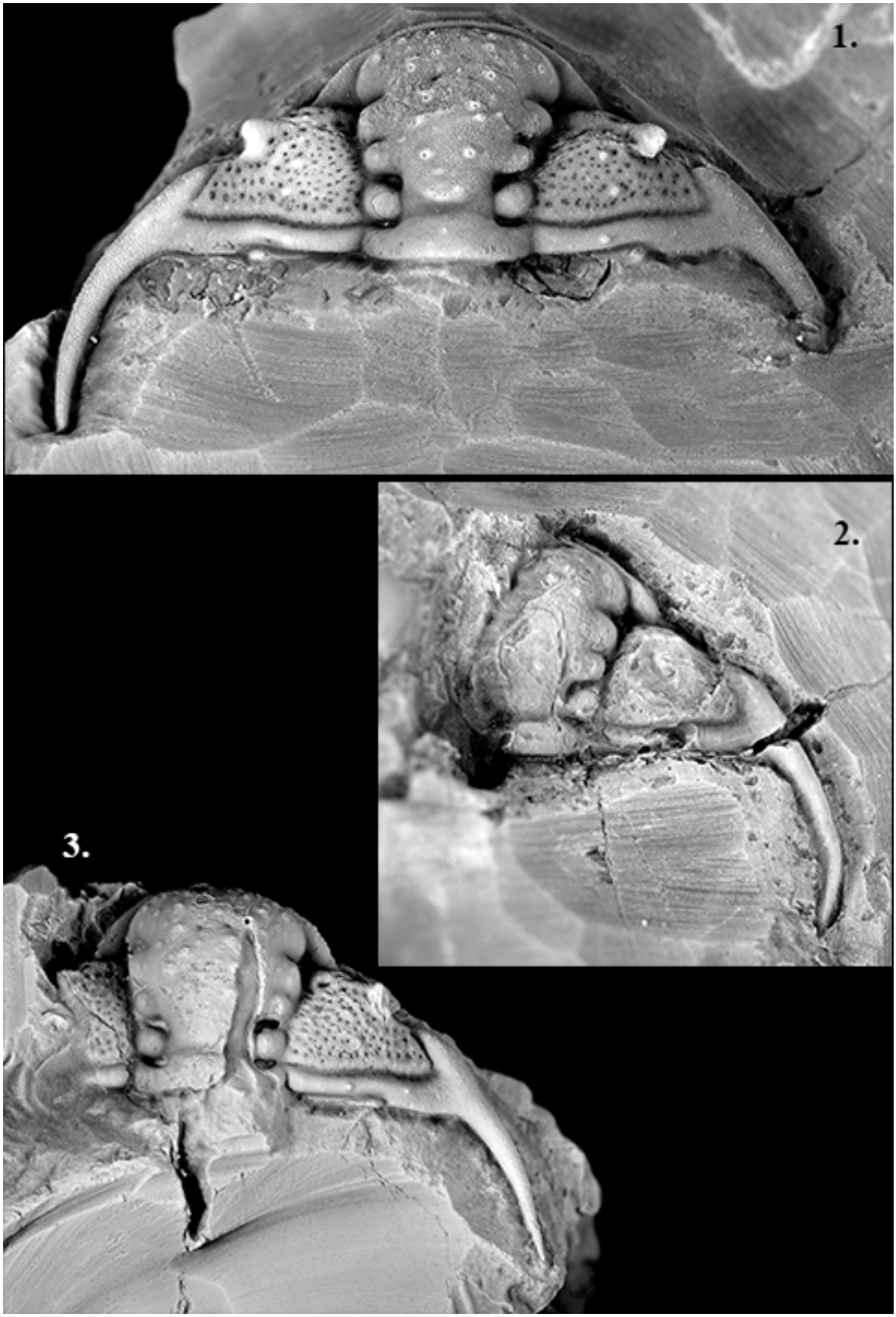
1.
2.
3.

Plate 9

Ceraurus walcotti sp. nov.

Figure 1: Holotype exoskeleton from the Rust Formation at Walcott Rust Quarry MCZ 111708, ×3.5.

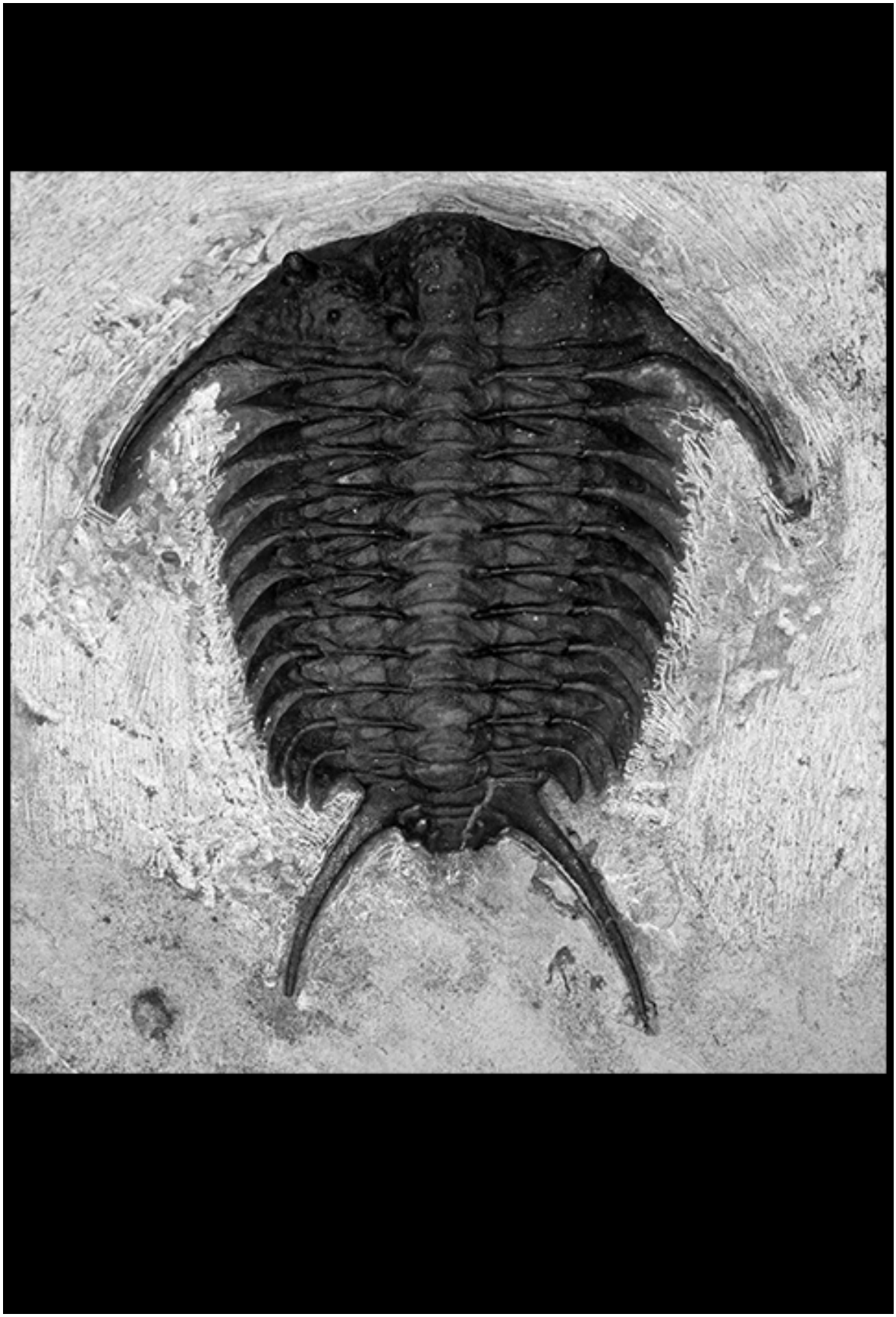

Plate 10

Ceraurus walcotti sp. nov.

Figure 1: Close up of holotype pygidium from the Rust Formation at Walcott Rust Quarry MCZ 111708, ×7.

Figure 2: Paratype upside down exoskeleton with hypostome in place from the Rust Formation at Walcott Rust Quarry MCZ 111715, ×3.6.

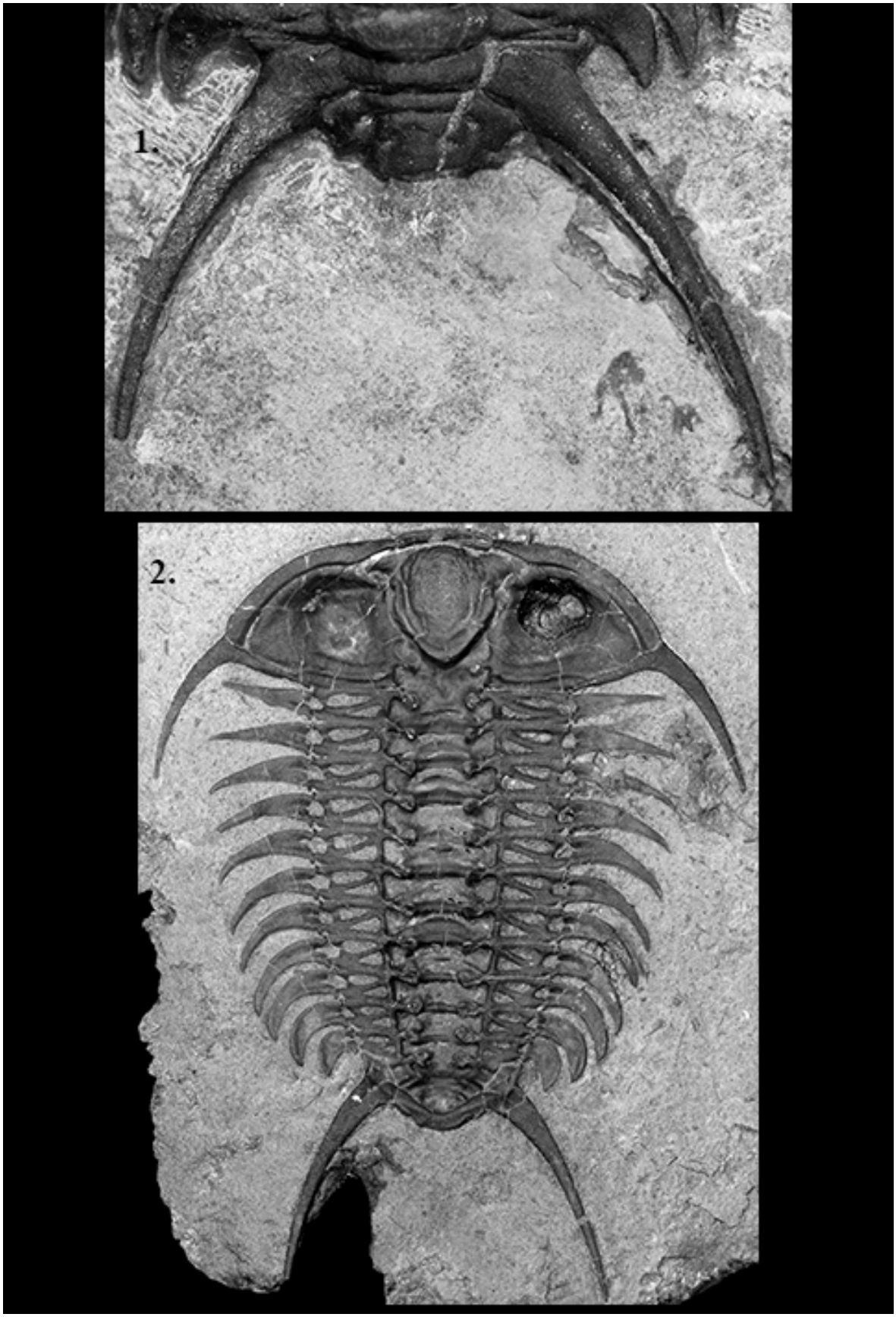
1.
2.

Plate 11

Ceraurus walcotti sp. nov.

Figure 1: Complete exoskeleton from the Neuville Formation at Neuville, Quebec, ROM 48568, ×3.7.

Figure 2: Ventral exoskeleton from the Neuville Formation at Neuville, Quebec ROM 48568, ×2.1.

Figure 3: Complete exoskeleton from the Neuville Formation at Neuville, Quebec ROM 48568, ×4.2.

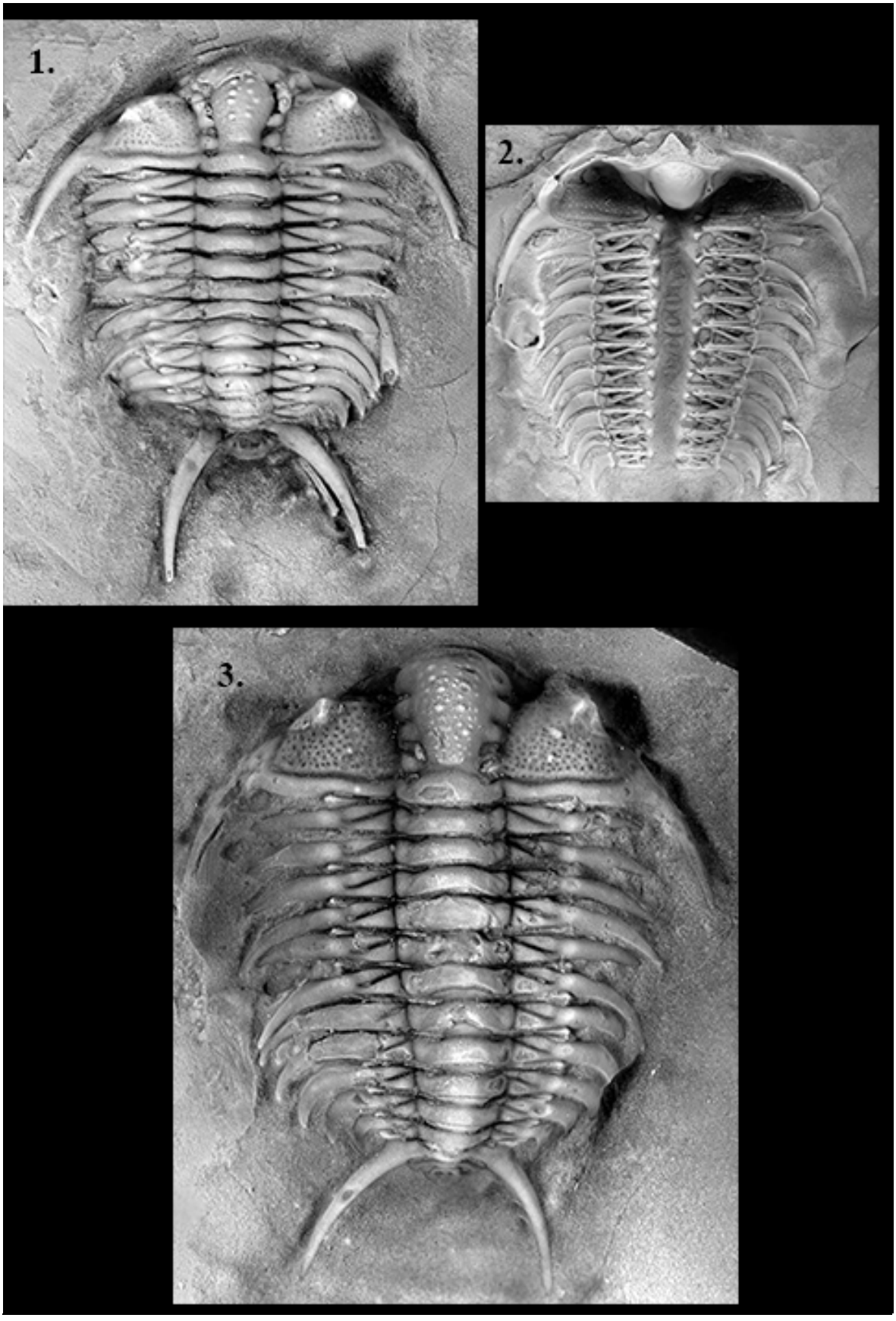
1.
2.
3.

Plate 12

Ceraurus plattinensis Foerste, 1920

Figure 1: Holotype exoskeleton from the Plattin Limestone near New London, Missouri USNM 78441, ×1.3. Photograph from Thomas Whitely.

Figure 2: Broken cranidium with bryozoans growing on the cheeks from the Kings Lake Limestone in the Decorah Formation near New London, Missouri KUMIP 325597, ×2.2.

Figure 3: Cranidium from the Kings Lake Limestone in the Decorah Formation near New London, Missouri KUMIP 325598, ×3.8.

Figure 4: Cranidium from Kings Lake Limestone in the Decorah Formation near New London, Missouri KUMIP 325599, ×2.5.

Figure 5: Pygidium from the Kings Lake Limestone in the Decorah Formation near New London, Missouri KUMIP 325600, ×4.5.

Figure 6: Cranidium from the Kings Lake Limestone in the Decorah Formation near New London, Missouri KUMIP 325601, ×3.

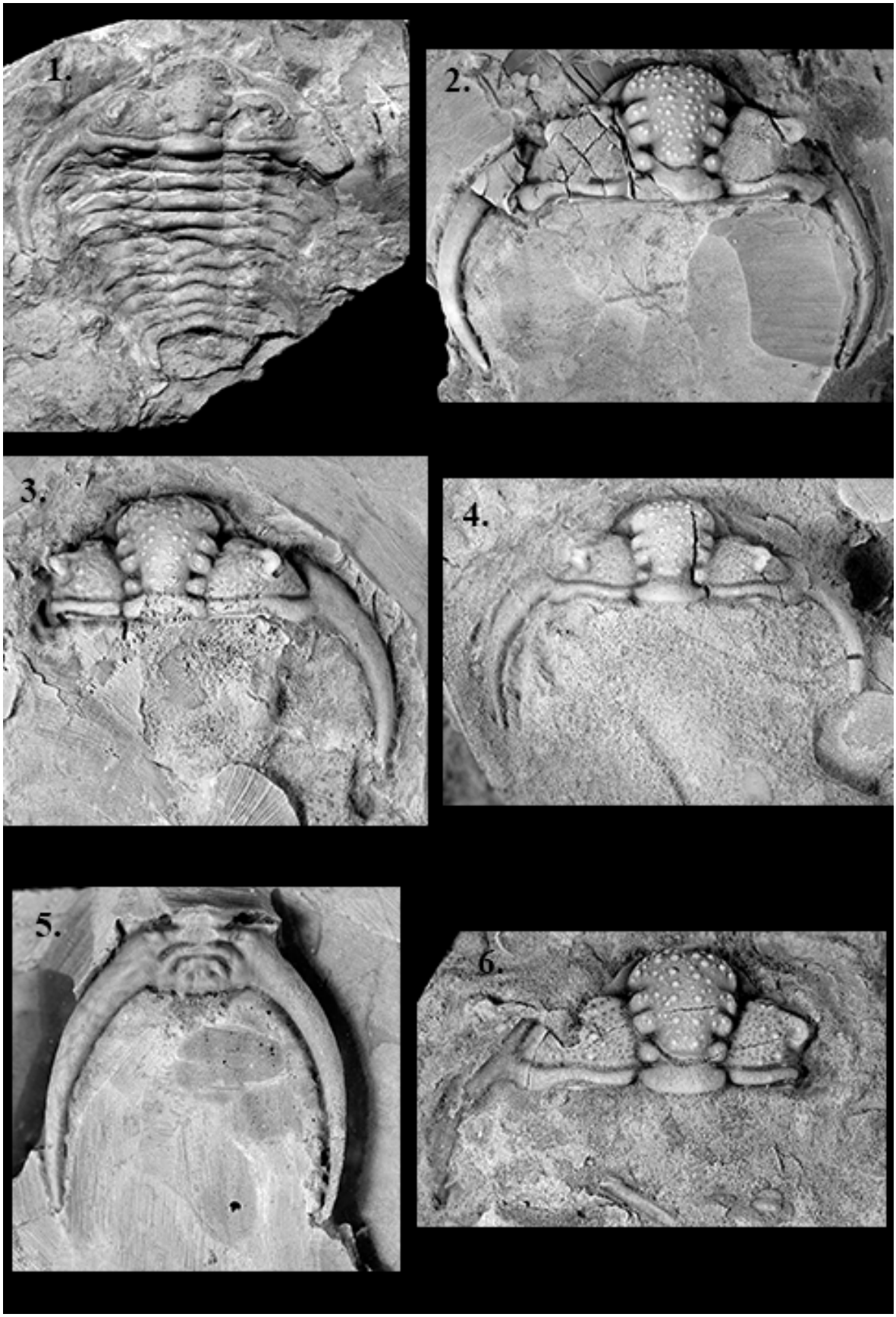
1.
2.
3.
4.
5.
6.

Plate 13

Ceraurus plattinensis Foerste, 1920

Figure 1: Nearly complete exoskeleton with a Pterygometopid cranidium from the Kings Lake Limestone in the Decorah Formation near New London, Missouri KUMIP 325602, ×2.8. Photograph from Thomas Whitely.

Figure 2: Hypostome from the Kings Lake Limestone in the Decorah Formation near New London, Missouri KUMIP 325603, ×6.6.

Figure 3: Three cranidia showing the variability of the posterior border lobe in the species from the Kings Lake Limestone in the Decorah Formation near New London, Missouri KUMIP 325604-6, ×3.3.

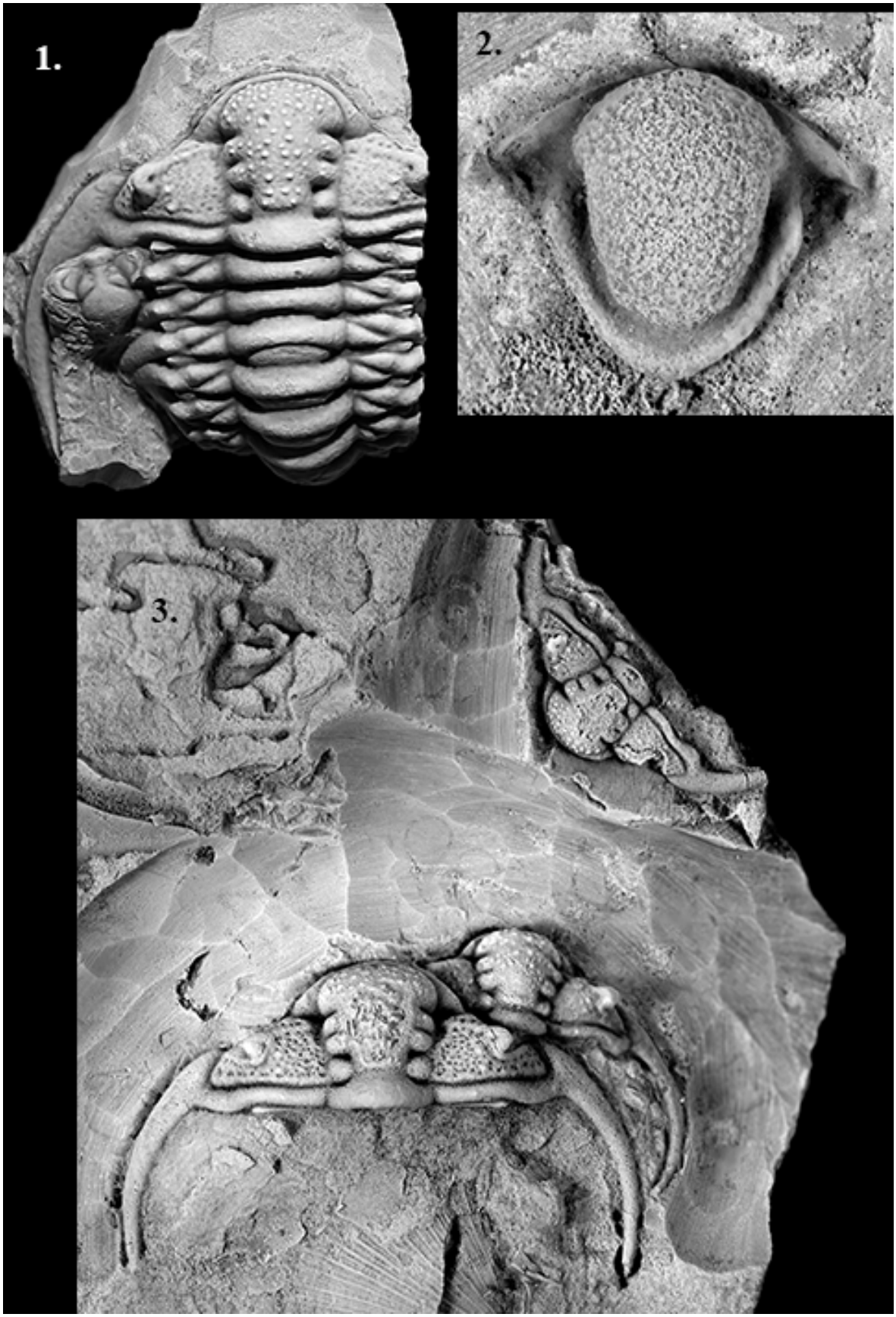
1.
2.
3.

Plate 14

Ceraurus plattinensis Foerste, 1920

Figure 1: Cranidium from the Kings Lake Limestone in the Decorah Formation near New London, Missouri KUMIP 325607, ×3.1.

Figure 2: Pygidium from the Kings Lake Limestone in the Decorah Formation near New London, Missouri KUMIP 325608, ×3.3. Dark substance on the specimen is a hard epoxy used to stabilize the specimen during the preparation.

Figure 3: Pygidium from the Kings Lake Limestone in the Decorah Formation near New London, Missouri KUMIP 325609, ×2.9.

Figure 4: Small pygidium from Kings Lake Limestone in the Decorah Formation near New London, Missouri KUMIP 325610, ×5.7.

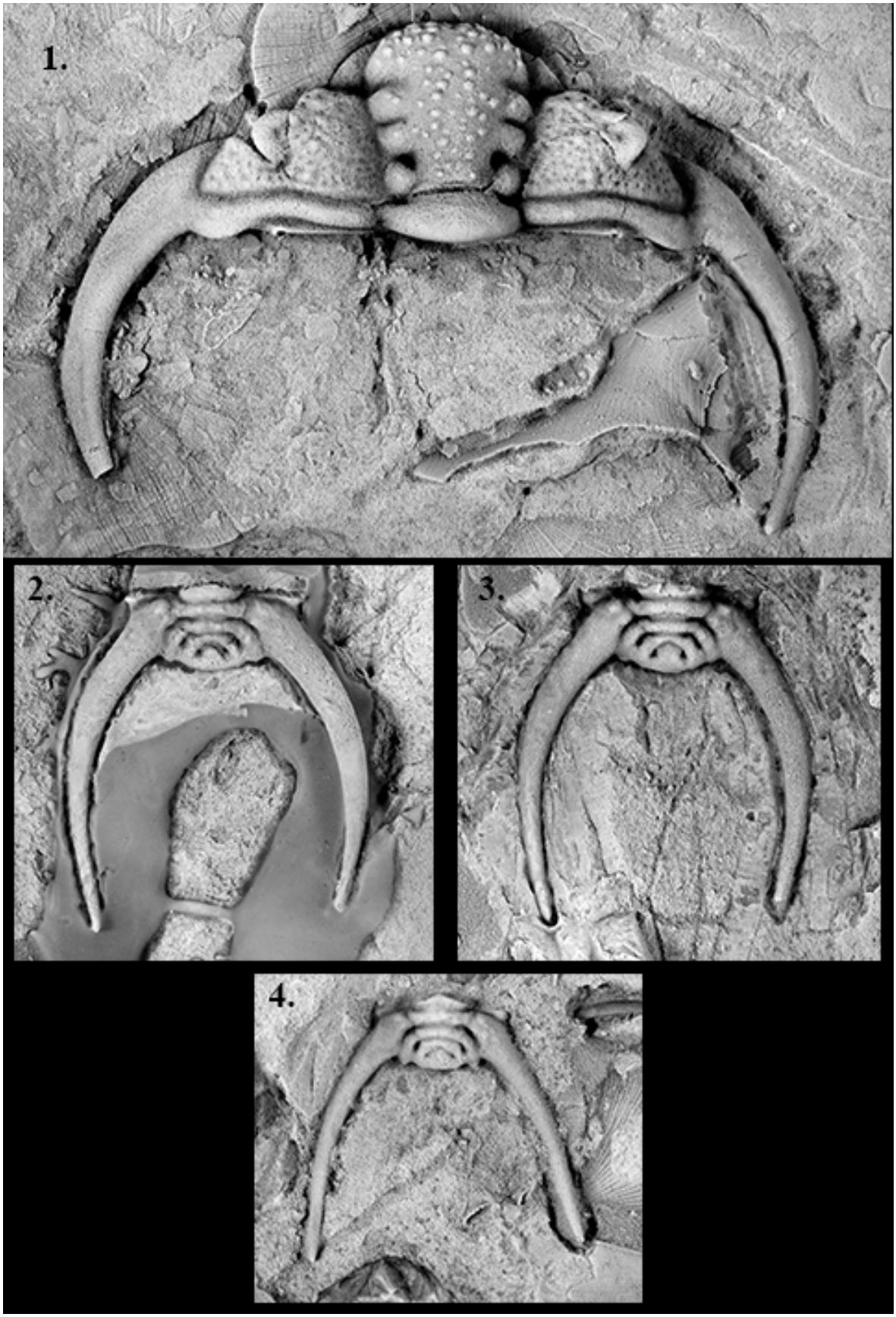
1.
2.
3.
4.

Plate 15

Ceraurus plattinensis Foerste, 1920

Figure 1: Cranidium and pygidium from the Kings Lake Limestone in the Decorah Formation near New London, Missouri KUMIP 325611-2, ×4.2.

Figure 2: Two pygidia from the Kings Lake Limestone in the Decorah Formation near New London, Missouri KUMIP 325613-4, ×8.3.

Figure 3: Hypostome from the Kings Lake Limestone in the Decorah Formation near New London, Missouri KUMIP 325615, ×5.8.

Figure 4: Partial pygidium from Kings Lake Limestone in the Decorah Formation near New London, Missouri KUMIP 325616, × 3.3.

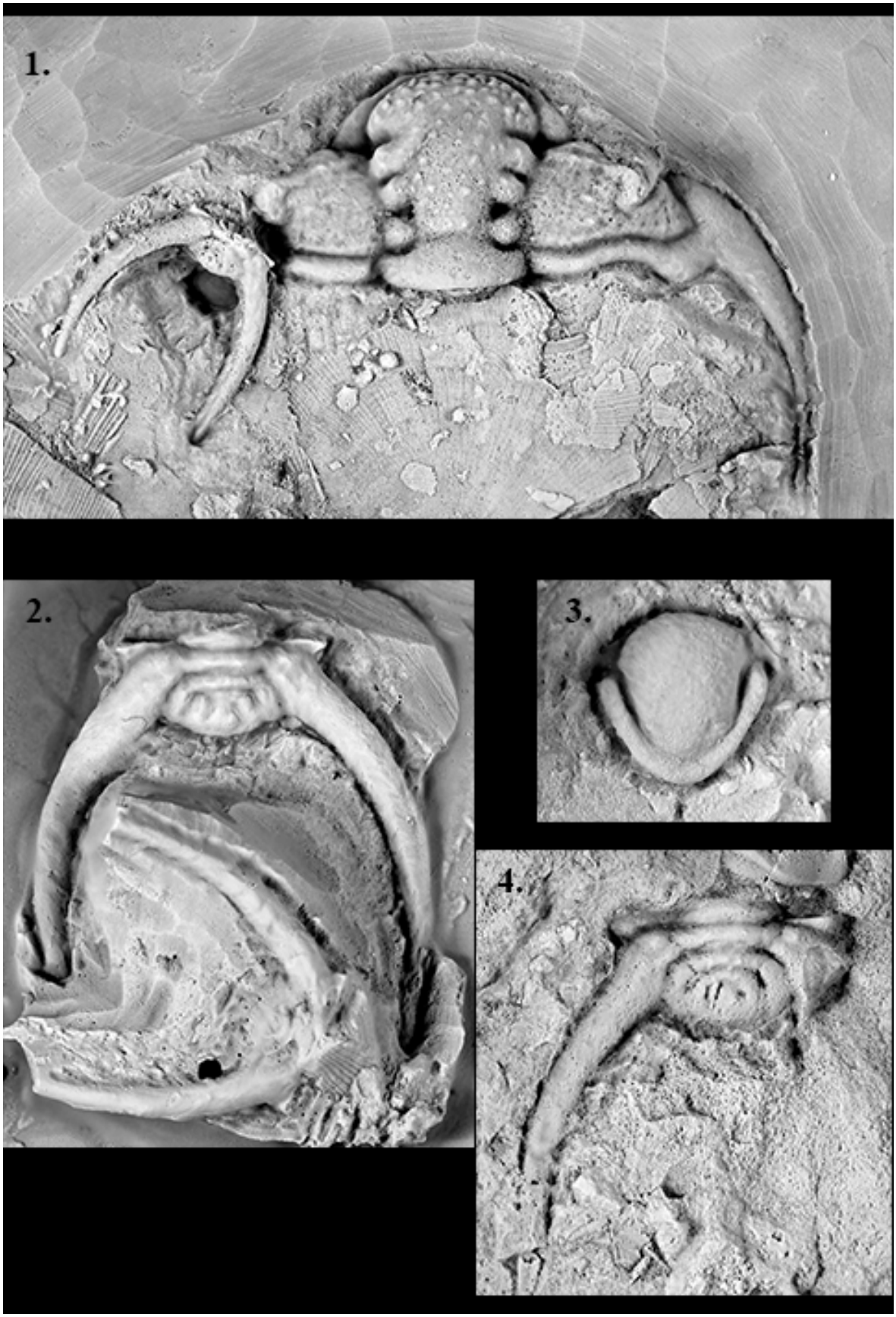
1.
2.
3.
4.

Plate 16

Ceraurus paraplattinensis sp. nov.

Figure 1: Cephalon and thorax of the holotype from the Bobcaygeon Formation near Brechin, Ontario ROM 48775, ×3.5.

Figure 2: Pygidium of the holotype from the Bobcaygeon Formation near Brechin, Ontario ROM 48775, ×7.4.

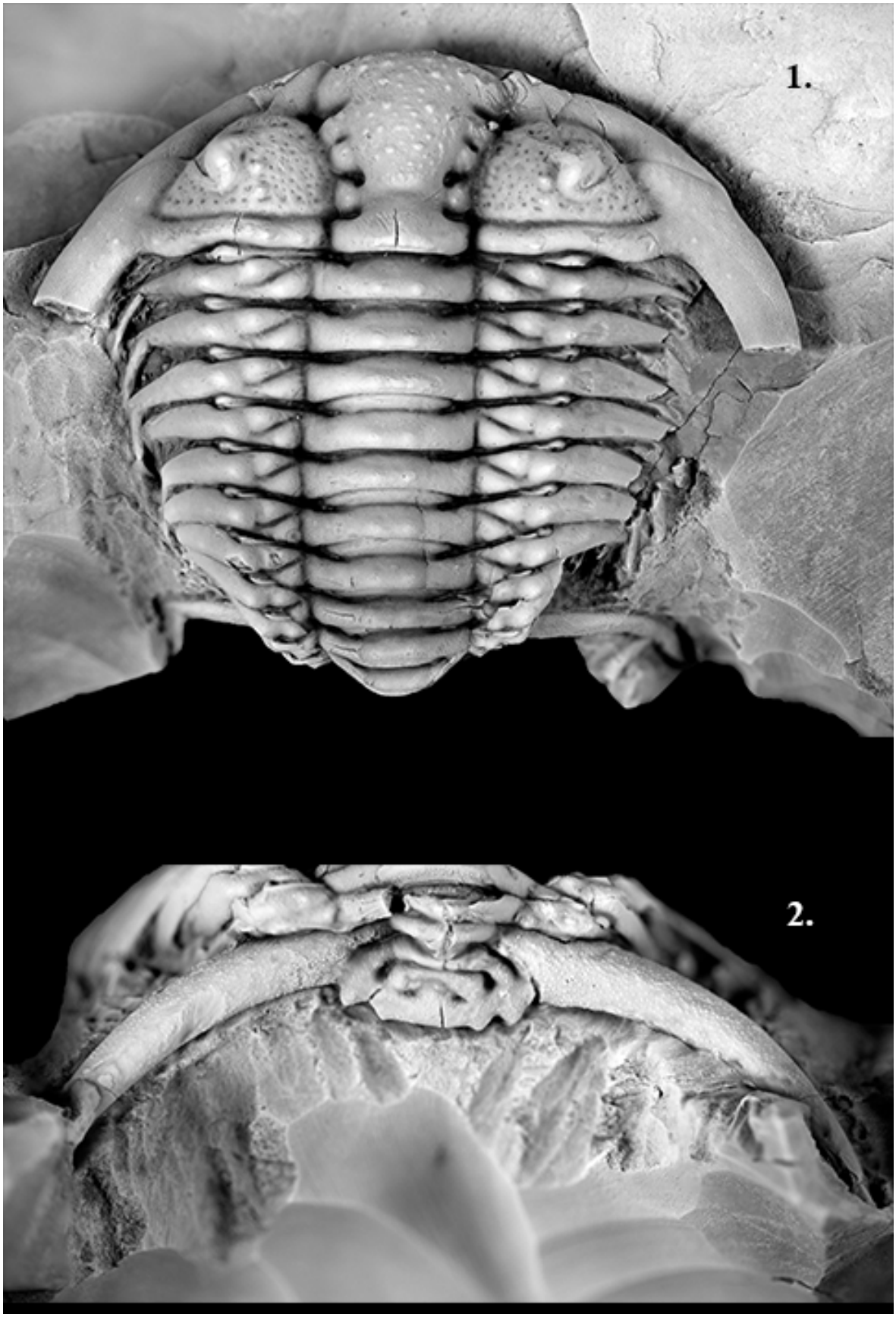
1.
2.

Plate 17

Ceraurus paraplattinensis sp. nov.

Figure 1: Exoskeleton from the Bobcaygeon Formation near Brechin, Ontario GSC 137131, ×5.3.

Figure 2: Hypostome of the same specimen from the Bobcaygeon Formation near Brechin, Ontario GSC 137131, ×6.3.

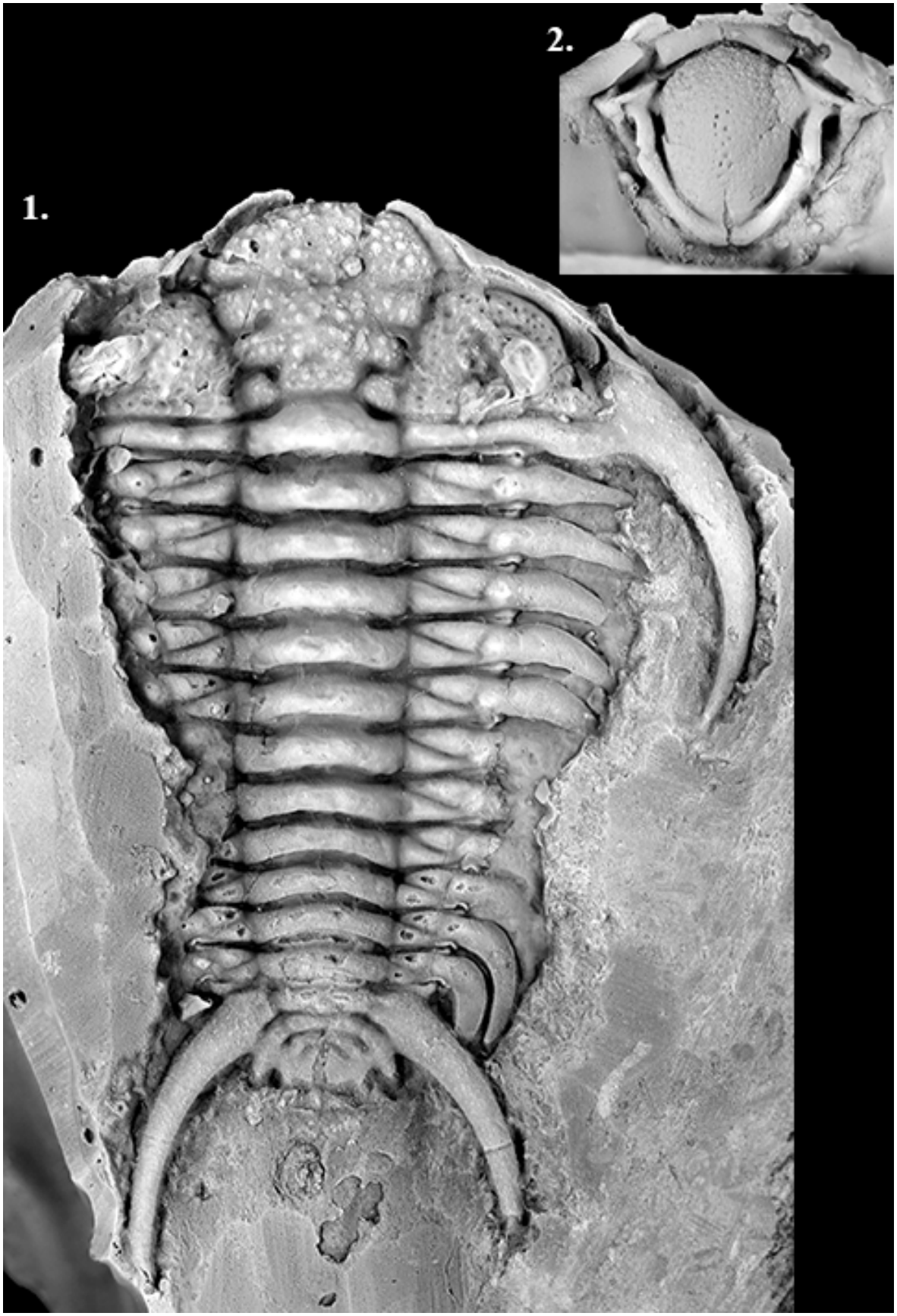
1.
2.

Plate 18

Ceraurus paraplattinensis sp. nov.

Figure 1: Complete exoskeleton from the Bobcaygeon Formation near Brechin, Ontario ROM 48565, ×3.4. Cephalon crushed and there is some evidence of restoration on the left genal spine, as well as the right anterior side of the cephalon and the anterior-most portion of the glabella.

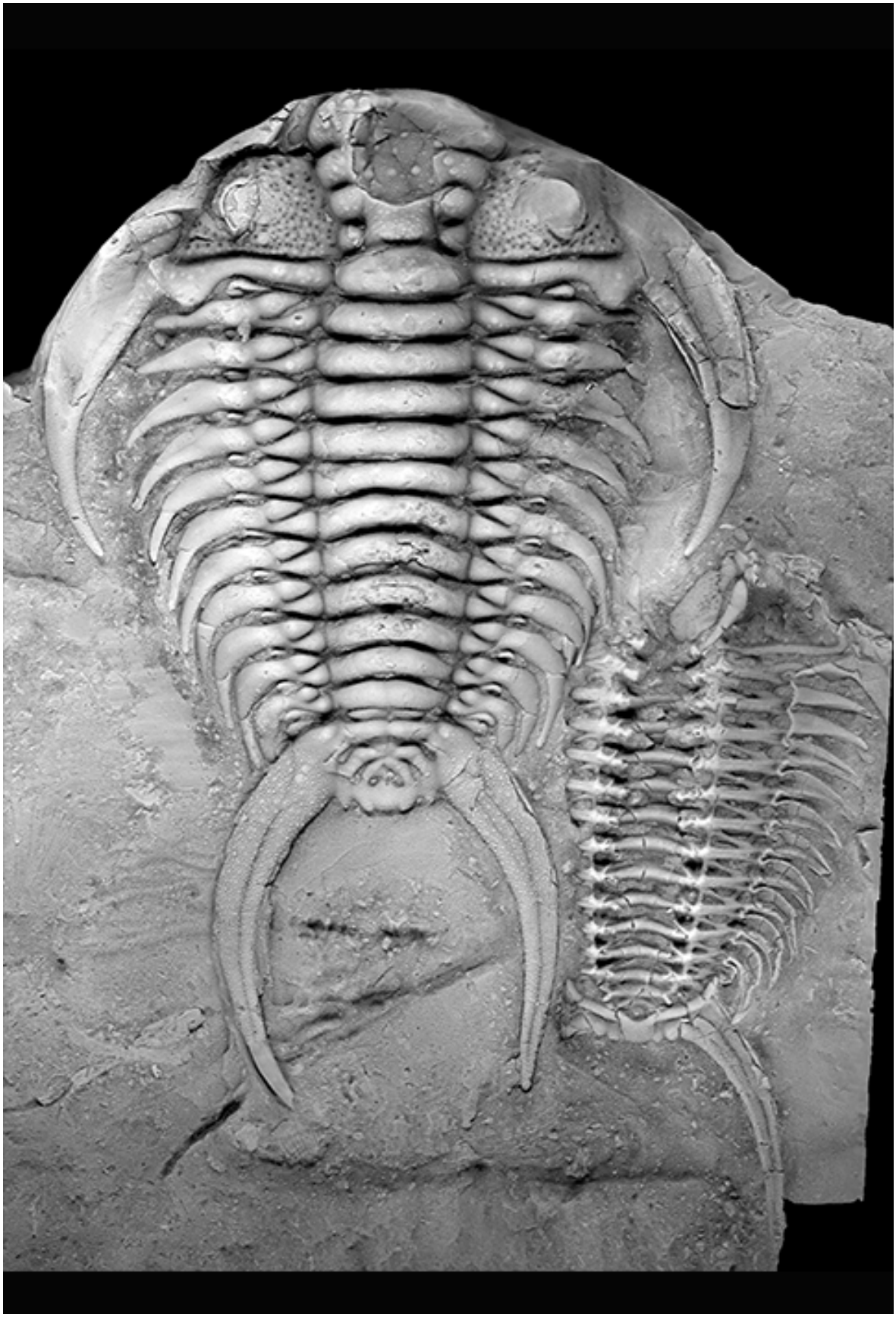

Plate 19

Ceraurus bispinosus Raymond and Barton, 1913

Figure 1: Dorsal view of holotype cranidium from the Leray? beds near Tetreauville, ROM 18682, ×3.1. Photograph from Janet Waddington.

Figure 2: Dorso-ventral view of holotype cranidium from the Leray? beds near Tetreauville, ROM 18682, ×2.6. Photograph from Janet Waddington.

Ceraurus matranseris Sinclair, 1947

Figure 3: Holotype cranidium from the Shipshaw Formation near Roberval, Quebec GSC 6801, ×8.1.

Figure 4: Paratype pygidium from the Shipshaw Formation near Roberval, Quebec GSC 7395, ×6.1.

Figure 5: Cranidium from the Lindsay Formation near Picton, Ontario GSC 137132, ×2.8.

Figure 6: Pygidium from the Shipshaw Formation near Chicoutimi, Quebec GSC 6801, ×3.2.


1.
2.
3.
4.
5.
6.

Plate 20

Ceraurus matranseris Sinclair, 1947

Figure 1: Cranidium from the Shipshaw Formation near Lake Manicouagan, Quebec, GSC 92985, ×4.5.

Ceraurus globulobatus Bradley, 1930

Figure 2: Cranidium from the Kimmswick Limestone near Defiance, Missouri KUMIP 325664, ×2.6.

Figure 3: Cranidium from the Kimmswick Limestone near Defiance, Missouri KUMIP 325665, ×3.0.

Figure 4: Cranidium from the Kimmswick Limestone near Defiance, Missouri KUMIP 325663, ×4.7.

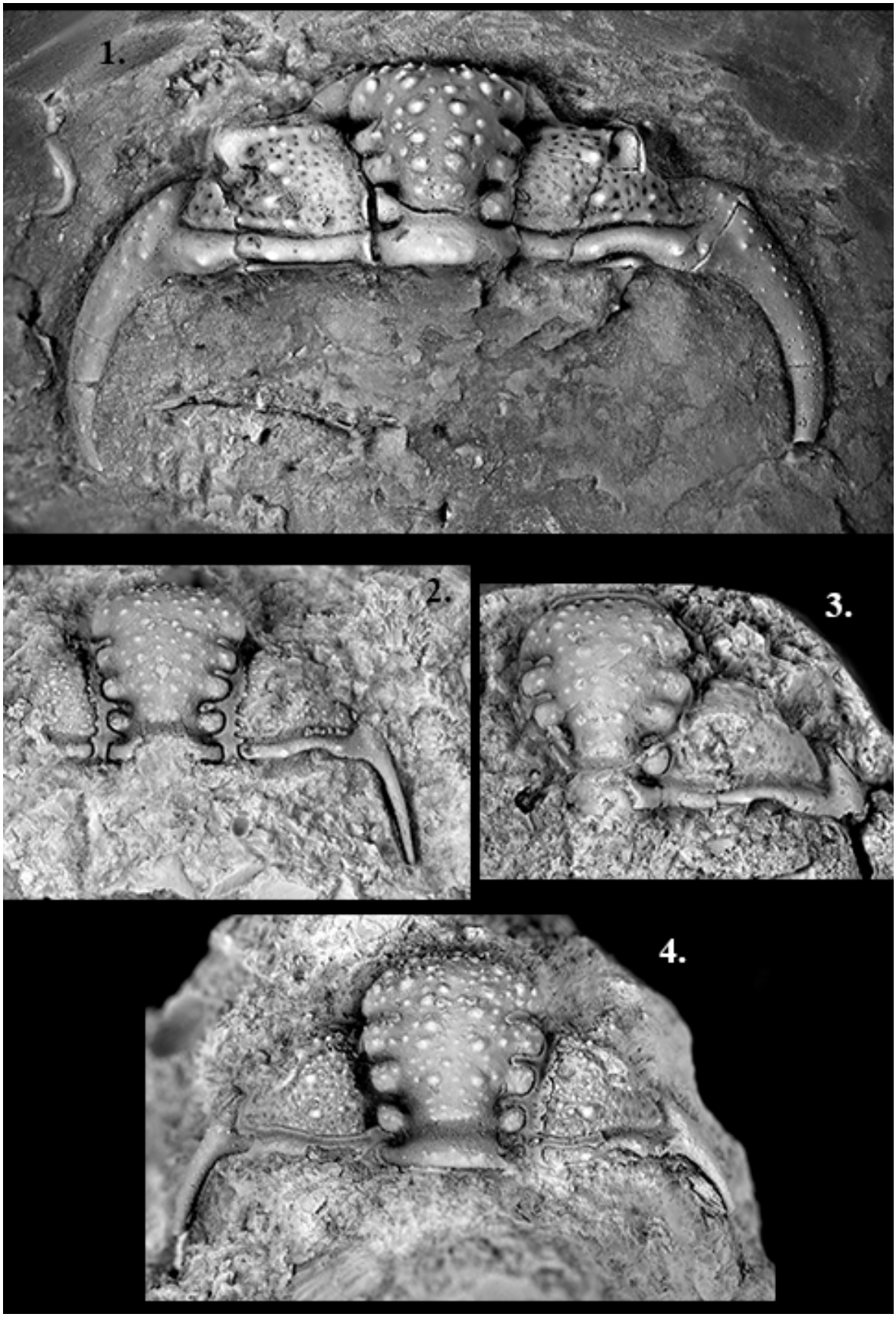
1.
2.
3.
4.

Plate 21

Ceraurus cf. *globulobatus* Bradley, 1930

Figure 1: Three complete exoskeletons from the Bobcaygeon Formation near Brechin, Ontario ROM 48566, ×2.5.

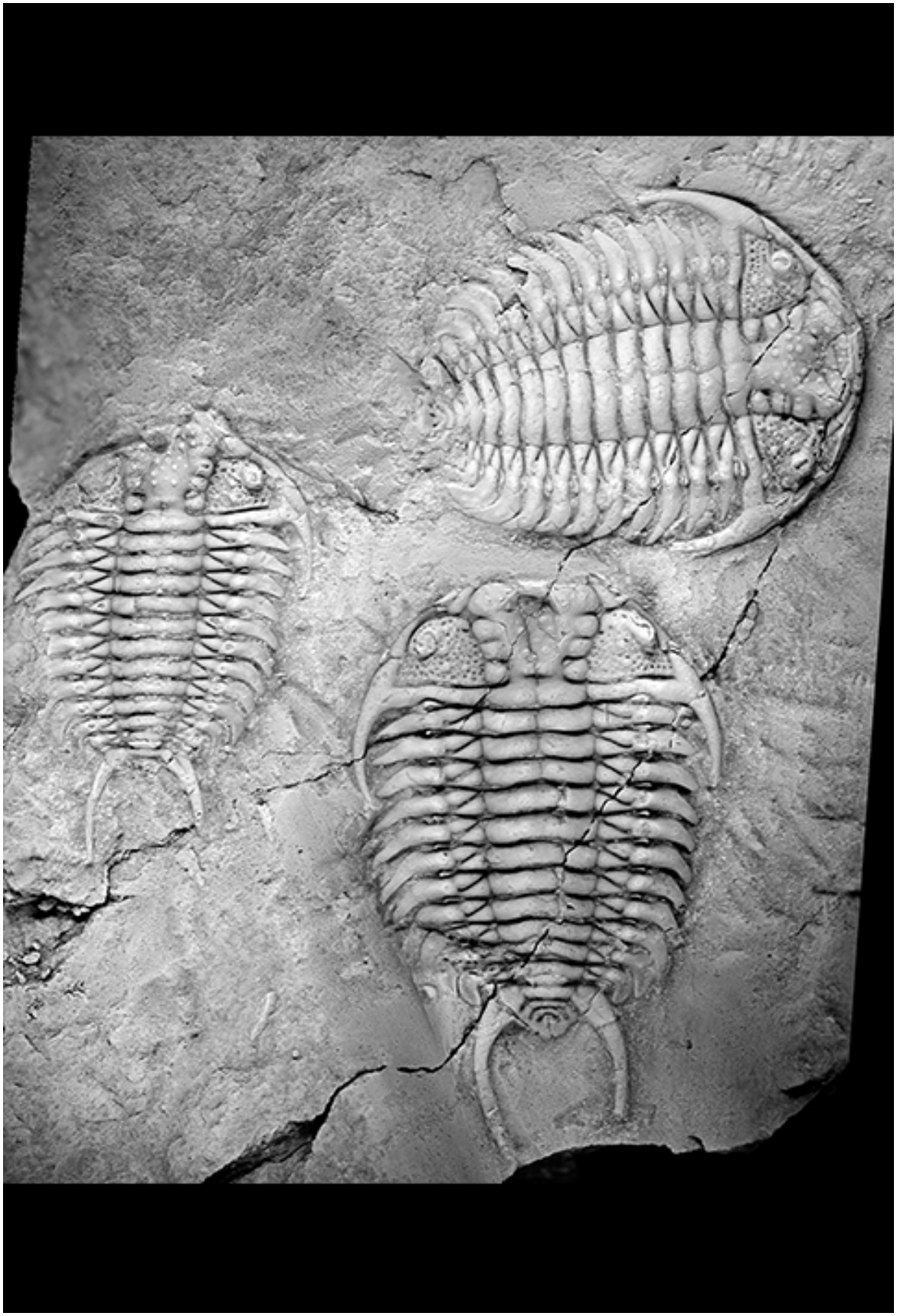

Plate 22

Ceraurus cf. *globulobatus* Bradley, 1930

Figure 1: Complete exoskeleton from the Bobcaygeon Formation near Brechin, Ontario GSC 137133, ×3.0.

Figure 2: Complete exoskeleton from the Bobcaygeon Formation near Ottawa, Ontario ROM 46075, ×3.0.

Figure 3: Cranidium from the Bobcaygeon Formation near Belleville, Ontario GSC 137138, ×2.3

Ceraurus ruidus Cooper, 1953

Figure 4: Holotype cranidium from the Edinburg Formation near Catawba Sanitorium, Virginia USNM 116466a, ×1.5. Photograph from Thomas Whitely.

Figure 5: Cranidium from the Edinburg Formation near Catawba Sanitorium, Virginia USNM 116466b, ×1.1. Photograph from Thomas Whitely.

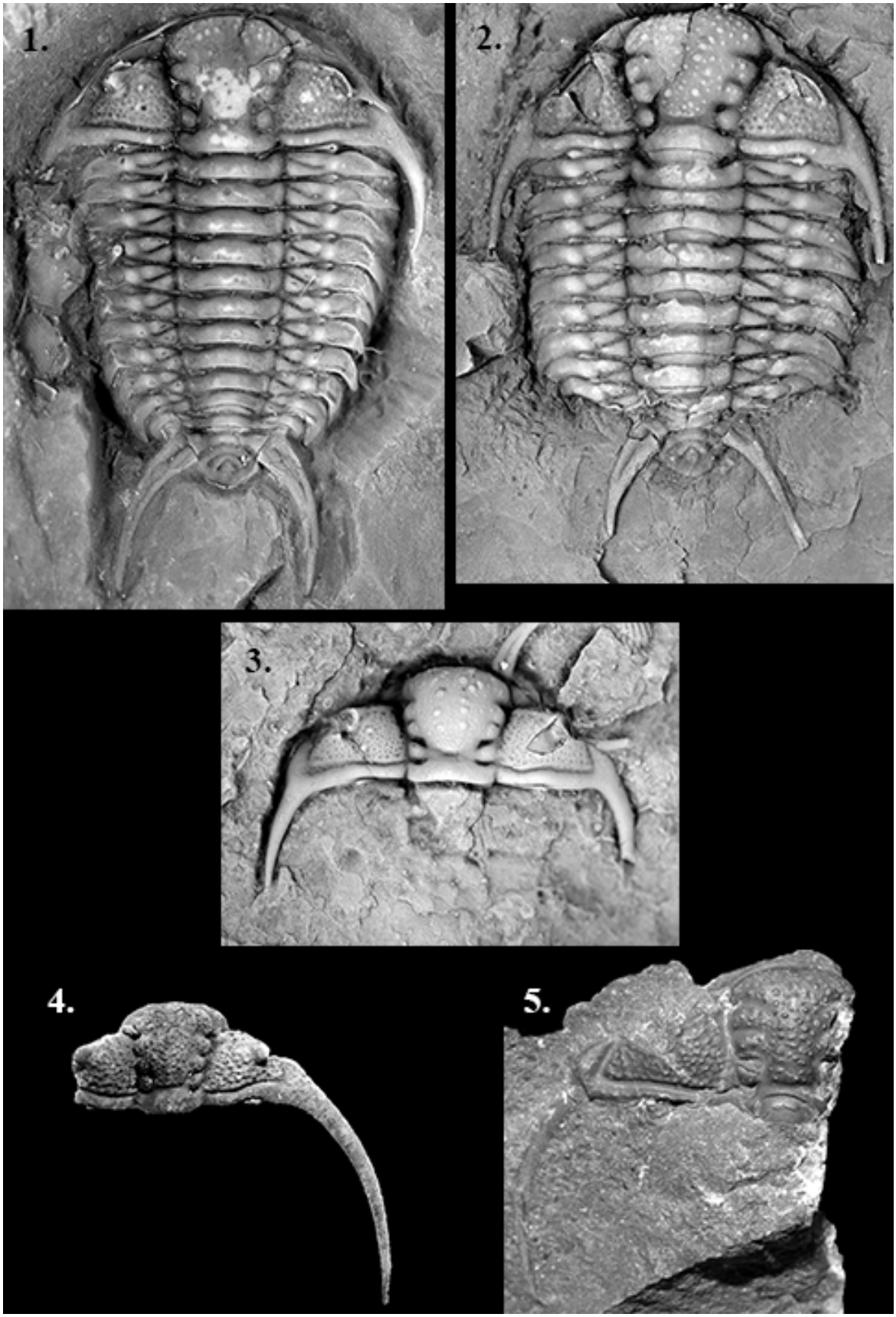
1.
2.
3.
4.
5.

Plate 23

Ceraurus mifflinensis (DeMott, 1987)

Figure 1: Cranidium from the Mifflin Member of the Plattville Group near Fennimore, Wisconsin KUMIP 325619, ×3.8.

Figure 2: Hypostome with smooth posterior border from the Mifflin Member of the Plattville Group near Fennimore, Wisconsin KUMIP 325620, ×3.6.

Figure 4: Two cranidia from the Mifflin Member of the Plattville Group near Fennimore, Wisconsin KUMIP 325622-3, ×3.4.

Figure 5: Cranidia from the Mifflin Member of the Plattville Group near Fennimore, Wisconsin KUMIP 325624, ×3.2.

Figure 6: Cephalon and thorax showing the large raised spines on the axial ring and pleurae of the thorax from Mifflin Member of the Plattville Group near Fennimore, Wisconsin KUMIP 325625, ×3.7.

Ceraurus jenlorum sp. nov.

Figure 3: Hypostome with spines on the posterior border from the Mifflin Member of the Plattville Group near Fennimore, Wisconsin KUMIP 325621, ×3.5.

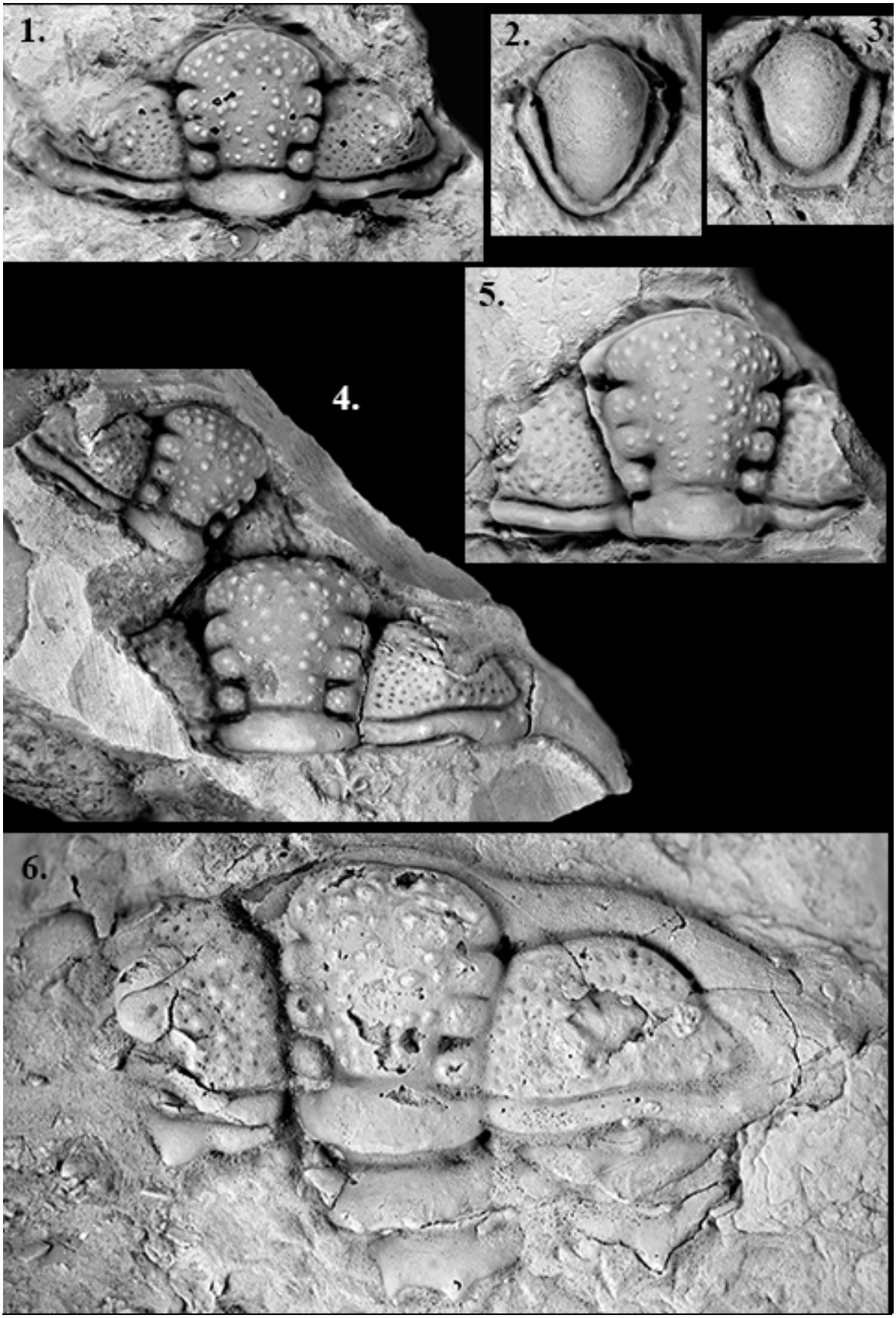
1.
2.
3.
4.
5.
6.

Plate 24

Ceraurus mifflinensis (DeMott, 1987)

Figure 1: Cranidium from the Mifflin Member of the Plattville Group near Fennimore, Wisconsin KUMIP 325626, ×3.5.

Figure 2: Partial pygidium from the Mifflin Member of the Plattville Group near Fennimore, Wisconsin KUMIP 325627, × 4.3.

Figure 3: Partial pygidium from the Mifflin Member of the Plattville Group near Fennimore, Wisconsin KUMIP 325628, × 2.8.

Figure 4: Partial pygidium from the Mifflin Member of the Plattville Group near Fennimore, Wisconsin KUMIP 325629, × 2.8.

Figure 5: Partial pygidium from the Mifflin Member of the Plattville Group near Fennimore, Wisconsin KUMIP 325630, × 2.6.


1.
2.
3.
4.
5.

Plate 25

Ceraurus mifflinensis (DeMott, 1987)

Figure 1: Hypostome from the Mifflin Member of the Plattville Group near Fennimore, Wisconsin KUMIP 325631, ×6.5.

Figure 2: Hypostome from the Mifflin Member of the Plattville Group near Fennimore, Wisconsin KUMIP 325632, ×6.8.

Figure 3: Oblique angle of thorax from the Mifflin Member of the Plattville Group near Fennimore, Wisconsin KUMIP 325633, ×6.

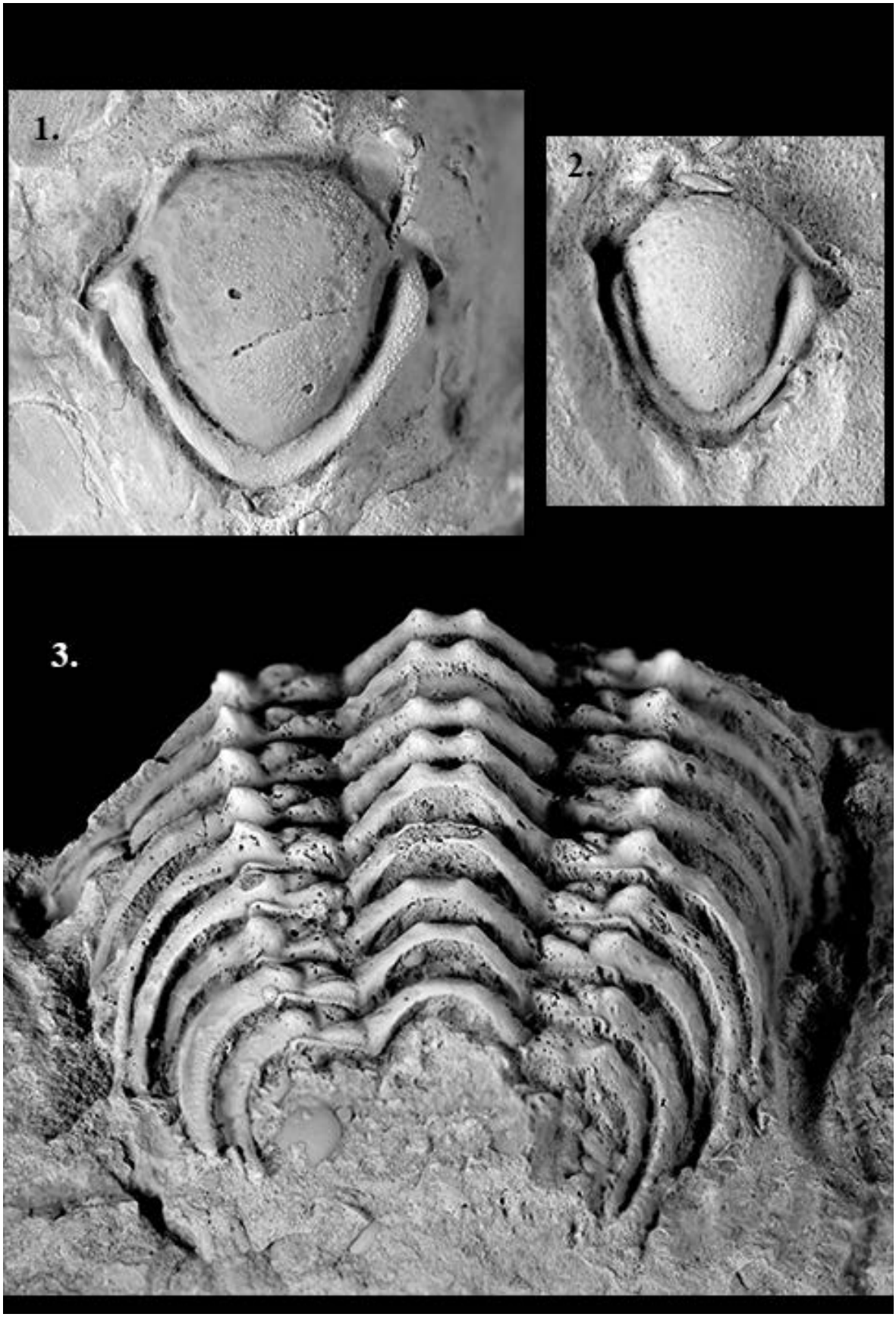
1.
2.
3.

Plate 26

Ceraurus jenlorum sp. nov.

Figure 1: Holotype exoskeleton from the Mifflin Member of the Plattville Group near Fennimore, Wisconsin KUMIP 325634, ×3.8.

Figure 2: Hypostome of the holotype specimen from the Mifflin Member of the Plattville Group near Fennimore, Wisconsin KUMIP 325634, ×3.9.

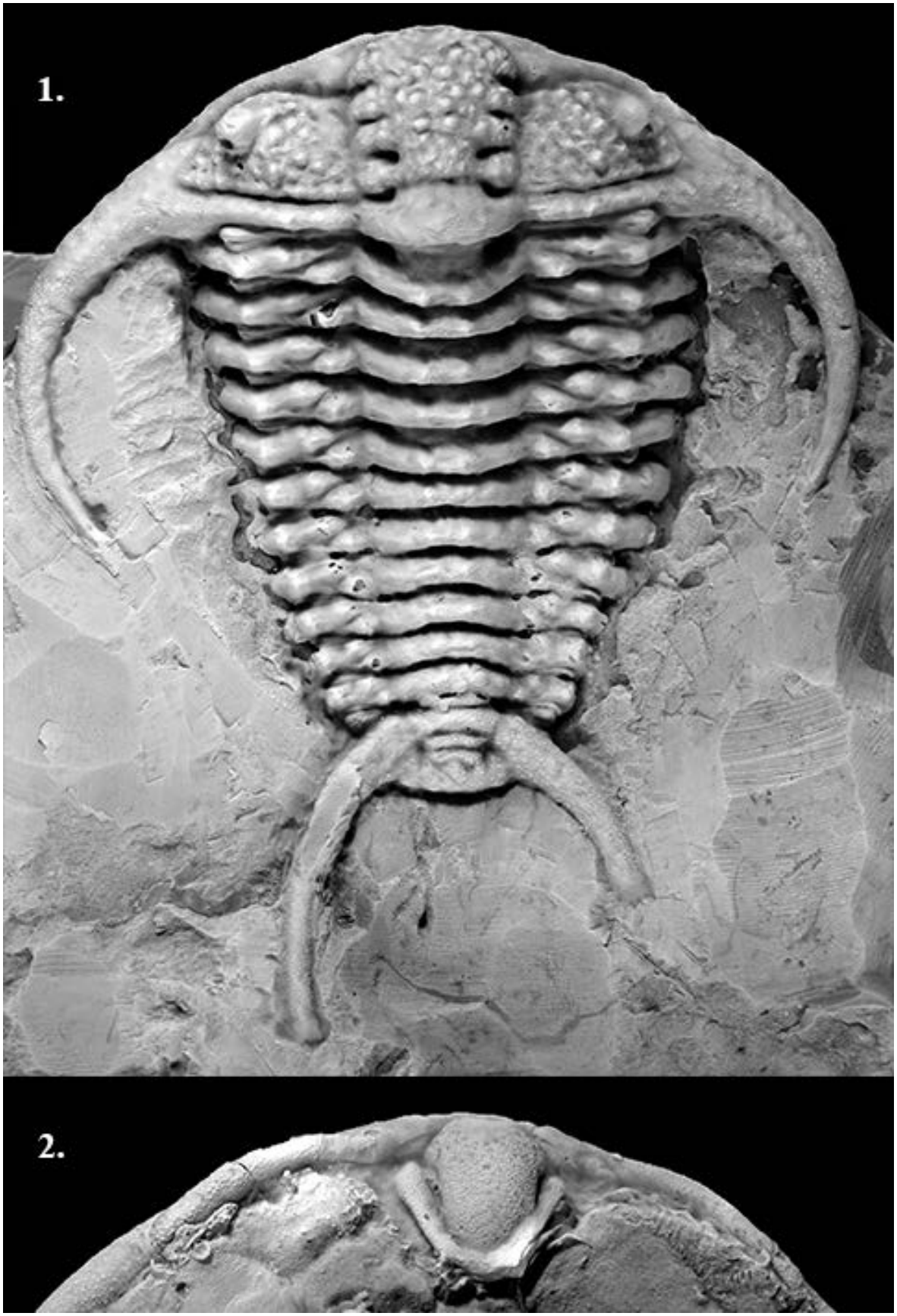
1.
2.

Plate 27

Ceraurus jenlorum sp. nov.

Figure 1: Cephalon of paratype exoskeleton from the Mifflin Member of the Plattville Group near Fennimore, Wisconsin KUMIP 325635, ×5.3.

Figure 2: Thorax and pygidium of paratype exoskeleton from the Mifflin Member of the Plattville Group near Fennimore, Wisconsin KUMIP 325635, ×4.6.

Figure 3: Pygidium from the Mifflin Member of the Plattville Group near Fennimore, Wisconsin KUMIP 325636, ×4.7.

Figure 4: Hypostome from the Mifflin Member of the Plattville Group near Fennimore, Wisconsin KUMIP 325637, ×6.1.

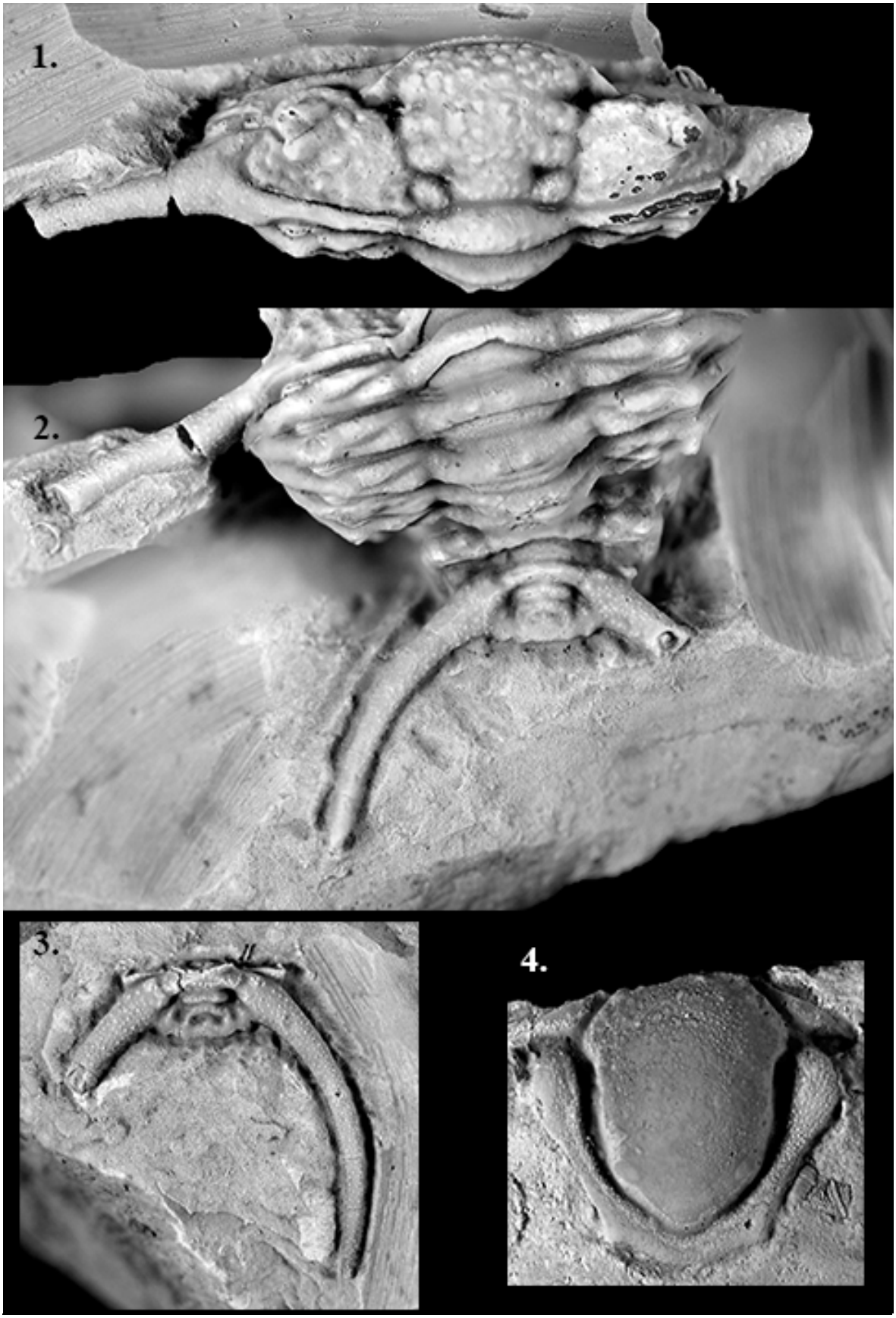
1.
2.
3.
4.

Plate 28

Ceraurus jenlorum sp. nov.

Figure 1: Cranidium and hypostome from the Mifflin Member of the Plattville Group near Fennimore, Wisconsin KUMIP 325638-9, ×4.2.

Figure 2: Cranidium from the Mifflin Member of the Plattville Group near Fennimore, Wisconsin KUMIP 325640, ×2.9.

Figure 3: Cranidium from the Mifflin Member of the Plattville Group near Fennimore, Wisconsin KUMIP 325641, ×2.5.

Figure 4: Cranidium from the Mifflin Member of the Plattville Group near Fennimore, Wisconsin KUMIP 325642, ×2.9.

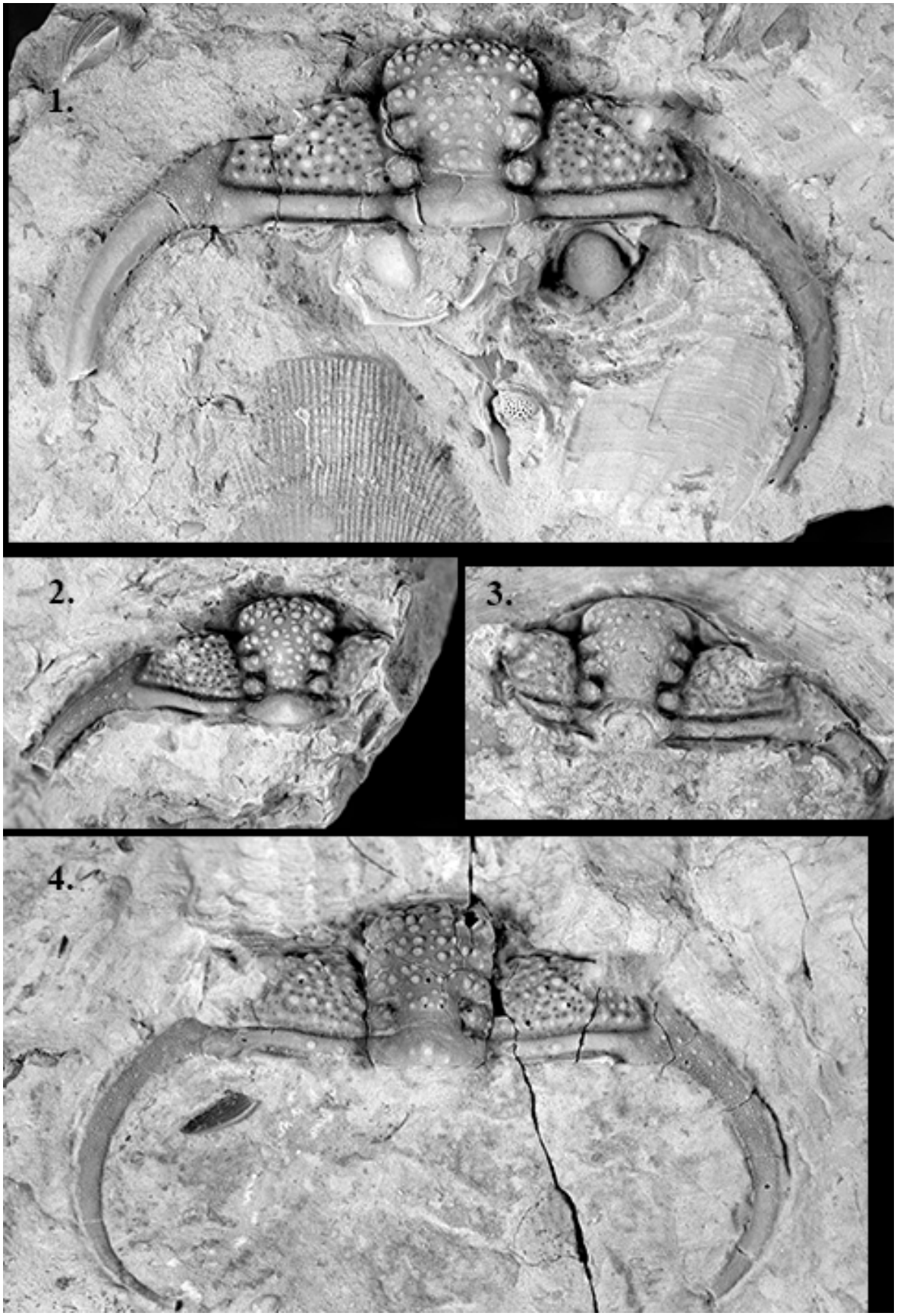
1.
2.
3.
4.

Plate 29

Ceraurus cf. *elginensis* Slocom, 1913

Figure 1: Pygidium from the Clermont Member of the Maquoketa near Clermont, Iowa KUMIP 325643, ×2.4.

Figure 2: Hypostome from the Clermont Member of the Maquoketa near Clermont, Iowa KUMIP 325644, ×6.7.

Figure 3: Pygidium from the Clermont Member of the Maquoketa near Clermont, Iowa KUMIP 325645, ×7.3.

Figure 4: Hypostome from the Clermont Member of the Maquoketa near Clermont, Iowa KUMIP 325646, ×7.1.

Figure 5: Hypostome from the Clermont Member of the Maquoketa near Clermont, Iowa KUMIP 325647, ×6.8.

Figure 6: Incomplete cephalon and thorax from the Clermont Member of the Maquoketa near Clermont, Iowa KUMIP 325648, ×6.

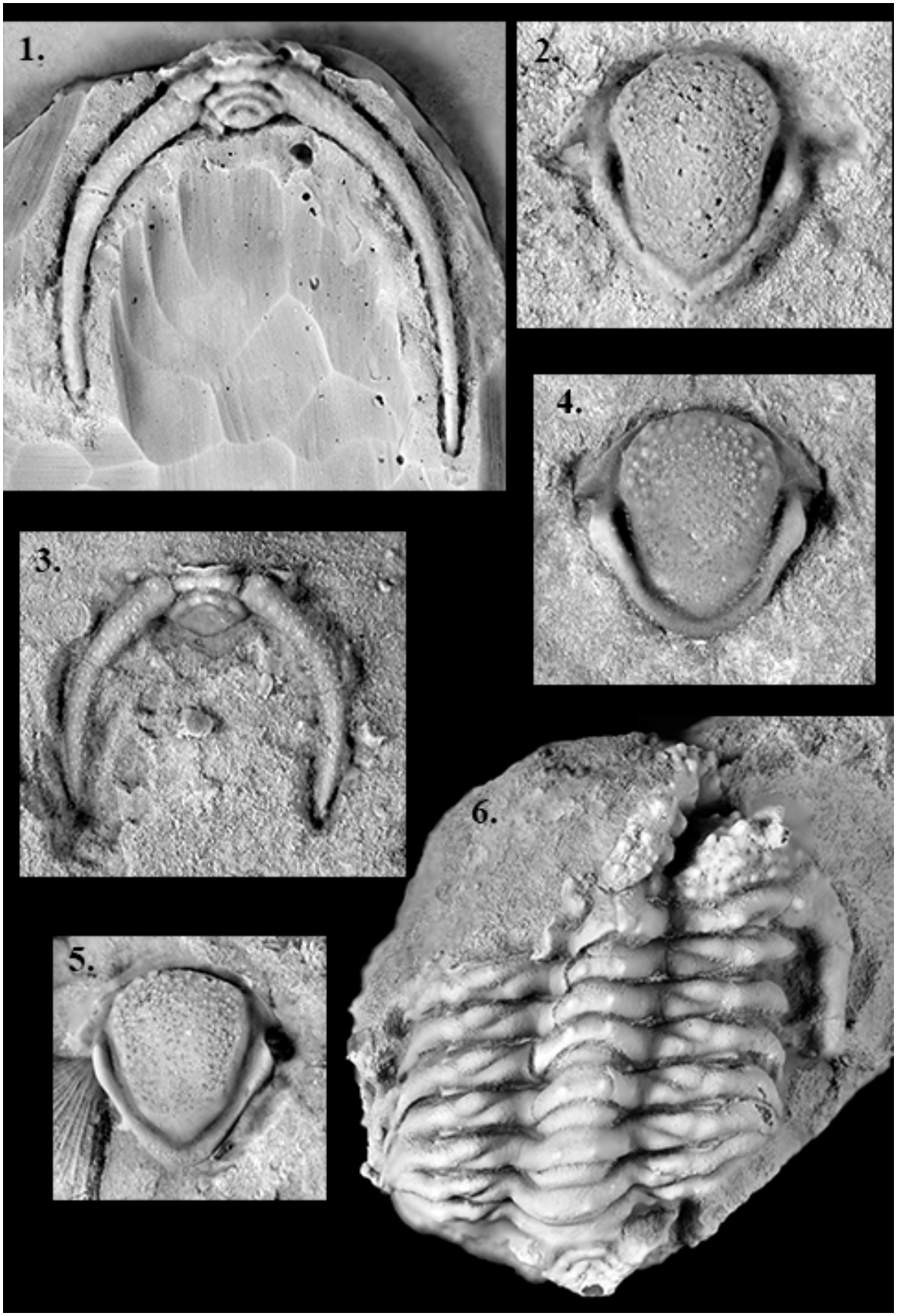
1.
2.
3.
4.
5.
6.

Plate 30

Ceraurus cf. *elginensis* Slocom, 1913

Figure 1: Cranidium and free cheek from the Clermont Member of the Maquoketa near Clermont, Iowa, KUMIP 325649-50, ×3.6.

Figure 2: Pygidium from the Clermont Member of the Maquoketa near Clermont, Iowa, KUMIP 325652, ×3.5.

Figure 3: Cranidium from the Clermont Member of the Maquoketa near Clermont, Iowa, KUMIP 325651, ×3.6

Ceraurus milleranus Miller and Gurley, 1894

Figure 4: Holotype exoskeleton from the Maysville Group near Cincinnati, Ohio UC 6062, ×1.7. Photograph from Thomas Whitely.

Figure 5: Exoskeleton from the Maysville Group near Cincinnati, Ohio USNM 33459, ×0.9. Photograph from Thomas Whitely.

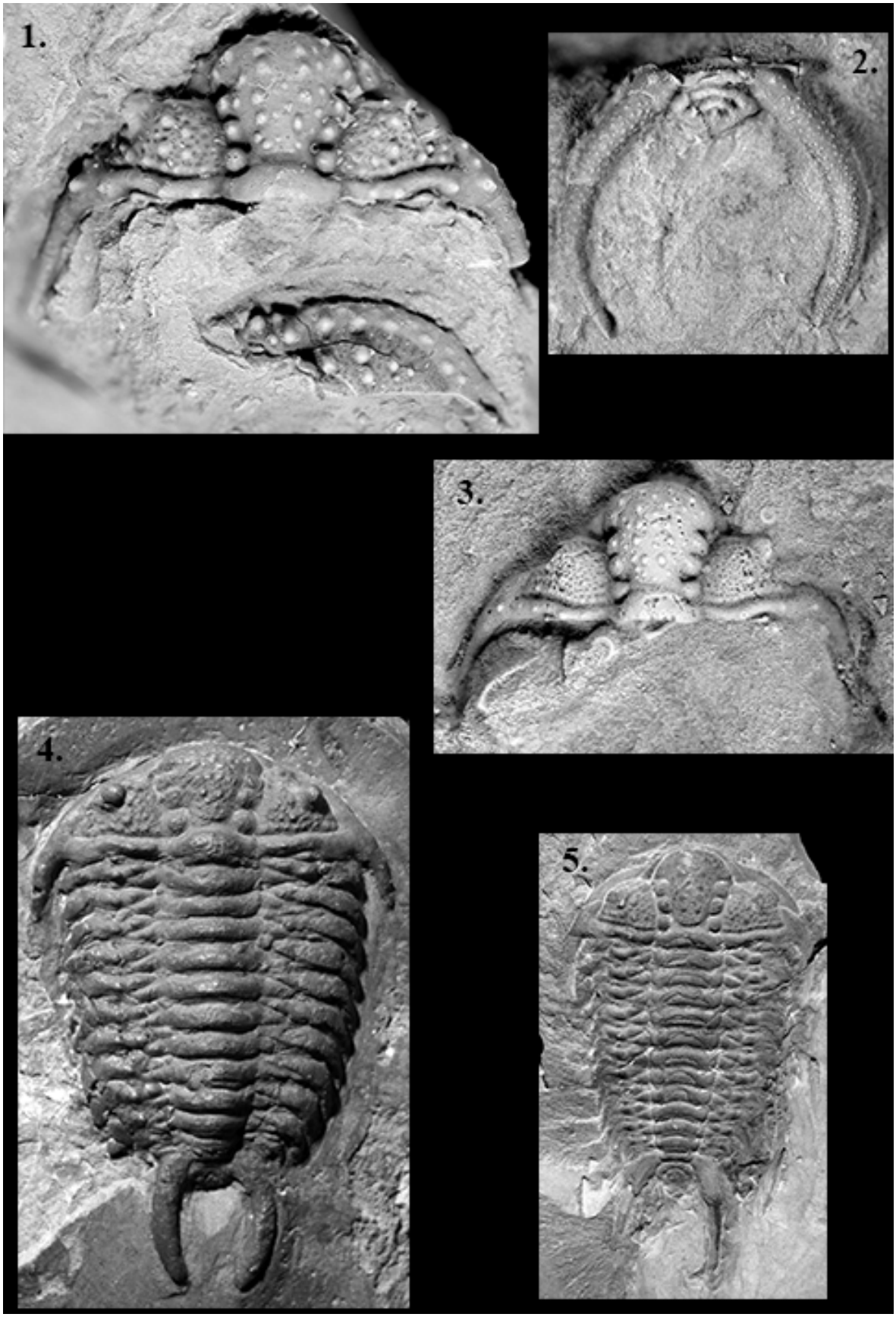
1.
2.
3.
4.
5.

Plate 31

Ceraurus furca sp. nov.

Figure 1: Holotype exoskeleton from the Cobourg Formation near Georgian Bay, Collingwood, Ontario, KUMIP 325617, ×4.

Figure 2: Exoskeleton from the Lindsay Formation near the Ogden Quarry near Colborne, Ontario ROM 45128, ×1.3. Photograph from Thomas Whitely.

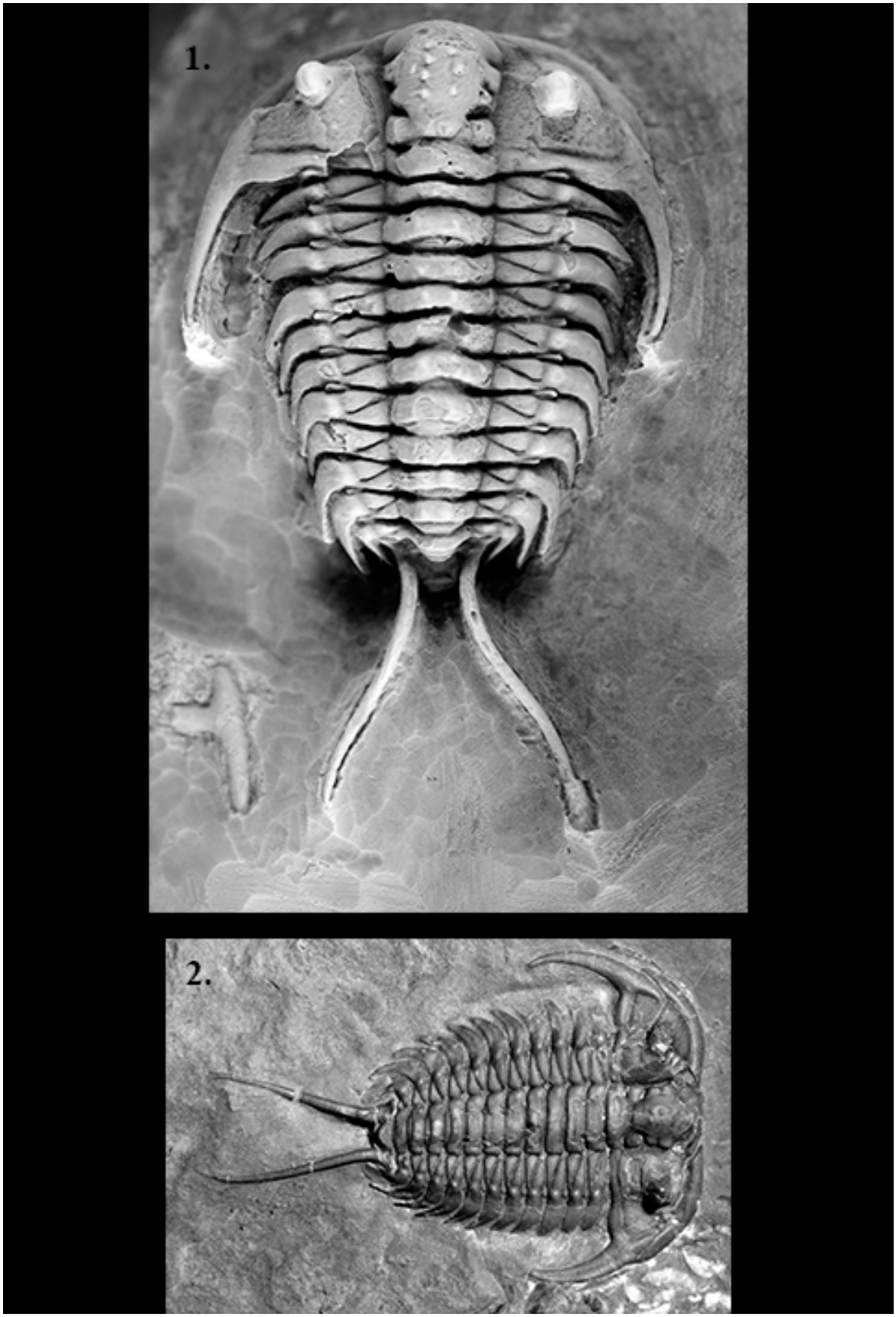
1.
2.

Plate 32

Ceraurus kirchmeieri sp. nov.

Figure 3: Holotype exoskeleton from the Elgin Member of the Maquoketa Formation in Fillmore County Minnesota KUMIP 325618, ×4.3.

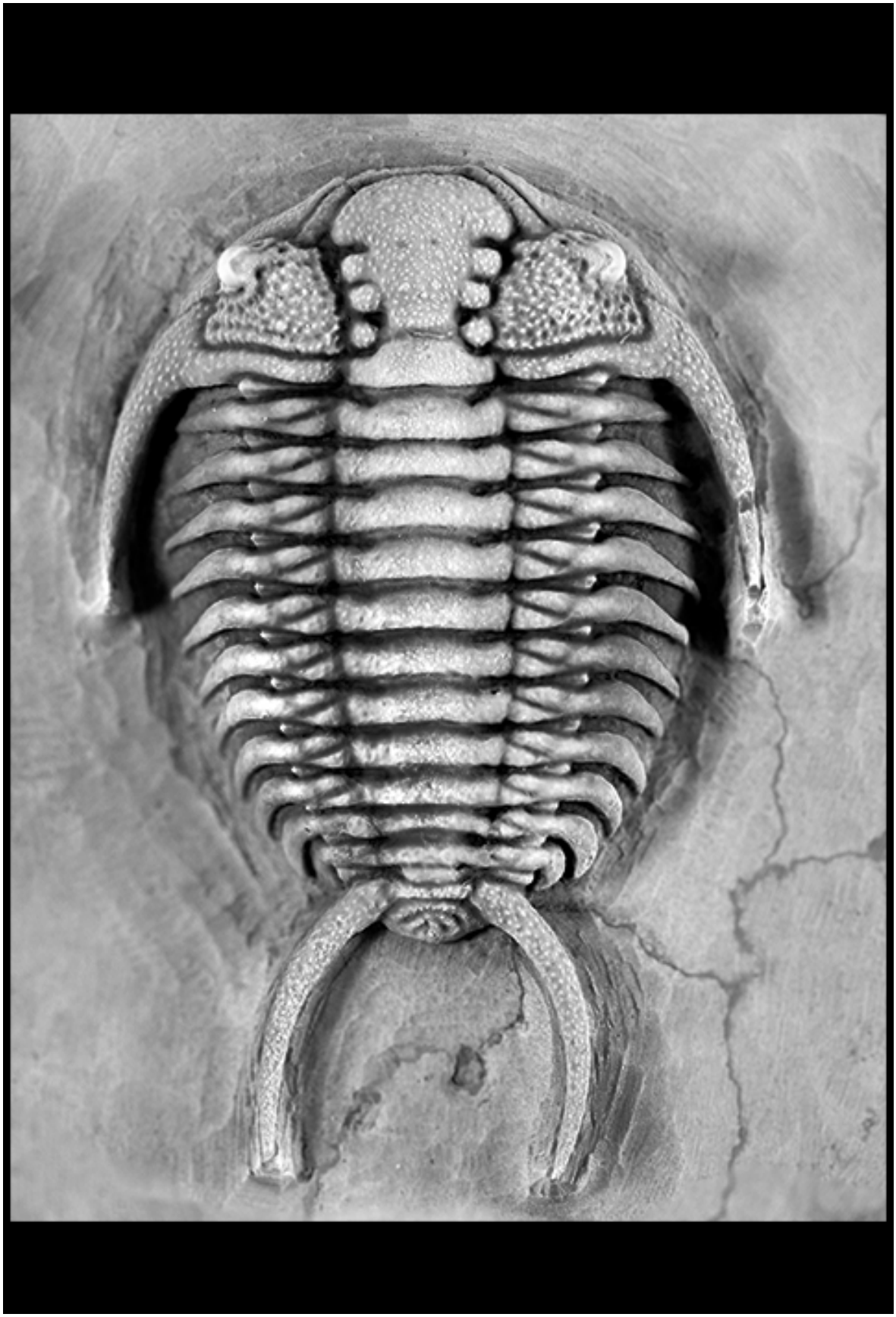

Plate 33

Ceraurus napaneei sp. nov.

Figure 1: Cranidium of holotype exoskeleton from the Napanee formation near Boonville, Oneida County, New York, KUMIP 325652, ×3.8.

Figure 2: Thorax and tail of holotype exoskeleton from the Napanee formation near Boonville, Oneida County, New York, KUMIP 325652, ×6.7.

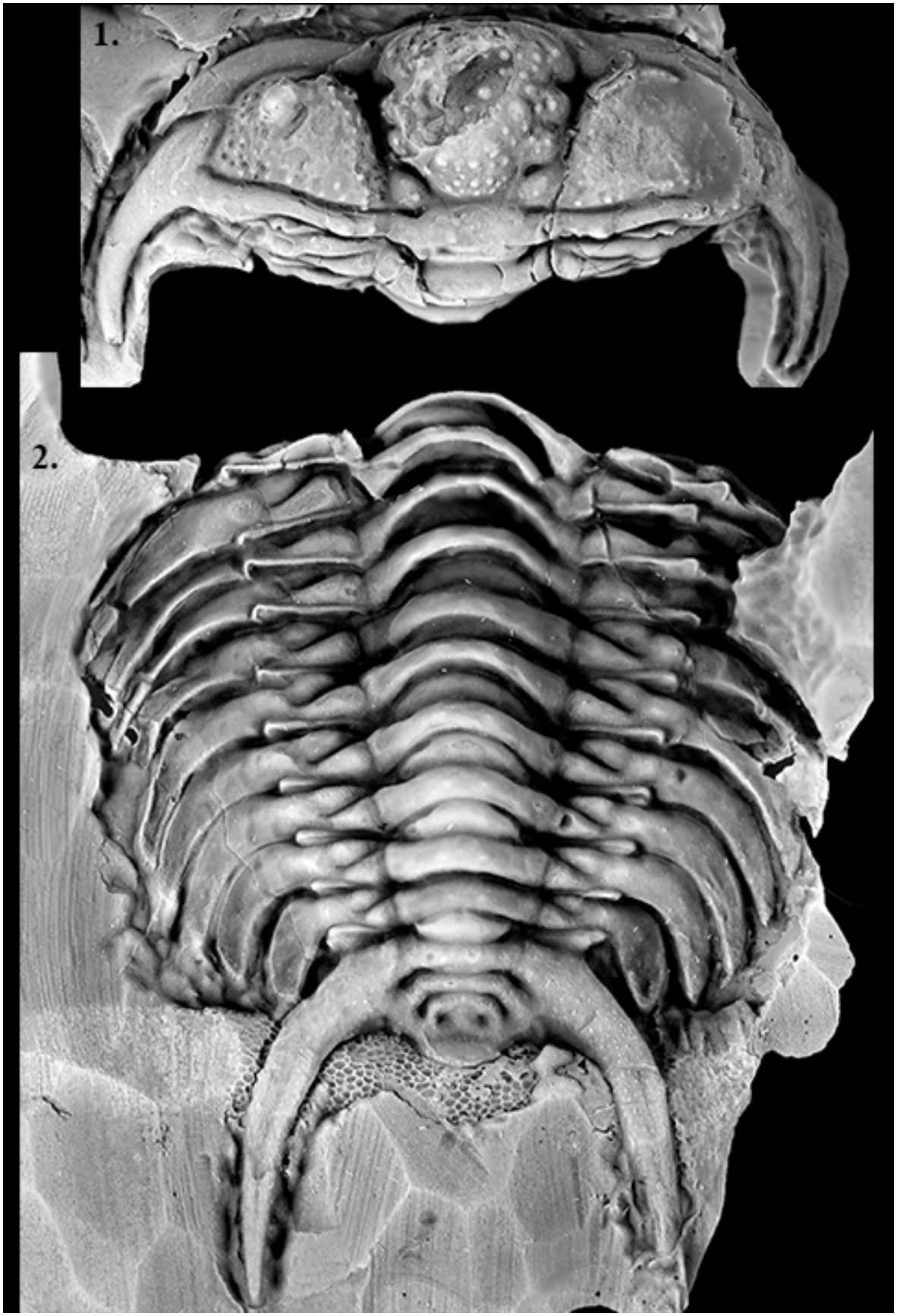
1.
2.

Plate 34

Ceraurus napaneei sp. nov.

Figure 1: Partial pygidium from the Napanee formation near Boonville, Oneida County, New York, KUMIP 325653, ×6.5.

Figure 2: Hypostome from the Napanee formation near Boonville, Oneida County, New York, KUMIP 325654, ×3.1.

Figure 3: Hypostome from the Napanee formation near Boonville, Oneida County, New York, KUMIP 325655, ×7.7.

Figure 4: Paratype pygidium from the Napanee formation near Boonville, Oneida County, New York, KUMIP 325656, ×6.1.

Figure 5: Cranidium from the Napanee formation near Boonville, Oneida County, New York, KUMIP 325657, ×5.


1.
2.
3.
4.
5.

Plate 35

Ceraurus napaneei sp. nov.

Figure 1: Paratype cranidium from the Napanee formation near Boonville, Oneida County, New York, KUMIP 325658, ×3.2.

Figure 2: Cranidium from the Napanee formation near Boonville, Oneida County, New York, KUMIP 325659, ×5.1.

Figure 3: Cranidium from the Napanee formation near Boonville, Oneida County, New York, KUMIP 325660, ×2.8.

Figure 4: Cranidium from the Napanee formation near Boonville, Oneida County, New York, KUMIP 325661, ×3.5.

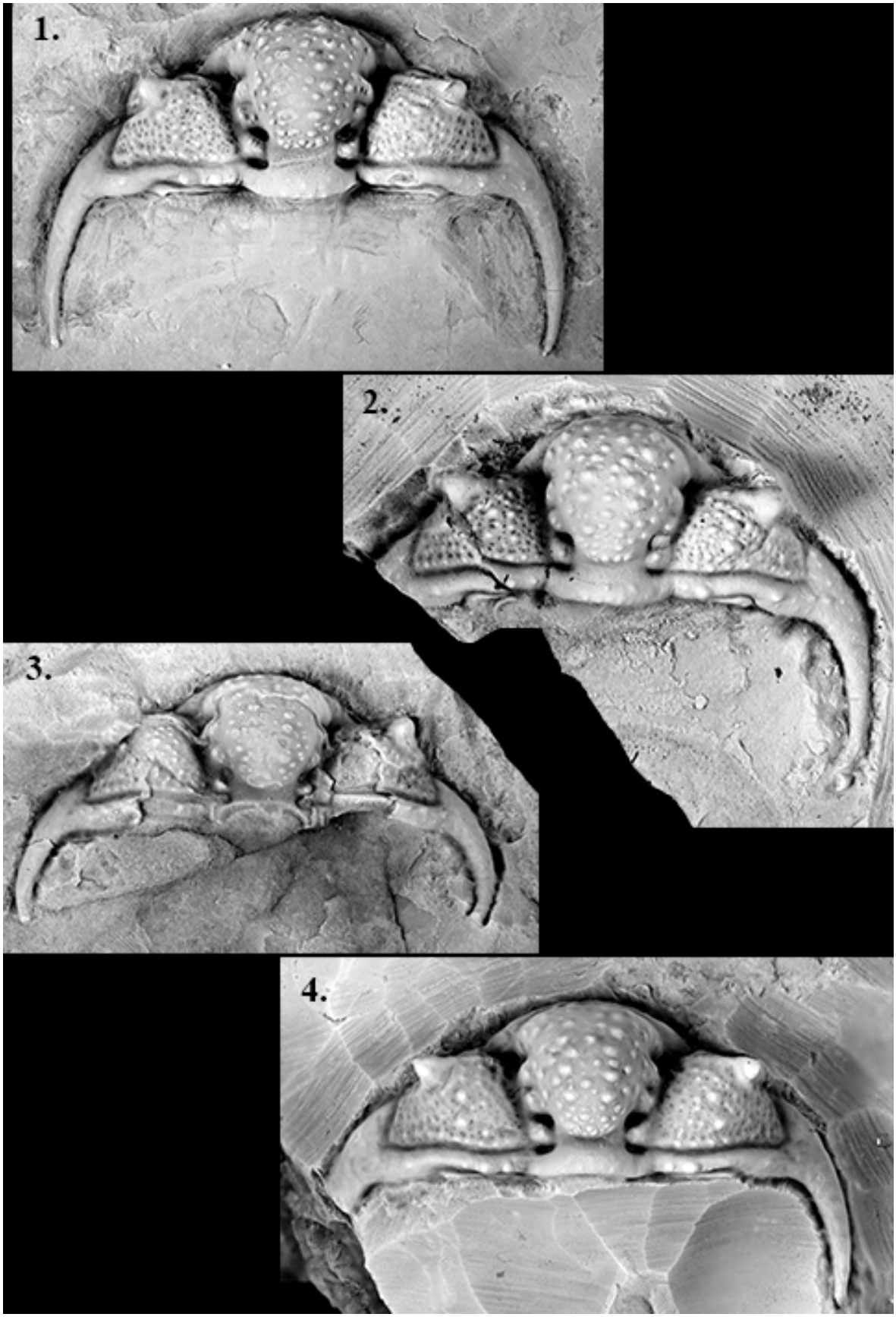
1.
2.
3.
4.

Plate 36

Ceraurus hillieri sp. nov.

Figure 1: Nearly complete holotype specimen from the Hillier Member in New York, NSYM 17000, ×8.1.

Plate 37

Ceraurus wilsoni sp. nov.

Figure 1: Partial exoskeleton from the Cobourg Formation at the St. Isodore Quarry, Ontario GSC 137134, ×3.8.

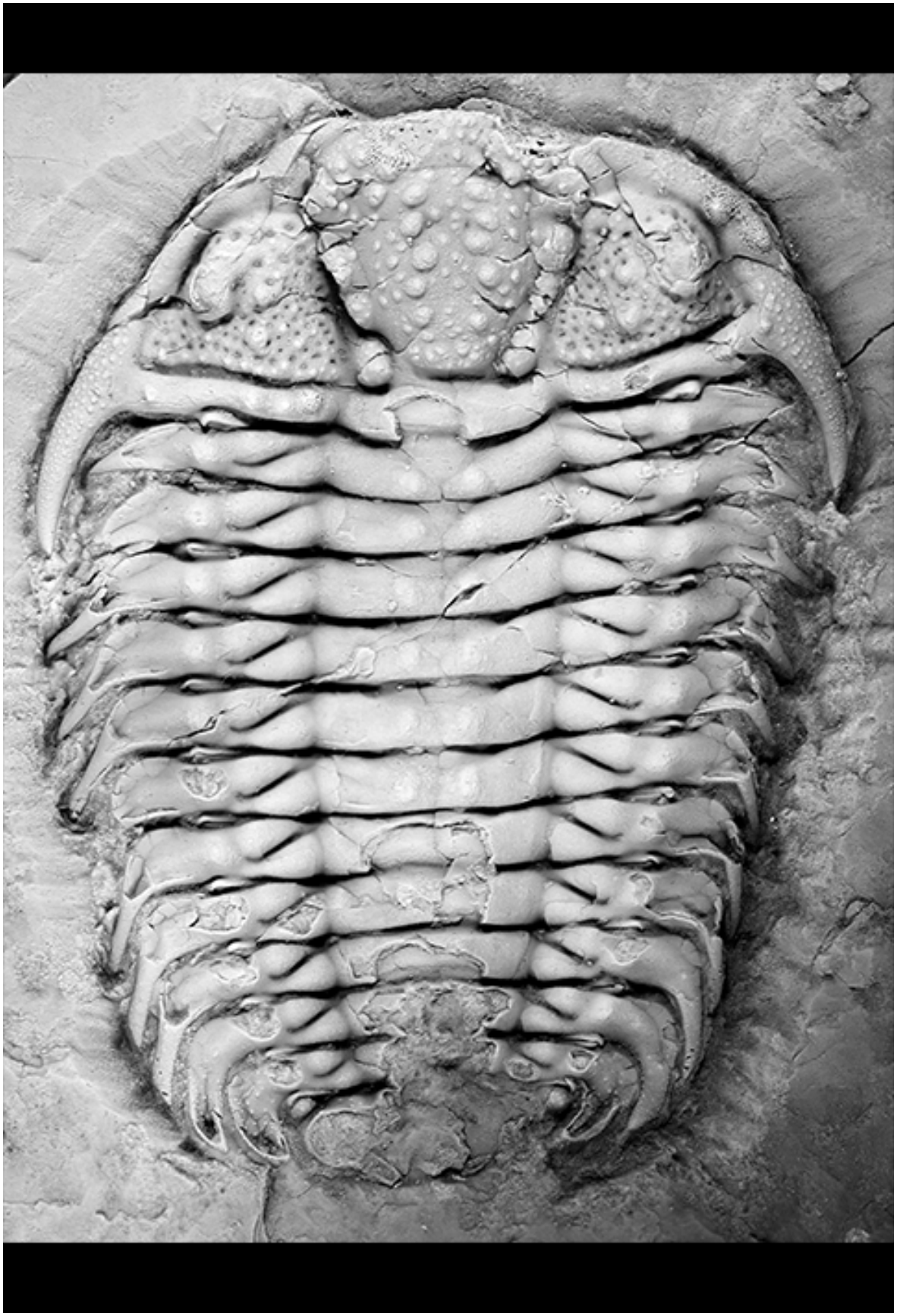

Plate 38

Ceraurus wilsoni sp. nov.

Figure 1: Holotype exoskeleton from the Lindsay Formation at Ogden Point Quarry, Ontario, ROM 45129, ×4.

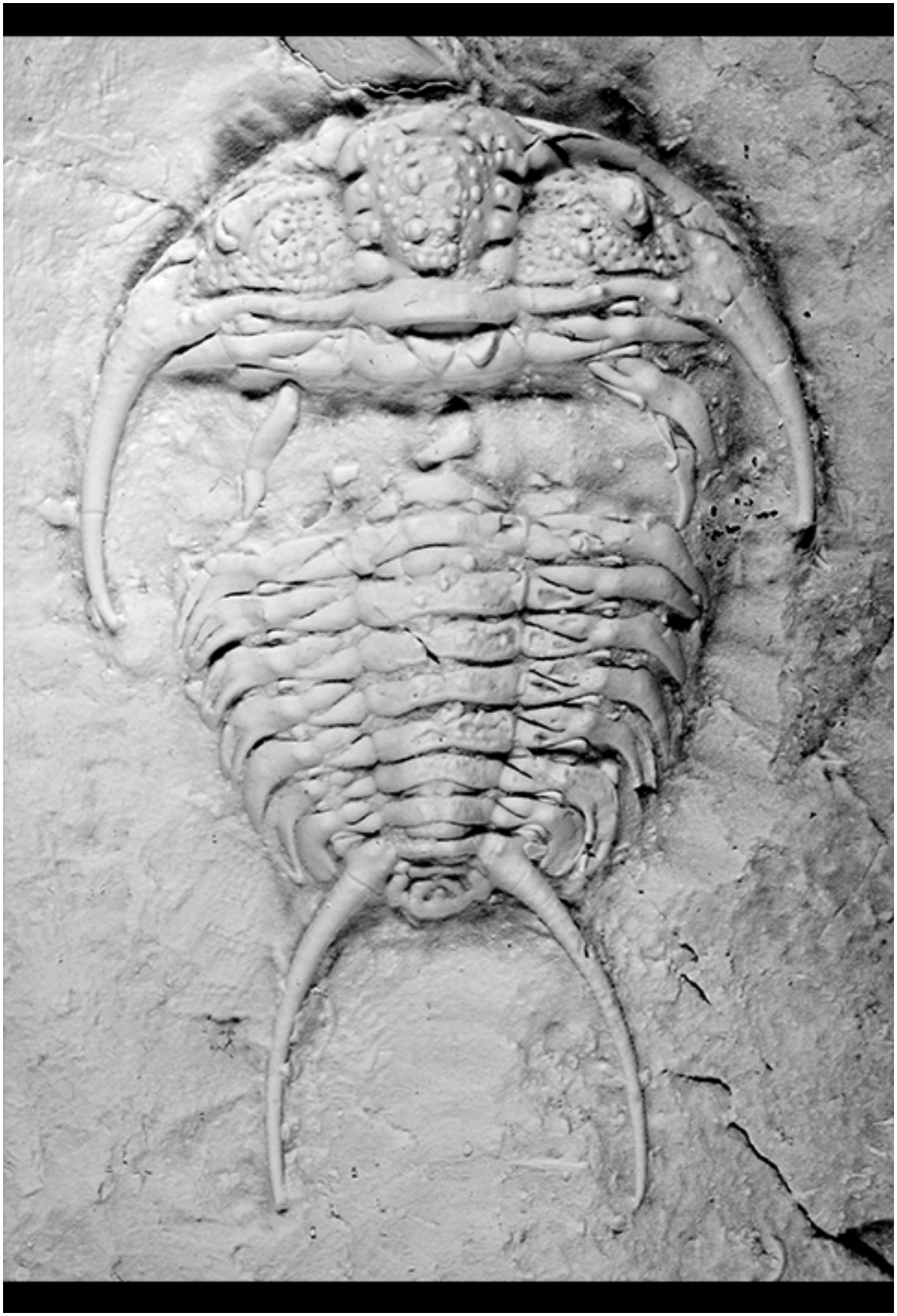

Plate 39

Ceraurus ottawaensis sp. nov.

Figure 1: Complete exoskeleton from the lower Bobcaygeon Formation near Ottawa, Ontario, KUMIP 325662, ×5.4.

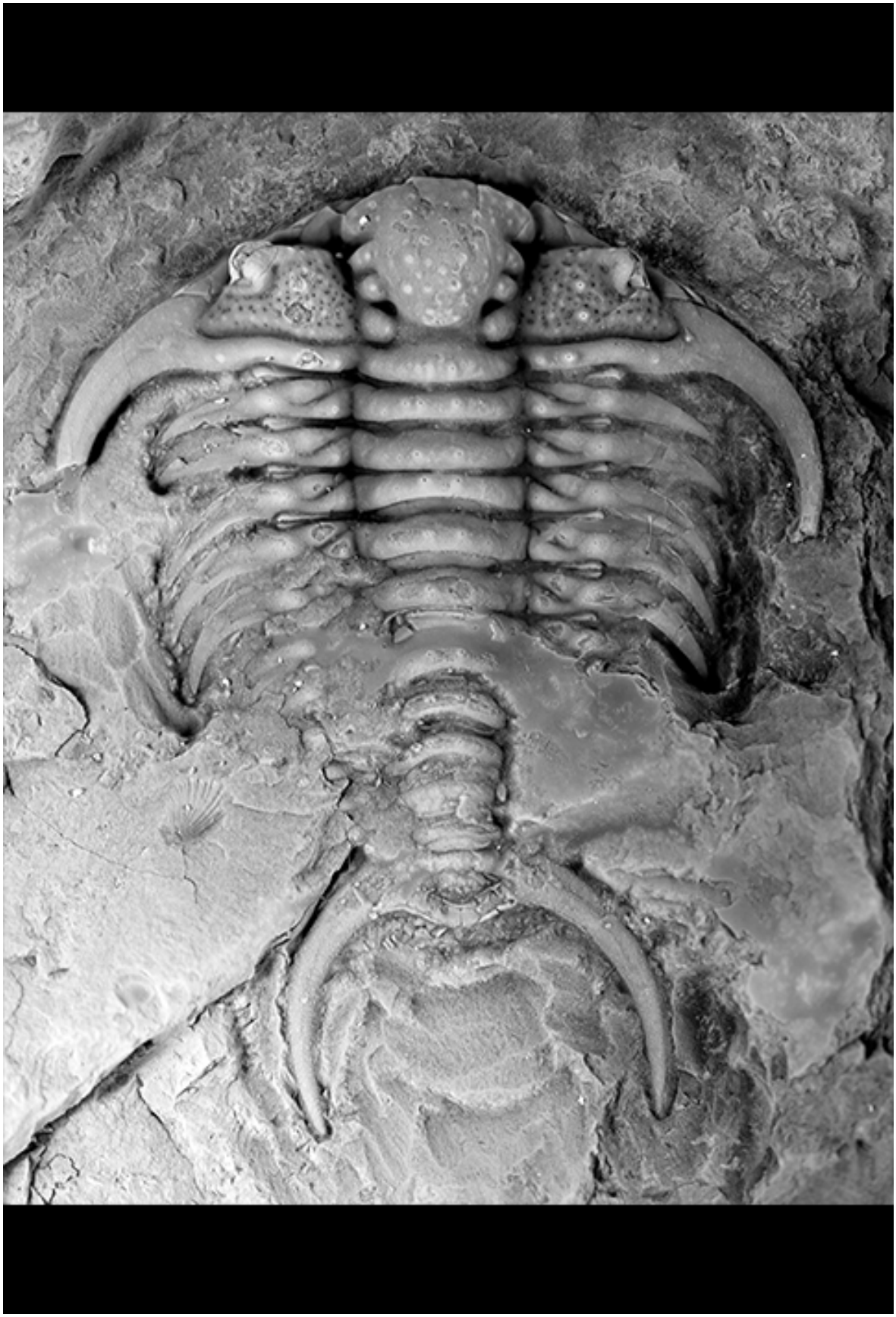

Plate 40

Ceraurus ottawaensis sp. nov.

Figure 1: Two complete exoskeletons from the lower Bobcaygeon Formation near Ottawa, Ontario, GSC 137135-6, as well as one complete *Ceraurus paraplattinensis* GSC 137137, ×2.4.

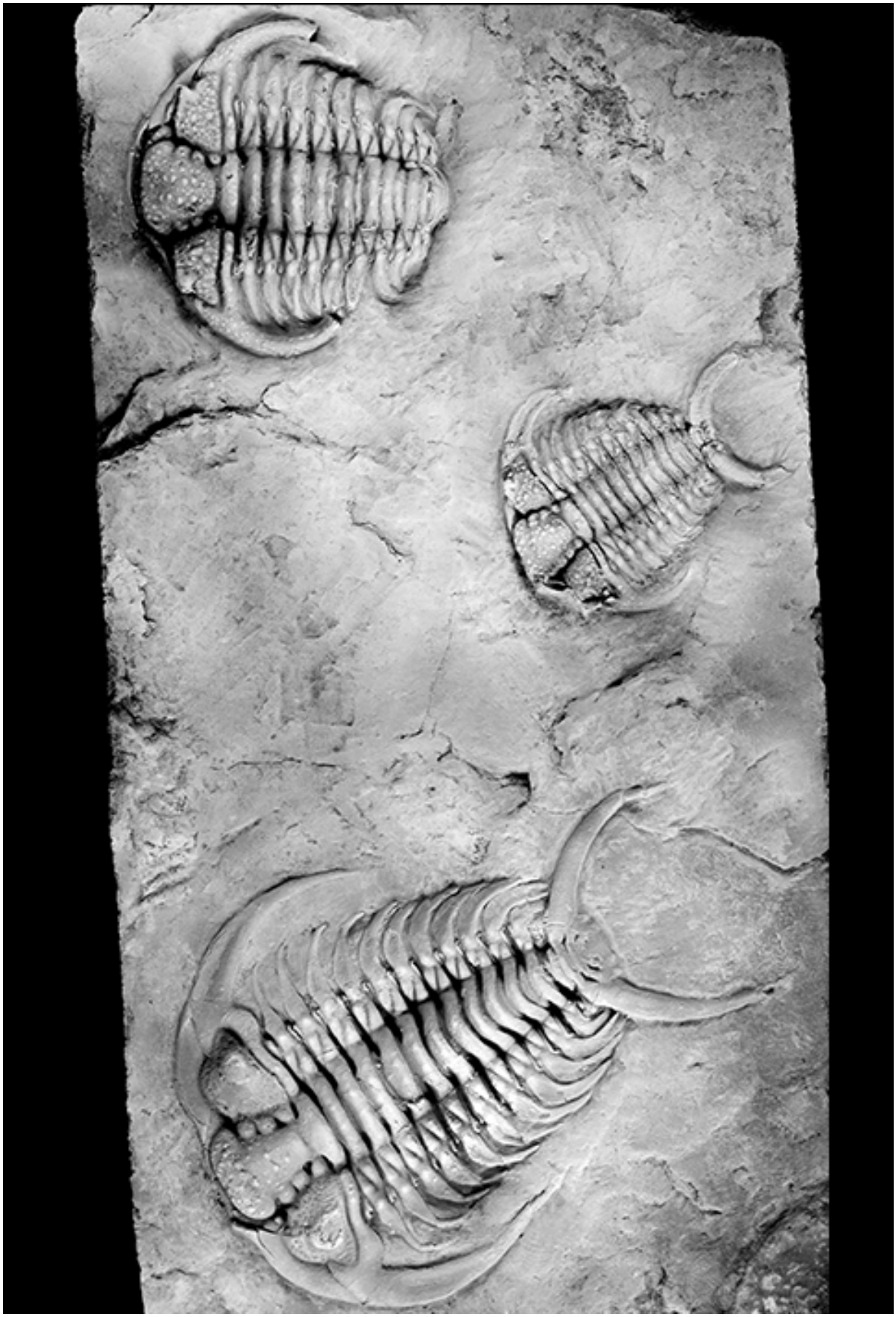

Chapter 4- CLADE TURNOVER: THE END ORDOVICIAN AS A LARGE SCALE ANALOG OF SPECIES TURNOVER

Curtis R. Congreve

(Formatted for submission to Palaeontology)

Abstract: Modern studies of individual populations have shown large cyclic shifts in phenotype/genotype that correlate with climatic variations. At the hierarchical level of the species, similar patterns can be observed in the climatically mediated turnover of species (i.e., Vrba's Relay Model). In turn, mass extinction events may have a similar analogous relationship to species turnover, while operating at the clade level. In this paper, such an analogous process is described and named the Cladal Turnover Model. The end Ordovician mass extinction event is used as a test case used to investigate the existence of such a phenomenon, with specific focus on the origin and extinction of the *Hirnantia* fauna. A test is outlined which can be used to determine if Cladal Turnover is occurring in the End Ordovician. An example case study is then performed on specific *Hirnantia* taxa, the trilobite genus "*Brongniartella*". The results of this test suggest that, while the taxon "*Brongniartella"* is derived from putatively cold-water high latitude stock (consistent with the classical definition of the *Hirnantia* taxa), the group does not go extinct at the end Ordovician event and instead gives rise to warm-water low latitude descendants. This result is consistent with the Cladal Turnover Model. The method proposed for testing the Cladal Turnover Model could be applied to look at other times of major evolutionary turnover preserved in the fossil record.

Key words: mass extinction, Ordovician, trilobite, evolution, Turnover Pulse

INTRODUCTION

THE end Ordovician marks the second largest mass extinction, in terms of percent genera and families extinguished, in the history of life (Sepkoski 1996). The cause of this extinction has classically been interpreted as the formation of a sudden and unstable icehouse in the middle of otherwise greenhouse conditions, which occurs contemporaneously with the extinction event (Berry and Boucot 1973, Sheehan 1973, Brenchley et al 1994, Sheehan 2002). The extinction is seen as occurring in two major pulses, related to the initial onset of glaciation and the return to greenhouse conditions (Hallam and Wignall 1997). The first extinction pulse has traditionally been interpreted to have been caused by habitat degradation due to a combination of the draining of epicontinental seaways (Sheehan 1973) and the shrinking of the tropical climatic belt (Berry and Boucot 1973, Stanley 1984). The initial episode of cooling and aspects of the extinctions may have been triggered by a gamma-ray burst (Melott et al. 2004). The second pulse of extinction has been interpreted to have resulted from a sudden return to warmer, pre-glacial conditions, with the newly icehouse-adapted taxa going extinct. More specifically, the presence of major glaciation may have increased ocean circulation, oxygenating oceanic deep water and opening up this habitat to oxygen demanding taxa (Hallam and Wignall 1997). When the glaciers quickly receded, dysoxic conditions may have returned to the ocean bottoms, killing off taxa with high oxygen requirements (Rong and Harper 1988, Briggs et al 1988, Fortey 1989, Sheehan

2002; Bapst 2012). While the interpreted cause of the extinction (ice maxima during the Hirnantian period) has remained consistent, modern studies have refined the timing. Modern geochemical evidence from carbon isotopes (Saltzman 2005, Finnegan et al. 2011), zooplankton biogeography (Vandenbroucke et al. 2010), and the results of ocean circulation modeling of the Ordovician (Hermann et al. 2004) suggests that the Ordovician icehouse transition likely occurred during the Late Ordovician (Sandbian or early Katian), with a polar front positioned between 55º -70ºS. However, tropical sea surface temperature estimates remain high throughout the late Ordovician and only drop sharply at the extinction event (Finnegan et al. 2011). The Hirnantian glaciation is then interpreted as an extreme glacial maximum within this late Ordovician icehouse, rather than a completely sudden transition from icehouse to greenhouse.

The *Hirnantia* fauna.-- The term *Hirnantia* fauna was first coined by Temple (1965) to describe a widespread brachiopod fauna that quickly came to dominance at the latest Ordovician (Hirnantian) and just as quickly died off at the Ordovician-Silurian transition. The most common elements of this fauna include *Hirnantia sagittifera, Dalmanella testudinaria, Kinnella kielanae, Paromalomena polonica, Eostropheodonta hirnantensis,* and *Plectothyrella crassicosta*. Although Temple's original recognition of the *Hirnantia* fauna comes from Late Ordovician beds in England, Wales, and Poland, subsequent authors have described equivalent faunas from around the world, including Morocco (Havlicek 1971), Austria (Schönlaub 1971), China (Rong 1979), Kazakhstan (Nikitin 1976), Sweden (Bergström 1968), and North America (Lesperance 1974, Neuman 1968). After Berry and Boucot (1973) suggested a link between the end Ordovician extinction and a global glacial period, Sheehan (1973) interpreted Temple's *Hirnantia* fauna as a cold-water adapted group, derived from high latitude Gondwanan forms, which spread due to the global cooling occasioned by glacial advance. Subsequently, the

majority of the *Hirnantia* fauna went extinct during the episode of global warming that ended the glaciation, presumably due to a combination of dysoxia and the restriction of "cold-water" habitats (Sheehan 2002). Implicit in this interpretation, although never directly stated, is the assumption that the *Hirnantia* fauna represented a real evolutionary and ecological unit with a history of "cold-water" habitat preference and not merely an amalgamation of the species that survived the first extinction pulse.

This original interpretation has remained unchanged (see Hallam and Wignall 1997, Sheehan 2002 for multiple references to the "cold-water" *Hirnantia* fauna), however it is important to note that a study by Rong (1984) (based on sedimentological proxies) suggests that the *Hirnantia* fauna was likely incredibly eurytopic, inhabiting a vast array of environments and temperatures. Essentially, Rong's results are expected under the hypothesis that the *Hirnantia* fauna were composed of the generalist survivors (or descendants of those survivors) of the first pulse of extinction, and not necessarily cold adapted taxa.

Some authors have claimed that groups other than brachiopods exhibit a pattern analogous to the *Hirnantia* fauna. One such analogous fauna has been identified in trilobites (Lespérance 1988). Much like the *Hirnantia* brachiopods, this fauna is interpreted as being a cold-water fauna descended from high latitude forms. The common members of this fauna consist of species assigned to the genera *Brongniartella, Platycoryphe, Dalmanitina,* and *Mucronaspis*. Unlike brachiopods, trilobites are character rich and thus excellent candidates for detailed phylogenetic study (see Lieberman 1994 and Lieberman and Kloc 1997 for phylogenetic evaluations of the status of Devonian fossil faunas). Consequently, it is possible to use phylogenetic analysis to determine if the *Hirnantia* fauna represents a cohesive evolutionary unit or if it is merely the accidental grouping of the taxa that survived the first pulse of extinction. If the *Hirnantia* fauna

are not a discrete evolutionary fauna derived from “cold-water” species, then our perception of the large scale patterns of extinction and speciation during the end Ordovician would need to change. In this case, a habitat-specific theory of evolutionary change, such as Vrba’s Relay Model, may be a more appropriate interpretation of this turnover event.

The Relay Model and its relationship to the end Ordovician. -- The Relay Model as proposed by Vrba (1995) is essentially a modified version of Vrba’s (1985, 1992) Turnover Pulse hypothesis. Turnover Pulse was proposed as a potential motor for speciation during a time of Plio-Pleistocene climate change. According to the model, global cooling and warming due to Milankovitch cycles caused the tropical climatic belt to contract and expand its range rhythmically through time. During periods of global cooling, the ranges of warm adapted species would be greatly constrained. Given sufficient cooling, these species would be separated into smaller isolated populations. Although a large portion of tropical species would go extinct during cold periods, the fractionation of populations would also be ideal to facilitate the necessary genetic isolation for speciation to take place. Therefore, the Turnover Pulse hypothesis predicts pulsed periods of extinction and speciation that coincide with Milankovitch cycles (Vrba, 1985, 1992). Vrba (1995) further refined this hypothesis into the Relay Model, which includes the effects that global warming periods have on cold-adapted species. The model suggests a back and forth pattern of turnover and extinction, with global cooling causing the warm adapted species to turnover and global warming causing the cold adapted species to turnover (Fig. 1). The Relay Model also states that taxa undergoing a turnover event may experience selective pressures to modify their temperature thresholds (i.e., taxa derived from the turnover of cold-adapted species during a warming phase could become more tolerant of warm temperatures and vice versa).

The Relay Model was initially invoked as a speciation motor within the confines of the Neogene icehouse. However, since Milankovitch cycles have operated throughout history, this model may explain turn-over patterns at other times (*sensu* Lieberman 1999). In this paper I explore analogous processes that may have been operating during the end Ordovician mass extinction event, i.e., how patterns of extinction and survivorship during the extinction event may be reinterpreted through the lens of Vrba's Relay Model. During the first extinction pulse (the initial glaciation), global cooling caused the tropical climatic belt to shrink, fractionating populations leading to increased extinction rates and potentially increased speciation rates. The new species generated from these fractionated populations of low-latitude taxa may have experienced strong selective pressures towards "cold-water" adaptations. Ergo, several of these independent surviving lineages may have given rise to the "cold-water" *Hirnantia* fauna and its equivalent faunas. When the glaciers receded and warmer conditions returned, the opposite pattern would have occurred. The second pulse of extinction reflected the *Hirnantia* fauna becoming increasingly restricted to higher and higher latitudes as the "cold-water" habitats receded to the poles. These high latitude populations may have fractionated, resulting in increased extinction and speciation rates. Some of the new species generated from these fractionated populations could experience strong selective pressures towards "warm-water" adaptations, thus potentially giving rise to taxa that could migrate to lower latitudes. Such a pattern represents a large-scale analogue of the Relay Model, hence forth referred to as the Cladal Turnover Model.

A crucial difference between the Relay Model and Cladal Turnover is the issue of scale. The Relay Model operates on Milankovitch timescales and deals with warm-cold cycles that are always constrained within an icehouse climate. On the other hand, the end Ordovician glacial

event is a transition from an ice-free greenhouse to an icehouse, and then back to a greenhouse state over million-year timescales. The prevalence of cold and warm adapted species is also an important difference between the end Ordovician and the Relay Model. In the Relay Model, the existence of cold and warm-adapted species is assumed because the model describes fluctuations between glacial and interglacial periods in an established icehouse. In the end Ordovician, the presence of cold-adapted taxa prior to the onset of glaciation in the Late Ordovician cannot be presumed because it follows on the heels of tens of millions of years of warm conditions. Ergo, the initial global cooling at the end Ordovician may result in a period of extinction and turnover, à la the Relay Model that may be expected to give rise to cold adapted taxa. A small scale pulse local to southern Gondwana would be expected during the onset of glaciation in the Sandbian or Katian when the glacier was forming, but the larger scale turnover would occur during what is typically treated as the first extinction pulse of the end Ordovician. Then, once the glaciers receded, a second period of turnover and extinction of the newly cold-adapted faunas would occur (second extinction pulse). In this case the formation and destruction of cold-adapted taxa is caused by similar, although not necessarily homologous, processes as those operating in the Relay Model. These processes, however, would be considered analogous because the forcing mechanism involved in this massive turnover involves the entire climate system of the planet switching from a greenhouse to an icehouse. If this is the predominant pattern for the end Ordovician extinction, then the event could be viewed as a large-scale analogue of the Relay Model.

It is also important to note that this type of pattern need not be limited strictly to temperature preference but could also be used for any environmental factors that could be oscillating through time (e.g. salinity, oxygen levels).

TESTING THE HYPOTHESIS

To test the Cladal Turnover Model the null hypothesis employed is Sheehan's (1973) view of the *Hirnantia* fauna, that it is a cold-adapted fauna derived from high latitudes that goes extinct, or is marginalized to high latitudes, at the end Ordovician. The alternative hypothesis is the Cladal Turnover Model, where the *Hirnantia* fauna is either derived from warm-water species that survive the first pulse of extinction, or gives rise to warm-water species during the second pulse. Phylogenetic analyses in conjunction with inferred cold- vs. warm-adapted ecology can be used to test the null and alternative hypotheses. This type of technique could also be applied to understanding the effects of other factors on survivability by mapping them onto the tree as characters, but for the purposes of this particular study we will be focusing solely on inferred ecology. Predicted outcomes of these analyses fall into five general scenarios:

Case 1: *The Hirnantia taxa are derived from historically cold-water lineages that extend well into the Middle Ordovician or beyond. The taxa either do not give rise to descendants that survive the end Ordovician or its descendants are all cold-water adapted.* This scenario fails to reject the null hypothesis. This result suggests the *Hirnantia* fauna is a real evolutionary unit with a long history of cold-water adaptation (*sensu* Sheehan 1973). That being said, this result cannot be used to prove the reality of the *Hirnantia* fauna since the assumptions of the test (i.e., high latitude taxa and members of the *Hirnantia* fauna are always cold-water adapted) bias the results in favor of the null hypothesis.

Case 2: *The closest putative ancestors to the Hirnantia taxa are cold-water adapted; however the cold-water lineages only extends back into the Late Ordovician and are derived from warm-*

water stock. This scenario provides weak evidence for rejecting the null hypothesis. Although in this scenario the actual *Hirnantia* taxon is derived from cold-water stock, the lineage is not historically cold-adapted. This suggests that the turnover event corresponding to the cold-water leg of the Relay Model may have occurred prior to the first pulse of extinction, possibly during the initial onset of glaciation. The Sandbian turnover resulted in the evolution of cold-water forms that would later give rise to the *Hirnantia* taxon.

Case 3: *The Hirnantia taxa are derived from a cold-water lineage. The taxa give rise to warm-water descendants that survive the end Ordovician.* This scenario rejects the null hypothesis, although it is not fully conclusive. Whereas the pattern of the origination and spread of the *Hirnantia* fauna after the first pulse of extinction fits well with the null hypothesis, the pattern observed during the second pulse of extinction is strongly in favor of the Clade Turnover Model. In this scenario only one of the two parts of the Relay Model is observed; the test recognizes the effects of the warming leg of the relay but not the cooling leg. This might imply that the glacial period began earlier in the Ordovician than expected, resulting in the origination of a cold-water, high-latitude taxon before the Sandbian. In order to test if the creation of these cold-water taxa are the result of an earlier pulse of the Cladal Turnover Model, rather than a deeply rooted cold water history, detailed speciation and extinction rates would need to be compared with paleoclimatic proxy data (such as oxygen and carbon isotopic curves). This addition test would determine if the taxa underwent a pulse of speciation/extinction that correlates with a climate shift.

Case 4: *The Hirnantia taxa are derived from a warm-water lineage. The taxa either do not give rise to descendants that survive the end Ordovician or their descendants are all cold-water adapted.* This rejects the null hypothesis for the same reasons as described in case 3, (this case is

merely the inverse of case 3). Here the test recognizes the effects of the cooling leg but not the warming leg. If the majority of analyses on *Hirnantia* taxa support case 3 and 4, there is good corroborative evidence for the Cladal Turnover Model.

Case 5: *The Hirnantia taxon is derived from a warm-water lineage. The taxon gives rise to warm-water descendants that survive the end Ordovician.* This is potentially the strongest evidence for rejecting the null hypothesis. In this example, both legs of the Cladal Turnover Model are recognized by the test: the lineage transitions from warm-water adapted to cold-water adapted and back to warm-water adapted. However, this interpretation depends upon the assumption that the *Hirnantia* taxa are cold-water adapted. If the *Hirnantia* taxa are instead warm-water eurytopes, then this interpretation breaks down since there is no transition between cold- and warm-water adaptation within the lineage in this scenario. Whenever possible independent evidence should be used to corroborate the assumption that the *Hirnantia* taxa lived in cold-water environments (e.g. geochemical proxies).

A Test Study on Homalonotid Trilobites.- The detailed phylogenetic data needed to test these hypotheses are currently limited to Ordovician trilobites. In particular, Congreve and Lieberman (2008) generated a phylogenetic hypothesis (Fig. 2) for Ordovician trilobites belonging to the Family Homalonotidae which contains the *Hirnantia* taxon "*Brongniartella"* (the group is designated with quote marks because the phylogeny suggests that "*Brongniartella*" is a paraphyletic grade leading to Silurian homalonotid forms, as well as the modestly diverse *Hirnantia* genus *Platycoryphe*). This analysis used 16 taxa and 26 characters and a branch and bound search in PAUP* (Swoford 1998), generating one most parsimonious tree of 54 steps. This phylogeny can be used to test if "*Brongniartella*" behave in a manner that would be

expected from traditionally defined *Hirnantia* fauna. This particular study is utilized as an example for how similar studies could be done in the future. Naturally, this type of analysis requires far more clades (and possibly multiple phyla) to ascertain if this pattern is shown consistently across the end Ordovician. This example is merely a proof of concept.

First, stratigraphic occurrence data was used to constrain origination times for each speciation event in the phylogeny. Then, all of the taxa included were classified into one of two groups: cold-water and warm-water adapted. For purposes here, all species that have previously been identified as cold-water *Hirnantian* forms were treated as cold-water adapted. For those taxa lacking previous determinations, estimates of a taxon's paleomagnetic latitudinal occurrence were used to infer cold/warm-water adaptation. Taxa occurring at palaeolatitudes of fifty degrees or higher were here considered to be cold-water taxa, while the rest are classified as warm-water taxa. This cutoff line is based on the discovery of putative cold-water Caradoc limestones with paleolatitude estimates of approximately fifty degrees (Cherns and Wheeley 2007) and is consistent with Sandbian climate models (Hermann et al, 2004). Environmental assignments were then mapped onto the tree as characters and a parsimony algorithm was used to obtain the most parsimonious reconstruction of the character states for the ancestral nodes (fig. 3). In this fashion, the preferred environments for the ancestors of the *Hirnantia* taxa were estimated (cold or warm water), as well as the timing of divergence of the *Hirnantia* fauna from its sister taxa.

The pattern found in *"Brongniartella"* most closely resembles the "case 3" scenario. In particular, *"Brongniartella"* is derived from a high-latitude putative cold-water stock. Furthermore, the species assigned to the group had a long evolutionary history of cold-water adaptation that extends well into the early Ordovician, which matches the expectation of the null hypothesis. However, "*Brongniartella*" is paraphyletic and therefore the lineage does not go

extinct at the end Ordovician mass extinction, instead giving rise to the ancestors of *Trimerus* and other warm water homalonotids. While the group does also give rise to a small monophyletic genus of *Hirnantia* taxa that goes extinct at the end Ordovician (*Platycoryphe*) the null hypothesis is an incomplete interpretation of the evolution of this group. Therefore, the patterns observed in the evolutionary history of *"Brongniartella"* is one of a cold-water adapted lineage evolving into a warm-water adapted lineage post the end Ordovician turnover. This pattern could represent one leg (in this case the global warming leg) of the Relay Model. Thus, in this particular case we would reject the null hypothesis. Again, it should be stated that this case is merely shown as an example and more studies must be made to determine if the Cladal Turnover Model is a repeated pattern across the end Ordovician.

DISCUSSION

If further testing reveals that the large-scale analogue to the Relay Model is indeed the correct model to explain the rise and fall of the *Hirnantia* fauna during the end Ordovician extinction event, then perhaps this model is a recurring pattern in Earth history. Theoretically, the Clade Turnover Model could explain turnover events observed during every transition from a greenhouse to an icehouse Earth and vice versa with either new cold-adapted forms derived from warm-adapted ancestors during the cooling leg or warm-adapted species derived from cold-adapted ancestors during the warming leg. The Clade Turnover Model would also explain some patterns of the attendant extinction. The approach detailed here could be applied to test for Relay Model-style turnover events during any major climatic transition, e.g., at the Eocene-Oligocene boundary, when the first Antarctic glaciers formed and ushered in a transition from a greenhouse to an icehouse climate (Ivany et al., 2000). Observations of a similar cold temperature leg of the

relay model during the Eocene-Oligocene transition would provide evidence for the prevalence of the Cladal Turnover Model.

If the cycles of the Cladal Turnover Model are shown to be consistent patterns throughout the history of life, then cyclical patterns of climatic variation may be important in directing evolution at all hierarchical levels. For example, at the level of the population, Grant and Grant (2002) observed large variations in beak morphology of Galapagos finches. Swings in beak morphology through time were correlated with dry and wet years resulting from the El Niño and La Niña cycles. These climatic oscillations affected the prevalence of the food sources the finches consumed, resulting in a shift of selective pressures that cycled between two favored morphologies. The Relay Model, as described by Vrba (1995) and van Dam et al. (2006), shows an analogous pattern of climatically mediated evolution at the species level. The processes occurring in the Relay Model are analogous to the climatically mediated morphological changes the Grants (2002) observed at the population level, but are not homologous because they cannot be explained through simple extrapolation of these population level variations to the species level. The smaller scale variations observed in the Galapagos finches are an example of the plasticity of adaptation in populations and are the direct result of directional selection, whereas the causal mechanism for the pulsed extinction and speciation patterns of the Relay Model are the result of the breakdown of population dynamics within a species which increases the potential for allopatric speciation.

In turn, mass extinction may also be correlated with even longer term cycles. For instance, Raup and Sepkoski (1982) argued that there was a 26 million year extinction cycle. Rohde and Muller (2005) presented a new analysis suggesting that there was a 62 million year cycle in biodiversity. Lieberman and Melott (2007, 2012) reconsidered these analyses and found strong

evidence for the 62 million year cycle and some evidence, albeit less profound, for a 26 million year and 32 million year cycle (Lieberman and Melott 2007). The Earth becomes more or less susceptible to extreme cosmogenic radiation and bolide impacts depending upon its position in the universe, which in turn can cause extreme and sudden shifts in the climate (Lieberman and Melott 2007, 2009, Alvarez et al. 1980, Melott et al. 2004). In this fashion, the history of life could be viewed as a series of climatic cycles nested within each other, with the longer term cycles resulting in more dramatic climatic swings and therefore more dramatic evolutionary reactions. This hierarchical arrangement of nested systems, with analogous climatic forcing mechanisms operating at each level, is a more complex and detailed extrapolation of Darwinian principles than the somewhat more reductionist viewpoint of macroevolution as merely population genetics scaled up that was the hardened view of the Modern Synthesis.

ACKNOWLDEGEMENTS

This research was supported by NSF DEB-0716162. I would like to thank the Panorama Society, Palaeontological Association, The International Palaeontology Congress, and the Association of Earth Science Club of Greater Kansas City for funding that was crucial to this research. I would also like to thank Bruce Lieberman, Corrine Myers, Keith Bennett, and one anonymous reviewer for edits that dramatically improved the quality of this manuscript, and Corinne Myers, Erin Saupe, Wes Gapp, Francine Abe, and James Lamsdell for scientific discussion that helped to formulate these ideas.

REFERENCES

Alvarez, L.W. and W. Alvarez, F. Asaro, H.V. Michel. 1980. Extraterrestrial Cause for the Cretaceous-Tertiary Extinction. *Science* 208(4448):1095-1108.

Bapst, D.W., P.C. Bullock, M.J. Melchin, H.D. Sheets, C.E. Mitchell. 2012. Graptoloid diversity and disparity became decoupled during the Ordovician mass extinction. *PNAS* vol. 109 no. 9:3428-33

Bergström, J. 1968. Upper Ordovician brachiopods from Västergötland, Sweden. *Geol. et Paleont.* 2:1-35.

Berry, W.B.N. and A.J. Boucot. 1973. Glacio-eustatic control of the Late Ordovician-Early Silurian platform sedimentation and faunal changes. *Geological Society of America Bulletin* 84:275-284.

Brenchley, P.J., J.D. Marshall, G.A.F. Carden, D.B.R. Robertson, D.G.F. Long. 1994. Bathymetric and isotopic evidence for a short-lived Late Ordovician glaciation in a greenhouse period. *Geology* 22:295-298.

Briggs, D.E.G., R.A. Fortey, E.N.K. Clarkson. 1988, Extinction and the fossil record of the arthropods. *In* Larwood, GP. (ed) Extinction and Survival in the Fossil Record. Clarendon. Oxford.

Cherns, L and J.R. Wheeley. 2007. A pre-Hirnantian (Late Ordovician) interval of glocal cooling- The Boda event re-assessed. *Palaeogeography, Palaeoclimatology, Palaeoecology* 251:449-460.

Congreve, C.R. and B.S. Lieberman. 2008. Phylogenetic and Biogeographic Analysis of Ordovician Homalonotid Trilobites. *Bentham Open; The Open Paleontology Journal* 1:24-32.

Finnegan, S. and K. Bergmann, J.M. Eiler, D.S. Jones, D.A. Fike, I. Eisenman, N.C. Hughes, A.K. Trípati, W.W. Fischer. 2011. The Magnitude and Duration of Late Ordovician-Early Silurian Glaciation. *Science*. 331:903-906.

Fortey, R.A. 1989. There are extinctions and extinctions: examples from the lower Palaeozoic. *Philosophical Transactions of the Royal Society of London B* 325:327-355.

Grant, P.R. and B.R. Grant. 2002 Unpredictable Evolution in a 30-Year Study of Darwin's Finches. *Science*. 296:707-711.

Hallam, A. and P.B. Wignall. 1997. Mass Extinctions and Their Aftermath. Oxford University Press. New York.

Havlicek, V. 1971. Brachiopodes de l'Ordovicien du Maroc. *Not. et Mem. Serv. Geol*. 230:1-135.

Hermann, A.D. and B.J. Haupt, M.E. Patzkowsky, D. Seidov, R.L. Slingerland, 2004, Response of Late Ordovician paleoceanography to changes in sea level, continental drift, and atmospheric pCO_2: Potential causes for long-term cooling and glaciation. Palaeogeography, Palaeoclimatology, Palaeoecology. 210:385-401.

Ivany, L.C., W.P. Patterson, K.C. Lohmann. 2000. Cooler winters as a possible cause of mass extinctions at the Eocene/Oligocene boundary. *Nature* 407:887-890

Lespérance, P.J. 1974. The Hirnantian Fauna of the Perce area (Quebec) and the Ordovician-Silurian boundary. *American Journal of Science* 274:10-30.

——., 1988. Trilobites. *Bulletin of the British Museum of Natural History Geology* 43:359-376.

Lieberman, B. S. 1994. Evolution of the trilobite subfamily Proetinae and the origin, evolutionary affinity, and extinction of the Middle Devonian proetid fauna of Eastern North America. *Bulletin of the American Museum of Natural History* 223:1-176.

——., 1999. Turnover pulse in trilobites during the Acadian Orogeny. Proceedings of the Appalachian Biogeography Symposium. *Virginia Museum of Natural History Special Publications* no 7:99-108.

——., and G. Kloc. 1997. Evolutionary and biogeographic patterns in the Asteropyginae (Trilobita, Devonian). *Bulletin of the American Museum of Natural History* 232:1-127.

——., and A. L. Melott. 2007. Considering the case for biodiversity cycles: reexamining the evidence for periodicity in the fossil record. *PLoS One* 2(8) e759:1-9., 2012

——., and A. L. Melott. 2012. Whilst this planet goes cycling on: What role for periodic astronomical phenomena in large scale patterns in the history of life? In J. Talent (Ed.), *Earth and Life: Global Biodiversity, Extinction Intervals, and Biogeographic Perturbations Through Time*. Springer, Berlin. In press.

Melott, A.L. and B.S. Lieberman, C.M. Laird, L.D. Martin, M.V. Medvedev, B.C. Thomas, J.K. Cannizzo, N. Gehrels, C.H. Jackman. 2004. Did a gamma-ray burst initiate the late Ordovician mass extinction? *International Journal of Astrobiology*. 3(1):55-61

Neuman, R.B. 1968. Paleogeographic implications of Ordovician shelly fossils in the Magog belt of the Northern Appalachian region. *In* Zen, e., WS White, JB Hadley, and JB Thompson (eds). Studies of Appalachian Geology: Nothern and Maritime. 35-48. Intersience Publ. New York

Nikitin, I.F. 1976. Ordovician of Kazahkstan. Pt. 1. Stratigraphy. Nauka Kaxakh. Ssr, Publishing House, Alma-Ata.

Raup, D.M. and J.J. Sepkoski. 1982. Mass Extinctions in the Marine Fossil Record. *Science*. 215(4539):1501-1503.

Rohde, R.A. and R.A. Muller, 1995. Cycles in fossil diversity. *Nature* 434:208-210

Rong, J.1979. The *Hirnantia* fauna of China with comments on the Ordovician-Silurian boundary. *Acta Stratigraphica Sinica* 3:1-8.

——., 1984. Distribution of the *Hirnantia* fauna and its meaning. *In* Bruton, DL. (ed) Aspects of the Ordovician System. Paleontological Contributions from the University of Oslo, No. 295:101-112. Oslo.

——., and D.A.T. Harper. 1988. A global synthesis of the latest Ordovician Hirnantian brachiopod faunas. *Transactions of the Royal Society of Edinburgh* 79:383-402.

Saltzman, M.R. and S.A. Young, 2005, Long-lived glaciation in the Late Ordovician? Isotopic and sequence-stratigraphic evidence from western Laurentia. Geology. 33(2):109-112.

Schönlaub, H.P. 1971. Palaeo-environmental studies at the Ordovician/Silurian Boundary in the Carnic Alps. *In* Colloque Ordovicien-Silurien, Brest, Setp. 1971. *Mem. Bur. Rech. Geol. Min.* 73:367-378.

Sepkoski, J.J. 1996. Patterns of Phaneroxoic extinction: a perspecitve from global data bases. *In* Valentine, JW (ed). Global Events and Stratigraphy in the Phanerozoic. Princeton University Press, Princeton.

Sheehan, P.M. 1973. The relation of Late Ordovician glaciation to the Ordovician-Silurian changeover in North American brachiopod faunas. *Lethaia* 6:147-154.

——., 2002. The Late Ordovician Mass Extinction. *Annual Review Earth Planet Science* 29:331-364.

Stanley, S.M. 1984. Temperature and biotic crises in the marine realm. *Geology* 23:205-208.

Swoford, D. 1998. PAUP* v.4.0. http://PAUP*.csit.fsu.edu/

Temple, J.T. 1965.Upper Ordovician braciopods from Poland and Britian. *Acta Paleontologica Polonica* 10:379-450.

Vandenbroucke, T.R.A. and H.A. Armstrong, M. Williams, F. Paris, J.A. Zalasiewicz, K. Sabbe, J. Nõlvak, T.J. Challands, J. Verniers, T. Servais. 2010. Polar front shift and

atmospheric CO_2 during the glacial maximum of the Early Paleozoic Icehouse. PNAS. 107(34):14983-14986.

van Dam, J.A. and H.A. Aziz, M.A.A. Sierra, F.J. Hilgen, L.W. van den Hoek Ostende, L.J. Lourens, P. Mein, A.J. van der Meulen, P. Pelaez-Campomanes. 2006. Long-period astronomical forcing of mammal turnover. *Nature*. 443:687-691.

Vrba, E. 1985. Environment and evolution: alternative causes of the temporal distribution of evolutionary events. *South African Journal of Science* 81:229-236.

——., 1992. Mammals as a Key to Evolutionary Theory. *Journal of Mammalogy* vol. 73,1:1-28

——., 1995. The fossil record of African Antelopes (Mammalia, Bovidae) in relation to human evolution and paleoclimate. *In* Vrba, E.S. and G.H Denton, T.C. Partridge, L.H. Burckle (eds). Paleoclimate and evolution, with emphasis on human origins Yale University Press

FIGURES AND CAPTIONS

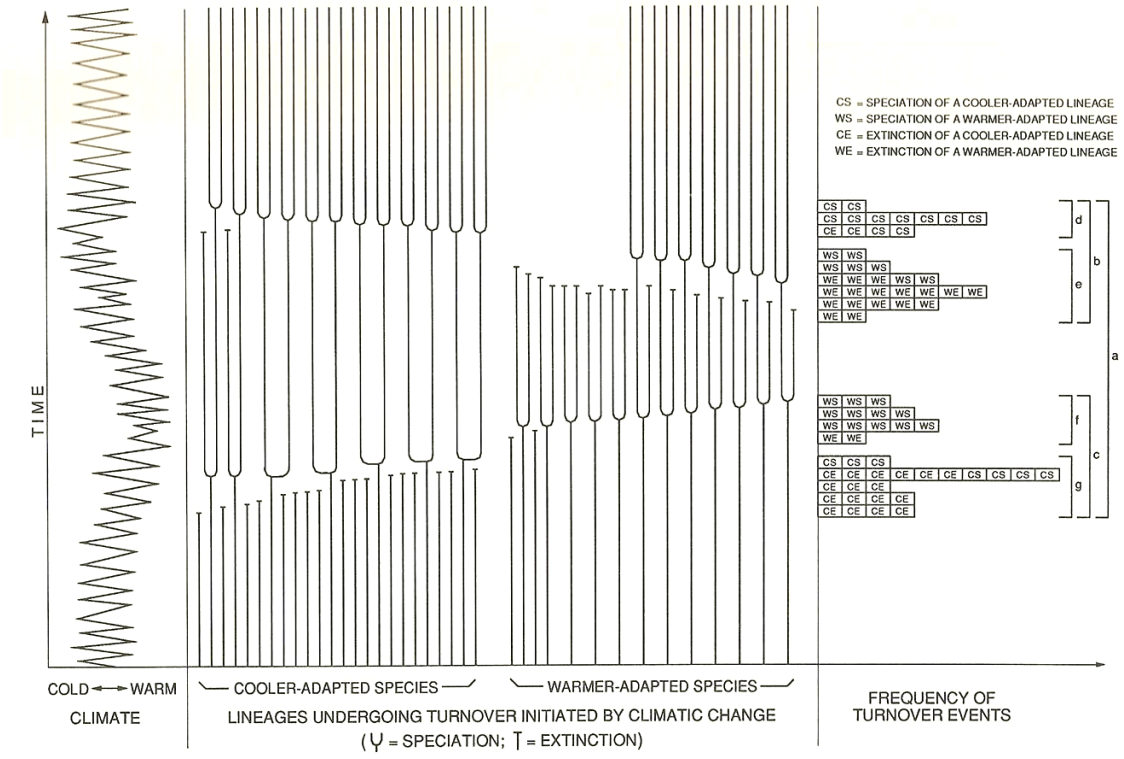

Figure 1: From Vrba (1995), a graphical depiction of the Relay Model. The short and long term oscillations on the left of the graph are temperature swings through time, while the middle of the

figure consists of hypothetical cold and warm adapted lineages. When long term climatic swings push strongly warm, the cold lineages go through a period of pulsed extinction followed by pulsed speciation while the warm lineages diversify. When the temperature swings extremely cold, the opposite pattern occurs.

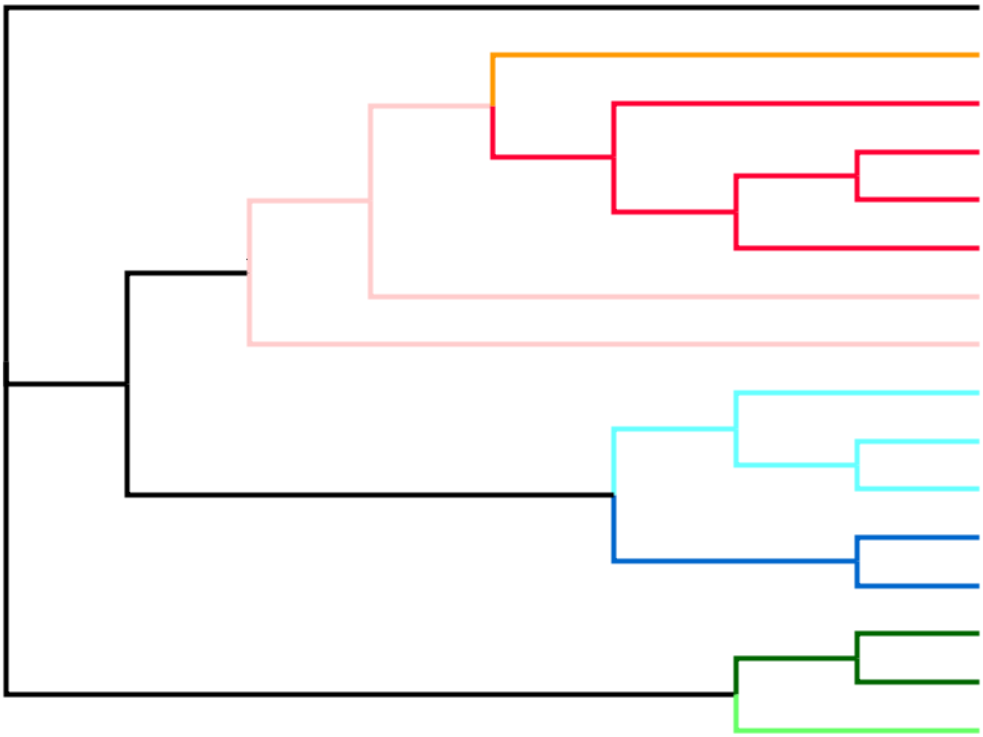

Figure 2: Phylogeny of Ordovician homalonotid trilobites generated by Congreve and Lieberman (2008). Taxa denoted by the pink limbs are members of the genus “Brongniartella”.

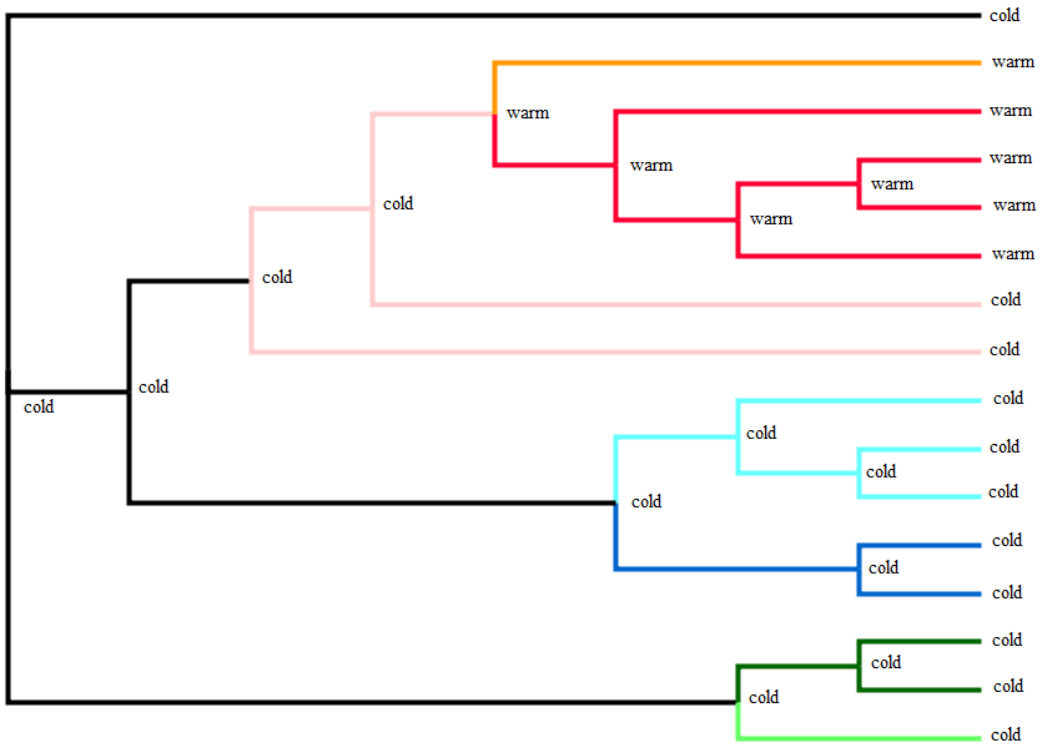

Figure 3: After Congreve and Lieberman (2008). The phylogeny of Ordovician homalonotid trilobites with the character states for warm and cold adaptation mapped to the tree.

Conclusion

Curtis R. Congreve

Extinction and Survivorship Patterns

There is potentially one factor that unites the trilobite clades that survive the extinction event: each clade that survives experienced some range expansion at the Hirnantian extinction event. The clade of deiphonines that survived the extinction dispersed to Australia from a Laurentia-Baltica complex (Congreve and Lieberman 2010), the sphaerexochines dispersed from Laurentia to South China at the end Ordovician (Congreve and Lieberman 2011), and the clade of homalonotids that survived the extinction geodispersed from Gondwana to a Laurentia-Baltica-Avalonia complex (although this dispersal likely originated due to the tectonic rifting of Avalonia off of Gondwana and subsequent drifting of the continent northward that began in the early Ordovician) (Congreve and Lieberman 2008). Conversely, the ceraurids remained endemic to Laurentia throughout the end Ordovician. As such, it is possible that dispersal during the extinction event could have proven advantageous for survivorship across the extinction event. It has previously been suggested that broadly adapted invasive species are more likely to survive the Devonian mass extinction event (Stigall 2010). While the Devonian mass extinction event is not directly comparable to the end Ordovician (as the Devonian event is likely caused by a substantial decrease in speciation rates as opposed to an increase in extinction rates), it is interesting that dispersal could be a factor affecting survivorship to taxa in both extinction events.

In the previous chapter, the Cladal Turnover Model was presented as an alternative hypothesis to explain the patterns of extinction and survivorship observed in the Hirnantia fauna. However, given that the Cladal Turnover Model is based upon the Relay Model, we would expect the model to also make predictions about extinction and survivorship patterns in non-Hirnantia taxa. Specifically, it would be expected that these taxa would undergo preferential extinction and range contraction during the first pulse of extinction, and would subsequently speciate and expand their ranges after the second pulse. Thus, we can compare the survivorship patterns of the cheirurid trilobite clades (deiphonines, ceraurids, and sphaerexochines) with the Cladal Turnover Model to determine if the model does in fact provide a more complete understanding of the extinction event. Of the three cheirurid trilobite taxa analyzed in this thesis, the ceraurids most exemplify the expected non-Hirnantia pattern given the Cladal Turnover Model. The group does not experience any range expansion/dispersal during the Hirnantian, remaining endemic to Laurentia, and goes extinct at the first pulse. The deiphonines show some support for the Cladal Turnover Model, in that they experience strong extinction at the first pulse and subsequently proliferate when the environmental conditions return to normal after the second pulse. However, the group does not appear to experience any range contraction during the event, but rather disperses during the Hirnantian from Laurentia-Baltica to Australia. Finally, the sphaerexochines do not show any support for the model, as the group does not appear to be strongly affected by the mass extinction event. That being said, the sphaerexochines might represent an odd outlier that either was lucky enough not to be affected by the environmental shifts associated with the extinction event, or consisted of strongly eurytopic species that could easily survive and adapt to the changing conditions.

Future Work

Given the data presented in this thesis, there is some evidence that the Cladal Turnover Model could explain extinction and speciation patterns observed in the end Ordovician mass extinction. The homalonotids and ceraurids show survivorship patterns that strongly corroborate the model, and the observed survivorship patterns of the deiphonines also appear to support the Cladal Turnover Model, although not as definitively. However, the survivorship patterns of the sphaerexochines would not be predicted given the Cladal Turnover Model. Given these contrasting results, and the relatively limited size of our original data set, more detailed phylogenetic and biogeographic studies need to be conducted on Ordovician taxa to determine if the Cladal Turnover Model is a general pattern for the majority of taxa. Ideally, these new studies should not only come from other trilobite groups, but also from other phyla. If the patterns of the Cladal Turnover Model can be found in other disparately related taxa, such as brachiopods and echinoderms, this would be strong evidence in support of the model, as it would be less likely that similar evolutionary patterns would be recovered in distantly related taxa through random chance. In turn, if subsequent studies suggest that the Cladal Turnover Model is occurring in the end Ordovician with a strong relative frequency, this type of research program could then be applied to other mass extinction events to determine if the model is generally applicable to different periods of life history, or if it is a pattern that is unique to the end Ordovician. In either case, the results of these types of studies would be intriguing. If the patterns of pulsed extinction and proliferation suggested by the Cladal Turnover Model do occur in other mass extinction events, then it suggests there are some intrinsic unifying elements common to all mass extinction events (possibly owing to how taxa respond to dramatic shifts in climate). If, however, the Cladal Turnover Model is found to only be applicable to the end Ordovician, then it

suggests that mass extinction events are likely independent events with survivorship patterns that are random with respect to each other. In either case, continued study into potential repeated survivorship patterns of mass extinctions will be an important research agenda for paleontology, partly because these unique periods of evolutionary upheaval are important turning points in the history of life and partly due to the current biodiversity crisis. Studying these important events in the past allows us to better understand the history of life, and potentially allows us to better understand and predict the long term ramifications caused by anthropogenic habitat destruction.

References

Congreve, C.R. and B.S. Lieberman. 2008. Phylogenetic and Biogeographic Analysis of Ordovician Homalonotid Trilobites. *Bentham Open; The Open Paleontology Journal* 1:24-32.

——., and B.S. Lieberman. 2010. Phylogenetic and Biogeographic Analysis of Deiphonine Trilobites. *Journal of Paleontology* 84: 128-136.

——., and B. S. Lieberman. 2011. Phylogenetic and biogeographic analysis of sphaerexochine trilobites. *PloS One* 6:e21304.

Stigall, A.L. 2010. Invasive Species and Biodiversity Crises: Testing the Link in the Late Devonian. *PloS One* 5:12 e15584